University of Alberta

Combinatorial synthesis and evaluation of polyamine libraries and oligoboronic acid based saccharide receptors.

Sukhdev Manku ©

A thesis submitted to the Faculty of Graduate Studies and Research in partial fulfillment
of the requirements for the degree of Doctor of Philosophy

Department of Chemistry

Edmonton, Alberta

Spring 2003

National Library
of Canada

Acquisitions and
Bibliographic Services

395 Wellington Street
Ottawa ON K1A 0N4
Canada

Bibliothèque nationale
du Canada

Acquisisitons et
services bibliographiques

395, rue Wellington
Ottawa ON K1A 0N4
Canada

Your file Votre référence
ISBN: 0-612-82137-4
Our file Notre référence
ISBN: 0-612-82137-4

The author has granted a non-exclusive licence allowing the National Library of Canada to reproduce, loan, distribute or sell copies of this thesis in microform, paper or electronic formats.

L'auteur a accordé une licence non exclusive permettant à la Bibliothèque nationale du Canada de reproduire, prêter, distribuer ou vendre des copies de cette thèse sous la forme de microfiche/film, de reproduction sur papier ou sur format électronique.

The author retains ownership of the copyright in this thesis. Neither the thesis nor substantial extracts from it may be printed or otherwise reproduced without the author's permission.

L'auteur conserve la propriété du droit d'auteur qui protège cette thèse. Ni la thèse ni des extraits substantiels de celle-ci ne doivent être imprimés ou aturement reproduits sans son autorisation.

Canada

University of Alberta

Library Release Form

Name of Author: Sukhdev Manku

Title of Thesis: Combinatorial synthesis and evaluation of polyamine libraries and oligoboronic acid based saccharide receptors.

Degree: Doctor of Philosophy

Year this Degree Granted: 2003

Permission is hereby granted to the University of Alberta Library to reproduce single copies of this thesis and to lend or sell such copies for private, scholarly or scientific research purposes only.

The author reserves all other publication and other rights in association with the copyright in the thesis, and except as herein before provided, neither the thesis nor any substantial portion thereof may be printed or otherwise reproduced in any material form whatever without the author's prior written permission.

25 Schroeder Drive
Cambridge, Ontario,
Canada
N1P 1B7

November 7, 2002

University of Alberta

Faculty of Graduate Studies and Research

The undersigned certify that they have read, and recommended to the Faculty of Graduate Studies and Research for acceptance, a thesis entitled "Combinatorial synthesis and evaluation of polyamine libraries and oligoboronic acid based saccharide receptors." submitted by Sukhdev Manku in partial fulfillment of the requirements for the degree of Doctor of Philosophy.

Dr. Dennis G. Hall

Dr. Ole Hindsgaul

Dr. Rik R. Tykwinski

Dr. Pierre-Nicholas Roy

Warren

Dr. Warren J. Gallin

Dr. Prabhat Arya

Date approved by committee: Nov. 5, 2002

Abstract

In order to facilitate the discovery of receptors for complex oligosaccharides capable of operating under physiological conditions, a combinatorial approach was taken towards the solid-phase synthesis and evaluation of a oligoboronic acid library. To obtain this library, a resin bound polyamine backbone was desired to provide the necessary scaffold for the alkylation with a 2-bromomethylphenylboronic ester to give the 2-(*N,N'*-dialkylamino)phenylboronic acid units required for saccharide binding. The polyamine library was prepared via the exhaustive amide reduction of a peptide (i.e., a polyamide) library using borane-tetrahydrofuran complex as the reducing agent. A method for reducing polystyrene-bound peptides was developed which employs iodine in a buffered medium to cleave the borane-amine adducts that form after the reduction. This method was found to be mild enough for use on peptides linked to polystyrene supports via the highly acid labile trityl linker. To encode each split-pool library, an efficient partial termination synthesis was developed during the preparation of the peptide library that allowed single beads, expressing a single compound, to be decoded by electrospray mass spectrometry coupled to liquid chromatography. This decoding method was found effective for both polystyrene and TentaGel® bound polyamine libraries, and for TentaGel® bound triboronic acids. Screening of a 289-membered, resin bound triboronic acid library was performed in on-bead assay against a fluorescently labeled Lewis-b glycoside. However, the binding of Lewis-b to any member of the library was never observed, perhaps due to the poor binding affinities that cannot be visually detected. This study has therefore led to a new approach which examines

smaller, tri- and diboronic acid parallel libraries in solution phase screenings against simpler disaccharides.

Since natural polyamines are known to be biologically active, our synthetic polyamine libraries were also evaluated as selective receptors for polyanionic targets. Using a polystyrene bound tetramine library, selective receptors for trisulfonated dyes and a synthetic peptide were discovered via on-bead assays. These preliminary studies will eventually lead to the screening of the polyamine libraries against biologically significant molecules such as oligonucleotides, ion channel proteins and polysulfated saccharides including heparin.

Acknowledgements

I would like to thank, firstly, my supervisor, Professor Dennis Hall for his guidance and support throughout my research. I would also like to acknowledge the members of my examination committee for their helpful comments that went towards the improvement of this thesis. In particular, Professor Ole Hindsgaul for taking an early interest in this project, providing a number of suggestions, and supplying some of the oligosaccharides for the library screenings.

I would also like to thank my scientific collaborators, Dr. Duane Stones, Dr. Fan Wang for their invaluable contributions to the research in this thesis. The assistance of Leon Lau is also appreciated. In addition, I am grateful to Dr. Stones and Michel Gravel for proofreading earlier versions of this thesis manuscript.

A warm thank you is given to the remaining members of the Hall group, both past and present, for creating an great environment for learning chemistry, conducting research and making friends.

I am indebted to the University of Alberta, Department of Chemistry for providing excellent research support, in particular the mass spectrometry and spectral services laboratories whose assistance was vital to the my research. Prof. Rik Tykwinski and his group for allowing me the use of their fluorimeter. Also, Dr. Mohammed Al-Sayah for his aid with the NMR titrations.

The studentship from the Alberta Heritage Foundation for Medical Research (AHFMR) for most of my period of research is greatly appreciated. Additional financial support from the Natural Science and Engineering Research Council (NSERC) of Canada, Research Corporation (Tucson, Az.) and the University of Alberta, Department of Chemistry is also thanked.

Finally, I would like to thank my parents for their constant support from so far away…

Table of Contents

Chapter One: Introduction

1.1: Small molecule recognition of biomolecules 1

1.2: Binding to carbohydrates in nature 5

  1.2.1: Hydrogen bonding. 5

  1.2.2: Metal coordination. 5

  1.2.3: Hydrophobic packing. 6

  1.2.4: Ionic interactions. 6

1.3: Synthetic carbohydrate receptors. 7

  1.3.1: Receptors in organic solvents. 7

  1.3.2: Saccharide binding in water using boronic acids. 8

  1.3.3: Boronic acid-saccharide complexes at neutral pH. 13

  1.3.4: Uses of boronic acids in binding oligosaccharides. 17

1.4: Combinatorial approaches to discovery of selective boronic acid-based oligosaccharide receptors. 18

  1.4.1: Solid-phase synthesis. 19

  1.4.2: Discovery of saccharide receptors from combinatorial libraries. 22

  1.4.3: Oligoboronate libraries on solid support: Towards the discovery of selective receptors for oligosaccharides. 25

1.5: Importance of polyamines in chemistry and biology. 27

1.6: Thesis goals. 30

Chapter Two: Polyamine Synthesis on Polystyrene Resin.

2.1: Solid-phase combinatorial synthesis of polyamines. 31

  2.1.1: Common strategies including exhaustive amide reduction. 31

  2.1.2: The use of iodine in the cleavage of borane-amine adducts. 33

2.1.3: Proposed Mechanism of Iodine-Promoted Oxidative Work-up. 39
2.2: Synthesis of model pentamines on polystyrene resin – extension of initial results. 41
2.3: Synthesis of philanthotoxin 433 and a branched analogue. 46
2.4: Preparation of polystyrene-supported split-pool polyamine and oligoboronic acid libraries. 49
2.4.1: Library encoding by partial termination synthesis. 49
2.4.2: First generation split-pool polyamine and oligoboronic acid libraries. 53
2.5: Conclusions. 61

Chapter Three: Dscovery of polyamines showing selective ion pairing to model polyanionic targets.

3.1: Objectives. 62
3.2: Model dye targets. 63
3.3: Library screening. 64
3.3.1: Screening of tetramine library against Acid Blue-92 (**57**). 65
3.3.2: Screening against dye **58**. 72
3.3.3: Screening against dye **59**. 76
3.4: Nature of the tetramine-dye interaction. 80
3.5: Determination of stability constants. 82
3.5.1: Solution versus solid phase binding. 82
3.5.2: Synthesis of triamine-amides. 82
3.5.3: ^{1}H NMR titrations 84
3.6: Selective extraction of dye **59** ('New Coccine') over dye **58**. 88
3.7: Screening of a glutamate rich peptide. 90
3.8: Conclusions. 93

Chapter Four: Synthesis of polyamines and oligoboronic acids on TentaGel® resin.

4.1: Hydrophobic versus hydrophilic supports. 94
4.2: Synthesis of polyamines on TentaGel® resin. 96
  4.2.1: Development of a borane-resistant TentaGel® resin. 96
  4.2.2: Polyamine and oligoboronic acid synthesis. 99
4.3: Synthesis of new, unnatural amino acid building blocks. 102
4.4: Split-pool synthesis of polyamines and oligoboronic acids on TentaGel® resin. 106
  4.4.1: Polyamine library synthesis. 106
  4.4.2: Polyamine library decoding on 90-150 μm beads. 107
  4.4.3: Polyamine library decoding on 250-300 μm beads. 110
  4.4.4: Triboronic acid library synthesis and decoding. 111
4.5: Conclusions. 117

Chapter Five: Screening of TentaGel® supported polyamine and oligoboronic acid libraries.

5.1: Targets for polyamine libraries. 119
5.2: Competitive assays for on-bead polyamine screening. 121
5.3: Indirect screening methods for oligosaccharide binding. 124
5.4: Screening of fluorescein labeled Lewis-b tetrasaccharide. 126
5.5: Synthesis and screening of NBD-labeled Lewis –b. 129
  5.5.1: Synthesis of labeled Lewis-b 129
  5.5.2: Screening against the triboronic acid library. 131
  5.5.3: Conclusions in the screening of Lewis-b. 131

Chapter Six: Synthesis and solution-phase evaluation of triboronic acid-based saccharide receptors.

6.1: Introduction. 133
6.2: Triboronic acid-based receptors. 134

6.2.1: Receptor design. 134
6.2.2: Receptor synthesis. 137
6.3: Disaccharide targets. 144
6.4: Measurement of binding affinities. 146
6.5: Recent Studies 151
6.6: Assay against blood group B trisaccharides. 153
6.7: Conclusions and future prospects. 154
6.7.1: Conclusions to triboronic acid saccharide receptors. 154
6.7.2: Future research into combinatorial approaches to boronic acid-based saccharide receptors. 155

Chapter Seven: Thesis conclusions. 159

Chapter Eight: Experimental.

8.1: General procedures. 162
8.2: General procedure for the synthesis of polyamides on aminotrityl resin. 164
8.3: General procedure for the exhaustive amide reduction of polystyrene-bound polyamides. 165
8.4: Typical cleavage of solid-supported polyamide/polyamines from trityl linkers. 165
8.5: Synthesis of polyamines on polystyrene resin. 166
8.6: Synthesis of PhTX-433 analogue. 174
8.7: Polyamine library synthesis and decoding on polystyrene resin. 177
8.8: Library screening against trisulfonated dyes. 180
8.9: Synthesis of triamine-amides, and determination of binding constants. 180
8.10: Dye extractions. 183
8.11: Synthesis of biphenyl amino acids. 185
8.12: Synthesis of trityl-TentaGel® resin. 194
8.13: Exhaustive amide reduction on TentaGel® bound polyamides. 197

8.14: Synthesis and decoding of split-pool polyamine and oligoboronic acid library on TentaGel® resin. 200
8.15: Synthesis and screening of anthracenyl-triboronic acids. 203
8.16: Acylation of amino acids. 210
8.17: Labeling of Lewis-b with nitrobenzodiazole 217

Bibliography 218

Appendix (with table of contents)

Table of Contents 226
A.1: ^{1}H and ^{13}C NMR spectra, and HPLC chromatograms of reported polyamines 229
A.2: ^{1}H and ^{13}C NMR spectra of diphenylamino acids and their intermediates 242
A.3: Examples of polyamines and triboronic acids decoded by LCMS 252
A.4: LC and NMR analyses of anthracenyl triboronic acids, **136** 266
A.5: Fluorescence titrations of **136** with disaccharides 274

List of Tables

Table 1.1: Stability constants for phenylboronic acid – polyol complexes. 10

Table 1.2: Stability constants between receptor **12** and mono- and disaccharides at pH 11.3. 12

Table 1.3: Stability constants for monosaccharide complexes with boronic acids **19** and **20.** 16

Table 3.1: Screening of PS-bound tetramine library against **57** ('Acid Blue-92') at pH 7. 66

Table 3.2: Frequency of individual tetramine residues out a total of 50 found in the screening of dye **57**. 67

Table 3.3: Calculated internitrogen distances (in Å) of library residues in their optimized, extended conformations (SYBYL). 69

Table 3.4: Clear beads isolated and decoded in the screening of PS-bound tetramine library against **57**. 71

Table 3.5: Screening of PS-bound tetramine library against **58**. 73

Table 3.6: Screening of PS-bound tetramine library against **59**. 77

Table 3.7: Frequency of individual residues found in the screening of **58** and **59**. 80

Table 3.8: Screening of tetramine library against peptide **72**. 18 beads were isolated. 92

Table 6.1: ESMS and HPLC purities of receptors **136** 142

Table 6.2: Stability constants (M^{-1}) between receptors **136** and disaccharides. 148

List of Figures

Figure 1.1: Examples of complex oligosaccharides. 4
Figure 1.2: Saccharide binding in Nature. 5
Figure 1.3: A and B faces of galactose and glucose. 6
Figure 1.4: Designed saccharide receptors in organic solvents. 7
Figure 1.5: Designed saccharide receptors suitable for neutral, aqueous conditions. 15
Figure 1.6: Complex **20a** and complex **20b**. 17
Figure 1.7: Cerium(IV) bis(porphyrinate) double decker – based receptor for oligosaccharides. 18
Figure 1.8: Parallel library synthesis. 20
Figure 1.9: Split-pool synthesis. 22
Figure 1.10: Structure of D-erythrose. 23
Figure 1.11: Boronic acid-based sialic acid receptor library. 24
Figure 1.12: Natural polyamines. 28

Figure 2.1: Stereoisomers of tetramine **31**. 36
Figure 2.2: HPLC traces of LD-**31** and DD-**31**. 37
Figure 2.3: Other linkers examined in the iodine-promoted work-up. 38
Figure 2.4: Model pentamines synthesized on polystyrene trityl resin. 41
Figure 2.5: LCUV and LCMS traces of pentamine **43**. 45
Figure 2.6: Acylpolyamine neurotoxins. 46
Figure 2.7: Structure-activity assignments for PhTX-433. 47
Figure 2.8: Schematic representation of mass spectrum decoding. 50
Figure 2.9: Fourteen amino acid building blocks used in the first polystyrene bound polyamine library. 53
Figure 2.10: Sample single bead analysis taken from the pentamine library. 57
Figure 2.11: Sample LCMS decoding of a triboronic acid library member. 60

Figure 3.1: Three polysulfonated dyes serving as model polyanionic 64

targets.
Figure 3.2: Hypothetical model of a resin bound tetramine coordinating to a trisulfonated dye. 64
Figure 3.3: Possible conformations of dye **57**. 69
Figure 3.4: Two examples of triamine library beads stained with dye **58** 74
Figure 3.5: Possible conformations of dye **58**. 76
Figure 3.6: Calculated oxygen-to-oxygen distances (in Å) for dye **59**. 79
Figure 3.7: ^{1}H NMR titration curves. 86
Figure 3.8: Job plot of **62** (8Aoc^{R}-8Aoc^{R}) with dye **59**. 87
Figure 3.9: Resin-supported tetramines used in the selective extraction of dyes **58** and **59**. 88
Figure 3.10: HPLC/UV chromatogram of a 1:1 mixture of dyes **48** and **49**. 89

Figure 4.1: Matrix of divinylbenzene cross-linked polystyrene resin. 94
Figure 4.2: Structures of commercially available PS-PEG resins. 95
Figure 4.3: New building blocks 103
Figure 4.4: Sample decoding from a 90 –150 μm TentaGel® resin bead. 110
Figure 4.5: Single bead decoding of 8Aoc^{B}-12Ado^{B} from a 250 – 300 μm TentaGel® bead. 113
Figure 4.6: LCMS of fragmented 8Aoc^{B}-γAbu^{B} 115

Figure 5.1: Repeating units in heparin. 120
Figure 5.2: Small polyanionic targets for TentaGel® bound polyamines. 121
Figure 5.3: Monosulfonated dyes used in displacement assays 122
Figure 5.4: Labeled Le^{b} used for the screening of the triboronic acid library. 126
Figure 5.5: "Controls" tested against Le^{b}-NBD (**125**). 128

Figure 6.1: "Sublibraries" of triboronic acid-based receptors. 136
Figure 6.2: Fluorescence enhancement of a receptor upon titration with disaccharide. 146

Figure 6.3: Titration curves of 4Acc^{B}Amb^{B}Anth^{B} with disaccharides. 147
Figure 6.4: Suspected binding profile of triboronic acid saccharide receptors. 151
Figure 6.5: Diboronic acids recently prepared and tested against lactulose. 152
Figure 6.6: Trisaccharide targets for Amb^{B}Amb^{B}Anth^{B} 153
Figure 6.7: Potential future library of diboronic acids. 156
Figure 6.8: Potential receptors for uronic acids and sialic acid. 157

List of Schemes

Scheme 1.1 9
Scheme 1.2 11
Scheme 1.3 11
Scheme 1.4 14
Scheme 1.5 15
Scheme 1.6 26

Scheme 2.1 32
Scheme 2.2 33
Scheme 2.3 35
Scheme 2.4 37
Scheme 2.5 39
Scheme 2.6 40
Scheme 2.7 42
Scheme 2.8 44
Scheme 2.9 48
Scheme 2.10 52
Scheme 2.11 54
Scheme 2.12 55

Scheme 3.1 83
Scheme 3.2 84
Scheme 3.3 91

Scheme 4.1 97
Scheme 4.2 98
Scheme 4.3 100
Scheme 4.4 101

Scheme 4.5 102
Scheme 4.6 104
Scheme 4.7 105
Scheme 4.8 105
Scheme 4.9 106
Scheme 4.10 108
Scheme 4.11 112
Scheme 4.12 115
Scheme 4.13 117

Scheme 5.1 124
Scheme 5.2 128
Scheme 5.3 130
Scheme 5.4 130

Scheme 6.1 135
Scheme 6.2 137
Scheme 6.3 138
Scheme 6.4 145
Scheme 6.5 158

List of Abbreviations

AcOH	acetic acid
Ac	acetyl
Ac_2O	acetic anhydride
12Ado	12-aminododecane acid
γAbu	4-aminobutyric acid
2(4)Acc	2(4)-aminocyclohexane carboxylic acid
Ala	alanine
εAhx	6-aminohexanoic acid
3(4)Amb	3(4)-aminomethylbenzoic acid
Amc	4-aminomethylcyclohexane carboxylic acid
1,4(3,3)Amp	1(3)-(4'(3')-aminomethylphenyl)benzoic acid
amu	atomic mass units
Anth	anthracenyl
8Aoc	8-aminooctanoic acid
aq.	aqueous
Asp	aspartate
APT	attached proton test
BOC	*tert*-butoxylcarbonyl
t-Bu	*tert*-butyl
°C	degrees Celsius
^{13}C NMR	carbon-13 nuclear magnetic resonance
calcd.	calculated
CBz	carboxybenzoyl
CDI	carbonyl diimidazole
Cy	cyclohexyl
δ	chemical shift downfield from 0 ppm
d	doublet
dd	double of doublets
Dde	1-(4,4-dimethyl-2,6-dicyclohexylidene)ethyl

DEAD	diethylazodicarboxylate
DHP	dihydropyran
DIPEA	*N,N*-diisopropylethylamine
DMF	*N,N*-dimethylformamide
DMS	dimethylsulfide
DNA	2'-deoxyribonucleic acid
EDCI	*N*-ethyl-*N*'-(3-dimethylaminopropyl)carbodiimide
Et	ethyl
ES	electrospray
ESMS	electrospray mass spectrometry
g	grams
GATS	D-glucosamine-2,3,6-trisulfate, trisodium salt
Glu	glutamate
Gly	glycine
FMOC	9-fluorenylmethoxycarbonyl
^{1}H NMR	proton nuclear magnetic resonance
HBTU	*O*-benzotriazol-1-yl-*N,N,N',N'*-tetramethyluronium hexafluorophosphate
HEPES	4-(2-hydroxyethyl)-1-piperazineethanesulfonic acid
HOBt	1-hydroxybenzotriazole
HMPA	hexamethylphosphoramide
HPLC	high performance liquid chromatography
HRMS	high resolution mass spectrometry
Hz	hertz
IP$_3$	inisitol triphosphate
IR	infrared
J	coupling constant
kDa	kiloDaltons
K_a'	stability constant
Le^b	Lewis-b tetrasaccharide
LCMS	liquid chromatography-mass spectrometry

LCUV	liquid chromatography-ultraviolet spectrophotometry
m	multiplet
M	molar
M^+	molecular ion
Me	methyl
MES	2-(*N*-morphorlino)ethanesulfonic acid
MH	protonated molcular ion
min	minutes
mg	milligrams
mL	milliliters
mmol	millimoles
MS	mass spectrometry
m/z	mass to charge ratio
NHS	*N*-hydroxysuccinimide
nm	nanometers
NBD	nitrobenzobenzodiazole
NMP	1-methyl-2-pyrrolidine
Nva	norvaline
obsd.	observed
PEG	polyethylene glycol
PET	photoinduced electron transfer
Ph	phenyl
Phe	phenylalanine
PMP	1,2,2,6,6-pentamethylpiperidine
ppm	parts per million
i-Pr	*iso*-propyl
PS	polystyrene
RNA	ribonucleic acid
rt	room temperature
R_f	retention factor
s	singlet

Su	succinimidyl
t	triplet
TEOF	triethylorthoformate
TIC	total ion current
TIPS	triisopropylsilane
TFA	trifluoroacetic acid
THF	tetrahydrofuran
TLC	thin layer chromatography
TMR	tetramethylrhodamine
TRIS	tris(hydroxymethyl)aminomethane
Trp	tryptophan
trt	trityl
Tyr	tyrosine
UV	ultraviolet
V	volts
Val	valine

Notes: An amino acid abbreviation with a superscripted R denotes a reduced amino acid residue. Example: $\varepsilon\mathrm{Ahx}^{\mathrm{R}}$ refers to a 6-aminohexanoic acid residue within an oligomeric sequence where its carbonyl group has been reduced to a methylene. The result is an amine rather than an amide linkage to the adjacent residue. An amino acid abbreviation with a superscripted B denotes a reduced amino acid residue that has been alkylated at the amine to give a 2-(*N*,*N'*-dialkylaminomethyl)phenylboronic acid derivative. Example: $\varepsilon\mathrm{Ahx}^{\mathrm{B}}$.

Chapter One:
Introduction

1.1: Small molecule recognition of biomolecules.

The discovery of small molecules that can interact with structurally complex biomolecules is a continuing quest in the areas of chemical biology and medicinal chemistry. These receptor molecules* can serve scientists by probing the function of the biomolecule by binding to it and perturbing it from its normal biological role. Finding a small molecule that can alter an undesired function of a specific biomolecular target forms the basis of most research in drug discovery today. However, the difficulty in designing these small molecule receptors lies in having them bind both specifically and with high affinity to a single target that exists within a complex biological environment. For this selectivity and affinity to be possible, each small molecule must possess specific structural elements, arranged in the proper orientation, that are complementary to the binding region of the targeted biomolecule. If the structure of the biomolecule is known and its function more or less understood, then a small molecule can often be obtained through carefully designing its binding elements to match those on the known target. However, in many cases little is known about the structure of the biomolecule, or its very existence is only speculative. In these cases, the only available option is to test large collections, or libraries, of known compounds, either synthetic or natural in origin, to determine if any produces a desired biological action.

The most often targeted class of biomolecules are proteins.[1] Proteins make ideal targets due to their large structural diversity that creates many unique binding sites for a small molecule receptor. This diversity arises through varying combinations of the twenty, naturally occuring amino acid building blocks that present a variety of binding elements that can anchor a small molecule. For instance, charged residues such as aspartate, glutamate or lysine, can bind via ionic interactions. Polar, uncharged residues like serine and threonine provide hydrogen bonding sites in addition to the hydrogen bonding that can occur to the amide backbone of the protein. Phenylalanine and valine are examples of nonpolar amino acids that can create hydrophobic pockets inside the protein, allowing the receptor to take advantage of hydrophobic interactions. In the case of aromatic residues like phenylalanine, tyrosine or trytophan, π-π interactions can also be exploited. Certain combinations of amino acid residues promote the formation of secondary structures such as α-helices and β-sheets, and thus provide motifs within the larger tertiary structure of the protein which a receptor can often target. With many options available for binding proteins, the area of protein recognition has seen many successes both in drug discovery and chemical biology.

---

* Throughout this thesis, the synthetic molecule designed to bind to a biological molecule is referred to as a "receptor" which is sometimes called a ligand by others.

The binding of small molecules to oligonucleotides has also been studied and many drugs that interact selectively with this class of biomolecule are being developed.[2-4] Both DNA and RNA are comprised of four nucleotide residues, each made from a purine or pyrimidine base, a pentose saccharide and a phosphate residue. The major bases are adenine, guanine, cytosine, thymine (in DNA) and uracil (in RNA). Although the number of building blocks in an oligonucleotide is less than with a protein, the complexity of the nucleotide residues in the oligonucleotides and the secondary structures they impart on the biomolecule as a whole, provide excellent opportunities for a small molecule to bind. For example, a molecule can bind electrostatically to the anionic phosphate groups along the outside of an oligonucleotide helix, or inside the major and minor grooves by hydrogen bonding with the edges of the base-pairs, or they can intercalate in between the aromatic rings of the base-pairs. Groove binding and intercalation provide the best opportunity for selective binding to a specific DNA or RNA sequence.

Small molecule receptors designed for the third major biomolecule, oligosaccharides (carbohydrates), have proven to be more elusive. This difficulty occurs despite the large structural diversity in these biomolecules that exists through the incorporation of a large number of monosaccharide building blocks, as well as in the method of linking these monosaccharides together. However, in many cases this diversity is subtle. Furthermore, their greater conformational flexibility compared to proteins and oligonucleotides, and the relatively small area where binding can occur, has made it extremely difficult to develop high affinity and selective synthetic receptors for oligosaccharides.

The lack of oligosaccharide receptors is unfortunate because of their importance as parts of glycoproteins, glycolipids and other conjugates in a variety of events such as intercellular communication, and molecular and cellular targeting.[5, 6] For instance, carbohydrate binding-proteins, also called lectins,[6] that are expressed on the surface of cells, enable the cell to recognize and take-up glycosylated molecules or microorganisms. This process is observed, for example, in the ingestion of pathogenic organisms by macrophages displaying the proper lectin. Lectins also allow cells to localize other cells expressing specific oligosaccharides on their surface. This process is exemplified in the early inflammation response involving the recruitment of leukocytes by a group of lectins, called selectins, to areas of injury.[7] Overrecruitment of leukocytes can lead to chronic inflammation diseases such as rheumatoid arthritis and psoriasis. One of the key oligosaccharides involved in this inflammation process is Sialyl Lewis X (Figure 1.1), and its interaction with the selectins is the subject of much research.[8, 9] Oligosaccharide antigens, such as Lewis b and y tetrasaccharides, are expressed on the surfaces of bacteria, red blood cells and tumor cells, and can provoke an immune response by binding selectively to a particular antibody. Another well known group of antigens are blood group determinants for blood group A and B which are recognized by blood group antibodies specific for each determinant.

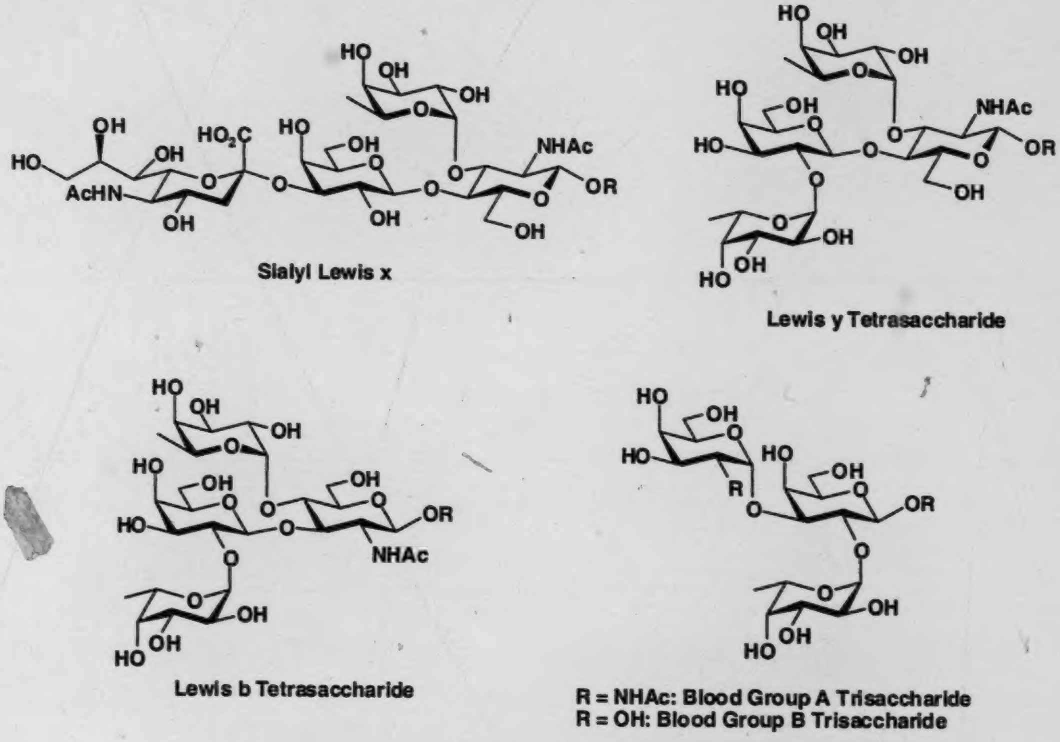

Sialyl Lewis x

Lewis y Tetrasaccharide

Lewis b Tetrasaccharide

R = NHAc: Blood Group A Trisaccharide
R = OH: Blood Group B Trisaccharide

Figure 1.1: Examples of complex oligosaccharides.

Although small molecules have been developed that can inhibit carbohydrate-protein recognition, they all operate by binding to the protein.[10] In order to complement this type of interaction, it would be useful to develop small molecules that can bind to the oligosaccharide. In addition, small molecules would have applications in diagnostics as sensors for oligosaccharides on the surface of a cell or protein. Carbohydrate sensors would also be valuable in the growing area of proteomics as a method of determining if a newly discovered protein exists as a glycoprotein.

1.2: Binding to carbohydrates in nature.

Before considering the design of a synthetic oligosaccharide receptor, it is useful to review the common binding modes found in natural carbohydrate-protein complexes.[6, 10] These binding modes include hydrogen bonding, metal coordination, hydrophobic packing and ionic interactions (Figure 1.2).

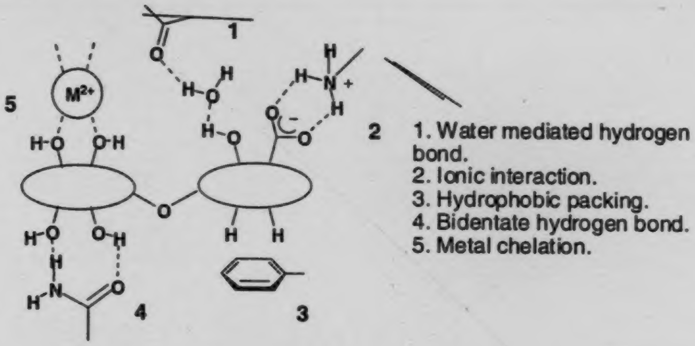

Figure 1.2: Saccharide binding in Nature.

1.2.1: Hydrogen bonding.

Hydrogen bonding often occurs between the hydroxyl groups of the saccharide and the carbonyl and NH groups on the protein amide backbone. Bonding to hydroxylated amino acids, such as serine and threonine, is less frequent due to the entropy loss of fixing two relatively flexible groups upon binding. However, bidentate hydrogen bonds involving the side chains in aspartate, glutamate, asparagine, glutamine, and arginine are more frequently observed and require a specific geometry leading to greater substrate specificity. Many hydrogen bonding interactions are bridged by water molecules. In many cases water can mediate complex networks of hydrogen bonds between the oligosaccharide and the protein.

1.2.2: Metal coordination.

Vicinal hydroxyl groups can also be coordinated to one or more metal ions, such as calcium or magnesium. Surrounding amino acid residues and water molecules complete the coordination sphere around the metal thus securing the saccharide within the protein.

1.2.3: Hydrophobic packing.

Although saccharides are normally considered to be polar molecules, it is recognized that the faces of the pyranose ring in some saccharides have significant hydrophobic character. For instance, galactose, looking at it from the face where the atoms progress from lower number to higher number in a clockwise manner (its "A" face), has its 4-OH group pointing upwards, whereas on its opposite face (its "B" face) its hydrogens are axial (Figure 1.3). As a result, the "A" face of galactose is more polar than its "B" face. It is therefore common to observe nonpolar or aromatic amino acid residues within a protein pressed against the "B" face of galactose.

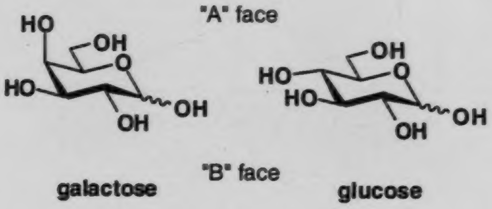

Figure 1.3: A and B faces of galactose and glucose.

With glucose, all the hydroxyls are equatorial and hydrogens axial making both faces of the monosaccharide nonpolar. Hydrophobic packing serves both to contribute to the stability of the protein-carbohydrate complex and to enhance ligand selectivity.

1.2.4: Ionic interactions.

Ionic interactions are often observed between ionic amino acid residues and charged or derivatized saccharides such as sialic acid, aminosaccharides and phosphorylated or sulfated saccharides. Many electrostatic interactions between a cation and an anion are nondirectional and do not require specific geometry unless hydrogen bonding is involved.

1.3: Synthetic carbohydrate receptors.

1.3.1: Receptors in organic solvents.

Initial attempts towards designing synthetic receptors for monosaccharides and oligosaccharides involved mimicking the interactions found within proteins.[11] An example is shown below in Figure 1.4.[12] Receptor **1** contains a cavity that selectively binds octyl pyrannosides **2** to **4** through a set of amide functionalities acting as hydrogen bond acceptor and donor sites, as well as aromatic rings that can press against the hydrophobic faces of the saccharide.

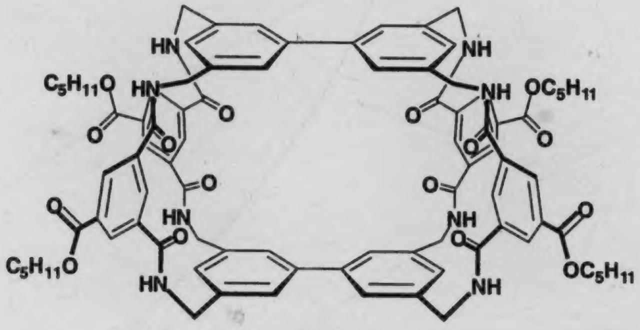
HN
NH
$C_5H_{11}O$
HN
NH
OC_5H_{11}
O
O
O
O
O
O
O
O
HN
NH
$C_5H_{11}O$
O
O
OC_5H_{11}
HN
NH

1

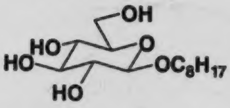
OH
HO
O
HO
OC_8H_{17}
HO

2

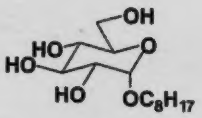
OH
HO
O
HO
HO
OC_8H_{17}

3

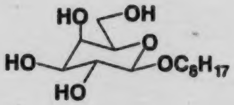
HO
OH
O
HO
OC_8H_{17}
HO

4

K_a by ^1H NMR titration (In $CDCl_3/CD_3OH$)	980 M^{-1}	20 M^{-1}	220 M^{-1}
K_a by fluorescence titration (In $CHCl_3$)	3×10^6 M^{-1}	1.3×10^5 M^{-1}	1.1×10^6 M^{-1}

Figure 1.4: Designed saccharide receptor in organic solvents.

It was found that octyl pyrannoside **2** possessed the greatest affinity towards receptor **1** by both ^{1}H NMR and fluorescence measurements. In order to obtain well resolved spectra, the ^{1}H NMR titrations were conducted in 98:2 $CDCl_3/CD_3OD$ (the methanol was required in order to improve spectral resolution), whereas the fluorescence measurements were performed solely in chloroform. The different stability constants in the two solvent systems illustrate the dramatic effect of even a small amount of polar protic solvent in competing for the hydrogen bonding sites and diminishing the overall binding affinity. This is typical of synthetic receptors that rely on hydrogen bonding and, as a consequence, their use has been restricted to nonpolar organic solvents such as chloroform. Ideally, one would prefer to develop a saccharide receptor that can operate in highly polar solvents, especially water, to make them more suitable for biological applications. Unfortunately, this goal has proven difficult to achieve through synthetic receptors that mimic proteins.

1.3.2: Saccharide binding in water using boronic acids.

In order to alleviate the problem of weak binding associated with receptors that rely on weak noncovalent interactions, researchers have begun turning their attention to reversible, covalent binding receptors. To date, the most promising receptors are based on boronic acids. This class of compounds has been known for a long time to bind covalently and reversibly to the diols of a saccharide via the formation of a boronate ester.[13, 14]

In 1959, Lorand and Edwards[15] first reported observing phenylboronic acid (**4**) and a diol in equilibrium with boronate ester **5** (Scheme 1.1). Under neutral, aqueous conditions, the equilibrium is in favour of the unassociated phenylboronic acid and the diol with only a small amount of **5** in solution. Under more basic conditions, the boronic acid forms the hydroxyboronate **6** which has a greater affinity towards the diol, forming the hydroxyboronate ester **7**. It is believed that coordination of a hydroxide ion to boronate **5** decreases the O-B-O bond angle resulting in the formation of the less strained and more favored tetrahedral boronate in **7**. In terms of pKa values, the pKa of ester **5** is about 1 to 2 units lower than the pKa of the acid **4**, due to the relief of the more strained boron in **5**.[16] (Note that with boronic acids, pKa 's refer to Lewis acidity not to Brönsted or protic acidity, although H_3O^+ is generated indirectly: $ArB(OH)_2 + H_2O \rightarrow ArB(OH)_3^- + H_3O^+$). The pKa of most typical arylboronic acids lies between 8 and 10, which means that boronate **7** will only be favorable at a pH above 8 or 10. For a boronate to be favourable under neutral conditions for biological applications, the boronic acid will need a pKa equal to or less than 7.

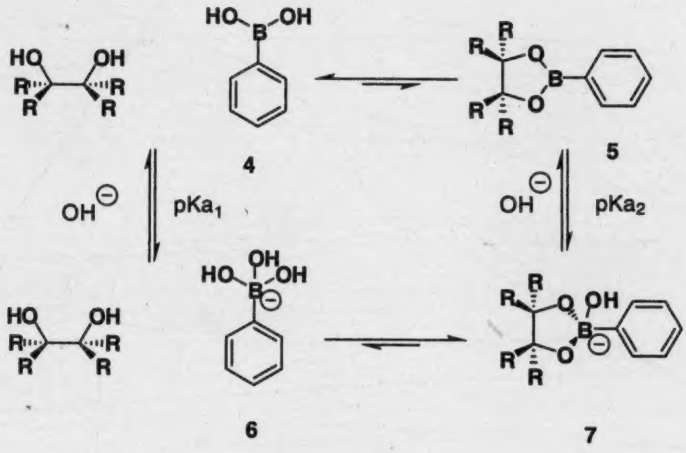

Scheme 1.1

Lorand and Edwards determined the stability constants between phenylboronic acid and various monosaccharides by monitoring the pH depression of the boronic acid upon titration with the sugar (see Table 1.1).[15] It was found that the greatest affinity was towards fructose over all other saccharides and ethylene glycol. However, in a recent investigation by Springteen and Wang[16] using spectroscopic methods, it was discovered that Lorand and Edwards' values reflect the equilibrium between the trigonal boronate **5** and the tetrahedral boronate **7** and not the overall boronic acid-diol stability constants. Both group of authors though show the same relative trend in affinities.

Table 1.1: Stability constants for phenylboronic acid – polyol complexes.

Polyol	K_a (M^{-1}) by pH depression[15]	K_a (M^{-1}) by spectroscopic methods (pH 8.5)[16]
D-fructose 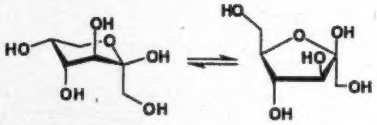	4370	560
D-galactose 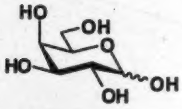	276	80
D-mannose 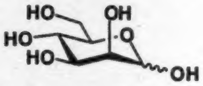	172	not determined
D-glucose 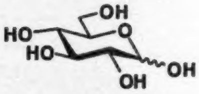	110	11
Ethylene glycol	2.76	not determined

The structure of an arylboronic acid complexed to fructose has only recently been elucidated by Norrild and Eggert using ^{13}C and ^{1}H NMR techniques.[17] It was found that upon mixing *p*-tolylboronic acid (**8**) with fructose at high pH, a mixture of complexes was formed (Scheme 1.2). When a one-to-one mixture of fructose and boronic acid were combined, it was discovered that complex **9**, which has the saccharide in its furanose form, is the most abundant boronate in the equilibrating mixture. With a large excess of *p*-tolylboronic acid, the bisboronate complex **11**, with fructose in its pyranose form becomes predominant.

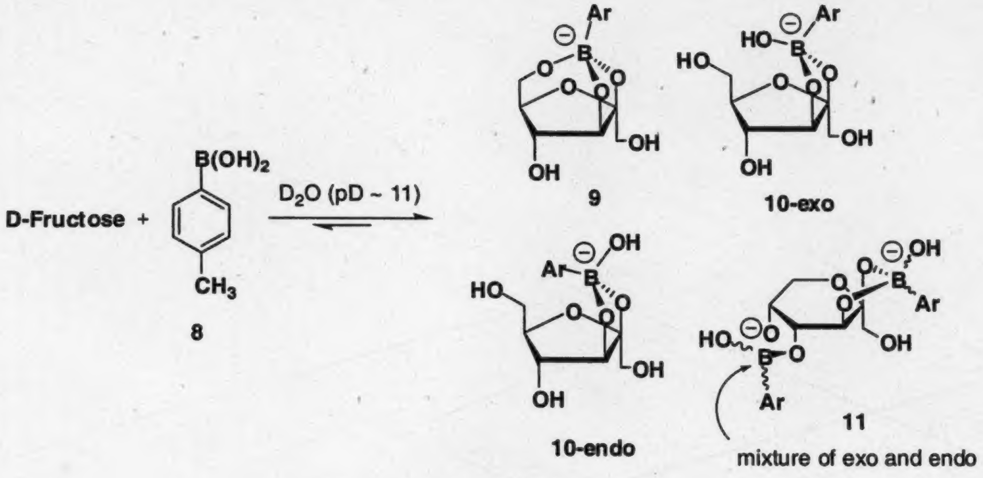
D-Fructose +
B(OH)₂
CH₃
8
D₂O (pD ~ 11)
9
10-exo
10-endo
11
mixture of exo and endo

Scheme 1.2

A noteworthy result in Table 1.1 is the rather weak binding displayed by D-glucose towards monoboronic acids when compared to fructose (110 M^{-1} vs. 4320 M^{-1}). However, Shinkai *et al.* have found that by incorporating two boronic acids in receptor **12** (Scheme 1.3 and Table 1.2), the selectivity turns towards D-glucose.[18] The binding of a series of saccharides to **12** was investigated by monitoring the receptor's circular dichroism (CD) spectrum as it transforms from an uncomplexed achiral molecule to a chiral 1:1 complex that is CD active upon binding to a single chiral saccharide. It is also interesting to note how the binding with disaccharides is much weaker than with simple monosaccharides.

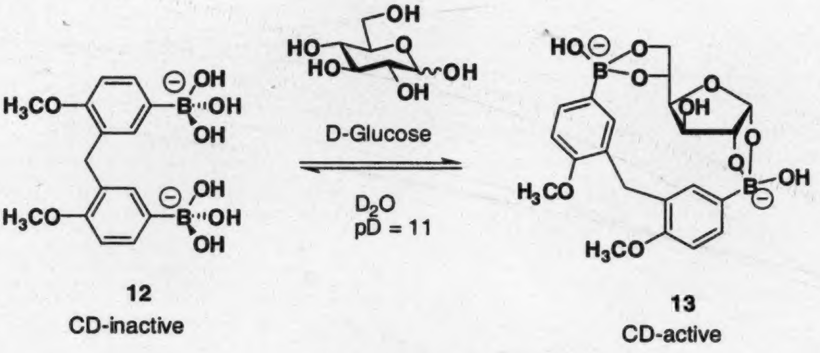
12
CD-inactive
D-Glucose
D₂O
pD = 11
13
CD-active

Scheme 1.3

Table 1.2: Stability constants between receptor **12** and mono- and disaccharides at pH 11.3 as measured by CD spectroscopy.

Monosaccharide	K_a (M^{-1})
D-glucose	19000
D-mannose	60
D-galactose	2200
D-talose 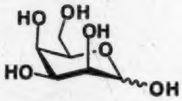 	4600
D-fructose	Too small to detect
Disaccharide	K_a (M^{-1})
D-maltose 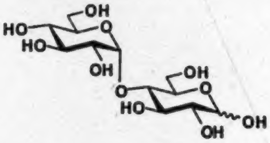 	100
D-cellobiose 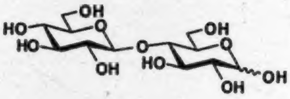 	80
D-lactose 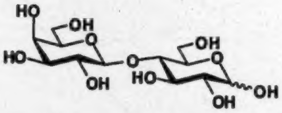 	15

Norrild and Eggert have shown through NMR spectroscopy that glucose binds to the diboronic acid receptor while in its furanose form, as shown in structure **13**.[19] The preference for the α-furanose form of glucose in binding to boronic acids is intriguing since in the absence of receptor **12** α-D-glucofuranose only exists in water as 0.14% of all possible anomers. This α-furanose preference offers a useful hint in explaining the relatively weak binding observed between **12** and the disaccharides shown in Table 1.2, which cannot convert to their furanose forms due to the glycosyl linkage at the 4-OH position at the reducing sugar.

1.3.3: Boronic acid-saccharide complexes at neutral pH.

With a strategy in place to bind saccharides in water, the next step was to lower the operating pH from 11 to 7. As described earlier, enabling a boronic acid to bind to a diol at pH 7 would require lowering its pK_a to a value less than 7. One method is to position an aminomethyl substituent *ortho* to the boronic acid on the phenyl ring.[20] The pH profile for this type of boronic acid is illustrated in Scheme 1.4.[21] At low pH the boronic acid exists as **14** with the protonated amine. Upon titration with base, the boronic acid **14**, with a pKa_1 of 5, converts to **15** where the amine is coordinated to the boron. This provides a tetrahedral boronate species that is reminiscent of the hydroxy boronate that was required to bind a diol at high pH, but now existing below pH 7. Since a given boronate ester is more Lewis acidic than its corresponding acid, the addition of a diol, such as a saccharide, will result in tighter coordination between the boron and the adjacent amine. However species **15**, can also be in equilibruim with its hydrate **17**, which in turn can convert to its zwitterionic species **18**. Increasing the pH to approximately 11 breaks the boron-nitrogen coordination in favour of the hydroxyboronate **16**. Both of the structures **15** and **18** are capable of binding a saccharide under neutral, aqueous conditions.

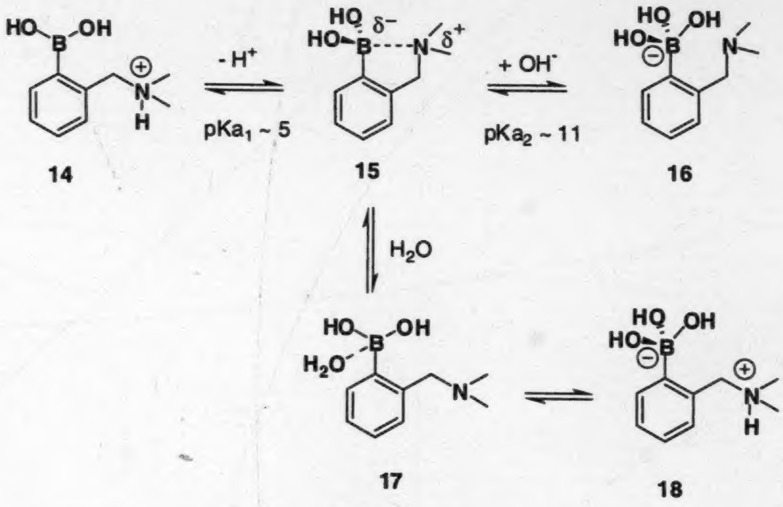

Scheme 1.4

Selective binding of monosaccharides under neutral conditions was first achieved by Shinkai *et al.* in the design of receptors **19** and **20** (Figure 1.5).[22] Each receptor incorporates the desired amine functionality adjacent to the boronic acid, along with an anthracene moiety to act as a PET (photoinduced electron transfer) sensor.[23] The pH profile of the receptor **19** is shown in Scheme 1.5. Under acidic conditions the amine is protonated (**19a**) causing inhibition of fluorescence quenching by the nitrogen lone pair via a PET mechanism. As the pH is increased to a value close to 7 the fluorescent species **19a** becomes the nonfluorescent boronic acid **19b** with the lone pair now exposed to quench the fluorescence of the anthracene moiety. Although coordination of the nitrogen to the boron does occur in **19b**, it is too weak to completely inhibit the PET process. However, in the presence of a saccharide, the boronate complex **19d** is formed and the increase in the Lewis acidity of the boron causes a stronger coordination with the nitrogen producing a highly fluorescent species. At basic pH, separation of the boron and the nitrogen results, giving the nonfluorescent species **19c** and **19e** without and with the saccharide present. Although exemplified here using the monoboronic acid receptor **19**, a similar pH profile also exists for the diboronic acid **20**. In both cases, a fluorescent species is only produced under neutral conditions when a saccharide is bound to the receptors.

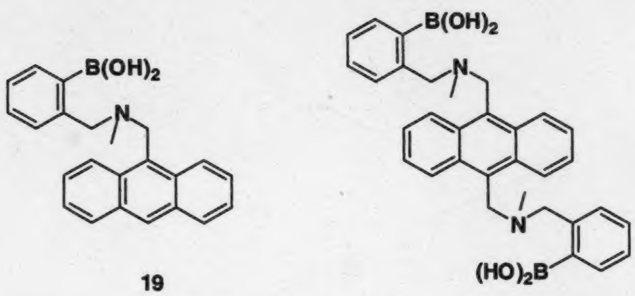
B(OH)₂
N
B(OH)₂
N
N
(HO)₂B

19

20

Figure 1.5: Designed saccharide receptors suitable for neutral, aqueous conditions.

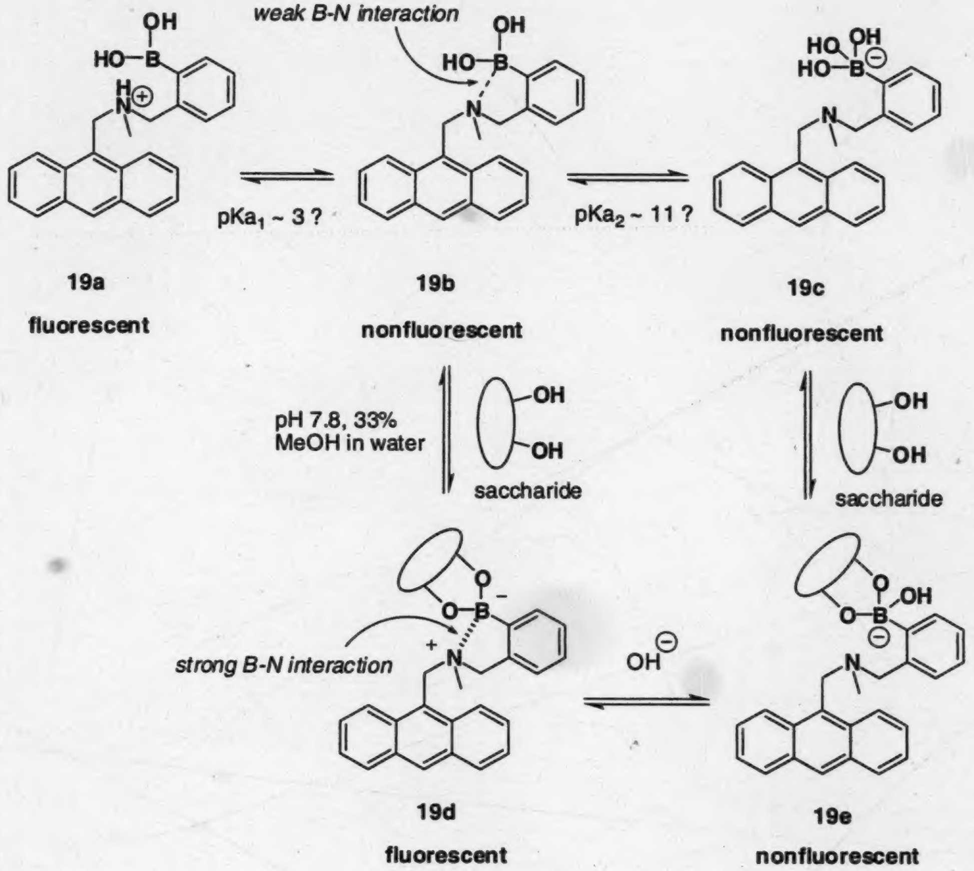
weak B-N interaction
OH
HO—B
H
N⊕
pKa₁ ~ 3 ?
pKa₂ ~ 11 ?
HO OH
HO—B⊖
19a
fluorescent
19b
nonfluorescent
19c
nonfluorescent
pH 7.8, 33% MeOH in water
OH
OH
saccharide
OH
OH
saccharide
O
O—B
strong B-N interaction
OH⊖
O
O—B⊖
OH
19d
fluorescent
19e
nonfluorescent

Scheme 1.5

Just as *p*-tolylboronic acid was more selective towards fructose at high pH, the monoboronic acid receptor **19** showed a similar preference for this monosaccharide under neutral conditions (Table 1.3). Likewise, the diboronic acid receptor **20** gave the largest affinity constant for glucose just as diboronic acid receptor **12** at pH 11.

Table 1.3: Stability constants for monosaccharide complexes with boronic acids **19** and **20** as determined by fluorometry measurements.

Saccharide or diol	K_a (M^{-1}) **19**	K_a (M^{-1}) with **20**
D-glucose	63	3200
D-fructose	1000	316
D-allose	320	630
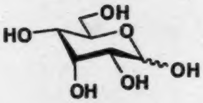		
D-galactose	160	160
Ethylene glycol	2.5	1.6

Following ^{1}H NMR studies in methanol, Shinkai *et al.* proposed the structure of the complex between receptor **20** and glucose to involve the monosaccharide in its pyranose form giving complex **20a** in Figure 1.6.[22] However, Norrild *et al.* have since shown that **20a** is initially formed in anhydrous methanol, but within 20 hours begins to convert to complex **20b** in where the glucose has converted to its α-furanose form.[24] In the presence of a small amount of water in the methanol, within 20 minutes **20b** is the most predominant complex due to the more rapid rate of mutarotation in water compared to methanol. It was argued that the ability of the amino-boronic acid to form the zwitterionic structure as in **18** (Scheme 1.4) at neutral pH, together with the superior stabilization of the tridentate boronates, enables the diboronic acid to bind in the observed 3,5,6-fashion, giving the more thermodynamically favoured α-D-glucofuranose complex.

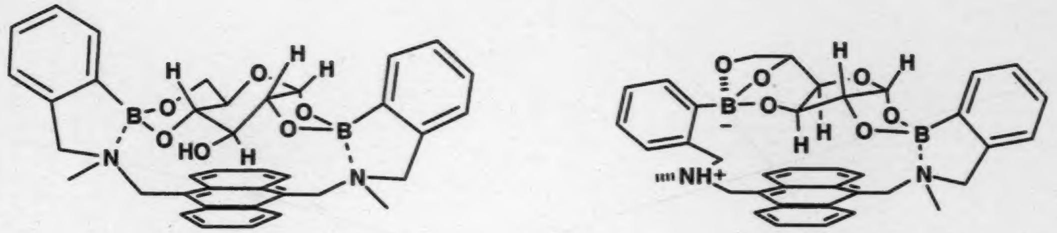

20a **20b**

Figure 1.6: Complex **20a** showing glucose binding to receptor **20** in its pyranose form and complex **20b** showing glucose in its furanose form.

1.3.4: Uses of boronic acids in binding oligosaccharides.

While the above receptors describe the recognition of mainly simple monosaccharides, the use of boronic acids in binding to more complex oligosaccharides has only recently been reported. One example is of a very elegant receptor described by Shinkai *et al.* based on a cerium(IV) bis(porphyrinate) double decker scaffold bearing boronic acids on each porphyrin rings **21** (Figure 1.7).[25, 26] This unique receptor operates in a positive homotropic allosteric manner whereby the binding of one oligosaccharide to a pair of boronic acids, located on the top and the bottom porphyrin ring double decker, suppresses rotation of the two porphyrin planes.[27] The subsequent alignment of the opposite pair of boronic acids allows the binding of another oligosaccharide in a cooperative fashion. The affinities of the receptor towards a series of maltooligosaccharides were shown to be quite remarkable – in the range of 10^5 to 10^6 M^{-2} for a 1:2 complex of receptor to the oligosaccharide in a 1:1 mixture of methanol and water at pH 10.5. Furthermore, receptor **21** has also become the first synthetic receptor to bind to Lewis oligosaccharides in aqueous media. It has even been shown to discriminate between Lewis^x and Lewis^a (K_a 9.0×10^5 M^{-2} and 4.2×10^5 M^{-2} respectively) via the opposite CD signs observed between their complexes with **21**.[28] Although unable to operate under conditions closer to pH 7, this impressive receptor has now opened up numerous possibilities in chemical biology and biotechnology in the selective detection of tumor-associated antigens.

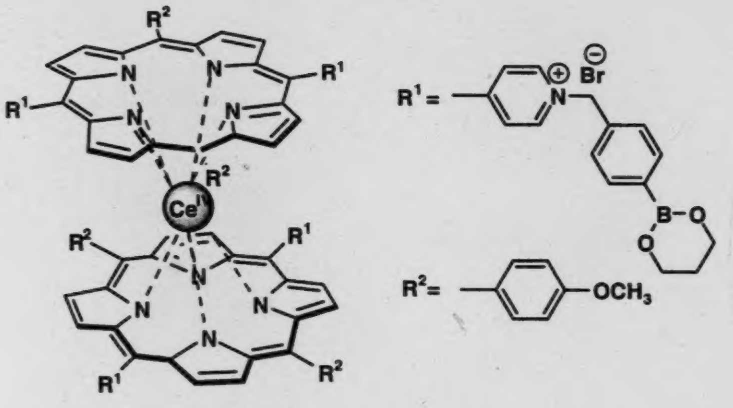

21

Figure 1.7: Cerium(IV) bis(porphyrinate) double decker – based receptor for oligosaccharides.

1.4: Combinatorial approaches to discovery of selective boronic acid-based oligosaccharide receptors.

While the rational design of oligosaccharide receptors has witnessed much progress recently, there is still much work to be done in designing both highly selective and high affinity receptors for increasingly complex oligosaccharides. This challenge is mainly due to the difficulty in predicting the conformation of the oligosaccharide and thus the location of the binding sites on the receptor molecule. To this end, a new approach could be employed to assist in discovering receptors in cases where little is known about the structure of the target biomolecule.

Combinatorial chemistry is a technique that first gained prominence in the 1980's by enabling the synthesis of large numbers of peptides over a short period of time. Combined with improved high-throughput screening technologies, these libraries of compounds can be screened against a target of interest to find an active receptor more quickly in many cases than if a rational design approach was taken. At this point the exact mode of binding of the newly discovered receptor can be investigated.

1.4.1: Solid-Phase Synthesis.

The popularity of combinatorial synthesis has been paralleled with increasing advances in solid-phase organic chemistry. In solid-phase chemistry the synthesis of the desired compounds is performed with its starting materials and intermediates immobilized onto an insoluble support. Typical solid supports used for this purpose are polymeric resin beads between 10 μm and 500 μm in diameter, and are often comprised of polystyrene crosslinked with 1 to 2% divinylbenzene, or polystyrene-polyethylene glycol copolymers.[29, 30] In each reaction, solvent is added to the resin beads causing them to swell and expose their inner reactive sites. This swelling allows reagents to enter the polymeric matrix and react with the resin-bound substrate. After completion of the reaction, the resin is simply rinsed with solvents to wash away the excess reagents. The ability to use large excesses of reagents to drive the reactions to completion, and the ease of removing them afterwards makes solid-phase synthesis attractive for the rapid construction of large compound libraries. The disadvantages of solid-phase synthesis compared to traditional solution-phase synthesis are the difficulties in monitoring the progress of the reaction and in characterizing each synthetic intermediate. At the end of each reaction step, a small amount of compound is cleaved from the resin for identification resulting in the unavoidable loss of material required in the next reaction step. However, recent advances in on-bead characterization (eg. IR microscopy[31] and NMR[32]) have alleviated some of the need to cleave material from the resin at each reaction stage. Solid-phase reactions need to proceed in high purity giving no resin-bound by-products or unreacted starting material, as purification techniques analogous to flash chromatography cannot be performed without cleaving the compound from the resin. As a result, impurities can accumulate on the resin. With these disadvantages, alternative combinatorial methods have been developed using modified versions of solution-phase chemistry that enable the preparation of large libraries.[33-37]

A solid-phase combinatorial library can be made in either of two ways: in parallel or by using a technique called split-pool (or split-mix) synthesis. Parallel synthesis involves keeping each library member separate from each other. Thus, at the end of the library synthesis, each member can be located and identified using standard analytical methods. Figure 1.8 illustrates the synthesis of a nine-membered library using hypothetical building blocks **A** to **F**.

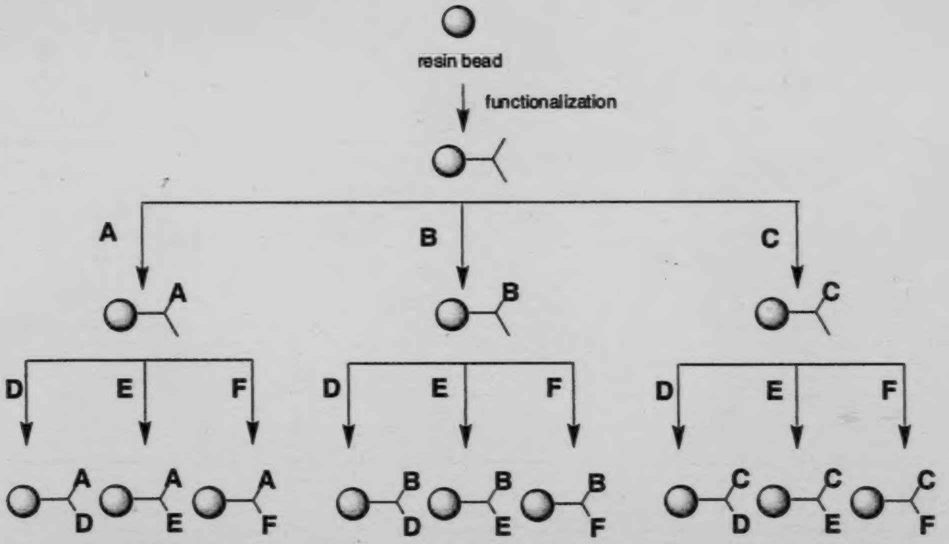

Figure 1.8: Parallel library synthesis showing the synthesis of 12 compounds (final products and intermediates) in 12 chemical steps. (**A** to **F** are individual building blocks)

Sometimes, if applicable, parallel libraries can be synthesized using solution-phase chemistry. One disadvantage of both solution and solid-phase parallel synthesis is that the number of chemical steps needed to make each final compound is not reduced. For instance the synthesis of a library of nine compounds as in Figure 1.8, requires at least twelve chemical steps. This problem often limits the size of parallel libraries.

Split-pool synthesis, first reported by Furka,[38] involves the generation of a library as a mixture of compounds. The technique is illustrated in Figure 1.9. A portion of underivatized resin is first split into separate batches. Into each of batch of resin a different building block is added. After the reaction is complete, all the batches are mixed together and then re-split into three new batches. Again, the building blocks are added, the reactions performed, and the batches re-mixed. If, for example, three building blocks (**A**, **B** and **C**) are added to three batches of resin over three split and mix cycles, then at the end of the synthesis, a total of 3^3 or 27 compounds are made in just 9 chemical steps. If this same library was made using parallel synthesis methods, a total of 3×27 or 81 chemical steps would be required. Now, if we imagine a library elaborated from the combination of 20 building blocks (amino acids for example), coupled 4 times, the result would be a 20^4 or 160000 member library assembled in just 80 chemical steps. In other words, split-pool synthesis provides the greatest efficiency in producing huge libraries, with a very minimal amount of effort. The entire library can even be converted to a new library by reacting the entire pooled resin in what is called a "library from library" approach.[39] Another unique facet of split-pool synthesis is that every resin bead expresses many copies of the same library member and, therefore, is sometimes referred to as the "one-bead, one-compound" approach.[40] Thus split-pool libraries can be screened as a pool of resin-bound compounds against a particular target in an on-bead assay. This type of on-bead assay provides for a high-throughput screening technique while isolating each library member as discrete compounds bound to individual resin beads. The greatest disadvantage of split-pool synthesis is the loss of identity of the compound on each bead due to each mixing step. However, special encoding methods have been developed that enable the identification of each compound on the resin bead even when the compound is only present in small quantities (picomole range sometimes).

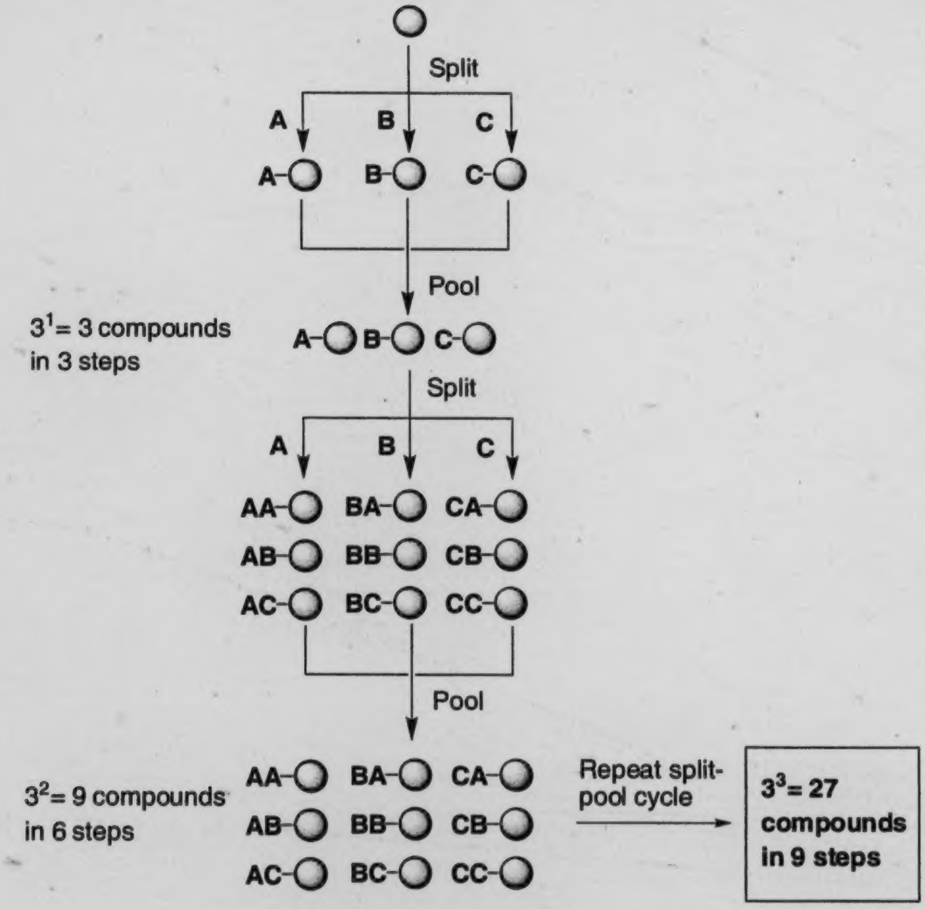
Split
A
B
C
A-
B-
C-
Pool
3¹= 3 compounds in 3 steps
A- B- C-
Split
A
B
C
AA- BA- CA-
AB- BB- CB-
AC- BC- CC-
Pool
3²= 9 compounds in 6 steps
AA- BA- CA-
AB- BB- CB-
AC- BC- CC-
Repeat split-pool cycle
3³= 27 compounds in 9 steps

Figure 1.9: Split-pool synthesis.

1.4.2: Discovery of saccharide receptors from combinatorial libraries.

One example of a saccharide-binding library is a group of pentapeptides that was synthesized towards the discovery of a monosaccharide receptor modeled after the naturally occuring saccharide-protein complexes.[41] The design of the library was around the motif Aro-X-X-X-Aro, where Aro was any aromatic L-amino acid residue, such as phenylalanine, trytophan or tyrosine, while X was any naturally occuring L-amino acid (except cysteine). The aromatic residues at the terminus of the peptide sequence provide the receptor with hydrophobic stacking ability, while the middle residues can potentially offer sites for hydrogen bonding with the monosaccharide. Altogether, a library of 62000 peptides was prepared via the split-pool method. Screening of the library was carried out using an on-bead assay under aqueous conditions buffered at pH 7.0. The target, D-erythrose (Figure 1.10), was reported to have a yellow colour and so when bound to any resin-supported peptide, should turn the corresponding resin bead yellow. A sample of the yellow-stained beads was isolated under a microscope, and their peptide structures determined by peptide sequencing.[42] Of the beads that were stained yellow many of them expressed a pentapeptide with the common motif Trp-N-N-N-Phe/Thr, where two of the three N residues were negatively charged amino acids (Asp or Glu). Using the data from the library screening, three model peptides were prepared as separate compounds and their binding constants to both D-erythrose and D-galactose, were measured by fluorescence spectroscopy to determine if the binding towards D-erythrose was selective. Indeed, the sequences Trp-Gly-Asp-Glu-Tyr and Trp-Ala-Asp-Glu-Phe showed greater affinities towards D-erythrose (K_a ~10^6 M^{-1}) compared to D-galactose (K_a ~10^4 M^{-1}), while another sequence that did not appear in the library screening (Lys-Trp-Ala-Ala-Ala-Trp) gave a rather low K_a value (~10^3 M^{-1}). It was postulated that while the aromatic residues provided the hydrophobic stacking capabilities to the peptide, the asparate and glutamate residues allowed for selective hydrogen bonding interactions to the D-erythrose hydroxyl groups. However, it should be mentioned that D-erythrose should normally be white in colour and what the authors reported to be yellow maybe oxidized impurities in the D-erythrose. Thus the binding that was detected may have been to this impurity and not the desired saccharide target.

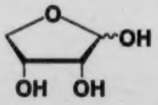

Figure 1.10: Structure of D-erythrose.

The only known saccharide receptor library to employ boronic acids is a library designed to bind sialic acid, and was prepared in a parallel fashion on a *soluble* polymer support, poly(allylamine) (Figure 1.11).[43] The library was designed to use a cooperative binding mechanism by having the boronic acids on the polymer binding to the saccharide diols while the neighbouring cationic amines associating with the carboxylic acid functionality on sialic acid. The synthesis of this library first involved coupling 2 % of the amine sites on the polymer with the carboxylic acid derivative of boronic acid **22** which had the anthracene moiety to allow for fluorescence detection. To introduce further diversity into the library, a small portion of the remaining amines (less than 10 %) were coupled to mixtures of various carboxylic acids. Screening of the library was carried out under aqueous conditions at pH 7.3. According to single point fluorescence measurements, fructose was still the strongest binding saccharide, except in two cases where the poly(allylamine) was derivatized with only 2% boronic acid **22** and when derivatized with 2% **22**, 3% **26** (IMA) and 3% **25** (OCT) as amide side chains. In these cases, sialic acid showed a slightly greater fluorescence response than fructose. All the poly(allylamine) derivatives showed greater binding to sialic acid compared to glucose, indicating the presence of some cooperative binding involving the hydroxyls and the carboxylic acid function of the sialic acid. One drawback of this library approach to boronic acid based receptors is that it uses an uncontrolled synthesis which inevitably leads to the screening of mixtures rather than discrete compounds. The deconvolution of this library mixture to isolate and identify the single most active receptor would be very difficult.

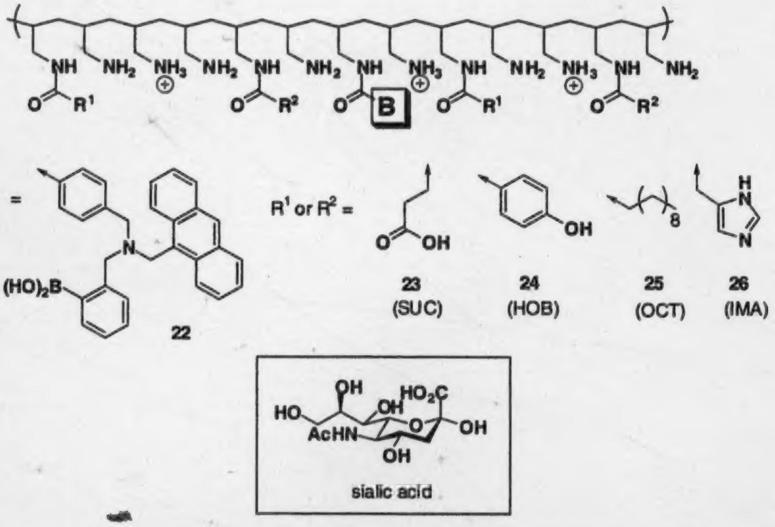

Figure 1.11: Boronic acid based sialic acid receptor library constructed on poly(allylamine) soluble polymer.

1.4.3: Oligoboronate libraries on solid support: Towards the discovery of selective receptors for oligosaccharides.

To date, only two saccharide receptor libraries are known in the literature and were described in the previous section. One is a split-pool library that utilizes binding motifs employed in natural lectins,[41] and the other is a solution-phase library that uses the boronic acid moiety first described by Shinkai *et al.*[43] What has not been reported is a split-pool oligoboronic acid library capable of binding a saccharide at neutral pH. Furthermore, a highly diverse boronic acid library may enable the discovery of selective receptors of saccharides for which no receptor currently exists. However, the production of a library of this kind must overcome three hurdles. First, a method of synthesizing these oligoboronic acids on solid-support must be developed that will allow the incorporation of molecular diversity into the library. In order to target complex saccharides with unique arrangements of diols, more than one boronic acid moiety may be needed in each library member, otherwise it will only bind to fructose (*vide supra*). In addition, to make the library functional at a pH of approximately 7, each boronic acid will need to have an adjacent amine to lower its pKa. Another challenge in any split-pool library is finding a suitable method of decoding each receptor on a single resin bead. Finally, a method of screening the library will need to be devised. The easiest screening method for a split-pool library is to screen it as a large pool of resin bound compounds, as described earlier with the pentapeptide library. Such an on-bead screening assay will require a method for visually detecting the binding event under a low-powered microscope. With the pentapeptide library described above, the detection was relatively simple as the saccharide target, D-erythrose, was reported as coloured. However, most saccharides are colourless. The use of an anthracene moiety on the boronic acid allows for fluorescence detection, but if it were to be used in a library, the anthracene would complicate the synthesis and compromise the diversity of the library.

A potential synthetic strategy for a split-pool oligoboronic acid library is to use the "library from library" approach mentioned earlier.[39] Towards this end, a split-pool library of peptides is an appropriate precursor, since these are the easiest to prepare in terms of synthesis and diversity (Scheme 1.6). The next stage would be to convert the entire library from a peptide, or polyamide, library to a polyamine library through exhaustive reduction of the amides on the peptide backbone. The amines on the polyamines will then provide sites for installing the required *N,N'*-dialkylaminomethylphenylboronic acid, affording an oligoboronic acid library of the type that may possess the ability to bind saccharides.

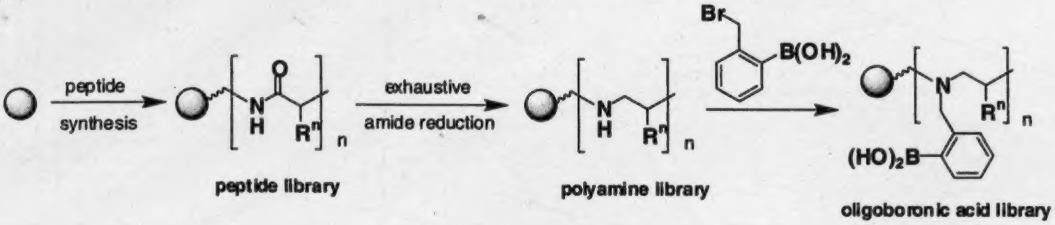

Scheme 1.6

To decode the library, various methods can be used, however, all require specialized instrumentation and/or some modification to the synthesis of the library. The most noninvasive encoding methods are by radio frequency (RF)[44] and optic encoding[45] whereby the resin and an RF or an optic storage device, which records the synthetic history of the resin, are placed inside a permeable polypropylene microreactor. Although ~~very~~ efficient, the major disadvantage is the prohibitive costs of the microreactors and the RF and optic "tag" reading equipment. An alternative method is to use inert chemical tags which work together as a binary encoding system for each building block that is used. The most popular chemical tags are haloaromatic derivatives that bind covalently to the polystyrene backbone of the resin bead.[46] These tags can be selectively cleaved and analyzed by gas chromatography (GC) using a very sensitive electron capture detector. The limitation of this encoding method is the need for an electron capture GC. Another common encoding method is by partial termination synthesis and then analysis by mass spectrometry (MS).[47] This method works best for oligomeric libraries, such as peptides, whereby the coupling of each amino acid building block is accompanied by a small amount of the corresponding capped amino acid. The capped amino acid terminates a small amount of the sequence, while the remaining amino acid allows for the continuation of the synthesis. A mass spectrum of the contents on the resin bead gives the full sequence as the major product and small amounts of the terminated sequences. The identity of each residue can then be determined by the mass differences between the observed MS signals. The disadvantages of this method are the limitations in using isomeric building blocks and the possibility that the terminated sequences may interfere with the screening of the resin-bound library.

The detection of the binding event to a resin-bound library of boronic acids without the use of a PET mechanism is perhaps the most serious challenge in the overall design of this project. One option available is a competitive assay whereby a coloured or fluorescent reagent bound to the boronic is displaced by the binding of a saccharide.[48, 49] However, this type of assay has only been used in solution and not on solid support. Another method is to tag the saccharide with a coloured or fluorescent labeled which can be visualized using a microscope. However, few tagged saccharides are commercially available, and so methods for their preparation may be required.

1.5: Importance of polyamines in chemistry and biology.

One advantage of the strategy depicted in Scheme 1.6 is that the polyamines used as the intermediate to the resin-bound oligoboronic acids could also be biologically active. Natural polyamines are important in biology as they fulfill essential roles in cell growth and differentiation.[50] They are also known to interact with ion channel proteins within the central nervous system and thus are the subject of much investigation in neurochemistry.[50-52] The rich biological properties of natural and synthetic polyamines have also been exploited in the development of potential antitumour[53] and antiinfective agents,[54, 55] carriers for drug[54, 56] and gene delivery.[57] Since high concentrations of natural polyamines seem to be vital in the growth of cancer cells, various polyamine derivatives have been synthesized to inhibit polyamine biosynthesis and transport.[58, 59] Polyamines can therefore be considered privileged structures in biology and medicinal chemistry, and an expansion on their diversity through combinatorial chemistry can potentially uncover new biologically active polyamines. Thus, efforts in optimizing the synthesis of the split-pool polyamine library are more than worthwhile. Examples of natural polyamines, which a synthetic library can diversify upon, are shown in Figure 1.12.

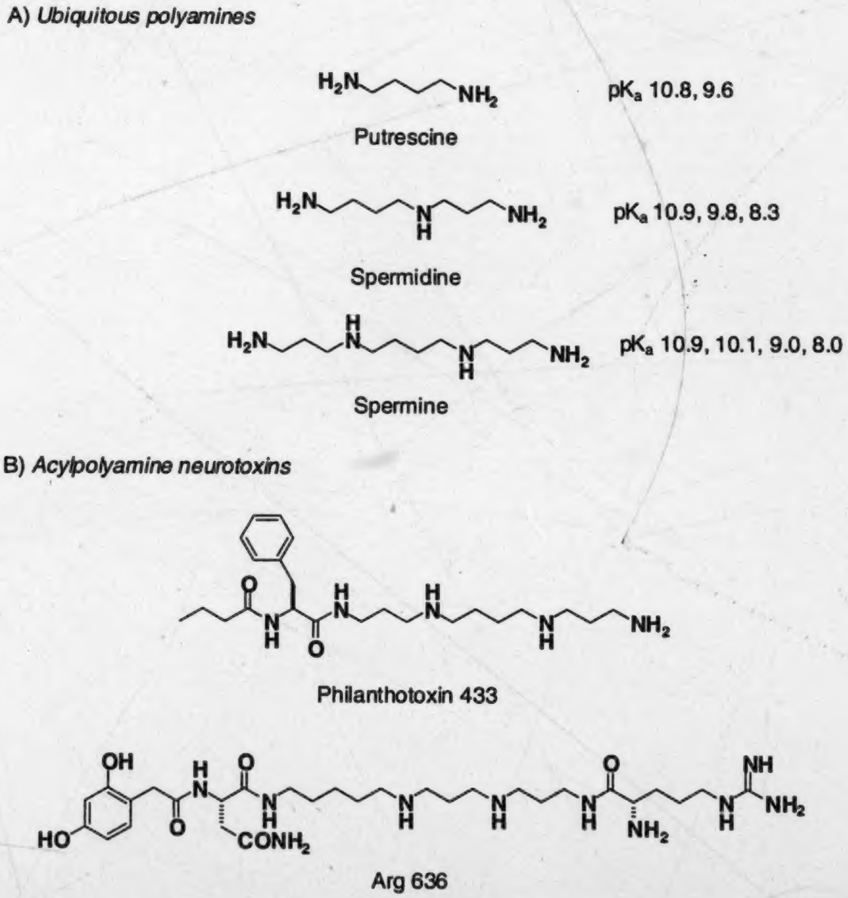
A) Ubiquitous polyamines
Putrescine
pKa 10.8, 9.6
Spermidine
pKa 10.9, 9.8, 8.3
Spermine
pKa 10.9, 10.1, 9.0, 8.0
B) Acylpolyamine neurotoxins
Philanthotoxin 433
Arg 636

Figure 1.12: A) Natural polyamines present in all cells (prokaryotic and eukaryotic) with pK_a values.[60] B) Polyamine neurotoxins found in the venom of wasps and spiders.

Putrescine, spermidine and spermine are the most ubiquitous of all the natural polyamines, present in both eukaryotic and prokaryotic cells in millimolar concentrations. The roles they play in cell growth are unclear, but it is generally accepted that they are involved in controlling gene expression by increasing the rate and accuracy of transcription and translation.[50] At low concentrations, polyamines increase the rate of DNA polymerase activity perhaps by inducing the dissociation of the polymerase from its complex with DNA. Polyamines may also help in DNA uncoiling, required for transcription, by interactions with topoisomerases. Under physiological conditions they become polycationic via polyprotonation. The pK_a's of each amine on putrescine, spermidine and spermine are given in Figure 1.12,[50] where the terminal amines are protonated before the secondary ones.[61, 62] Due to their polycationic nature, it is reasonable to assume that they have particular high affinity for polyanionic biomolecules such as certain proteins, oligonucleic acids and even sulfated oligosaccharides such as heparins.[63]

Several crystal and NMR structures have revealed that the mode of binding between polyamines and short oligodeoxyribonucleotides depends on the specific sequence of the DNA. In general, spermidine and spermine are more active in to binding and stabilizing the A-form of DNA over the B-form.[64-66] With A-DNA, the polyamines have been found to bind in one of three ways:

1. Within the major or minor grooves by hydrogen bonding its cationic ammonium groups to the nitrogen on the nucleotide bases either directly or mediated through water. Additional stabilization can occur through hydrophobic interactions between the methylenes and either the methyls of the thymine or the DNA pentose units.
2. Binding via electrostatic interactions between the ammonium groups and the phosphates along the edge of the DNA sequence. In these cases the binding is believed to be less specific.
3. Binding both to the bases in the major groove and to the phosphates.

All three of the above binding modes have also been observed in tRNA structures stabilized by spermidine or spermine.[67, 68]

The role of polyamines in the activity of ligand-gated ion channel membrane proteins in neuronal cells is complex and poorly understood.[51, 52] For instance, it has been found that with certain ion channel proteins, spermine and spermidine can act allosterically to either enhance or inhibit the binding of regulatory ligands to the protein. At low concentrations, the polyamines will bind to one site of the ion channel, enhancing ligand-protein complexation (i.e. an agonistic effect) while at higher concentrations they will bind to a different site to inhibit complex formation (i.e. antagonistic effect). Acylpolyamine neurotoxins[69] such as philanthotoxin 433 (PhTX 433) and Arg 636 (Figure 1.12) are isolated from the venom of wasps and spiders, respectively, and inhibit the ion conductance of cation channels in their prey by blocking the inside of the ion channel. It is believed that with PhTX 433, binding occurs via electrostatic and hydrogen bonding interactions with glutamate, aspartate and other polar residues along the walls of the channel.[70, 71] This activity towards neural channels has led to investigations into their applications as therapeutic and preventative agents in neurotoxicity, epilepsy and neurodegenerative diseases.

1.6: Thesis goals.

The ultimate goal throughout much of this thesis was directed towards the preparation and screening of a split-pool library of oligoboronic acids for the discovery of receptors with high affinity and selectivity for a complex oligosaccharide. The preparation of this library followed the synthetic route depicted in Scheme 1.6. A polyamide library was made using a partial termination synthesis amenable to decoding by electrospray mass spectrometry. In order to convert the polyamide library to the key polyamine intermediates, an amide reduction method needed to be developed that was suitable for solid-phase synthesis. Finally, installation of the aryl boronic acid units was accomplished by alkylation of the polyamines. With this library in hand, an attempt was made to screen it in an on-bead assay against an oligosaccharide. This screening required a method of detecting the binding of the oligosaccharide to the resin supported oligoboronic acids. In addition to the split-pool library, a smaller, more focused parallel library was also prepared and evaluated for saccharide binding in solution.

While the oligoboronic acid project progresses, some research was directed at the resin bound polyamine libraries as receptors to polyanionic targets. Towards this end, the libraries were screened against appropriate model targets in order to determine if a selective receptor can be discovered that binds using highly ordered ionic interactions as mimics of polyanionic biomolecules.

Chapter Two:
Polyamine Synthesis on Polystyrene Resin.

2.1: Solid-phase combinatorial synthesis of polyamines.

2.1.1: Common strategies including exhaustive amide reduction.

The synthesis of natural and unnatural polyamines both in solution and on solid support has been extensively reported in the literature and has been the subject of two recent review articles.[72, 73] For the synthesis of a library, solid-phase synthesis is the preferred method due to the ease with which it allows one to derivatize the polyamine without resorting to tedious aqueous isolation procedures. The majority of work done on solid-support has basically relied on three methods. The first is the attachment of a natural polyamine building block, like spermidine, to the resin followed by derivatization and then cleavage.[74-77] This method is the simplest and leads to the synthesis of numerous polyamine conjugates by derivatization of the amines. However, it is also limited by the diversity that can be incorporated between the nitrogen spacers on the polyamine chain. The second method is a sequence of protection, alkylation and deprotection steps resembling the traditional methods used in solution phase polyamine synthesis.[78-81] In principle, greater diversity can be achieved between the nitrogens, but overall the method is too laborious for a very large library synthesis. The final method that has been reported is via the exhaustive amide reduction of a resin-bound peptide.[82, 83] This method appears to be the most suitable for a library synthesis since the peptide library intermediates can be easily prepared and diversified. With these advantages in mind, this method was the one we chose to synthesize our polyamine library.

The reduction of amides on solid-support is best achieved by the use of borane (BH_3) as the reducing agent. Although lithium aluminium hydride is commonly used in solution, the need for an excess amount of this reagent in a solid phase reaction would lead to alternative cleavage of the amide to give the alcohol. The mechanism of the reduction of secondary amides by excess borane is depicted in Scheme 2.1.[84, 85]

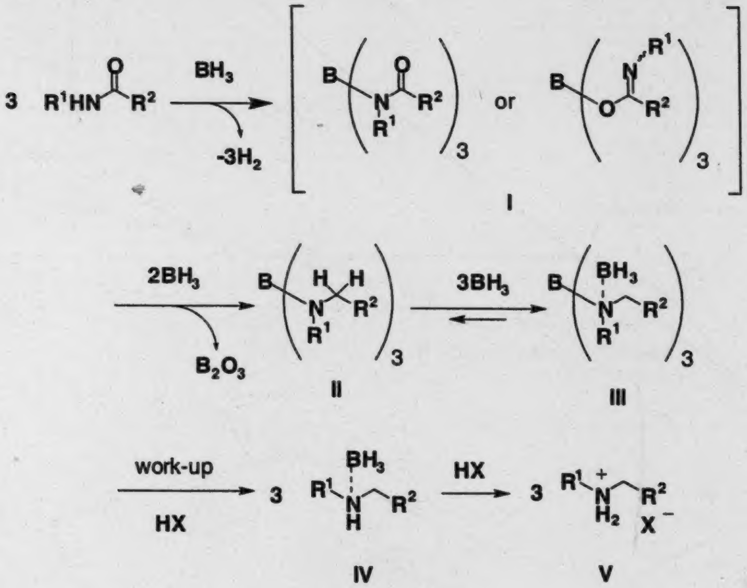

Scheme 2.1

The initial step is an acid-base reaction between one equivalent of borane (three hydride equivalents) and the amidic hydrogens on three equivalents of the amide to give complex **I**. Two hydride equivalents are then delivered to each amide leading to reduction of the carbonyl and the formation of the triaminoborane intermediate **II**. At this point, an additional equivalent of free borane complexes to **II** to afford the borane-amine aminoborane adduct **III**. The hydrides on adduct **III** are not sufficiently activated to continue further reduction, meaning that excess borane is required to complete the reaction. Overall, a total of six hydride equivalents are necessary to reduce one equivalent of a secondary amide. The B—N bonds of triaminoboranes are rather labile and can be easily cleaved under mild conditions, such as weak acid. On the other hand, the borane-amine on **III** and **IV** is more robust and requires harsher methods to effect its cleavage.[86, 87] The traditional solution-phase procedure uses protolytic conditions such as refluxing concentrated HCl or trifluoroacetic acid (TFA)[88] to give the amine salt **V**, or aqueous ammonium chloride (for tertiary amides).[89] Others have reported the use of either basic hydrolysis in aqueous carbonate,[90] or prolonged exposure to refluxing methanol.[91]

The disadvantage of these borane-amine cleavage methods in solid-phase synthesis is that the substrates are usually bound to the resin support via an acid or base sensitive linker. For example, Houghten and co-workers have reported on the reduction of resin-bound peptide derivatives **27** with borane followed by borane-amine cleavage using HCl/methanol at 65 °C. (Scheme 2.2).[92] These strongly acidic conditions can only be employed using linkers, such as methylbenzhydrylamine (MBHA), that are cleaved using anhydrous hydrogen fluoride - a rather inconvenient reagent in solid-phase chemistry that requires specialized equipment.

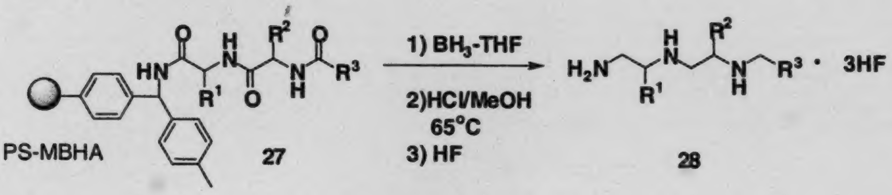

Scheme 2.2

A similiar strategy employed by another group uses TFA to concomitantly cleave the borane-amine adduct and release the product from a 2-chlorotrityl linker on polystyrene.[82] The disadvantage with this approach is that it does not allow the modification of the secondary amines on the solid support after the reduction. A milder protocol is an exchange reaction between the borane-amine and excess piperidine at elevated temperatures over 12 hours.[83] This last method is more suitable for use with acid sensitive linkers allowing the polyamine to remain on the resin for further derivatization. It would be, however, preferred if the borane-amine cleavage could be done at room temperature over a shorter period of time, making it more amenable to rapid parrallel synthesis.

2.1.2: The use of iodine in the cleavage of borane-amine adducts.

In order to perform simpler solid-phase amide reductions on the most convenient acid labile linkers, an investigation was made into alternative procedures towards the cleavage of the borane-amine adducts. One idea came from the early literature describing the titration of these adducts with iodine to liberate the free amine (Eq. 1).[86, 93] It seemed reasonable to assume that the use of iodine could be transferred to solid-phase chemistry on polystyrene resin.

$$R_3N\text{-}BH_3 \;+\; I_2 \;+\; 3\,H_2O \longrightarrow R_3\overset{\oplus}{N}H \;+\; B(OH)_3 \;+\; 6\,\overset{\ominus}{I} \;+\; 5\,\overset{\oplus}{H} \qquad \text{Eq. 1}$$

Our first attempt at reducing a resin-bound amide by this procedure was carried out on trityl-polystyrene bound $H_2N(CH_2)_3NH$-LPhe-LAla-Ac, prepared via FMOC-amino acid peptide synthesis employing HBTU/HOBt as the coupling reagents (Scheme 2.3).[94] The reduction was performed on the triamide **29**, using 30 equivalents of a 1.0 M solution of BH_3 in THF (10 equivalents per amide) at 65 °C for 24 hours, followed by treatment with 15 equivalents of iodine in a buffered media consisting of diisopropylethylamine (DIPEA) and acetic acid in THF (1:2:7 ratio). The buffer system is required as the DIPEA traps the hydroiodic acid that is released, while the acetic acid acts as a protic/nucleophilic source (*vide supra*). A major proportation of THF in the buffer ensures that the resin swelling is maintained in spite of the polar buffer components. After four hours at room temperature the resin was rinsed with THF to remove excess iodine. The bound polyamine was then neutralized with several washes of Et_3N in DMF, followed by washes with methanol to remove polar byproducts, such as boric acid, to furnish tetramine **30**. Cleavage of **30** from the trityl linker was achieved by exposure to 5% TFA in dichloromethane to give the tetrakis(trifluoroacetate) salt **31** in 95% crude yield and 91% purity by HPLC under UV detection. In addition, a sample of resin **30** was also acetylated to with acetic anhydride to give the triacetylamine **32** in 96% crude yield and 95% purity by HPLC following cleavage from the resin. (Note that the colour of the resin upon addition of BH_3-THF complex changes from pale yellow to white. Subsequent treatment with iodine turns it dark brown, then it finally returns to its original pale yellow colour after washing with Et_3N/DMF. It has been observed throughout this work that if the resin failed to turn to its original colour after the Et_3N/DMF washings, the cleaved polyamine was of poorer quality by HPLC and NMR spectroscopy. To ensure a successful reaction it was found necessary to use argon or a fast flow of nitrogen as an inert atmosphere coupled with a high concentration of iodine – between 0.25 to 0.50 g/mL).

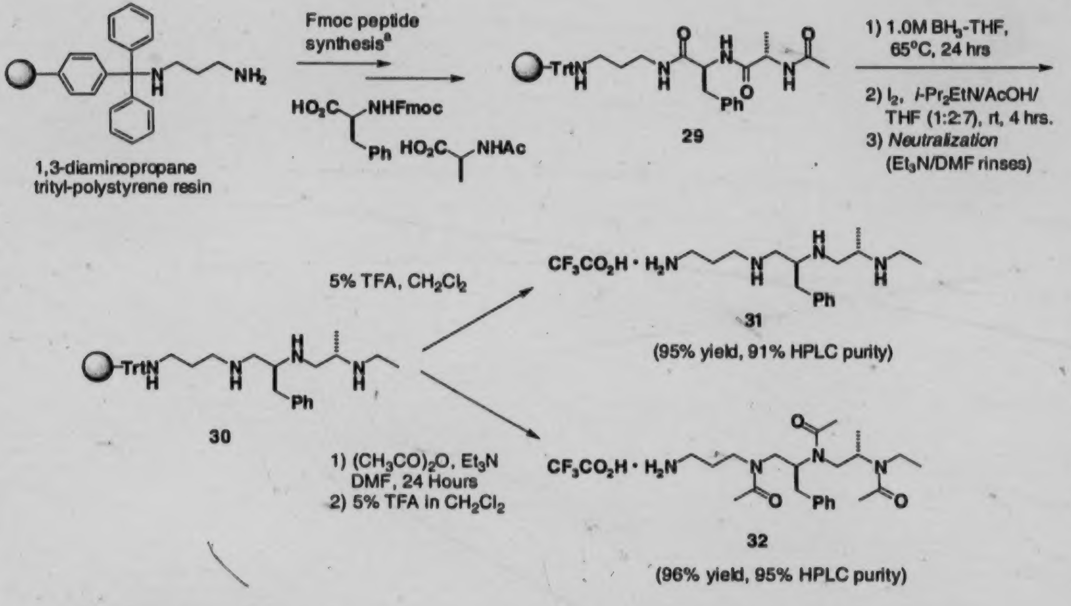
Fmoc peptide synthesis^a
1,3-diaminopropane trityl-polystyrene resin
HO$_2$C NHFmoc
Ph
HO$_2$C NHAc
Trt
29
1) 1.0M BH$_3$-THF, 65°C, 24 hrs
2) I$_2$, i-Pr$_2$EtN/AcOH/THF (1:2:7), rt, 4 hrs.
3) Neutralization (Et$_3$N/DMF rinses)
5% TFA, CH$_2$Cl$_2$
CF$_3$CO$_2$H · H$_2$N
31
(95% yield, 91% HPLC purity)
30
1) (CH$_3$CO)$_2$O, Et$_3$N DMF, 24 Hours
2) 5% TFA in CH$_2$Cl$_2$
32
(96% yield, 95% HPLC purity)

^{a} i)HBTU, HOBt and HO-LPhe-FMOC (2 eq. each), i-Pr$_2$EtN (4 eq.), DMF, 2 hours; ii) 1:4 piperidine/DMF, 0.5 hours; iii) repeat i) with HO-LAla-Ac.

Scheme 2.3

At this stage, a comparison was made between the iodine-promoted work-up and borane-exchange with piperidine.[95] To this end, the reduction was repeated on the same substrate, but this time the work-up was divided into three portions: a) the iodine procedure described above, b) neat piperidine for 24 hours at 65°C, and c) direct addition of acetic anhydride and triethylamine to the borane-amine intermediate. Interestingly, acetic anhydride was found to be sufficiently electrophilic to breakdown the borane-amine adduct to provide **32** in 78% crude yield, albeit in a reduced purity of 78%. The tetramines resulting from the iodine procedure and piperidine exchange were independently acetylated with acetic anhydride to provide **32** in quantitative yield. The purities of **31** and **32** from the piperidine protocol were comparable to those obtained using the iodine, yielding values of 89% and 94% respectively.

One concern was the possibility of epimerization at the stereogenic centers, either during the reduction or in the iodine treatment. To investigate this further, the other three stereoisomers of **31**, shown in Figure 2.1 (DD-**31**, LD-**31**, and DL-**31**), were individually prepared using the same exhaustive reduction and iodine-promoted work-up. Their NMR spectra and HPLC traces were then compared to determine the extent of any epimerization.[95] For instance, if DD-**31** were to undergo partial or complete epimerization at one or both stereogenic centers then its diastereomers, LD-**31** and DL-**31**, would be observed in both the NMR spectrum and HPLC trace. Fortunately, no detectable epimerization was observed as illustrated, for example, in Figure 2.2 which shows the HPLC traces of diastereomerically pure polyamines DD-**31** and LD-**31**. Traces A and B show the independent injection of LD-**31** and DD-**31**, respectively, eluting as single diastereomers. If complete epimerization had occurred both traces would resemble trace C which corresponds to the co-injection of pure LD-**31** and DD-**31**. The apparent lack of epimerization was also evident from the clean ^{1}H and ^{13}C NMR spectra obtained for each of the four diastereomers.

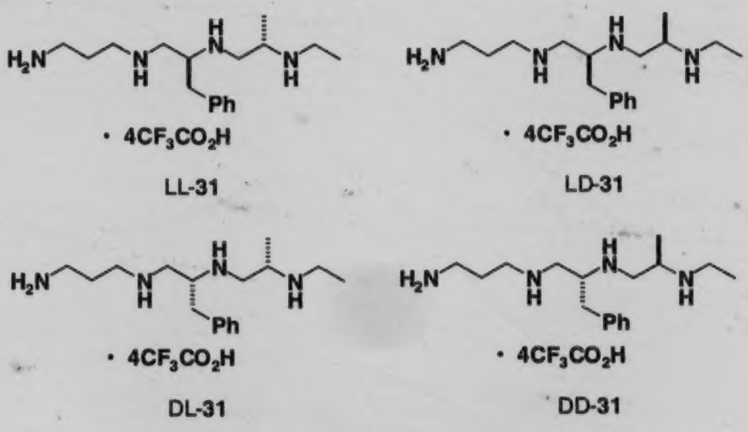

Figure 2.1: Stereoisomers of tetramine **31**.

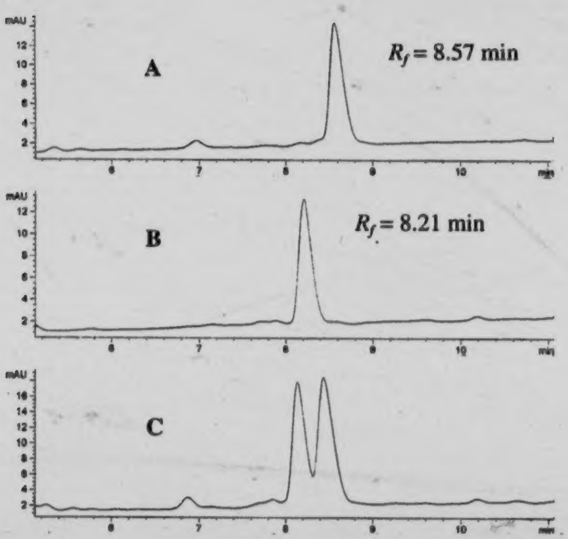

Figure 2.2: **A** - HPLC trace of LD-**31**. **B** - HPLC trace of DD-**31**. **C** Co-injection of LD-**31** and DD-**31**. (See experimental section for HPLC conditions).

The advantages of using a trityl linker in the above reaction sequences are the ease in which substrates can be attached and then conveniently removed by exposure to dilute TFA. However, the utility of the borane reduction/iodine-promoted work-up would be further enhanced if it could be performed on resins and linkers other than trityl polystyrene. To this end, an attempt was made to reduce the same dipeptide attached to a Rink amide linker **33** (Scheme 2.4). Using identical reaction conditions described above, followed by cleavage using 95% TFA with 2.5% triisopropylsilane (TIPS) and 2.5% water, tetramine **31** was isolated, however, in much lower yield and purity.

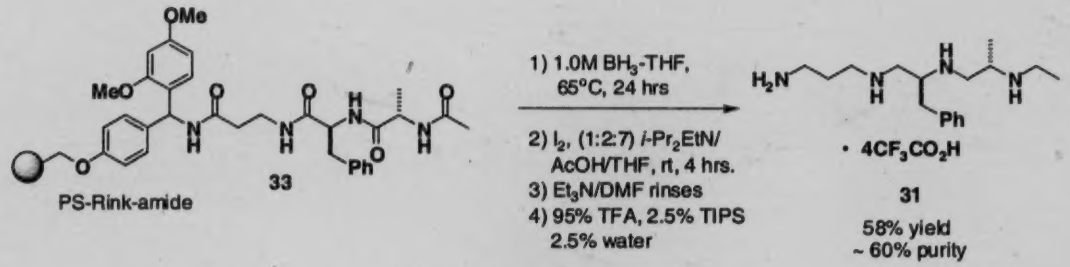
OMe
MeO
PS-Rink-amide
33
1) 1.0M BH_3-THF, 65°C, 24 hrs
2) I_2, (1:2:7) i-Pr_2EtN/ AcOH/THF, rt, 4 hrs.
3) Et_3N/DMF rinses
4) 95% TFA, 2.5% TIPS 2.5% water
H_2N
Ph
· $4CF_3CO_2H$
31
58% yield
~ 60% purity

Scheme 2.4

Interestingly, the reduction and iodine treatment of peptides linked to the resin via a trityloxy functionality instead of a tritylamine led to almost no polyamine product after attempting to cleave the product from the resin by TFA (Figure 2.3). On the other hand, the use of piperidine in the work-up on the trityloxy linker was more sucessful. A similiar observation was made when the peptide was linked via an hydroxy group to dihydropyran (DHP) and Wang linkers; that is, the iodine procedure failed while the use of piperidine gave the product in reasonably good yield and purity. Furthermore, earlier studies in this laboratory have shown that reductions of amides linked to the resin via an ester bond (e.g. bound to Wang linkers) gave reduced yields, presumably due to reductive cleavage of the ester under the extreme conditions of excess borane over high temperature and long reaction times. (These reactions on Wang linkers were done by C. Laplante and D.G. Hall of our labs.)

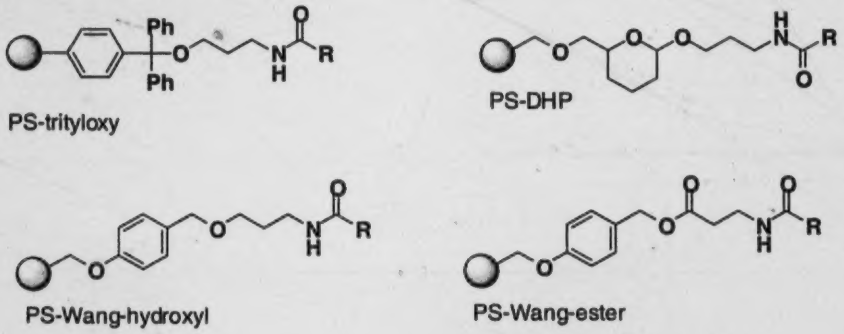

Figure 2.3: Other linkers examined in the iodine-promoted work-up.

Our future interests in screening resin bound polyamine derivatives against biological targets led us to examine the tolerance of hydrophilic polystyrene-polyethylene glycol (PS-PEG) resins, such as TentaGel® resin, towards our reduction/work-up procedure (Scheme 2.5). At this stage, we were required to use the only commercially available trityl PS-PEG supports whereby the trityl linker is attached to the resin backbone either through a 4-carboxamide or 4-phenoxy anchor. Attempts with the latter linker met with failure, yielding a small amount of very impure product after reduction, iodine-promoted work-up and TFA cleavage. It is suspected that the phenoxymethylene is reducible under these conditions leading to premature cleavage of resin-bound material. The 4-carboxamide anchored trityl linker, on the other hand, was more successful. When the model peptide substrate was bound to this PS-PEG resin (**34**, Scheme 2.5) and subjected to reduction and iodine treatment we were able to obtain **31** although in lower yield (65%) and purity (62% by LCUV) than that obtained with the polystyrene support. Although somewhat promising, we were still concerned with the lower purity and the likelihood that the 4-carboxamide anchor was being reduced to the amine. The latter issue would be problematic as the extra amine would be functionalized with the rest of the polyamine nitrogens and no doubt interfere in any on-bead library screening that would be planned for the future. Thus, we began to consider developing a PS-PEG resin with a novel method of anchoring the trityl linker (*vide supra*).

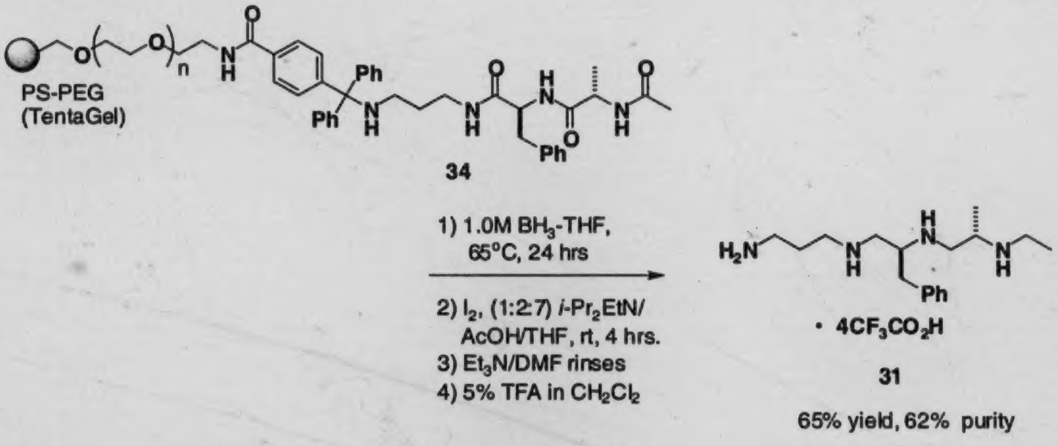

Scheme 2.5

2.1.3: Proposed mechanism for iodine-promoted oxidative work-up.

By combining known data on the reactivity of iodoboranes[93, 96] and other observations made in our laboratory,[95] we have been able to propose a plausible pathway for the breakdown of borane-amine adducts under the iodine conditions that were employed (Scheme 2.6) (Much of the work on the mechanism of the iodine-promoted work-up was done by Timothy Chan of our lab). Firstly, any oxygen nucleophile, such as acetate ion from the buffer, or methanol in some cases,[94] will be able to cleave the highly labile aminoborane unit of adduct **I** (recall Scheme 2.1). This cleavage is driven by the formation of the more thermodynamically favoured boron-oxygen bonds. In the presence of iodine, the borane-amine adduct in **II** is expected to undergo substitution of its hydrides with the iodine to initially give the monoiodoborane species **III**. Successive substitution of each hydride can continue leading to diiodoborane and triiodoborane species, but studies in solution have revealed that only one equivalent of iodine is required in the work-up procedure. Thus, we believe that cleavage of the borone-amine adduct likely occurs through the monoiodoborane **III**, although under the conditions of excess iodine used in the solid-phase method, it is possible that di- and triiodoboranes are also formed and subsquently cleaved from the amine. According to the general order of Lewis acidities for trihaloboranes ($BF_3 < BH_3 < BCl_3 < BBr_3 < BI_3$) it is expected that substitution of the hydrides in **II** with iodine would enhance the boron-nitrogen coordination in **III**. However, the iodide, being an excellent leaving group, may be displaced by a charged nucleophile,[97, 98] such as an acetate anion, via an S_N2 type mechanism analogous to substitutions at a primary alkyl halide.[99] The resulting acetoxyborane adduct **IV** is now a much weaker adduct than the monoiodoborane due to back-bonding of the oxygen, and thus is expected to dissociate readily under these conditions. The acetic acid irreversibly traps the free amine as the amine salt and captures the librated borane species as triacetoxyborane.

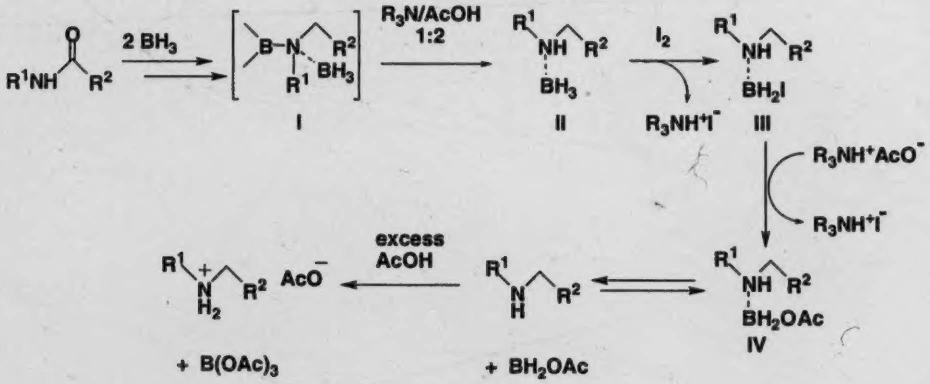

Scheme 2.6

2.2: Synthesis of model pentamines on polystyrene resin – extension of initial results.

Before attempting the synthesis of a polyamine library, we desired to further test the capabilities of the borane reduction and the iodine promoted borane-amine cleavage on the synthesis of two model pentamines, **35** and **36**, supported on trityl polystyrene resin (Figure 2.4). These compounds represent the two opposite ends in the structural range of polyamines that would be included in our planned polyamine library. Although Houghten and co-workers[83, 100] have used borane to reduce many solid-supported amino acids for their own polyamine libraries, our primary concern lay with the effectiveness of the iodine-promoted work-up on substrates that are more complex than the examples shown earlier. Furthermore, as our first steps towards the preparation of potential saccharide binding oligoboronic acids, we needed to optimize the polyalkylation on both pentamines with 2-bromomethylphenylboronate **40** (Scheme 2.7). Thus our goal was to synthesize and then alkylate pentamine **35**, a flexible long-chained polyamine, and the more rigid pentamine model **36**.

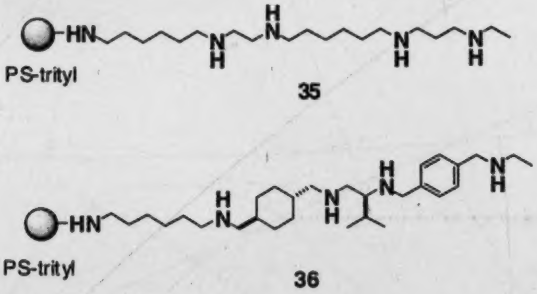

Figure 2.4: Model pentamines synthesized on polystyrene trityl resin.

To prepare **35**, we began from tetramide **38**, prepared by coupling the *N*-FMOC derivatives of glycine (Gly), ε-aminohexanoic acid (εAhx), and β-alanine (β-Ala) sequentially to 1,6-diaminohexane trityl resin **37** via standard coupling protocols using HBTU/HOBt as coupling reagents (Scheme 2.7). Exhaustive amide reduction of **38** using 1.0 M BH$_3$/THF for 48 hours followed by iodine promoted work-up led to the resin-bound pentamine **35**. Cleavage from the resin gave the crude pentakis(trifluoroacetate) salt **39** in 77% crude yield from the trityl chloride resin. After precipitation from methanol and ether, **39** was obtained in 44% purified yield.

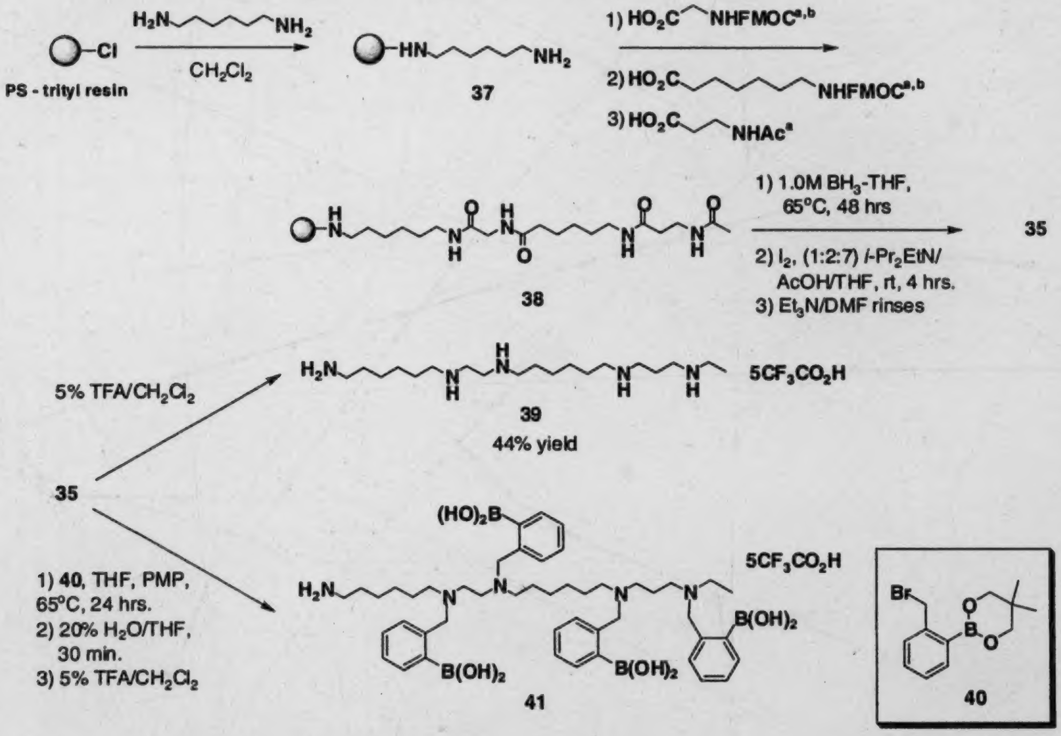

PS - trityl resin
CH₂Cl₂
37
1) HO₂C NHFMOC^a,b
2) HO₂C NHFMOC^a,b
3) HO₂C NHAc^a
38
1) 1.0M BH₃-THF, 65°C, 48 hrs
2) I₂, (1:2:7) i-Pr₂EtN/AcOH/THF, rt, 4 hrs.
3) Et₃N/DMF rinses
35
5% TFA/CH₂Cl₂
5CF₃CO₂H
39
44% yield
1) 40, THF, PMP, 65°C, 24 hrs.
2) 20% H₂O/THF, 30 min.
3) 5% TFA/CH₂Cl₂
41
40

[a]HBTU, HOBt and FMOC-amino acid (2 eq. each), i-Pr$_2$EtN (4 eq.), DMF, 2 hours; [b]1:4 piperidine/DMF, 0.5 hours

Scheme 2.7

Although **39** was quite pure by ^{1}H NMR (above 90%), its purity by LCMS was 85% with the most apparent impurity coming from a compound with a mass 28 units above that of the desired pentamine. This impurity appeared to be from incomplete reduction of two amides in **39**. However, IR microscopy of the resin-bound pentamine revealed no amide stretches, and acetylation by acetic anhydride followed by electrospray mass spectroscopic analysis of the resulting tetracetylamine, showed no unwanted amides left over from the tetramide **38**. Analysis by high resolution electrospray MS suggested the addition of a –CH_2CH_2- unit. It was thought that this unit may be arising from the only possible two-carbon source in the reaction mixture – acetic acid, but the use of propanoic acid as a replacement did not eliminate the addition of the 28 mass units.

Since the ^{1}H NMR spectrum appeared to be fine, it is possible that this extra signal in the LCMS is the result of a compound that is very responsive in the electrospray mass spectrometer which exaggarates its proportion in the crude product.

Alkylation of **35** with 40 equivalents of **40**[22] in the presence of 40 equivalents of 1,2,2,6,6-pentapiperidine (PMP or 'pempidine'), followed by hydrolysis of the boronate ester and cleavage from the resin gave the tetraboronic acid **41**. As a library of oligoboronic acids is to be decoded by LCMS, we were interested in the type of mass spectrum this compound would give when analysed by ESMS. Previous experience in our laboratory with diboronic acid compounds and ESMS has revealed the formation of intramolecule anhydrides in the gas phase, yet the effects of having three or four boronic acids on the same molecule was unknown at this time. With the tetraboronic acid **41** it was found that it typically lost three water molecules, but was made to lose four if the voltage of the spectrometer increased. As will be shown later, the amount of water lost also depends on the structure of each particular oligoboronic acid molecule.

The synthesis of the resin-supported rigid pentamine **36** began from tetramide **42** which was subjected to the same reduction conditions described for **38** (Scheme 2.8). Cleavage from the resin provided crude **43** as its penta(trifluoroacetate) salt in 69% yield. Unfortunately, precipitation of the polyamine salt from a methanol solution with ether failed. Its crude purity by HPLC was determined to be 72% MS detection or 78% by UV detection. The impurities by MS detection arose from signals with 24 and 14*n* ($n = 1$ and 2) mass units greater than the expected pentamine mass (MH). The MH+14 signal as well as the MH+28, which was the most intense of the three impurities, again appeared to be from the incomplete reduction of two amides, but as before, on-bead IR microscopy, high resolution mass spectrometry, and acetylation revealed no amides were left over from tetramide **42**. The same signals eluting in the LCUV chromatograph appeared with lower intensity than in the LCMS trace suggesting that these compounds are highly active in the electrospray mass spectrometer and thus exaggerating their proportion in the crude mixture (Figure 2.5).

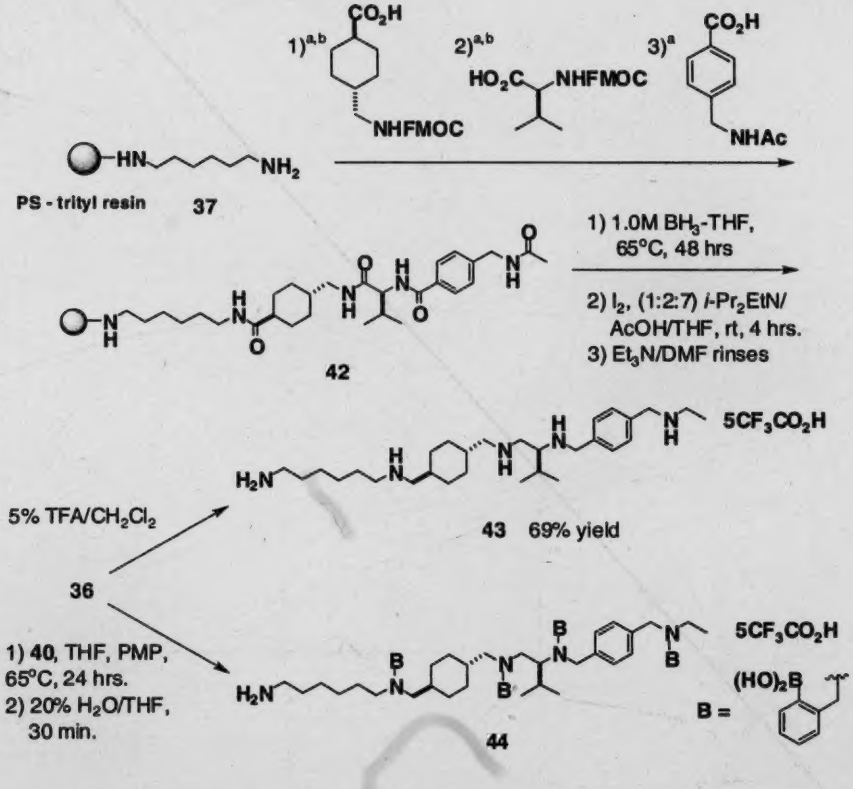
1)a,b
CO2H
NHFMOC
2)a,b
HO2C NHFMOC
3)a
CO2H
NHAc
HN
NH2
PS - trityl resin
37
42
1) 1.0M BH3-THF, 65°C, 48 hrs
2) I2, (1:2:7) i-Pr2EtN/AcOH/THF, rt, 4 hrs.
3) Et3N/DMF rinses
5CF3CO2H
H2N
43 69% yield
5% TFA/CH2Cl2
36
1) 40, THF, PMP, 65°C, 24 hrs.
2) 20% H2O/THF, 30 min.
44
5CF3CO2H
B =
(HO)2B

[a] HBTU, HOBt and FMOC-amino acid (2 eq. each), *i*-Pr_2EtN (4 eq.), DMF, 2 hours; [b] 1:4 piperidine/DMF, 0.5 hour

Scheme 2.8

The MH+24 mass impurity, however, is even more puzzling. Although 24 mass units would equal the mass of a B_2H_2 unit, high resolution electrospray MS indicated there were no boron atoms in the compound. A comparison between piperidine and iodine-based work-ups suggested that the MH+24 impurity was the result of the iodine procedure, for the use of piperidine gave a cleaner compound (89% purity by LCUV) with no such impurity being detected. However, the MH+28 impurity was still present in the mass spectrum, abeit in a smaller amount when compared to the product of the iodine work-up (see Figure 2.5) meaning that the impurity could have arisen from the borane reduction itself. One possibility is that both the MH+24 and MH+28 impurities form as a result of the borane treatment and that the work-ups, with either iodine or piperidine, somehow removes them, but to varying degrees. In addition to the LCMS data, the ^1H NMR spectrum of **43** prepared through the piperidine-based work-up appeared somewhat more pure than when iodine was used (see Appendix). The fact that there are impurites present, which are highly active by ESMS, is a concern since future polyamine libraries will be decoded by this method.

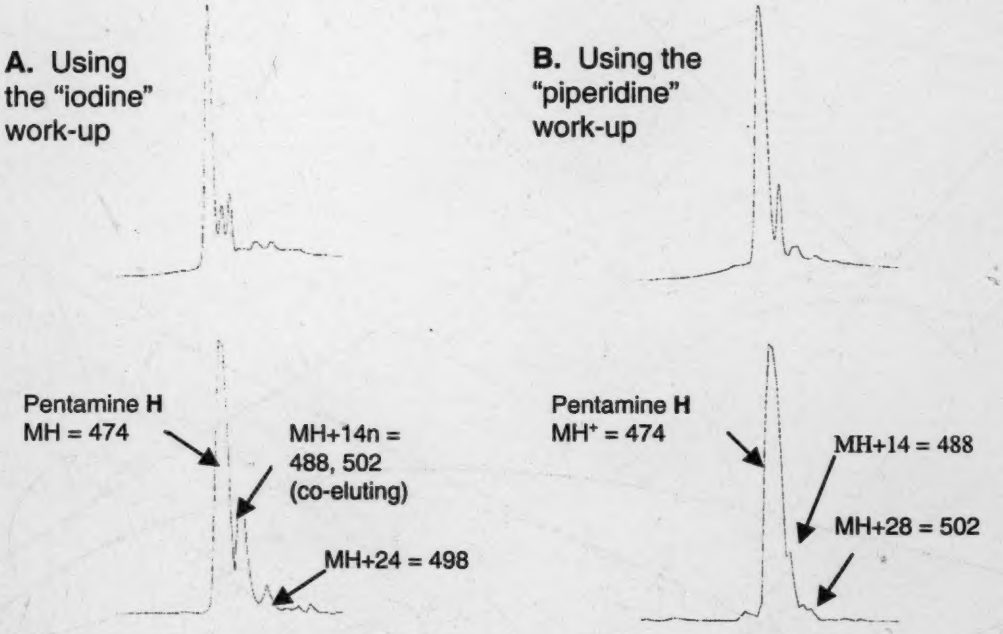

Figure 2.5: LCUV (top) and LCMS (bottom) traces of pentamine **43.** (See Experimental section for full conditions).

Alkylation of **36** with ester **40** was performed using similar conditions described for **35**. However, even after two and a half days at 65 °C complete alkylation proved to be difficult as a significant amounts of di- and triboronic acid were obtained. It is believed that the *iso*-propyl group was too sterically demanding to allow complete alkylation of its neighbouring nitrogens. The ESMS of the fully boronated polyamine **44** showed the loss of three water molecules both under high and low voltage conditions instead of four as observed with **41**. Presumably the rigidity of the molecule restricts the formation of certain internal anhydrides so that only three waters are lost. However, the dehydration pattern of the underalkylated impurities also proved to be enlightening. The diboronic acid, which elutes as a single LC peak gave a mass spectrum with two masses:

one mass with a single water lost, the other with two. The triboronic acid showed a similar mass spectrum as the diboronic acid with the loss of both one and two water molecules. Thus, these impurites may prove useful in helping in predicting the extent of dehydration for different oligoboronic acids during the library decoding by electrospray mass spectrometry.

2.3: Synthesis of philanthotoxin 433 and a branched analogue.

Our ability to synthesize complex polyamines led us to attempt the synthesis of naturally occuring acylpolyamine neurotoxins, isolated from the venom of spiders and wasps.[69] This would serve as another test for our methodology and at the same time could establish openings into the systematic generation of analogue libraries. Most suited to our methodology is the synthesis of natural products, such as philanthotoxin-433 (PhTX-433) and HO-416b toxins (Figure 2.6), which both feature a simple polyamine chain capped by a short amide chain containing an aromatic appendage. While acylpolyamines of this type have been prepared in a linear fashion on solid-support[77, 81, 101] none have been made via an exhaustive amide reduction strategy, a more convergent and potentially simpler route.

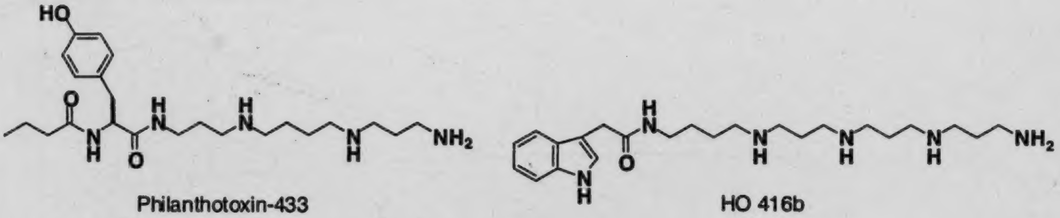

Philanthotoxin-433

HO 416b

Figure 2.6: Acylpolyamine neurotoxins.

HO-416b is obtained from the venom of the funnel web spider *Hololena curta* [102] while PhTX-433 is isolated from the Egyptian solitary digger wasp *Philanthrus triangulum*.[103] The latter, for instance, produces PhTX-433 in order to paralyze its insect prey by inhibiting the ionic conductance in cationic channels located at the postsynaptic neurons. Interest in this class of neurotoxins is due to their potential as human therapeutic agents towards conditions affecting the central nervous system, and as probes in studying the interactions between polyamine receptors and ion channel proteins. Hundreds of synthetic analogous of PhTX-433 have been synthesized by traditional solution-phase methods for structure-activity assignments.[70, 71, 104, 105] A summary of such assignments between PhTX-433 and the nicotinic acetylcholine receptor is depicted in Figure 2.7.[71]

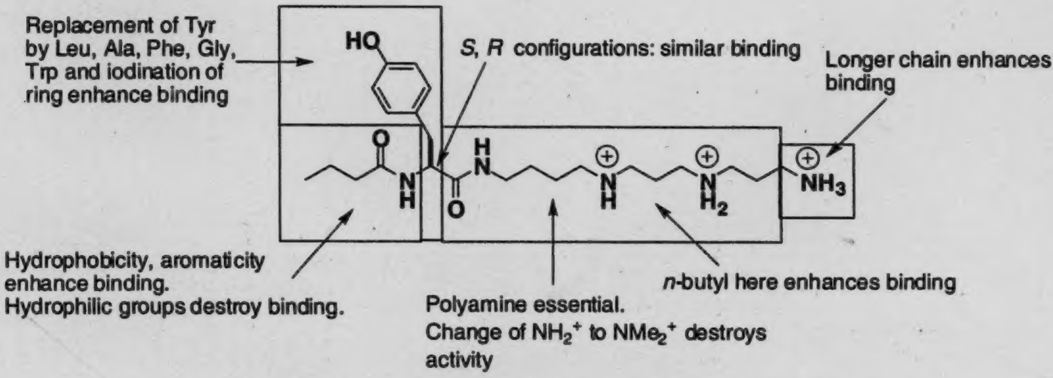

Replacement of Tyr by Leu, Ala, Phe, Gly, Trp and iodination of ring enhance binding

S, *R* configurations: similar binding

Longer chain enhances binding

Hydrophobicity, aromaticity enhance binding.
Hydrophilic groups destroy binding.

n-butyl here enhances binding

Polyamine essential.
Change of NH_2^+ to NMe_2^+ destroys activity

Figure 2.7: Structure-activity assignments for PhTX-433.[71]

Although a great deal of structure-activity information has been gained from recent reports on PhTX-433 analogues, very little has been learned about the effects of stereogenic side chains on the polyamine portions of these neurotoxins. This problem is largely due to the difficultly in synthesizing such compounds. It was envisioned that the exhaustive amide reduction of short peptides on solid-support would offer a viable route to analogs of acylpolyamine neurotoxins for a sizable combinatorial library. No large libraries were prepared in our case, but the examples presented illustrate the use of this strategy in providing a class of derivatives that until now has not been prepared.

Scheme 2.9 shows the solid-supported synthesis of an analogue of PhTX-433 (PhTX-43'3) featuring a stereogenic methyl group on the polyamine chain.[106] It began by coupling the amino acids alanine and then β-alanine onto 1,3-diaminopropane trityl polystyrene resin (**45**) to form the dipeptide intermediate **46**. Reduction of the two amides followed by iodine-promoted work-up led to the tetramine **47**. A portion of **47** was cleaved from the support to give the tetrakis(trifluoroacetate) salt in 77% yield which was verified by NMR spectroscopy and ESMS. To selectively functionalize the polyamine chain, we employed the strategy described by Nash *et al.*[77] in their hemisynthesis of PhTX-433 from spermine. Selective protection of the primary amine on **47** as a bis-*N*-[1-(4,4-dimethyl-2,6-dioxocyclohexylidene)ethyl] (Dde)[107] derivative using 2-acetyldimedone was followed by conversion of the secondary amines to BOC derivatives. Removal of the Dde group with hydrazine liberated the primary amine, and the resulting intermediate **48** was coupled to FMOC-Tyr(*t*-Bu)-OH and then butyric acid to give **49**. Exposure of the resin to a TFA/water/triisopropylsilane cocktail afforded the tris(trifluoroacetate) ammonium salt of PhTX-43’3 in 75% yield from the dipeptide after precipitation from methanol and ether, and 88% purity by HPLC under UV detection.

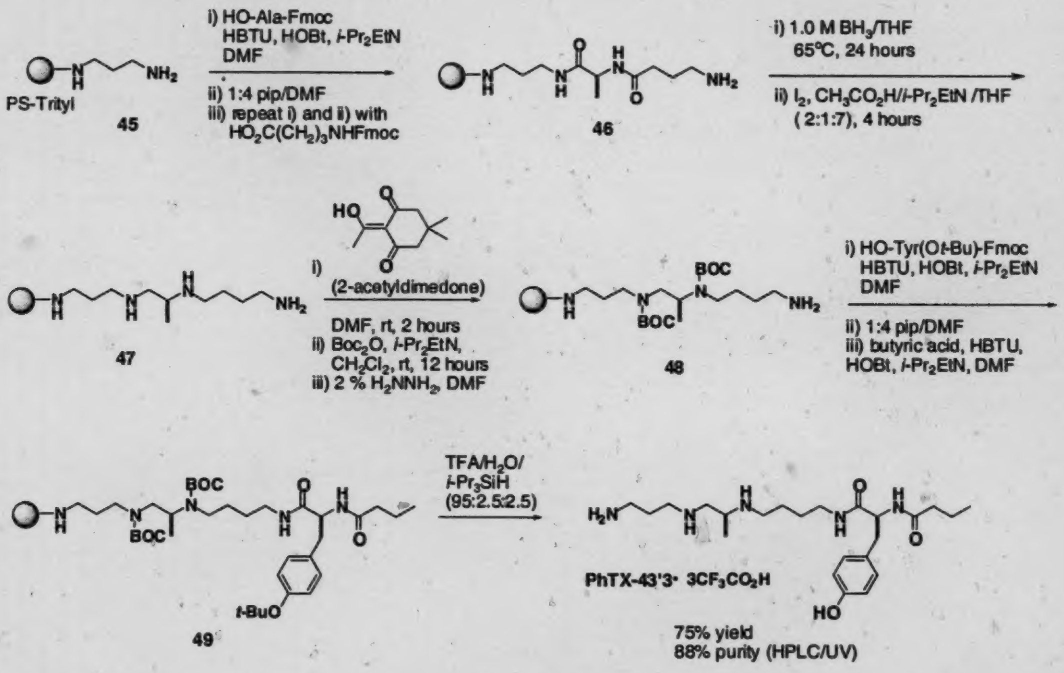
PS-Trityl
45
i) HO-Ala-Fmoc HBTU, HOBt, i-Pr2EtN DMF
ii) 1:4 pip/DMF
iii) repeat i) and ii) with HO2C(CH2)3NHFmoc
46
i) 1.0 M BH3/THF 65°C, 24 hours
ii) I2, CH3CO2H/i-Pr2EtN /THF (2:1:7), 4 hours
47
i) (2-acetyldimedone)
DMF, rt, 2 hours
ii) Boc2O, i-Pr2EtN, CH2Cl2, rt, 12 hours
iii) 2 % H2NNH2, DMF
48
i) HO-Tyr(Ot-Bu)-Fmoc HBTU, HOBt, i-Pr2EtN DMF
ii) 1:4 pip/DMF
iii) butyric acid, HBTU, HOBt, i-Pr2EtN, DMF
49
t-BuO
TFA/H2O/ i-Pr3SiH (95:2.5:2.5)
PhTX-43'3· 3CF3CO2H
75% yield
88% purity (HPLC/UV)

Scheme 2.9

The synthesis of the natural compound, PhTX-433, was also achieved using a similar route to that outlined above except replacing FMOC-Ala-OH with FMOC-βAla-OH in the first coupling round.[106] The yield of the tris(trifluoroacetate) ammonium salt was 77% and its purity by HPLC/UV was found to be 80 % after precipitation. Comparison of this sample with the natural PhTX-433, kindly donated to us by Professor Koji Nakanishi (Columbia University), helped to further comfirm its identity. In addition, HO-416b was prepared by an analogous route in our laboratory in 54% overall yield and 81% purity. (Note that both PhTX-433 and HO-416b were prepared by postdoctoral collaborator, Dr. Fan Wang.)

The important feature in all three of these syntheses is the potential to use widely available amino acid building blocks to form both the acyl "head" and the polyamine "tail" in a library of toxins. Although only three compounds were prepared, it has been shown in our laboratory that a diverse set of natural and unnatural amino acids can tolerate the key amide reduction step and iodine treatment.[95] (In particular, a wide range of protected α-amino acid derivatives were successfully employed by graduate student Carmen Laplante). Thus, a library of acylpolyamine neurotoxins by the above route should, in principle, be achievable.

2.4: Preparation of polystyrene-supported split-pool polyamine and oligoboronic acid libraries.

2.4.1: Library encoding by partial termination synthesis.

The preferred method for decoding our split-pool libraries is a partial termination synthesis, whereby during the peptide (i.e., polyamide) elongation stage a small amount of the growing sequence is terminated. These terminated sequences are then carried over during the reduction and alkylation steps with the polyamine and oligoboronic acid library respectively. Mass spectrometric analysis of a library member from a single resin bead will then allow us to determine the identity of each residue simply from the mass differences between the full sequence and the smaller amounts of the terminated sequences. The expected mass spectrum is depicted schematically in Figure 2.8. Partial termination synthesis and MS decoding was originally developed by Youngquist and co-workers[47] for peptide libraries using MALDI (Matrix Assisted Laser Desorption Ionization) MS, but in principle, it should also be applicable to other oligomeric libraries using ESMS coupled to an HPLC column. The advantages of this decoding technique over other indirect methods (examples: chemical,[46] RF,[44] or optical tags[45]) is that it also allows for the simultaneous evaluation of the compound purity as it is being decoded, alleviating the need to make smaller "test libraries" of individual compounds for characterization. The main disadvantage is the unavoidable "impurities" that are accumulated by continually terminating the sequence, but this can be somewhat lessened by terminating very small amounts during the synthesis. Another disadvantage is the use of isomeric (or "isobaric") building blocks which, of course, cannot normally be distinguished by mass spectrometry. However, this limitation can be solved in many cases by employing different terminating groups with different masses.

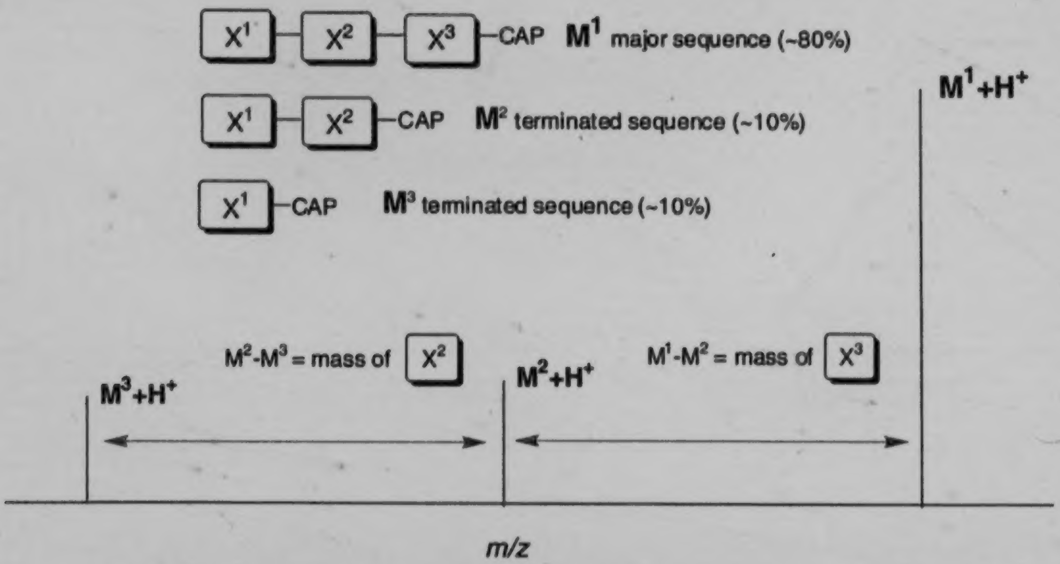
X1 – X2 – X3 –CAP M1 major sequence (~80%)
X1 – X2 –CAP M2 terminated sequence (~10%)
X1 –CAP M3 terminated sequence (~10%)
M1+H+
M2-M3 = mass of X2
M1-M2 = mass of X3
M3+H+
M2+H+
m/z

Figure 2.8: Schematic representation of mass spectrum decoding of a partially terminated library member from a single bead.

Before setting out to find a suitable termination strategy it was considered necessary for, any future on-bead binding assay, to artifically reduce the loading of the highly substituted, commercially obtained PS-trityl resin (typically between 0.7 and 1.2 mmol/g). This would hopefully "dilute" the receptors in the resin bead and, as a consequence, favour the formation of a 1:1 complex between the receptor and the target as opposed to higher ordered complexes. The loading reduction was performed by either capping a portion of the 1,6-diaminohexane spacer with 0.7 equivalents of phenylisocyanate, or by reacting a submolar quantity of butylamine (0.8 equivalents) to the tritylchloride resin before attaching the 1,6-diaminohexane. As will be seen later, this would prove to be detrimental to the library decoding.

Different termination strategies were tested during the synthesis of a single sequence, Gly-Phe-Ala (Scheme 2.10). The first one examined was the addition of a small amount of a capping reagent to the terminal amine of a growing peptide prior to coupling the next amino acid in the sequence. Initially isocyanates were used since they react rapidly with amines to give the urea without the aid of coupling reagents, and therefore, from a practical standpoint, made them easy to use. In addition, isocyanates of different molecular weight can be used to partially terminate two separate isomeric residues making them distinguishable by MS analysis. In order to partially terminate the growing peptide, 0.2 equivalents of isocyanate was added to the resin to cap about 20% of the sequence before the next FMOC amino acid was added. Although all sequences were observed at the peptide stage, after prolonged exposure to BH_3 at 65°C and subsequent iodine-based treatment the urea terminated sequences could no longer be observed by ESMS. After alkylation with boronic ester **40** they were still not visible. It was never certain if the urea functionality was being reduced to unknown products, or if it was just extremely difficult to detect the expected peaks among the background noise of the mass spectrum. (Note that at the time of these experiments an LCMS instrument was not readily available to us and so most samples were injected directly into an ESMS detector without column purification. Thus, mass signals not observed at that time may actually have been present, but only observed if they were chromatographically resolved and not hidden under the heavy background noise throughout the entire spectrum).

The next strategy used small amounts of acid anhydrides, such as acetic anhydride, to partially terminate some of the growing peptide with an amide which, of course, becomes reduced and alkylated in later steps (Scheme 2.10). This time all the sequences were visible after each stage of the synthesis after cleaving *multi-milligrams* of resin. However, ESMS analyses of *single* beads taken after alkylation were more discouraging. Out of twelve single beads only one produced a mass spectrum showing both the terminated sequences and the full tetraboronic acid sequence. The rest gave no signal corresponding to any sequence.

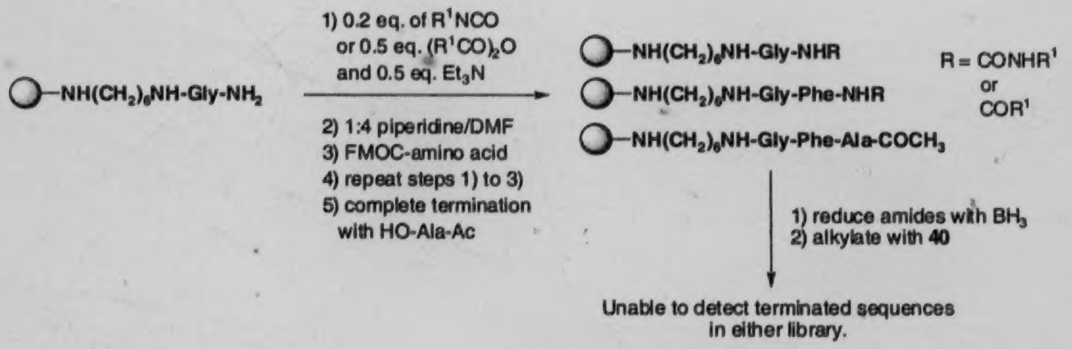
NH(CH2)6NH-Gly-NH2
1) 0.2 eq. of R1NCO or 0.5 eq. (R1CO)2O and 0.5 eq. Et3N
2) 1:4 piperidine/DMF
3) FMOC-amino acid
4) repeat steps 1) to 3)
5) complete termination with HO-Ala-Ac
NH(CH2)6NH-Gly-NHR
NH(CH2)6NH-Gly-Phe-NHR
NH(CH2)6NH-Gly-Phe-Ala-COCH3
R = CONHR1 or COR1
1) reduce amides with BH3
2) alkylate with 40
Unable to detect terminated sequences in either library.

Scheme 2.10

It is believed that the lack of signals in the mass spectrum from most beads was due to reactivity differences among the resin beads themselves. It is known, that smaller beads will react more rapidly than larger ones due to different rates of reagent diffusion into the beads,[108] and unfortunately the bead size distribution of our resin was rather broad. Thus, in the attempt to reduce the loading of the resin it was likely that many of the beads reacted completely with the phenyl isocyanate or butylamine thereby making them completely unreactive in subsequent steps. The same phenomenom may have occurred in the partial termination steps, where many beads became completely terminated instead.

With this lesson behind us, we decided to forego the loading reduction and use higher quality beads with a more uniformed size distribution (~90 μm). Furthermore, a alternative termination strategy was investigated. Rather than employing a 'precapping' strategy, the new plan was to couple a mixture of an FMOC amino acid (~90%) and its corresponding *N*-terminated derivative (~10%). Initially, *t*-BOC and CBz protected amino acids were used as the terminated derivatives, but the carbamates did not appear to survive the excess borane or the iodine-based work-up according to their electrospray mass spectra. As a result, *N*-acylamino acids were examined in order to terminate the sequence with a secondary amide which has more predictable chemical behaviour. The disadvantage to using these derivatives is that only a few are commercially available, and they become reduced and alkylated during the library syntheses making the terminated sequences potentially active in any library screening. However, as it turns out, they work very well in decoding all libraries.

2.4.2: First generation split-pool polyamine and oligoboronic acid libraries.

With a new termination method at hand, we were set to initiate our first library synthesis. We choose as our building blocks a set of straight chain, cyclic and sterically diverse mixture of 14 natural and unnatural amino acids (Figure 2.9).

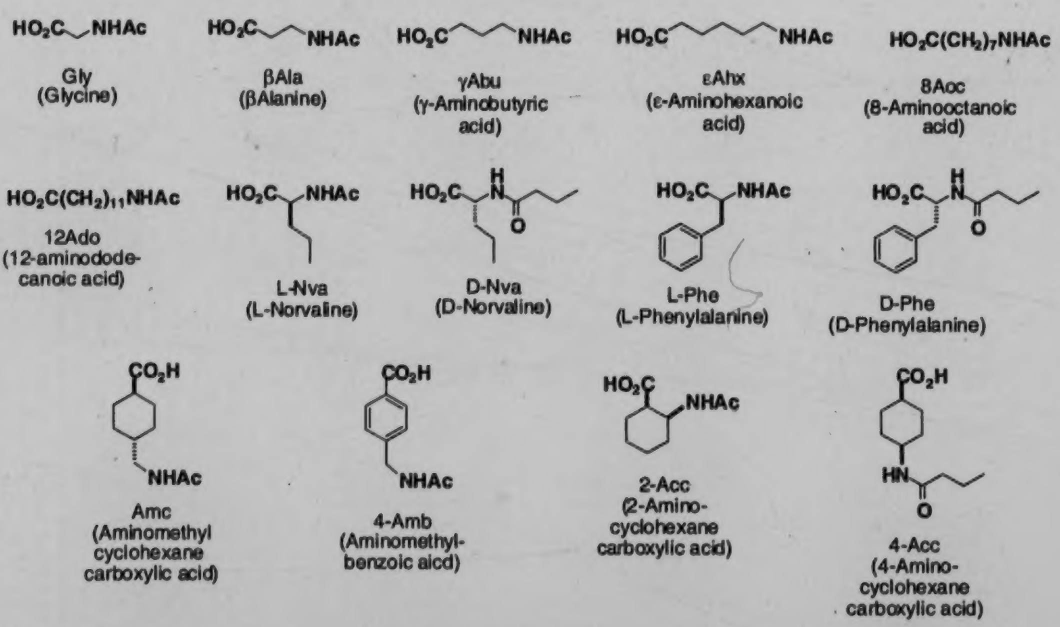
HO₂C NHAc
Gly (Glycine)
HO₂C NHAc
βAla (βAlanine)
HO₂C NHAc
γAbu (γ-Aminobutyric acid)
HO₂C NHAc
εAhx (ε-Aminohexanoic acid)
HO₂C(CH₂)₇NHAc
8Aoc (8-Aminooctanoic acid)
HO₂C(CH₂)₁₁NHAc
12Ado (12-aminododecanoic acid)
HO₂C NHAc
L-Nva (L-Norvaline)
HO₂C H N O
D-Nva (D-Norvaline)
HO₂C NHAc
L-Phe (L-Phenylalanine)
HO₂C H N O
D-Phe (D-Phenylalanine)
CO₂H NHAc
Amc (Aminomethyl cyclohexane carboxylic acid)
CO₂H NHAc
4-Amb (Aminomethyl-benzoic aicd)
HO₂C NHAc
2-Acc (2-Amino-cyclohexane carboxylic acid)
CO₂H HN O
4-Acc (4-Amino-cyclohexane carboxylic acid)

Figure 2.9: Fourteen amino acid building blocks, shown as their *N*-acyl derivatives, used in the first polystyrene bound polyamine library.

A number of factors determined the choice of these amino acids. Firstly, they had to be readily available, either commercially or synthetically. The minimum derivatization required was either the attachment of the FMOC protective group[109] or the *N*-acyl group[110] onto a free amino acid (Scheme 2.11).

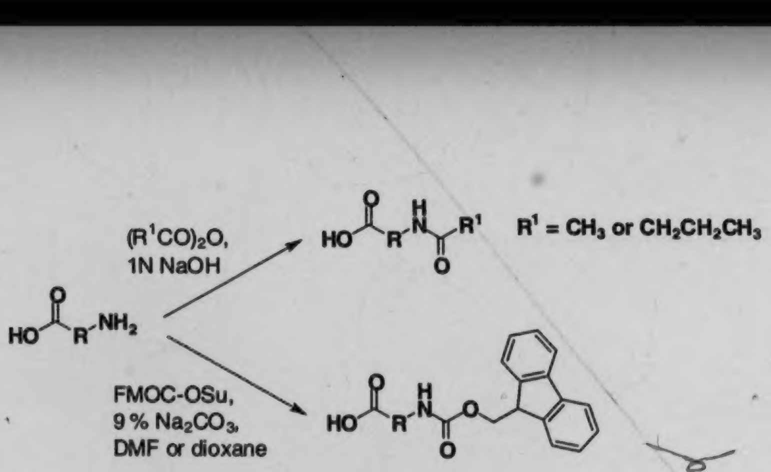

Scheme 2.11

In addition, the building blocks should not present any functionality that may affect the amide reduction or the alkylation with boronic ester **40**. For instance, valine which was used in the synthesis of **43**, was not used because it seemed to sterically hinder the alkylation step. The building blocks also needed to be as structurally diverse as possible in order to cover a wide range of structural variations. Finally, the masses of the amino acids need to be considered since our decoding method is by mass spectrometry. By using two different *N*-acyl groups (acetyl and butyryl) we were able to include isomers of phenylalanine, norvaline and aminocyclohexane carboxylic acid. However, other possible amino acid candidates had to be rejected because of conflicting masses with amino acids that have already been chosen. Using 14 amino acids, each coupled three times, will make a tripeptide (i.e., tetramide) library of 2744 compounds which can be converted to an equal number of pentamines and tetraboronic acids in subsequent 'library-to-library' transformations.[39] Coupling each amino acid twice provides a 196-membered dipeptide (i.e., triamide), and subsequently the tetramine and triboronic acid libraries.

The synthesis of the library was carried out as shown in Scheme 2.12. From chlorotrityl polystyrene resin (loading ~ 0.8 mmol/g, 90-150 μm diameter beads), a twelve carbon diamine spacer was attached to give resin **50**. Such a long spacer should help minimize any possible interactions between the screening target and the polymer backbone. For the synthesis of a pentamine library, an encoded tripeptide library **51** was initially prepared. During the first two amino acid additions a 9:1 mixture of an FMOC-protected amino acid and its corresponding *N*-acyl derivative were coupled in NMP (*N*-

methylpyrrolidinone) using HBTU and HOBt as the coupling reagents. For the final amino acid coupling, only the *N*-acylamino acid was added. During each coupling, a portion of resin was removed from each pool to determine if single beads could be decoded at each stage and to see if the beads were showing uniform reactivity. In all cases, the beads were easily decoded by ESMS. The peptide library was then converted to the pentamine library **52** by exhaustive amide reduction with borane at 65°C for 3 days followed by iodine-promoted cleavage of the borane-amine adducts. Alkylation of the pentamines with **40** over 3 days gave the tetraboronic acid library **53**. The triamide library could be obtained by removing a portion of the resin en route to the tripeptide and then converting it to the corresponding tetramine and triboronic acid libraries. Alternatively, it can be made separate from the tetramides by first coupling the FMOC and *N*-acylamino acid mixture, and then the *N*-acyl amino acid by itself.

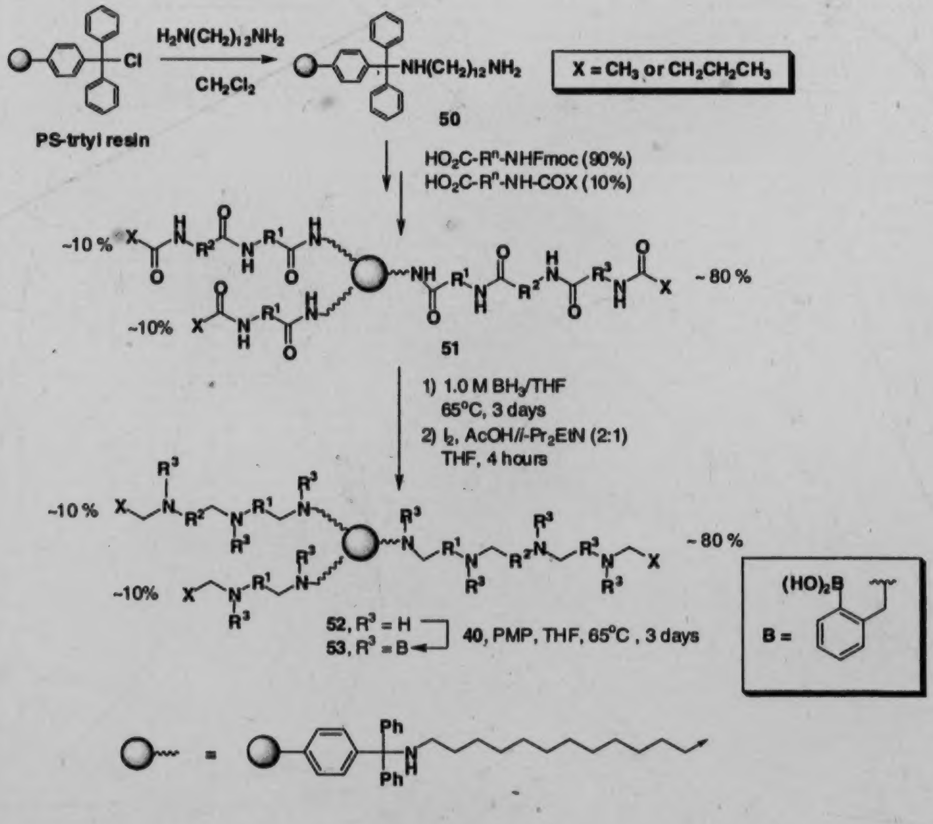
H₂N(CH₂)₁₂NH₂
CH₂Cl₂
PS-trityl resin
NH(CH₂)₁₂NH₂
50
X = CH₃ or CH₂CH₂CH₃
HO₂C-Rⁿ-NHFmoc (90%)
HO₂C-Rⁿ-NH-COX (10%)
~10 %
~10%
~ 80 %
51
1) 1.0 M BH₃/THF
65°C, 3 days
2) I₂, AcOH/i-Pr₂EtN (2:1)
THF, 4 hours
~10 %
~10%
~ 80 %
52, R³ = H
53, R³ = B
40, PMP, THF, 65°C , 3 days
(HO)₂B
B =
Ph
Ph

Scheme 2.12

Of all the beads isolated from the pentamine library 79% of them were successfully decoded by LCMS. An example of a decoding LCMS is illustrated in Figure 2.10 for the pentamine sequence Amc^R-Amc^R-DPhe^R (**54**) (the superscripted R denotes a reduced amino acid residue). The top section of Figure 2.10 shows the fully drawn structure of the pentamine along with its written abbreviation using a system commonly used throughout this Thesis (Note that two of the amines arise from the diamine spacer, while the other three originate from the reduction of the amino acid building blocks, Amc and DPhe). The middle part of the figure is the total ion current (TIC) chromatograph while on the bottom is the ESMS of the TIC peaks eluting between 5 and 6 minutes. Clearly observed in the mass spectrum are the two terminated sequences and the full pentamine along with a few minor impurities. At around 8.7 minutes in the TIC is another impurity peak but an injection of a control sample (that is, everything except the bead) revealed that it was not from the bead but likely from an external source (examples: syringe, vial, or solvent). Those pentamines that were only partially decoded (13% in total) were due mainly to the absence of one of the terminated sequences from the mass spectrum – usually the first sequence. A small number (8%) gave absolutely no MS signal perhaps because of poor handling of the bead or its contents after it was cleaved. In some cases the decoding was aided by the comparison of LC retention times with known sequences.

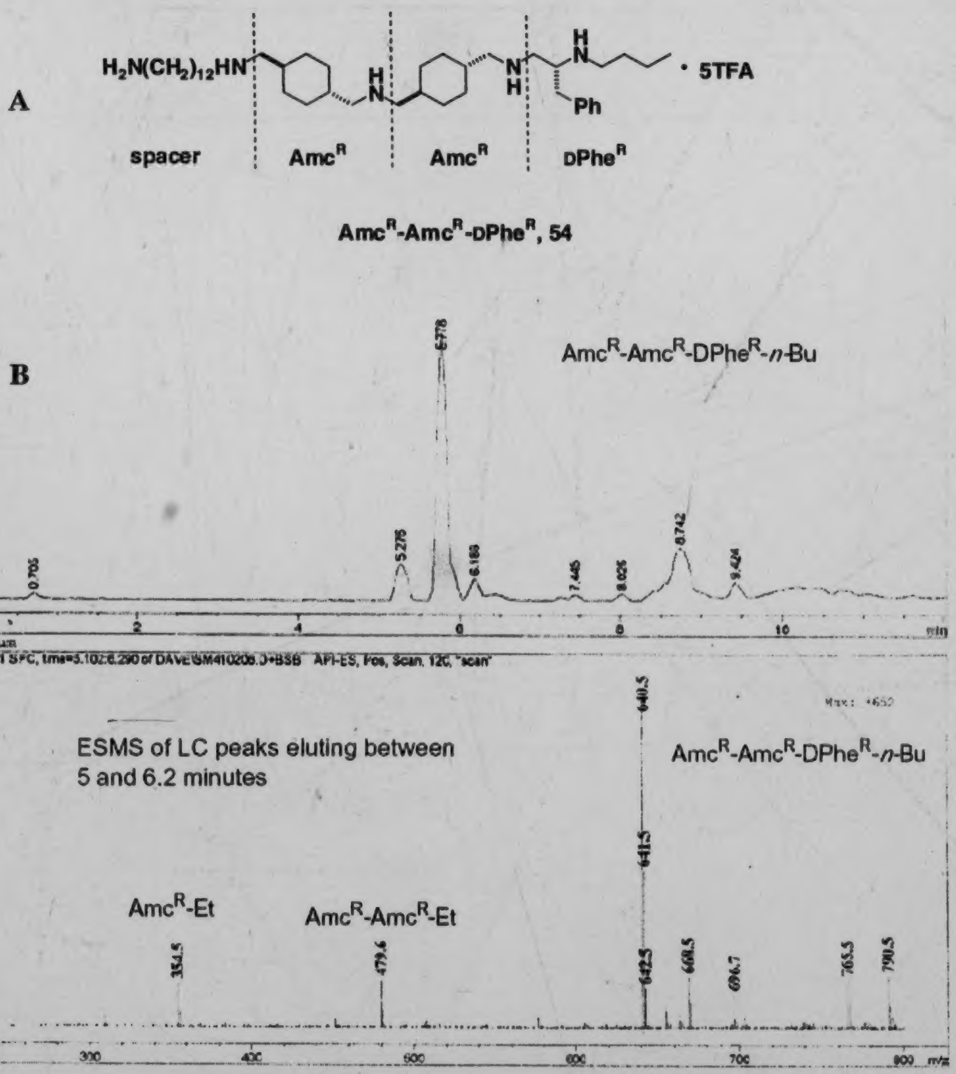

Figure 2.10: **A**: common abbreviation of a polyamine sequence used throughout this thesis. **B**: single bead analysis by LCMS of Amc^{R}Amc^{R}DPhe^R taken from the pentamine library.

It was noticed that with all pentamine successfully decoded, impurities with 24 mass units greater than the full pentamine sequences (MH+24) were rarely observed in significant amounts, unlike with **35**. This observation seems to suggest that this particular impurity is specific to the pentamine sequence in **35**. On the other hand, the impurities with an extra 28 mass units were frequently observed in many samples. The pentamine sequence depicted in the example above is one such case were the MH+28 impurity can be seen, and its the intensity shown in the Figure is typical to what is observed in other samples.

With the decoding of the tetraboronic acid library, we were initially concerned that it would be complicated by varying amounts of dehydration due to anhydride formation between each boronic acid units. Fortunately, as we began analysing the beads, a clear pattern began to emerge making it simple to predict the number of water molecules that each sequence would lose during the LCMS analysis. The first terminated sequence, with two boronic acid units, often loses one and two water molecules in the mass spectrometer. Thus the LC peak of this sequence can be clearly identified by its MS as it gives two distinct mass peaks differing by 18 amu. Both the second terminated sequence and the full seqence always show the loss of three water molecules.

However, the decoding efficiency of the tetraboronic acid library still requires some improvement. Of 38 beads analysed, 19 were fully decoded, 8 were partially decoded, often with one mass peak missing. 10 beads could not be decoded at all, perhaps due to isolation or cleavage problems with the resin bead. In the majority of samples the major impurties did not show a characteristic boron isotope pattern in the mass spectrum, and so may not have arisen from any side reactions between **40** and the polyamine. Instead they may have come from external sources. In six of the decoded sequences the identifiable boron containing impurity was determined to be an unreduced amide leftover from the polyamine precursor rather than under alkylation. However, nine samples revealed boron-containing impurities that could not be identified.

An ideal LCMS is shown in Figure 2.11 for the sequence DNva^B-Gly^B-εAhx^B (**55**) (the superscripted B denotes a boronated, reduced amino acid residue). It shows the LC peaks of each of the terminated sequence and the full sequence along with an impurity containing no boron. The combined mass spectrum of the three boronic acid sequences is also shown. The spectrum of the first terminated sequence containing DNva^B clearly shows the loss of both one and two water molecules (MH – xH$_2$O = 574.5 and 592.5). The LC signal of the full sequence (MH – 3H$_2$O = 966.6) overlaps a small amount of overalkylated material (MH – 3H$_2$O = 1082.7) in the TIC. However, quarternization by overalkylation of a tertiary amine may led to species that are highly active by electrospray mass spectrometry due to the existence of a positive charge on the compound. Therefore, the intensity of quarternized compounds in the mass spectrum may exaggerate the actual proportion in the sample. The bottom of Figure 2.11 illustrates the postulated structures of the boronic anhydrides that are frequently formed in the mass spectrometer.

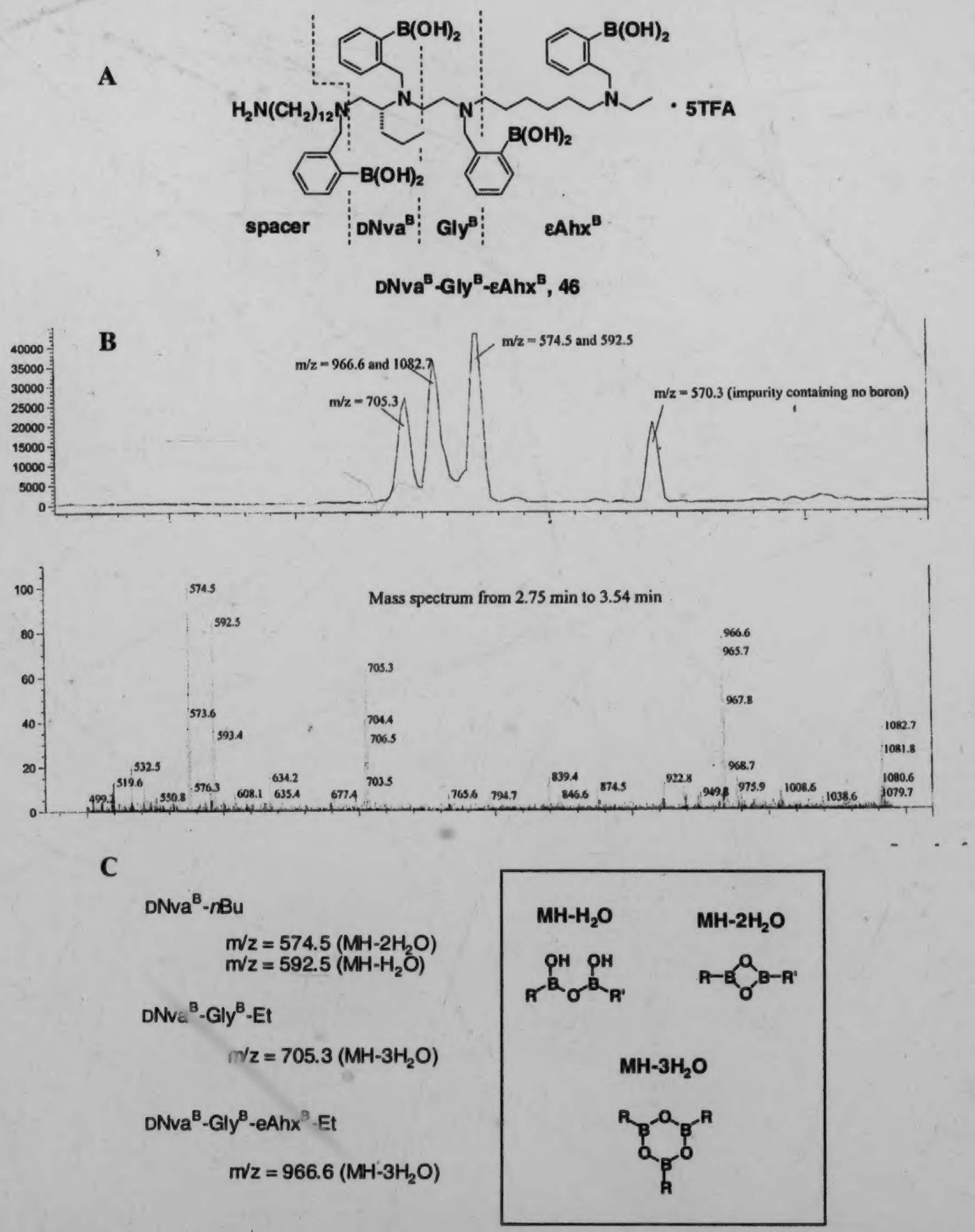

Figure 2.11: **A:** Structure of sample tetraboronic acid with common abbreviation. **B**: LCMS decoding of a triboronic acid library member. **C**: Postulated structures of boronic anhydrides observed in the mass spectrum.

2.5: Conclusions.

A relatively mild method was developed which allows for the reduction of solid-support bound amides by borane. This method employs iodine, in a buffered medium, that cleaves the borane-amine adducts that appear immediately after the reduction step. It has been shown that this procedure is mild enough to be used on highly acid sensitive linkers such as the trityl linker. The iodine-based work-up performs best after the reduction of polyamides (i.e., peptides) on polystyrene trityl amine resins, giving very pure polyamines. With more complex polyamines the impurities appearing as MH+24 and MH+14*n* in the electrospray mass spectrum are sometimes observed in small amounts. The use of iodine, however, affords lower yields and purities after the reduction of polyamides bound to PS-PEG trityl amine resins. Furthermore, iodine fails when the polyamides are linked to the resin as an ether to trityl, DHP, and Wang linkers. In these cases, the use of piperidine to cleave the resin-bound borane-amine adducts is recommended.

With a suitable reduction protocol in hand, a polystyrene-bound polyamine and oligoboronic acid libraries were synthesized using the split-pool technique. A successful decoding strategy was developed for these libraries which involved the partial termination synthesis of the intermediate polyamide library. This partial termination was achieved by coupling a 9:1 mixture of an FMOC-protected amino acid, which elongates the sequence, and the corresponding *N*-acylamino acid, which terminates the sequence. The full sequence and the terminated sequences were fully observed in the electrospray mass spectrum of polyamines and oligoboronic acids on single beads.

Unfortunately, libraries bound to polystyrene resin may not be suitable in on-bead screening assays against water-soluble biomolecules since polystyrene swells poorly in water. Therefore, the polyamine and oligoboronic acid synthesis described above will eventually need to be performed on a more hydrophilic resin. In the meantime, organic soluble molecules can still make ideal targets for the polyamine libraries in the search for selective receptors.

Chapter Three:

Discovery of polyamines showing selective ion pairing to model polyanionic targets.

3.1: Objectives.

Natural polyamines, such as spermine and spermidine, exist as polyammonium ions under physiological pH conditions, giving them high affinity towards polyanionic biological molecules through the formation of ion pairs. The biological and medical implications of the polyamines' affinity towards proteins and nucleic acids was described earlier in Chapter One. Given the importance of polyamines, and the need to further understand their biological roles, it would be advantageous to synthesize a diverse set of polyamine analogues using combinatorial chemistry, and to develop high-throughput screening techniques for discovering new active compounds of this class.

The split-pool synthesis of polyamine libraries, described in the previous chapter, could be an ideal method for the preparation of novel polyamine structures. However, this library is more easily screened as an on-bead mixture and, therefore, would require a method for visually detecting the polyanionic target bound to the resin bead expressing the active polyamine sequence. Unfortunately, no on-bead screening assays exists involving resin bound polyamines. Furthermore, for this kind of screening to be performed against water-soluble biological targets, the resin support needs to swell in aqueous solutions. However, the polyamine libraries prepared up this point have been on polystyrene, a matrix that swells poorly in water. Despite these difficulties, our interest was to determine, as a proof-of-principle, whether resin-bound polyamine libraries could be screened against a polyanionic target via the formation of selective ion-pairing interactions under aqueous conditions.[111-114]

To date, the majority of work on selective anion recognition has involved designed synthetic receptors containing cationic sites such as amines (including polyamines) or guanidinium groups.[115] Results have been achieved in the recognition of peptides[116] and nucleotides[117-119] through designed receptors that employ ion pairing interactions and can operate in water. However, only two known report exists into the screening of a combinatorial library of anion receptors.[120, 121]

With our resin-supported polyamines, the ideal targets are organic soluble polysulfonated azo dyes.[121] The advantage of these dyes is that they allow the easy detection of the binding event by changing the colour of the bead upon binding the supported polyamine. In addition to these polyanionic dyes, a short peptide conjugated with a coloured, uncharged dye, and containing three glutamate residues was also tested for resin-supported selective ion pair interactions.

3.2: Model dye targets.

In order to ensure high affinity between the polyamine and the target, polyanionic dyes were sought that contained at least an equal number of anionic sites to the ammonium sites on the polyamine libraries. Unfortunately, few commercially available dyes exist which contain four anionic sites suitable for the pentamine library. (Note that the amine bound to the trityl linker is inactive due to the bulkiness of the surrounding trityl group. Therefore, it effectively behaves as a 'tetramine' library. See Figure 3.2). On the other hand, a full range of trisulfonated dyes are available that would be ideal for the 196-membered tetramine library (effectively a 'triamine' library). Of these trisulfonated dyes, we choose three, **57**, **58** and **59** (Figure 3.1), which are all dark in colour (red and blue) to help visualize them binding to the bead, and which maintain the same colour over the pH range that was studied. These dyes differ mainly in the relative distances and positions of the sulfonates, which could lead to different selectivities among the tetramines in the library. In other words, could a polyamine, or group of polyamines, target one dye selectively over another (Figure 3.2)?

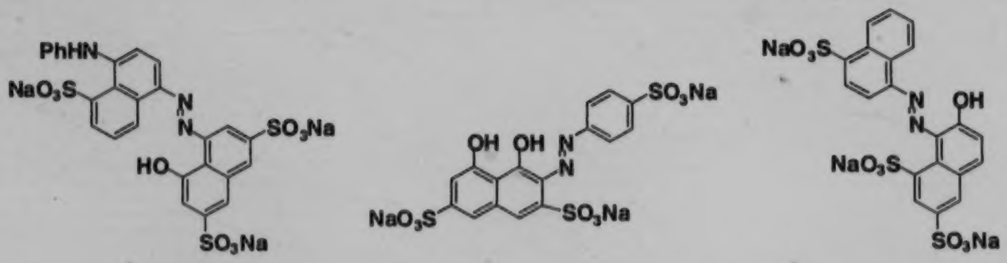

"Acid Blue-92," 57

58

"New Coccine," 59

Figure 3.1: Three polysulfonated dyes serving as model polyanionic targets.

Although rotation can occur about one of the C-N bonds in each dye, it is assumed that the second C-N bond would be locked into position by an intramolecular hydrogen bond between the phenolic hydrogen and the lone pair on the azo nitrogen. Thus these dyes provide sufficiently rigid targets for our tetramine library.

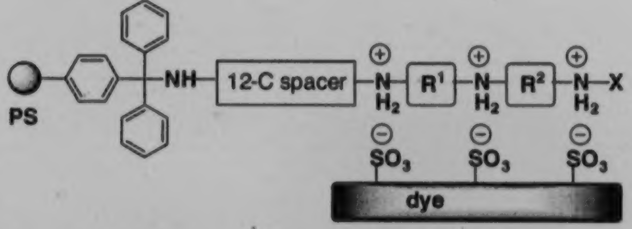

Figure 3.2: Hypothetical model of a resin bound tetramine coordinating to a trisulfonated dye.

3.3: Library screening.

It was found that the best solvent system for performing the on-bead assays was a 10% mixture of aqueous buffer in *N*, *N*-dimethylformamide (DMF). The large proportion of organic solvent was required in the mixture to ensure the resin beads remained swollen during the assays. The aqueous buffer was added to determine if selective ion-pairing on resin-bound polyamines can occur in the presence of water.[122] Before screening against the polyamines, the dye was tested against a suspension of underivatized polystyrene resin and the resin bound tripeptide library in the same solvent and buffer conditions to verify that nonselective binding would not occur to the polystyrene resin matrix. In a typical screening, approximately 3-mg of polystyrene-supported tetramine library (approximately 10 000 beads) was added to a small volume of buffered solution inside a small, shallow Petri dish. Small amounts of the dye were then added to the swirling suspension until a visible colour change in the resin was observed. Only a minimum amount of the dye was added in order to avoid saturation and reduced selectivity. The darkest of the beads were then removed from the dish using a narrow capillary tube and transferred to a separate dish where they were washed with 10% water/DMF (containing no buffer), and then dichloromethane. The beads were individually cleaved in a conical microvial using a small volume of 5% TFA in dichloromethane (5 - 7.5 μL) and then analysed by LCMS. Each screening was performed more than once to ensure reproducibility. For a more detailed procedure see the experimental section in Chapter Seven.

3.3.1 Screening of tetramine library against Acid Blue-92 (**57**).

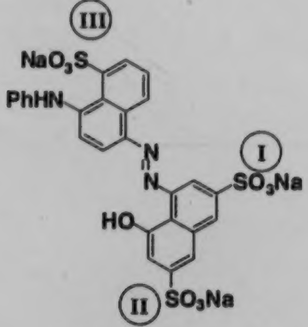

"Acid Blue-92," **57**

The blue coloured dye was screened against the tetramine library as a 5.0×10^{-5} M solution in 0.01 M MES-TRIS buffer (pH 7.0) in 10% water/DMF. After about one hour of swirling the suspension, the dye solution became clear. Under a low-powered microscope, about 50% of the beads appeared as various shades of blue, while the remaining beads stayed colourless. Of the blue beads 40% (or 20% overall) were considered very dark and worth isolating. Altogether, 25 beads were isolated, cleaved and then analysed for their specific tetramine sequence. The results are shown in Tables 3.1 and 3.2.

Table 3.1: Screening of PS-bound tetramine library against **57** ('Acid Blue-92') at pH 7. See text for details.

Residue pair	Number of occurrences	Residue pair	Number of occurrences
εAhx^{R}, εAhx^{R} 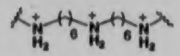	4	8Aoc^{R}, 8Aoc^{R} 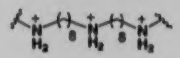	1
8Aoc^{R}, 12Ado^{R} 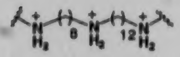	2	8Aoc^{R}, LNva^{R} 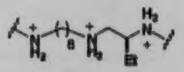	1
γAbu^{R}, γAbu^{R} 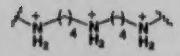	2	βAla^{R}, DPhe^{R} 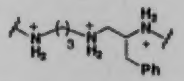	1
βAla^{R}, 12Ado^{R} 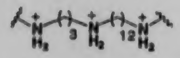	2	βAla^{R}, Gly^{R} 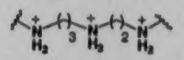	1
εAhx^{R}, γAbu^{R} 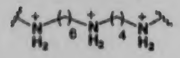	2	γAbu^{R}, Amc^{R} 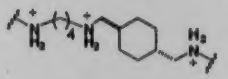	1
βAla^{R}, LNva^{R} 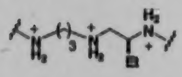	2	2Acc^{R}, εAhx^{R} 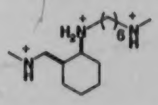	1
8Aoc^{R}, LPhe^{R} 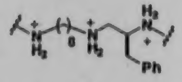	2	DNva^{R}, 4Amb^{R} 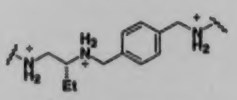	1
8Aoc^{R}, γAbu^{R} 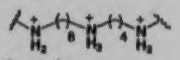	1	βAla^{R}, 4Acc^{R} 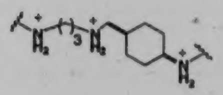	1

Table 3.2: Frequency of individual tetramine residues out a total of 50 found in screening of dye **57**.

Residue	**Number of Occurences**	**Percentage of total residues (frequency)**
12Ado^{R}	4	8%
8Aoc^{R}	8	16%
εAhx^{R}	11	22%
γAbu^{R}	8	16%
βAla^{R}	7	14%
Gly^{R}	1	2%
LNva^{R}	3	6%
DNva^{R}	1	2%
LPhe^{R}	2	4%
DPhe^{R}	1	2%
2Acc^{R}	1	2%
4Acc^{R}	1	2%
Amc^{R}	1	2%
4Amb^{R}	1	2%

It became apparent in the screening of **57** that the sequences themselves were less important than the individual residues. In other words, the dye would not be able to distinguish the tetramine sequence R^1-R^2 over the same sequence expressed in the opposite direction, R^2-R^1, from the polymer support. Thus it makes more sense to depict the results as residue pairs (Table 3.1) and the frequency at which individual residues are observed out of the total residues decoded (Table 3.2). The most favoured residues found with this dye were the flexible, linear ones containing 3, 4, 6, 8, and 12 carbon spacers (βAla^{R}, γAbu^{R}, εAhx^{R}, 8Aoc^{R}, and 12Ado^{R} respectively). The most frequent individual residues were the 6-carbon εAhx^{R}, appearing a total of 22% of the time, followed by the

8-carbon residue of 8Aoc^{R} and the 4-carbon of γAbu^{R}, which both appear in a 16% frequency.

Examination of the relative positions of the sulfonates on dye **57** can provide some rationale into the rather modest selectivity that is observed. Hand-held molecular models revealed that the most reasonable planar conformation of the dye would be **57-A** in Figure 3.3, as **57-B** suffers from steric clashing between the hydroxyl group and the naphthyl ring. Using structure **57-A**, single point SYBYL calculations were used to determine the approximate range of distances between oxygens. In addition, the nitrogen-to-nitrogen distances on preferred triamine residues, which were also determined by single point calculations with the same force field on the predicted extended conformation. All calculations were done on the neutral molecules in the gas phase, and thus, are used solely as a guide in comparing the oxygen-to-oxygen distances between the internitrogen distances. From this simple analysis, it would appear that the εAhx^{R} and 8Aoc^{R} residues would fit ideally between sulfonates **I** and **II** on the naphthyl moiety, and even between **I** and **III**. The distance between the furthest sulfonates, **II** and **III**, could be reached by the longest residues, 8Aoc^{R} and 12Ado^{R}. It is also conceivable that sulfonates **II** and **III** can be accessed by the most distant amines on tetramine sequence made of two shorter residues (example: εAhx^{R}-βAla^{R}) leaving the middle amine uncomplexed.

Table 3.3: SYBYL calculations on internitrogen distances (in Å) of library residues in their optimized, extended conformations (see text for details).

12Ado^{R}	16.6
8Aoc^{R}	11.5
εAhx^{R}	8.9
γAbu^{R}	6.2
βAla^{R}	4.9
2-carbon spacers[1]	3.8
2Acc^{R}	4.5
4Acc^{R}	5.6 to 5.2
4Amc^{R}	7.6 (extended) to 6.7
4Amb^{R}	7.4 (extended) to 6.8

[1] residues derived from α-amino acids.

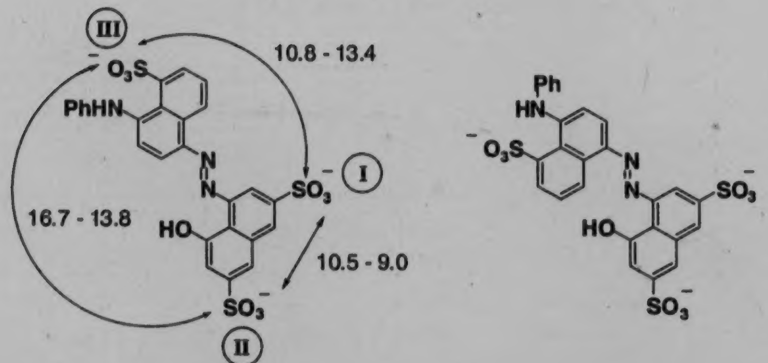

57 - A **57- B**

Figure 3.3: Possible conformations of dye **57** with average oxygen-to-oxygen distances calculated between sulfonates.

The low selectivity observed between the library and dye **57** is possibly due the difficulty the resin bound tetramines have in accessing all three sulfonates with each of their three available amines. To form three ion pair interactions many of the tetramines will need to 'bend' around the dye to properly position their ammonium units. However, hand-held models have shown that when linear tetramines rotate their bonds, they create a significant amount of unfavoured gauche interactions between the carbon atoms on the tetramine chain. This bending of the chain would result in a higher energy state in the molecule that may not be compensated by the stabilization of an ion pair. Furthermore, the presence of the bulky aniline unit may also have a role in restricting access to sulfonate **III**. The high degree of variability among residues may suggest a nondirected electrostatic interaction, rather than a highly selective ion pair that is geometrically defined via hydrogen bonding. For example, the γAbu^{R} and βAla^{R} residues may be long enough to allow their ammonium units to be attracted by the electronic charge spheres of the sulfonates, although probably without a defined geometric orientation. Alternatively, one residue on the resin bound tetramine sequence may be dominating the interaction with the dye while the remaining one is left uncomplexed, or two residues together may be long enough to span two sulfonates by leaving its middle nitrogen uncomplexed (i.e. two point binding over three point binding). These two latter scenarios may explain the frequent appearance of the 2-carbon spacers (16% frequency in total) which, according to their internitrogen distances, should not be expected to span the distance between two sulfonates by itself. One cannot also rule out the possibility of higher order complexes involving more than one resin supported tetramines binding to a single trisulfonated dye as a result of the rather high loading of the resin.

Ten beads that stayed clear (that is 'nonbinding' beads) during the screening were also isolated and sequenced in order to determine the degree of ligand exchange between supported tetramines. Adequate exchange would be indicated if selective sequences found previously in the blue beads were absent in the clear ones. This test would determine if the binding is thermodynamically controlled, whereby an equilibrium is established which favours the active tetramines, or kinetically controlled, whereby the dye binds to the most accessible polyamine available immediately upon being added to the beads. Effective ligand exchange would indicate a thermodynamically controlled process. The decoded sequences are given in Table 3.4.

Table 3.4: Clear (nonbinding) beads isolated and decoded in the screening of PS-bound tetramine library against **57**.

Residue pair	Number of occurrences	Residue pair	Number of occurrences
LPhe^{R}, LNva^{R} 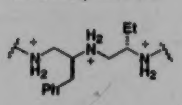	3	LPhe^{R}, LPhe^{R} 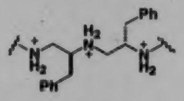	1
12Ado^{R}, 4Amb^{R} 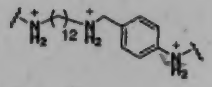	2	εAhx^{R}, Amc^{R} 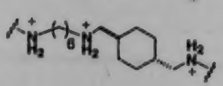	1
DNva^{R}, 4Amb^{R} 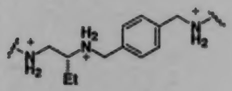	1	βAla^{R}, 12Ado^{R} 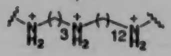	1
εAhx^{R}, 4Acc^{R} 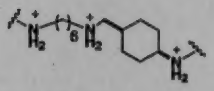	1		

The analysis of the clear beads revealed mainly the presence of 2-carbon residues, namely Phe^{R} and Nva^{R}, as well as the cyclic residues of 4Amb^{R}, 4Acc^{R}, and Amc^{R}. This group of residues was generally avoided by the dye target, perhaps due to the inappropriate spacing of the nitrogens relative to the sulfonates. However, the degree of polyprotonation is an additional factor in the ability of some residues to bind to the dye. It has been shown that the extent of complete protonation in a given polyamine at neutral pH will depend on the number of carbon units between the nitrogens.[60, 111, 112] Long carbon chains will allow a greater degree of protonation, while shorter ones will disfavour protonation at two adjacent nitrogens due to greater electronic repulsion felt by the two positively charged centers. Thus, in our dye screening exercise, the tetramines composed of two carbon spacers would not be completely protonated at pH 7, resulting in reduced affinity for the trisulfonated dye. The fact that they do occasionally appear in the coloured beads suggests that they are involved in sequences that bind the dye through a two point binding interaction rather than three point interaction.

In a few instances, residues observed in the blue-coloured, 'binding' beads were also found in some of the clear ones. The discovery of these residues indicates that ligand exchange among the solid-supported library members is slow, suggesting that the binding is, to some extent, kinetic in nature. However, the relative consensus in the binding indicates binding under thermodynamic control. These results indicate that further study is needed to learn more of the thermodynamics of the binding of the dye to the resin bound tetramine (*vide infra*).

3.3.2. Screening against dye **58**.

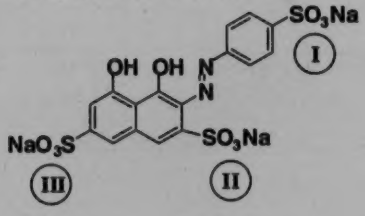

58

In order to further study the selectivity of the tetramine library, a different trisulfonated dye, **58**, was chosen. Dye **58** has its three sulfonate groups positioned almost along the same line with each other so that the tetramines would not need to twist themselves to reach each anionic center. The screenings with **58**, which is red in colour, was done under three different conditions and the results are depicted in Tables 3.5 and 3.7. In the first screening, the library beads were suspended in a solution of the dye in 1:9 water/DMF, buffered at pH 7. The effect of a competitive inhibitor was then tested by the addition of spermidine to the screening mixture. Finally, a third screening was performed at a lower pH to observe any possible changes in selectivity upon increasing the extent of polyprotonation on the tetramines.

Table 3.5: Screening of PS-bound tetramine library against **58**.

pH 7.0 without spermidine – condition A (31 beads)		**pH 7.0 with spermidine – condition B (26 beads)**		**pH 5.5 with spermidine – condition C (23 beads)**	
Residue pair	Frequency	Residue pair	Frequency	Residue pair	Frequency
8Aoc^{R},12Ado^{R}	4	8Aoc^{R},12Ado^{R}	5	12Ado^{R},4Acc^{R}	6
8Aoc^{R}, 8Aoc^{R}	4	8Aoc^{R}, 8Aoc^{R}	5	12Ado^{R}, 12Ado^{R}	5
8Aoc^{R}, εAhx^{R}	3	12Ado^{R},4Acc^{R}	4	8Aoc^{R},12Ado^{R}	2
8Aoc^{R}, 4Acc^{R}	3	8Aoc^{R}, εAhx^{R}	3	8Aoc^{R}, 4Acc^{R}	2
8Aoc^{R}, Amc^{R}	3	12Ado^{R}, 12Ado^{R}	3	LPhe^{R}, D/LNva^{R}	2
εAhx^{R}, Amc^{R}	3	8Aoc^{R}, Amc^{R}	2	12Ado^{R},LPhe^{R}	2
12Ado^{R}, 12Ado^{R}	3	8Aoc^{R}, 4Acc^{R}	2	εAhx^{R}, εAhx^{R}	1
8Aoc^{R}, γAbu^{R}	2	12Ado^{R},βAla^{R}	1	12Ado^{R},LNva^{R}	1
12Ado^{R},4Acc^{R}	2	βAla^{R}, Amc^{R}	1	12Ado^{R},βAla^{R}	1
Amc^{R}, Amc^{R}	1			12Ado^{R},Amb^{R}	1
8Aoc^{R}, βAla^{R}	1				
εAhx^{R}, εAhx^{R}	1				
Amc^{R}, 2Acc^{R}	1				

Conditions - approximately 3 mg of resin suspended in a 3.75×10^{-5} M solution of **58** in 1:9 water/DMF and: (A) 0.050 M MES-TRIS (pH 7.0); (B) 3.16×10^{-4} M spermidine with 0.050 M MES-TRIS (pH 7.0); (C) 3.22×10^{-4} M spermidine with 0.025 M MES (pH 5.5).

In the first screening (without spermidine, pH 7.0) about 5% of the beads were dark red, 30% were clear and the remaining were various shades of pink (see Figure 3.4). Thirty-one beads that were among the darkest were isolated and decoded for their tetramine sequences. The results revealed a preference for the 6, 8, and 12-carbon linear chains (εAhx^{R}, 8Aoc^{R}, and 12Ado^{R} respectively) with the 8-carbon chain the most favoured overall. In addition, two cyclic residues, 4Amc^{R} and 4Acc^{R}, frequently appeared in the decoding. In the presence of spermidine, the selectivity for 12Ado^{R} increased, appearing in 33% frequency (that is, 17 times out of a possible 52 residues found) compared to 20% without spermidine as an additive (see Table 3.7). Lowering the pH of the screening to 5.5 resulted in an unexpected change in the selectivity.

A.

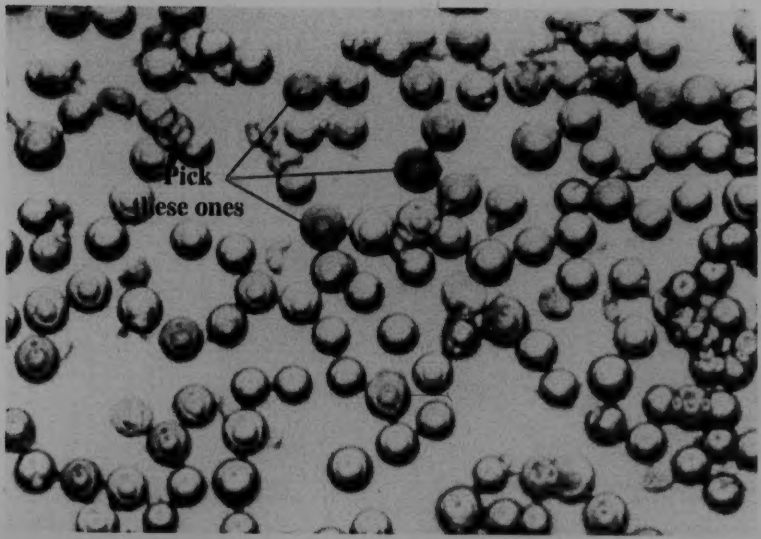
Pick
these ones

B.

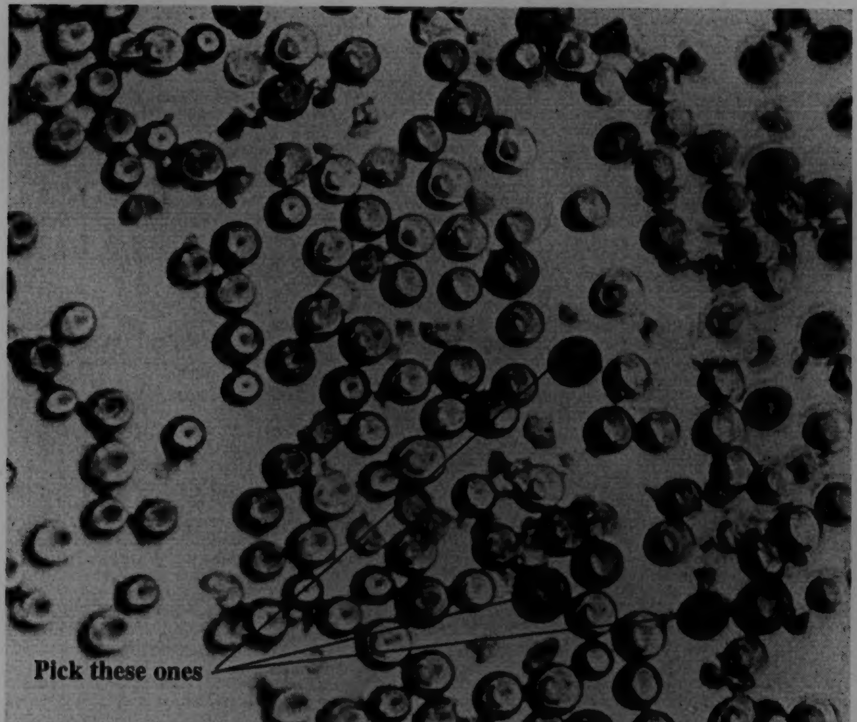
Pick these ones

Figure 3.4: Two examples of triamine library beads stained with dye **58** viewed under a microscope with 4×'s magnification. (Diameter of one bead is approximately 150 μm).

Although the appearance of 2-carbon residues was somewhat expected due to higher degree of protonation, there was also a marked increase for 12Ado^R, up to 50% frequency, as well as the cyclic 4Acc^R residue (10% to 17%). The increase in these residues seems to come at a cost of 8Aoc^R which drops to 9% frequency from 40%. One possible explanation for the decrease in 8Aoc^R is the greater ability at pH 5.5 for the spermidine, which spans eight atoms in between the terminal amines, to completely inhibit the 8-carbon residue from binding the dye. Each of these screenings were repeated a number of times, and on each occasion the same general pattern of selectivity was observed.

A number of clear beads were also randomly isolated from the screening at pH 7 with spermidine. In almost all cases, at least one two-carbon residue (Phe^R, Gly^R or Nva^R) or the residue 2Acc^R was found in each sequence, with many tetramines containing various combinations of these shorter residues. In only a few instances were these residues paired up with ones found commonly in the red beads.

Calculations (SYBYL force field) on both dye **58** and the tetramine residues have shown similarities in the distances between the sulfonates on the dye and nitrogens on the 6 to 12-carbon residues. From hand-held molecular models, two reasonable planar conformations for the dye have been identified, and from these the range of oxygen-to-oxygen distances between sulfonates were measured (see Figure 3.5). These calculations revealed only a slight change in the sulfonate distances between the two conformations. The 8Aoc^R (11.9 Å, N to N) and εAhx^R (8.9 Å) residues have distances very close to those between neighbouring sulfonates (**I** to **II** and **II** to **III**), while 12Ado^R (16.6 Å) by itself is capable of spanning the distance between the furthest sulfonates (**I** to **III**). However, the fact that 12Ado^R is often found paired with another linear residue may indicate that 12Ado^R does not bind alone. It is possible that under the aqueous conditions of the screening, the long hydrocarbon spacer contracts itself in order to maximize hydrophobic interactions, thereby shortening its length and making it capable of binding two sulfonates that are positioned more closely.

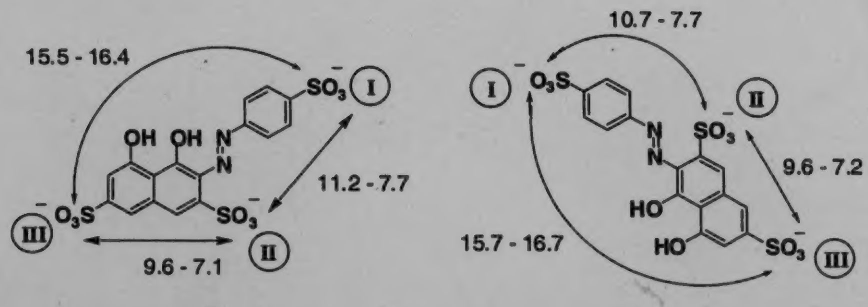
15.5 - 16.4
SO3 I
OH OH
N
N
O3S
III
SO3
11.2 - 7.7
9.6 - 7.1
II
10.7 - 7.7
I
O3S
II
N
N
SO3
9.6 - 7.2
HO
HO
15.7 - 16.7
SO3
III

58 - A

58 - B

Figure 3.5: Possible conformations of dye **58** with measured oxygen-to-oxygen distances (in Å) between remote sulfonate oxygens.

3.3.3: Screening against dye **59**.

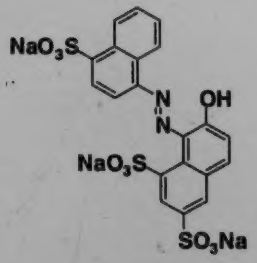
NaO3S
N
OH
N
NaO3S
SO3Na

"New Coccine," 59

A good way to further demonstrate ion pair selectivity with the tetramine library is to screen another dye whose sulfonate groups are spaced over different distances than that of dye **58**. To this end we selected dye **59** ('New Coccine') which possesses three sulfonate groups in closer proximity with the expectation that they will attract different residues containing shorter internitrogen distances than those observed with **58**. The screening of the library was done in the presence of spermidine both at pH 7 and 5.5. In each assay, around 12% of the beads appeared dark red. The results are shown in Tables 3.6 and 3.7.

Table 3.6: Screening of PS-bound tetramine library against **59**.

PH 7.0– condition A (40 beads)		**pH 5.5 – condition B (31 beads)**	
Residue pair	Frequency	Residue pair	Frequency
8Aoc^R, εAhx^R	4	12Ado^R, 4Acc^R	3
8Aoc^R, 12Ado^R	4	8Aoc^R, 12Ado^R	2
8Aoc^R, 8Aoc^R	3	2Acc^R, 2Acc^R	2
εAhx^R, 4Acc^R	3	2Acc^R, Amc^R	2
8Aoc^R, 2Acc^R	2	2Acc^R,12Ado^R	2
εAhx^R, Amc^R	2	εAhx^R, Amc^R	2
12Ado^R, 4Acc^R	2	εAhx^R, DNva^R,	2
2Acc^R, εAhx^R	2	εAhx^R, Amb^R,	2
εAhx^R, βAla^R	2	εAhx^R, 2Acc^R	1
8Aoc^R, D/LPhe^R	2	εAhx^R, 4Acc^R	1
2Acc^R, Amc^R	1	2Acc^R, 4Acc^R	1
8Aoc^R, 4Acc^R	1	2Acc^R, 8Aoc^R	1
2Acc^R, βAla^R	1	4Acc^R, DNva^R	1
8Aoc^R, LNva^R	1	4Acc^R, DPhe^R	1
8Aoc^R, γAbu^R	1	12Ado^R, LNva^R	1
Amc^R, Amc^R	1	12Ado^R, 12Ado^R	1
4Acc^R, γAbu^R	1	12Ado^R, Amc^R	1
12Ado^R, Amc^R	1	Gly^R, DPhe^R	1
12Ado^R, εAhx^R	1	εAhx^R, 8Aoc^R	1
Amc^R, Gly^R	1	8Aoc^R, 8Aoc^R	1
8Aoc^R, Amc^R	1	8Aoc^R, Amc^R	1
εAhx^R, DNva^R	1		
8Aoc^R, 4Amb^R	1		
βAla^R, γAbu^R	1		

Conditions - approximately 3 mg of resin suspended in a 3.75×10^{-5} M solution of **59** in 1:9 water/DMF and: (A) 3.16×10^{-4}M spermidine with 0.050 M MES-TRIS (pH 7.0); (B) 3.22×10^{-4} M spermidine with 0.025 M MES (pH 5.5).

The higher proportion of dark red beads in the Petri dish immediately indicated that the overall selectivity for this dye was lower than for **58**. Indeed, decoding of isolated beads gave an increased variation in both the tetramine sequences and individual residues under both pH conditions. There are, however, some similarities, namely the preference for long, linear residues, as well as some ring-containing ones over the 2-carbon spacers. The shorter residues, however, are more frequently encountered with dye **59** at pH 7 compared to **58**. An interesting difference between the two dyes is the reduction in the frequency of 12Ado^R binding to **59**. For instance, at pH 7 with spermidine the frequency of the 12 carbon unit goes from 33 % with **58** to only 10 % when screened against **59**. Alternatively, the 6-carbon unit, εAhx^R, is found more frequently with **59** than with **58** (19 % versus 6 %). The shift towards shorter length residues reflects the shorter distances between the sulfonates on the dye. Another striking difference is the discovery of the 2Acc^R residue as a binding unit which was rarely observed in the screening of **58**. In terms of frequencies, the 2Acc^R unit was encountered 8 % of the time at pH 7, and then 18 % at pH 5.5, apparently at the cost of 8Aoc^R.

Again, some rationale for the observed selectivity can be provided by comparing the atomic distances in both the dye and the residues. Two possible conformations exist for the dye (Figure 3.6), however, the relative positions of the sulfonates are almost identical in both. The internitrogen distance for the extended conformation of εAhx^R is 8.9 Å which is close to the distance between sulfonates **I** and **II**. The nitrogen distance for the optimized conformation of the 2Acc^R residue is 4.5 Å which should be able to fit reasonable between the *meta* sulfonate groups **II** and **III**. In addition, the residues 4Acc^R and Amc^R, which are also strong binders according to Table 3.6, have calculated distances of 5.2 to 5.6 and 7.4 Å respectively and, therefore, should also be able to interact with the *meta* sulfonates. Once again, when the screenings were repeated almost the same results were obtained.

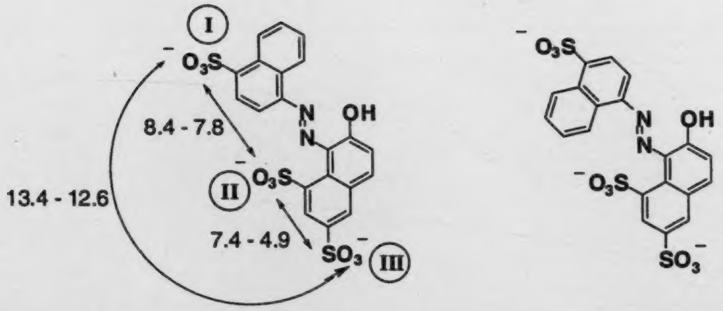
I
II
III
8.4 - 7.8
13.4 - 12.6
7.4 - 4.9
OH
N
N

59-A 59-B

Figure 3.6: Calculated oxygen-to-oxygen distances (in Å) for dye **59**.

Table 3.7: Frequency of individual residues (number of occurrences and percentage out of total residues) found in the screening of **58** and **59**.

Dye:	**58**	**58**	**58**	**59**	**59**
pH:	7.0	7.0	5.5	7.0	5.5
spermidine:	no	yes	yes	yes	yes
no. of beads decoded:	30	26	23	40	31
no. of residues:	60	52	46	80	62
12Ado^{R}	12, 20%	17, 33%	23, 50%	8, 10%	11, 18 %
8Aoc^{R}	23, 39%	21, 40 %	4, 9 %	23, 29 %	7, 11 %
εAhx^{R}	[illegible] 12%	3, 6 %	2, 4 %	15, 19 %	10, 16 %
γAbu^{R}	1, 2 %	0, 0 %	0, 0 %	3, 4 %	0, 0 %
βAla^{R}	2, 3 %	3, 6 %	1, 2 %	4, 5 %	0, 0 %
Gly^{R}	0, 0 %	0, 0 %	0, 0 %	1, 1 %	1, 2 %
LNva^{R}	0, 0 %	0, 0 %	2, 4 %	1, 1 %	1, 2 %
DNva^{R}	0, 0 %	0, 0 %	1, 2 %	1, 1 %	4, 6 %
LPhe^{R}	0, 0 %	0, 0 %	2, 4 %	1, 1 %	0, 0 %
DPhe^{R}	0, 0 %	0, 0 %	2, 4 %	1, 1 %	2, 3 %
2Acc^{R}	1, 2 %	0, 0 %	0, 0 %	6, 8 %	11, 18 %
4Acc^{R}	5, 8 %	5, 10 %	8, 17 %	6, 8 %	7, 11 %
Amc^{R}	9, 15 %	3, 6 %	0, 0 %	9, 11 %	6, 10 %
4Amb^{R}	0, 0 %	0, 0 %	1, 2 %	1, 1 %	2, 3 %

3.4: Nature of the tetramine-dye interaction.

In order to verify that ion pairing is responsible for the observed selectivity, a series of control experiments were conducted to determine the nature of the binding between the dyes and the resin-bound tetramines. As mentioned earlier, nonspecific binding of the dyes to the underivatized polystyrene support was not observed in the mixed organic/aqueous solvent. (Interestingly, when attempting the same dye screening experiments on TentaGel® supported polyamines (see Chapter Five), the dyes where found to bind strongly to the underivatized resin). The large number of long, hydrophobic residues that were selected in the screenings (example: $12Ado^R$, $8Aoc^R$) suggested the possibility of hydrophobic interactions as a dominant binding mode in the polar solvent. However, screening of the tetramine libraries in the presence of 0.1 % Triton X-100®, a nonionic detergent that is supposed to minimize nonspecific hydrophobic interactions, did not reduce the appearance of the beads after mixing with the dye targets. Furthermore, no coloured beads resulted when the peptide library, which could only bind via hydrophobic interactions, or when the neutral tetramine library (at pH 11) were suspended in the dye solution. If electrostatic interactions are indeed important, then increasing the salt concentration of the solution should inhibit the binding of the dyes. Indeed, mixing the tetramine library in the presence of 0.5 M tetrabutylammonium bromide failed to decolourize the dye solution and resulted in only clear beads.

The occasional appearance of active residues in the clear, nonbinding beads seems to suggest a very slow exchange of dyes between beads in the suspension. To determine if any dye exchange can occur, an experiment was designed where tetramine beads, saturated with an excess amount of dye **58** and suspended in the water/DMF mixture at pH 7, were placed on one side of a chamber partitioned by a coarse filtration frit. On the opposite side of the partition were library beads, not previously exposed to the dye, suspended in the same solvent mixture. Within a few days, the some of the resin on the later side of the chamber began to turn pink, and after one week, the all the resin on both sides had the same dark red appearance. This experiment verifies that dye exchange does occur slowly between the resin-bound tetramines despite the high loading of the resin. The slowness of the dye exchange between the partitioned resin may be due to limitations in the experiment, such as the inability to constantly agitate the resin without having them cross the partition barrier. In addition, performing the on-bead screenings for longer periods of time (48 hours) did not greatly change the selectivity among beads that were decoded. However, it is expected that the high local concentration of tetramines within the resin would retard the migration of the dyes between the beads.

3.5: **Determination of stability constants.**

3.5.1: Solution versus solid phase binding.

The screening results suggest that the length of the polyamine residue determines its affinity for the dye target. These results imply a geometrically defined interaction that depends on the precise positioning of the ammonium ions relative to the sulfonates, rather than a general electrostatic attraction. Similar kinds of observations have been reported in the literature for solution phase guest-host complexes that rely on ion pair interactions. For instance, Dougherty *et al.* have shown, using a carboxylate-based host, that by increasing the length of a dicationic guest by increments of a single methylene group, the binding affinity towards the host reaches a maximum once a specific length of the guest is reached.[122]

Although our solid phase screening observations seems to agree with the solution phase studies reported in the literature, various factors may influence the outcome of the on-bead binding assays. The high loading of the resin may result in higher order binding of more than one tetramine to a single dye target, and thus, cause difficulty for the dye to diffuse out of the resin bead to provide sufficient exchange with other supported polyamines. Therefore, to show that this type of library screening is still beneficial in identifying high affinity receptors for more general applications, individual polyamine receptors were synthesized and examined in solution with both dye **58** and **59**.

3.5.2. Synthesis of triamine-amides.

From the screening results given above, a most likely polyamine to have high affinity towards **58** in solution is the sequence 8Aoc^{R}-8Aoc^{R}. Synthesis of this polyamine (as a triamine) was performed on trityl polystyrene resin (Scheme 3.1). Initial attempts involved the use of an amino-alcohol spacer attached to the support as a trityloxy. The alcohol functionality was incorporated to avoid an unwanted primary amine at the end of the polyamine following cleavage from the solid-support. However, as mentioned in Chapter Two, the reduction of the amino-alcohol linked triamide followed by iodine-promoted borane-amine cleavage resulted in very little yield of product. (It was not until a year later that it was discovered that the piperidine-based work-up would have worked well with this linker). As a result of this failure, the trityldiamine **37** linker was employed, which unfortunately required additional synthetic steps in order to block the terminal amine after cleavage. Thus, after reduction of triamide **60**, the resulting resin-supported tetramine was treated with (BOC)$_2$O (di-*t*-butyldicarbonate) to provide the BOC protected tetramine derivative **61**. Cleavage of **61** from the resin was effected by exposure to dilute TFA (1 %) in dichloromethane. Acetylation of the primary amine by acetic anhydride was followed by removal of the BOC protective groups with concentrated TFA to give the triamine-amide **62** in 19 % overall yield from triamide **60**. Compound **62** would be used in subsequent NMR binding assays.

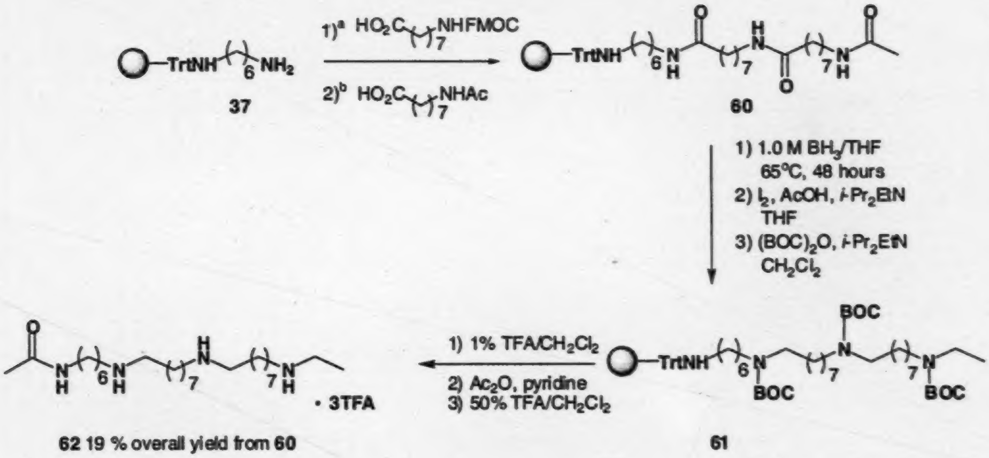

TrtNH
NH2
6
37
1)a HO2C NHFMOC 7
2)b HO2C NHAc 7
60
1) 1.0 M BH3/THF 65°C, 48 hours
2) I2, AcOH, i-Pr2EtN THF
3) (BOC)2O, i-Pr2EtN CH2Cl2
61
BOC
1) 1% TFA/CH2Cl2
2) Ac2O, pyridine
3) 50% TFA/CH2Cl2
· 3TFA
62 19 % overall yield from 60

a) HBTU, HOBt, *i*-Pr$_2$EtN, HO-8Aoc-FMOC. b) 1:4 piperidine/DMF; HBTU, HOBt, *i*-Pr$_2$EtN, HO-8Aoc-Ac

Scheme 3.1

A solution phase triamine expected to have a lower affinity for dye **58** than triamine-amide **62** (8Aoc^R-8Aoc^R) would be one with shorter internitrogen residues. We selected, based on the library screening results, the sequence 2Acc^R-εAhx^R which has the poorly selected 2Acc^R residue. However, although this particular sequence should have a weaker affinity for **58**, it should be a strong ligand for dye **59**. Our solution phase version of the 2Acc^R-εAhx^R sequence is triamine-amide **66**.

The synthesis of **66** on solid-support was carried in a manner analogous to that of **62** (Scheme 3.2). One unexpected complication was the isolation of a diaminoborohydride **64** after amide reduction of **63** and iodine-promoted borane-amine cleavage. This type of aminoborohydride species has been observed previously in this laboratory during the reduction of resin-bound tertiary amides.[95][123] As in those cases, the diaminoborohydride **64** was treated with excess ethylene glycol under basic conditions to affect the exchange of the boron to the diol, providing the resin-supported tetramine. (It should be noted that the aminoborohydride was never observed in decoding single resin beads expressing the sequence 2Acc^{R}-εAhx^{R}, or any other tetramine). BOC protection of the amines proceeded to give **65** which was cleaved from the resin and subsequently acetylated and deprotected, as described previously for **62**, to give the triamine-amide **66** in 15 % overall yield from the triamide **63**.

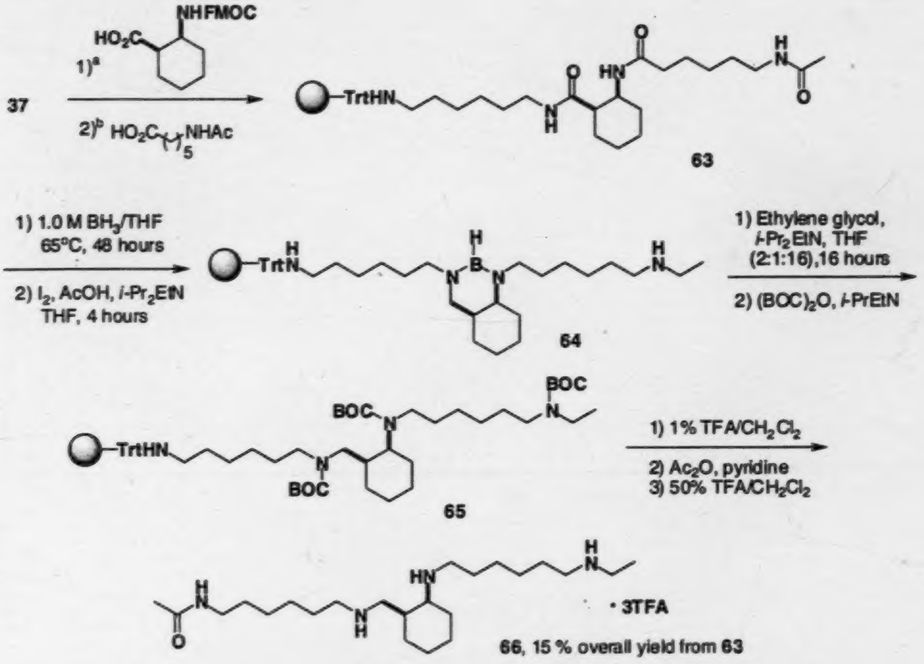
37
NHFMOC
HO2C
1)a
2)b HO2C(CH2)5NHAc
TrtHN
63
1) 1.0 M BH3/THF 65°C, 48 hours
2) I2, AcOH, i-Pr2EtN THF, 4 hours
64
1) Ethylene glycol, i-Pr2EtN, THF (2:1:16),16 hours
2) (BOC)2O, i-PrEtN
BOC
65
1) 1% TFA/CH2Cl2
2) Ac2O, pyridine
3) 50% TFA/CH2Cl2
• 3TFA
66, 15 % overall yield from 63

a) HBTU, HOBt, i-Pr$_2$EtN, HO-2Acc-FMOC. b) 1:4 piperidine/DMF; HBTU, HOBt, i-Pr$_2$EtN, HO-εAhx-Ac

Scheme 3.2

3.5.3: ^{1}H NMR titrations.

Initial attempts at determining the stability constants (*K_a*'s) by UV/visible spectroscopy failed as no detectable change in the UV/visible spectra of the dyes were observed upon titration with the triamine-amide ligands. Therefore, ^{1}H NMR was employed[124] using 20 % D_2O in DMSO-d_6 as the solvent mixture. This particular solvent system was used due to solubility issues. The *K_a*'s were then obtained from the titration curves, shown in Figure 3.7, using curve fitting software developed by C.A. Hunter.[157]

With dye **58** the stability constants for **62** (8Aoc^R-8Aoc^R) and **66** (2Acc^R-εAhx^R) were found to be 6400 M^{-1} and 1100 M^{-1} respectively. Both fit a binding curve that had assumed a 1:1 stoichiometry over other higher order complexes. In addition, a Job plot of **62** with the dye provided further evidence of a 1:1 complex between this pair (Figure 3.8). There are a few important differences between the solution phase and the solid phase assays that should be discussed. Firstly, the solvent systems employed were different; the NMR titrations were performed in 20% D_2O in DMSO-d_6, which is a more polar medium than the 10% water in DMF used for the solid phase work. The higher polarity solvent may reduce the solution phase binding affinities by increasing the desolvation energy of the uncomplexed ions.[122, 125] Different counter ions in both cases can also affect the binding affinities. Of course the very high local concentrations of resin bound tetramines in the resin may also cause differences in the binding stoichiometries observed between the solution and solid-supported experiments. However, despite these differences, the larger binding constant obtained for **62** adds credibility to the library screenings that led towards this ligand.

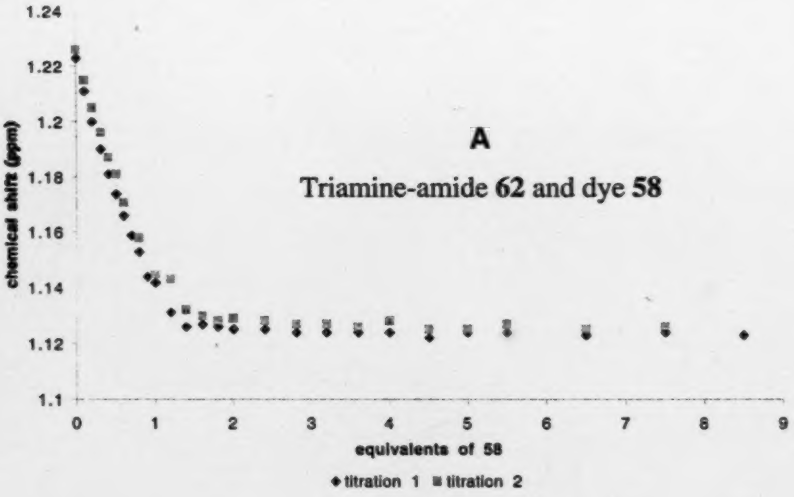

A

Triamine-amide **62** and dye **58**

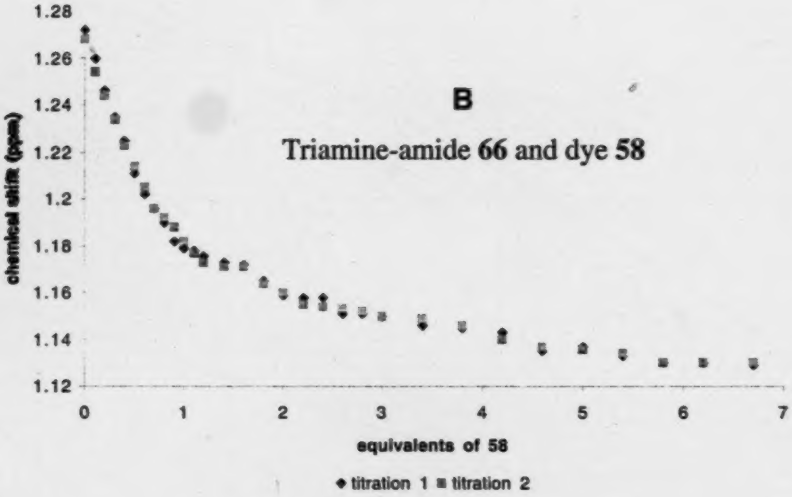

B

Triamine-amide **66** and dye **58**

66 and dye **59** ('New Coccine')

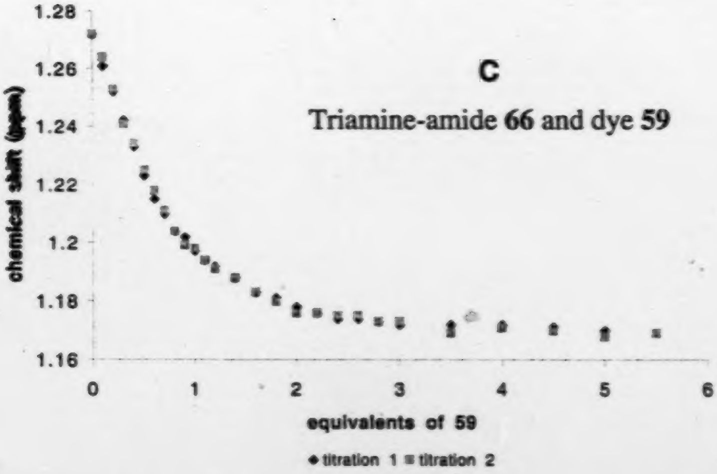

Figure 3.7: A: ^{1}H NMR titration of **62** with dye **58**, monitoring the change in chemical shift of the methylenes at 1.226 ppm. **B**: Titration of **66** with dye **58**, monitoring the chemical shift of the methylenes at 1.271 ppm. **C**: Titration of **66** with dye **59**, monitoring the chemical shift of the methylenes at 1.271 ppm.

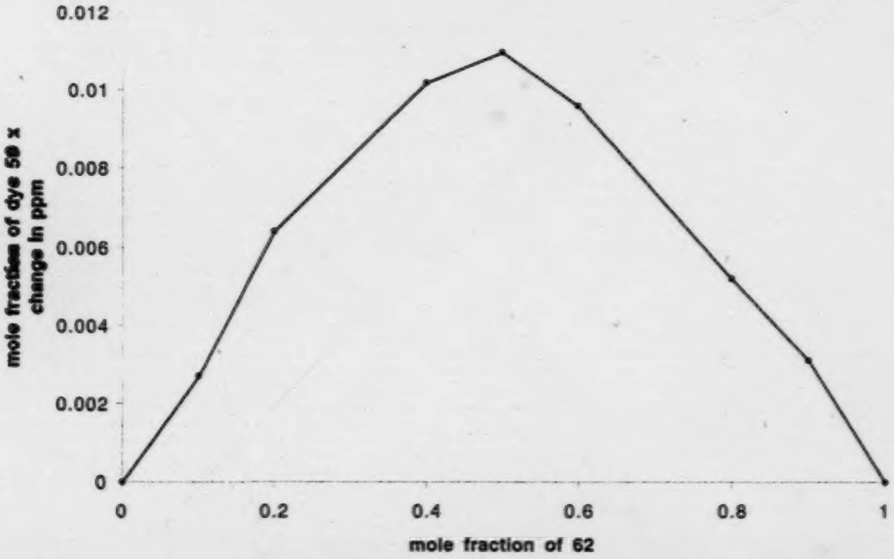

Figure 3.8: Job plot of **62** (8Aoc^R-8Aoc^R) with dye **59**, monitoring the naphthalene protons of the dye at 7.445 ppm.

Stability constant measurements with dye **59** ('New Coccine') were also performed with triamine-amides **62** and **66**. Unfortunately, titration of **59** with **62** resulted in precipitation of the complex in the NMR tube, so a K_a value could not be determined for this pair. Between **59** and **66** the stability constant was determined to be 2700 M^{-1}, which is higher than with the dye **58**, a result that was predicted from the on-bead screening data.

3.6: Selective extraction of dye 59 ('New Coccine') over dye 58.

The library screening results and the different stability constants between triamine-amide **66** (2Acc^R-εAhx^R) and the two dyes suggested the possibility of an alternative binding assay that involves using resin-supported tetramines to selectively remove a particular trisulfonated dye from a mixture of dyes. This binding assay would alleviate the tedious synthesis of the triamine-amides for solution-phase studies, yet still provide useful information into the selectivity of a given polyamine towards a particular polyanionic dye target.

To investigate the feasibility of this type of selective extraction, the resin bound tetramine sequences 2Acc^R-εAhx^R and 8Aoc^R-8Aoc^R (**67** and **68**, Figure 3.9) were prepared by the amide reduction of a triamide precursor on trityl polystyrene.

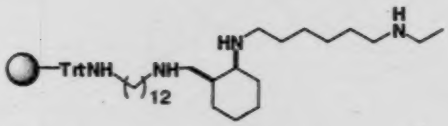

67, (2Acc^R-εAhx^R)

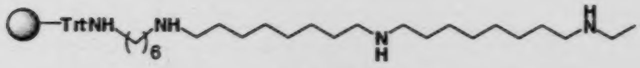

68, (8Aoc^R-8Aoc^R)

Figure 3.9: Resin-supported tetramines used in the selective extraction of dyes **58** and **59**.

In the preparation of **67**, just as for the triamine-amide **66**, additional treatment with basic ethylene glycol was required following the reduction with borane and work-up with iodine. The resin-supported tetramine **67** was then suspended in a 1:1 mixture of **58** and **59** in 1:9 water/DMF with 0.050 M MES-TRIS at pH 7. The resin, which immediately turned deep red, was filtered and washed three times with a 0.1 M DMF solution of phenylsulfonate, sodium salt (PhSO$_3$Na) to remove any weakly bound material, and then three times with a 0.5 M solution to elute the bound dyes. After each wash the filtrate was collected as a separate fraction. Analysis of the third fraction with 0.5 M PhSO$_3$Na gave dye **59** in 79% purity by HPLC/UV. An additional wash eventually produced the dye in approximately 97% purity (Figure 3.10).

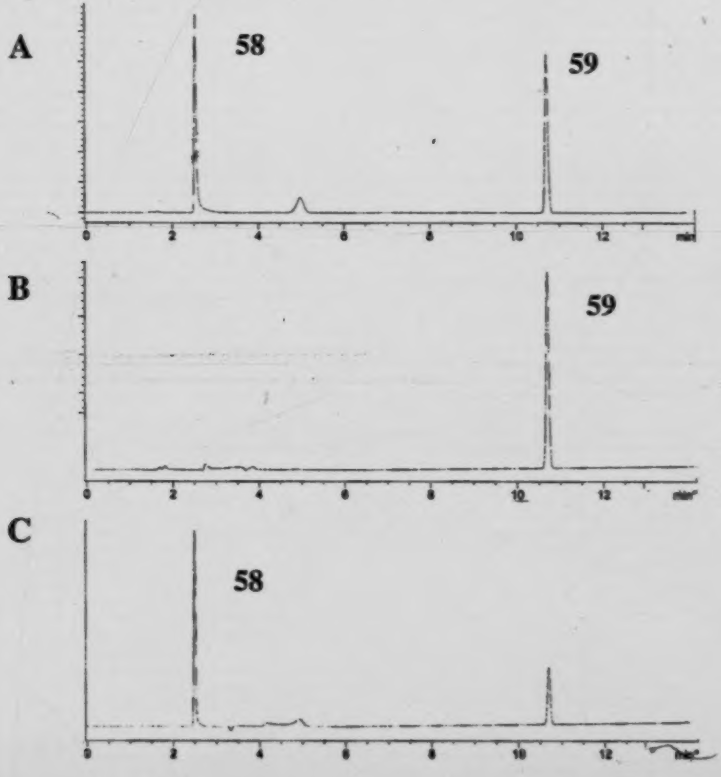

Figure 3.10: A: HPLC/UV chromatogram of a 1:1 mixture of dyes **58** and **59**. **B:** After washing resin **67** (2Acc^R-εAhx^R) with 0.5 M PhSO$_3$Na. **C:** After washing resin **68** (8Aoc^R-8Aoc^R) with 0.5 M PhSO$_3$Na.. (Detailed HPLC conditions in Chapter 7, Section 7.10).

The sequence 8Aoc^R-8Aoc^R (**68**) was also tested in the same type of extraction experiment. It was synthesized again via the usual amide reduction/iodine-promoted work-up without incident. As expected from the library screening data (Table 3.7) **68** selectively extracted dye **58** over **59**, for after three washes with 0.5 M $PhSO_3Na$, the resin-supported tetramine recovered **58** in 68 % purity by HPLC/UV (Figure 3.10).

From the on-bead library screening, two tetramine sequences have been identified that are capable of sensing, rather selectively, the subtle geometrical differences between anionic groups on the two dye targets. For real chromatographic-type applications one would prefer to immobilize the tetramines to silica gel which has a higher separation efficiency than polystyrene resin due to smaller particle size.

3.7: Screening of a glutamate rich peptide.

So far all the screening experiments described with the tetramine library have been with trisulfonated dyes which were used due to their easy detection on the resin bead. However, alternative targets would be desired to expand the applicability of the library to other polyanionic molecules with more biological relevance. To this end, we choose a nonameric peptide sequence, rich with glutamate residues, that is found within an α-helical motif in hemoglobin protein (Gly-Glu-Tyr-Gly-Ala-Glu-Ala-Leu-Glu).[116, 126] In order to visualize the binding to the resin, the peptide was labeled with a red-coloured dye. By itself the peptide is too short to exist as an α-helix, but we were interested in whether a resin bound tetramine sequence could be discovered that can stabilize and promote α-helix formation.

The synthesis of the labeled peptide **72** began by preparing the protected peptide **69** by standard FMOC peptide synthesis on Rink amide resin using orthogonally protected glutamate and tyrosine amino acids (Scheme 3.3). An εAhx residue was attached to the *N*-terminal end of the sequence to act as a spacer between the hemoglobin peptide and the Disperse Red-1 dye (**71**). Before linking the dye onto the peptide, the FMOC protective group on the εAhx was removed and an *O*-2-chlorotrityl protected FMOC-tyrosine was coupled, then *N*-terminated with an acetyl group to provide the peptide intermediate **70**. The 2-chlorotrityl group was then removed from the tyrosine using dilute TFA, liberating the phenolic hydroxyl which allowed for a Mitsunobu coupling to attach the dye **71**. Concomitant deprotection of the glutamates and the internal tyrosine residues with cleavage of the peptide from the resin was achieved by treatment with 95/2.5/2.5 TFA/water/*i*-Pr_3SiH, affording the labeled peptide **72**. This tagged peptide was used in crude form for subsequent screenings.

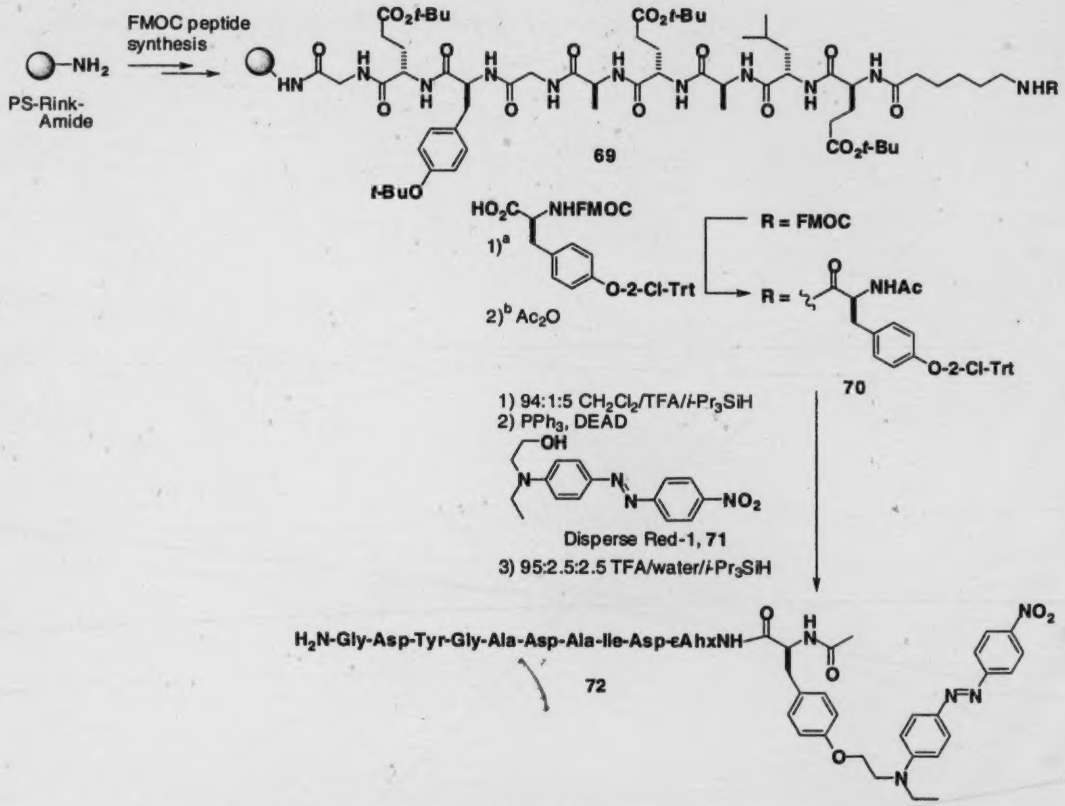
FMOC peptide synthesis
PS-Rink-Amide
NH2
CO2t-Bu
CO2t-Bu
CO2t-Bu
t-BuO
NHR
69
HO2C
NHFMOC
1)a
2)b Ac2O
O-2-Cl-Trt
R = FMOC
R =
NHAc
O-2-Cl-Trt
70
1) 94:1:5 CH2Cl2/TFA/i-Pr3SiH
2) PPh3, DEAD
OH
NO2
Disperse Red-1, 71
3) 95:2.5:2.5 TFA/water/i-Pr3SiH
H2N-Gly-Asp-Tyr-Gly-Ala-Asp-Ala-Ile-Asp-eAhxNH
72
NO2
N=N

[a] 1:4 piperidine/DMF; HO-Tyr(2-Cl-Trt)FMOC, HBTU, HOBT, *i*-Pr_2EtN [b] 1:4 piperidine/DMF; Ac_2O, Et_3N.

Scheme 3.3

The on-bead screening was performed with a 2.0×10^{-5} M solution of peptide **72** in 0.010 M MES-TRIS (pH 7.0) in 10% water/DMF. About 5% of the beads were dark red and a total of 18 of these were isolated and decoded by LCMS. Table 3.8 shows the sequences that were selected by the library.

Table 3.8: Screening of tetramine library against peptide **72**. 18 beads were isolated.

Residue pair	No. of occurrences	Residue	Frequency
8Aoc^{R}, 12Ado^{R}	5	12Ado^{R}	11, 31 %
12Ado^{R}, 4Acc^{R}	3	8Aoc^{R}	11, 31 %
8Aoc^{R}, 4Acc^{R}	2	εAhx^{R}	3, 8 %
εAhx^{R}, 12Ado^{R}	2	γAbu^{R}	1, 3 %
Amc^{R}, 8Aoc^{R}	1	βAla^{R}	0, 0 %
Amc^{R}, Amc^{R}	1	Gly^{R}	0, 0 %
εAhx^{R}, Amc	1	LNva^{R}	0, 0 %
8Aoc^{R}, γAbu^{R}	1	DNva^{R}	0, 0 %
8Aoc^{R}, 8Aoc^{R}	1	LPhe^{R}	0, 0 %
Amc^{R}, 12Ado^{R}	1	DPhe^{R}	0, 0 %
		2Acc^{R}	0, 0 %
		4Acc^{R}	5, 14 %
		Amc^{R}	5, 14 %
		4Amb^{R}	0, 0 %

In the past, tetracationic ligands such as spermidine[126] and synthetic tetraguanidinium[116, 127, 128] receptors have induced tetraglutamate and tetrasparate peptide sequences into forming α-helices. When spermidine was employed, the peptide had its glutamate residues spaced in an i, i+4, i+7, i+11 orientation, which is the same as in peptide **72**. In other words, the distances between each anionic site along the α-helix of the peptide is complimentary to the internitrogen distances in spermidine, which are relatively short. However, the selection of long residues (12Ado^{R} and 8Aoc^{R}) from our library screening would seem to indicate that peptide **72** remains as an elongated sequence as it binds to the resin-bound tetramine. This means that the glutamate residues on the peptide are far apart from each other and not likely part of a α-helical structure. In addition, the use of DMF as the screening solvent has an unknown effect on the propensity for α-helix formation.

3.8: Conclusions

In this work, a combinatorial library was used to discover polyamine receptors towards various trisulfonated dyes through the formation of selective ion pair interactions. It appears that the strongest complexes are the result of geometrically defined ion pairing, possibly mediated by hydrogen bonding. This belief is supported by the similar distances between each sulfonate group on the dye molecules compared to each internitrogen distance on the most selected tetramine residues. The weaker complexes may involve weaker, nondirectional electrostatic attractions between the positively charged ammoniums on the polyamine and the negatively charged sulfonates. The results from these on-bead screenings were also used to identify individual polyamines that exhibit the same selectively towards particular dye targets, both in solution and on solid-support during a solid-phase extraction experiment. Overall, the results show that it is possible to achieve reasonably good selectivity based on ion pairing interactions between a resin-supported polyamine library and a polyanionic target. The eventual goal for this work is screening polyanionic biomolecules, including oligonucleic acids, proteins and polysulfated oligosaccharides such as heparin, and perhaps smaller molecules like the inositol phosphates. However, before these screenings can be achieved, the polyamine libraries need to be synthesized on a more hydrophilic, water swelling, resin.

Chapter Four:

Synthesis of polyamines and oligoboronic acids on TentaGel® resin.

4.1: Hydrophobic versus hydrophilic supports.

In all the work described thus far, the solid-support used was a polystyrene 'gel-type' resin, lightly cross-linked with 1% divinylbenzene (DVB), which possesses highly nonpolar properties typical of polystyrene polymers (Figure 4.1).[29, 30] For gel-type resins to be effective as solid-supports in organic synthesis, they need to swell in some appropriate solvent in order to expand their polymeric framework. Once swollen, reagents can enter the interior of the resin where up to 99 % of bound substrate resides. Polystyrene resins typically swell best in dichloromethane, toluene, THF, dioxane and DMF. They swell poorly in diethyl ether, hexane, and especially polar protic solvents like methanol and water. Thus, if a reaction is performed on a polystyrene matrix and requires the presence of water, then a large amount of co-solvent such as THF or DMF is needed. For this reason, the dye screening experiments with polystyrene-bound tetramines (Chapter Three) could only be performed with no more than 10 % water in DMF. However, even in these conditions, the polystyrene matrix maintains a highly nonpolar environment that polar molecules in solution may be reluctant to diffuse into. (This is one reason why some organic reactions are slower on solid-support compared to solution-phase).

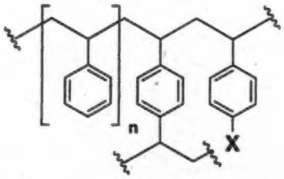

Figure 4.1: Matrix of divinylbenzene cross-linked polystyrene resin. (X represents the linker).

In order to screen water soluble biological molecules against bead-supported polyamine or oligoboronic acid libraries, the resin needs to tolerate complete aqueous conditions with little or no organic co-solvent. Among the most suitable resins for these conditions are PS-PEG based resins which have polyethyleneglycol (PEG) chains grafted into a polystyrene matrix. The PEG chains make up to 70 % of the resin by weight and, therefore, dominate its chemical properties over the polystyrene backbone. The resin will swell in any solvent that dissolves PEG. In other words, resin will tolerate both polar and nonpolar solvents as a result of PEG's amphipilic nature. The outcome is a wider range of solvents that can be employed with these resins, from dichloromethane to pure water.

The chemical structures of the commercially available PS-PEG resins are given in Figure 4.2. One of the first hydrophilic resins to become available was TentaGel®[129] from Rapp Polymere. Although it has excellent swelling properties, its one disadvantage is the rather acid labile benzylic linkage of the PEG chain to the polystyrene matrix. In order to provide more acid resistant supports, alternative resins such as ArgoGel® (Argonaut Technologies) and NovaSyn® (Novabiochem), which both use more stable PEG linkages, have become commercially available. However, despite TentaGel®'s problems, it has now become the most popular type of hydrophilic resin used in solid-phase synthesis. In all cases PS-PEG resins occasionally suffer from leaching of the PEG chains regardless of the method linking the PEG to the polystyrene matrix. Their loading levels are also much less than that of polystyrene resins, typically between 0.2 and 0.3 mmol/g, although some can approach 0.6 mmol/g such as the bifurcated ArgoGel®.

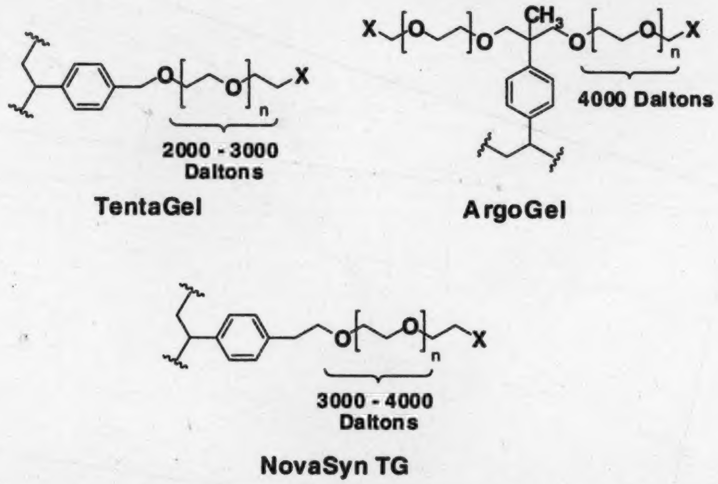

Figure 4.2: Structures of commercially available PS-PEG resins.

4.2: Synthesis of polyamines on TentaGel® resin.

4.2.1: Development of a borane-resistant TentaGel® resin.

In the early stages of our work, we began to examine the transfer of our polyamine synthesis from polystyrene to PS-PEG by attempting the exhaustive amide reductions and subsequent iodine-promoted work-up on commercially available resins pre-derivatized with the trityl linker. There are two methods used by commercial resin manufacturers to attach the trityl linker to the PEG spacer: via an amide bond or through a phenoxy ether linkage (Scheme 4.1).[95] With the amide-linked trityl, used in Rapp Polymere's TentaGel® resins, the same model triamide, LPhe-LAla-Ac (shown as **34** in the scheme), used in the polystyrene optimization experiments (see Chapter Two) was prepared and then subjected to the usual borane treatment and iodine-promoted work-up furnishing bound tetramine **73**. The result after cleavage from the resin was crude polyamine **31** in 65% yield and 62% purity by HPLC/UV which are both noticeably lower than the polystyrene example. An additional cause for concern was the formation of an undesired amine on the opposite side of the trityl group that would undoubtedly hamper any on-bead screening of a polyamine or an oligoboronic acid library. However, the outcome was no better with the phenoxy ether linkage, used on NovaSyn® TG resin (**74**), as in this case only a low yield of impure product was obtained.

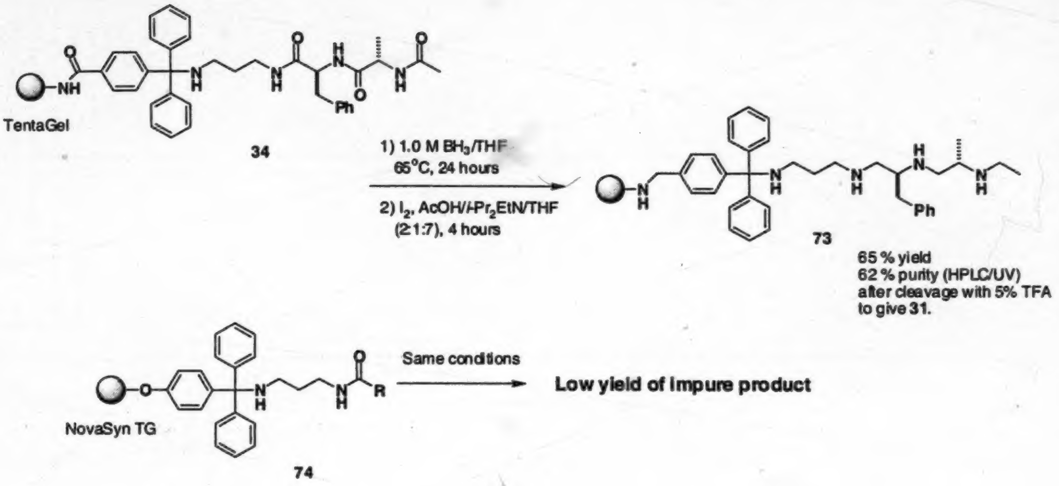
TentaGel
34
1) 1.0 M BH$_3$/THF
65°C, 24 hours
2) I$_2$, AcOH/i-Pr$_2$EtN/THF
(2:1:7), 4 hours
73
65 % yield
62 % purity (HPLC/UV)
after cleavage with 5% TFA
to give 31.
NovaSyn TG
Same conditions
Low yield of impure product
74

Scheme 4.1

Thus an alternative trityl-PS-PEG resin was required that did not include the amide or phenoxy functionalities and, consequently, would be more stable to the borane reduction and work-up. To this end, we looked at attaching the trityl linker to the PEG spacer through an inert methylene bridge. (The early development of this new linker was carried out by Dr. Fan Wang of our laboratory). The synthesis of this resin (Scheme 4.2) was performed beginning with brominated TentaGel® resin **75** using two bead sizes. Initially the standard sized resin (90-150 μm bead diameter) was employed, but in order to aid in the single bead LCMS decoding of the resin, larger (250 - 300 μm) beads ('TentaGel® MB') were also used. With the macrobeads the reaction times were longer than the standard sized resin due to the slower rates of reagent diffusion into the larger beads

Beginning from resin **75**, a copper catalysed Grignard reaction with **76** displaced the bromide giving the resin bound benzophenone **77** after acid-mediated cleavage of the acetal protective group. Through elemental analysis, the amount of unreacted bromide on resin **77** was found to ranged from 7 to 0.4% on both standard and macrobead resins. Formation of hydroxy trityl resin **78** was achieved by reacting **77** with freshly prepared phenylmagnesium bromide. A successful reaction in this case was indicated by the disappearance of the carbonyl stretch and the appearance of the hydroxyl band in the IR spectrum of the resin. Activation of **78** by treatment with thionyl chloride gave the trityl chloride resin which was subsequently coupled with a PEG-mimicking diamine spacer to give **79**. Among the standard beads, the yields of the diamine resin, starting from the brominated TentaGel®, and according to elemental analysis on the nitrogen, was up to 95%, while with the macrobeads, the yields ranged from 56 to 70%. The lower yield with the macrobeads may be attributed in part to the incomplete addition of the phenylmagnesium bromide to **77**, perhaps arising from an inability to constantly stir the resin due to its increasing fragility (*vide infra*). In fact, a tiny amount of carbonyl stretching was observed by IR microscopy after the reaction. Unfortunately, even longer reaction times could not improve the yields.

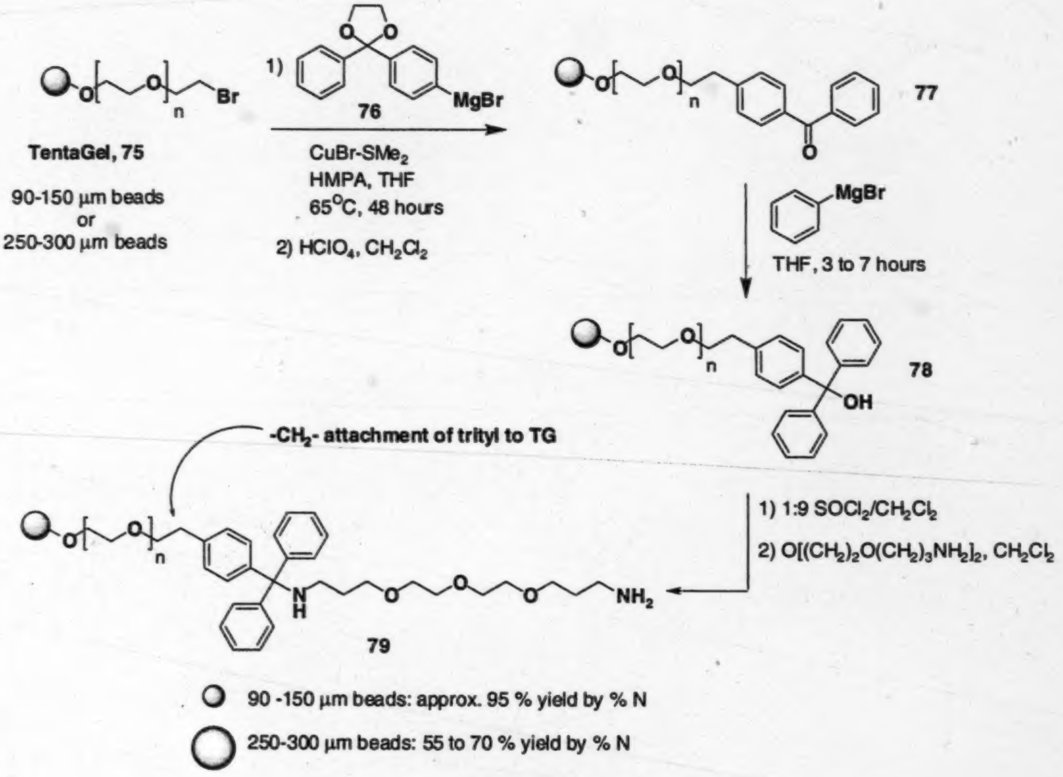
TentaGel, 75
90-150 μm beads
or
250-300 μm beads
1)
76
CuBr-SMe$_2$
HMPA, THF
65°C, 48 hours
2) HClO$_4$, CH$_2$Cl$_2$
77
THF, 3 to 7 hours
78
1) 1:9 SOCl$_2$/CH$_2$Cl$_2$
2) O[(CH$_2$)$_2$O(CH$_2$)$_3$NH$_2$]$_2$, CH$_2$Cl$_2$
-CH$_2$- attachment of trityl to TG
79
90 -150 μm beads: approx. 95 % yield by % N
250-300 μm beads: 55 to 70 % yield by % N

Scheme 4.2

It was found by the end of the synthesis the resin becomes noticeably softer and easily breakable, presumably as a result of some of the harsh reaction conditions it was subjected to. This fragility meant that the use of stir bars and magnetic agitators, often employed by automated synthesizers, were avoided to prevent further damage to the resin beads to the point of making it impossible to conduct an on-bead screening assay. Even the act of weighing out the resin could result in damage to the beads, so extreme care was required at all times when working with it.

4.2.2: Polyamine and oligoboronic acid synthesis.

As in the early stages of the polystyrene bound polyamine library, the synthesis of a few individual polyamines was attempted to see how well this new TentaGel®-trityl resin could endure some of the key reactions. The first polyamine attempted was analogous to the resin-supported pentamine **43** described in Chapter Two (Scheme 4.3). The reduction was of the tetramide **80**, which featured a twelve carbon spacer instead of six-carbon spacer used in the tetramide percursor for **43**, and a phenylalanine amino acid to substitute for the valine. (The synthesis and study of the polyamine described in this paragraph was performed by Dr. Fan Wang). Reduction of **70** under the same conditions employed in the polystyrene examples was followed by cleavage from the resin to provide pentamine **81**. Analysis of **81** by electrospray mass spectrometry gave the expected compound as the major component, along with a significant amount of the mysterious MH+24 signal. However, replacing the iodine-promoted work-up with piperidine gave no detectable MH+24 suggesting that it was somehow being caused by the buffered iodine reaction. A closer examination of the iodine-promoted work-up resulted in an alteration of the procedure using propionic acid instead of acetic acid in the buffer, with a slightly higher concentration of iodine (0.30 to 0.40 g/mL) and greater proportion of THF (THF:propionic acid:DIPEA equaled 15:2:1). Although these new conditions did not entirely remove the MH+24 signal, it was reduced to about 5 % of intensity of the desired peak in the mass spectrum.

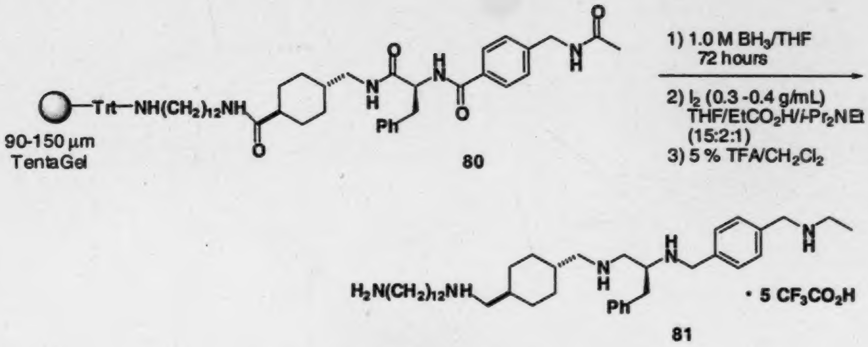

Scheme 4.3

A second model polyamine was prepared to evaluate the synthesis on the larger 250-300 μm beads and to determine whether there were any differences in reactivity between these and the standard sized beads (Scheme 4.4). Tetramine **84** was constructed from the TentaGel®-trityl resin with the PEG-like diamine spacer in order to stay closer to what would actually be used in the eventual library synthesis. The triamide precursor **82** was prepared from resin **79** (250 - 300 μm) using the standard FMOC coupling protocol with *N*-FMOC-norvaline and *N*-acetylaminomethylbenzoic acid as the amino acid derivatives, and HBTU/HOBt as the coupling reagents. The choice of amino acid building blocks was based on the reasonable degree of complexity that they would provide to the tetramine, testing both the presence of a side chain and an aromatic residue, while keeping its NMR spectra relatively simple for characterization purposes. Exposure of triamide **82** to 1.0 M BH_3 in THF for 24 hours at 65°C was sufficient to afford complete reduction of the amides. Subsequent borane-amine cleavage using the amended iodine protocol described for pentamine **81** led to the resin-supported tetramine **83**. The tetramine was then cleaved from the support to provide **84** as a tetrakis(trifluoroacetate) salt. LCMS analysis of **84** gave only 59% purity by MS, 65% by UV (210 nm) with a significant amount of MH+24 despite the new work-up conditions. The use of piperidine to cleave the borane-amine adducts led to a much higher purity (84% by MS, 90% by UV at 210 nm) with little detectable MH+24 present in the mass spectrum. The difference in purity was also noticed in the ^{1}H NMR spectra of **84** as the piperidine protocol gave a cleaner spectrum compared to the iodine method.

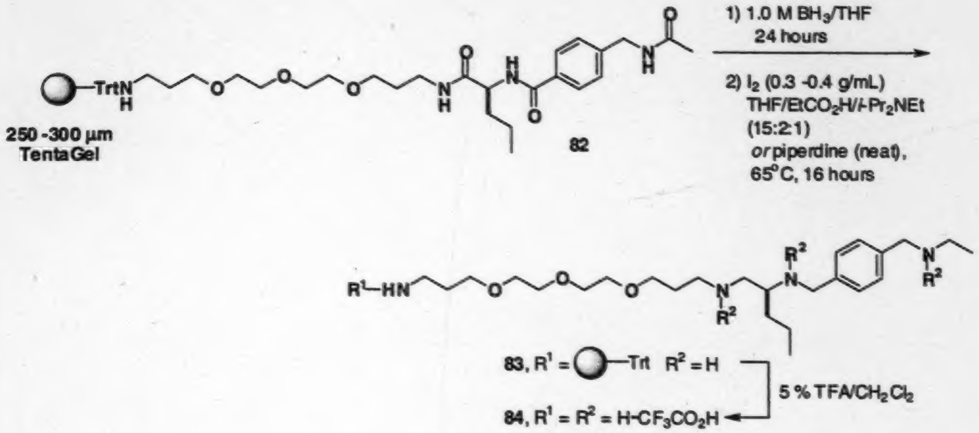
250-300 µm
TentaGel
TrtN
82
1) 1.0 M BH3/THF
24 hours
2) I2 (0.3-0.4 g/mL)
THF/EtCO2H/i-Pr2NEt
(15:2:1)
or piperdine (neat),
65°C, 16 hours
R1-HN
83, R1 = Trt R2 = H
84, R1 = R2 = H·CF3CO2H
5 % TFA/CH2Cl2

Scheme 4.4

Boronation was performed on the bound tetramine **83** obtained through the piperidine-based work-up to ensure higher purity of the final compound. The reaction was achieved by alkylation of the tetramine with benzyl bromide **40** over 48 hours, followed by hydrolysis to provide **85**, which was cleaved from the resin giving the triboronic acid **86** (Scheme 4.5). Purity by HPLC was determined to be 59% by MS, 75% by UV detection at 210 nm. (Note that oligoboronic acids become more difficult to ionize in the mass spectrometer as the number of boronic acid units increased, and as a result they produce weaker signals compared to impurities such as incompletely boronated products, which may ionize more readily. Thus, purity by MS will appear lower than actuality due to these differences in ionization). The only impurities detected in the MS were small amounts of under alkylated tetramines and an unidentified compound with a mass ten units less than the mass of **86** (*vide infra*).

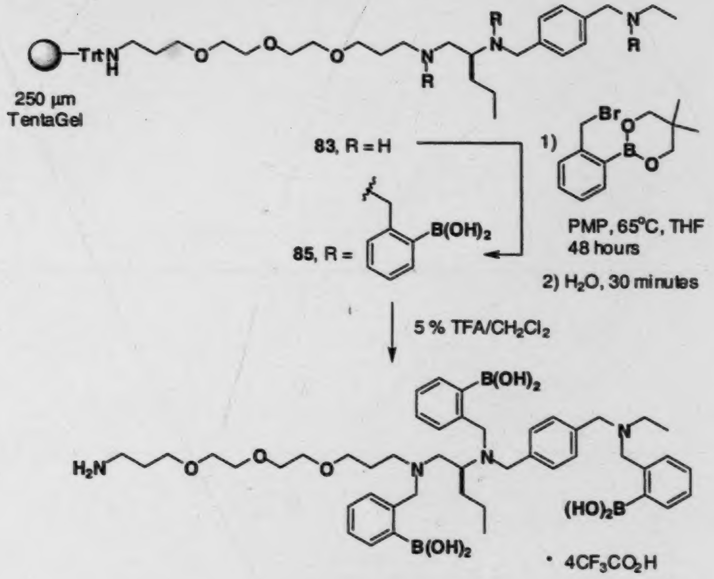
Trt
N
H
O
O
O
N
R
R
N
N
R
250 µm
TentaGel
83, R = H
1)
Br
O
B
O
85, R =
B(OH)₂
PMP, 65°C, THF
48 hours
2) H₂O, 30 minutes
5 % TFA/CH₂Cl₂
B(OH)₂
H₂N
O
O
O
N
N
N
(HO)₂B
B(OH)₂
· 4CF₃CO₂H

86

Scheme 4.5

4.3: Synthesis of new, unnatural amino acid building blocks.

The relatively large proportion of linear building blocks in the original polystyrene supported library unfortunately restricted its structural diversity, and therefore required attention before synthesizing a more advanced library on TentaGel®. However, most commercial amino acids are based on natural α-amino acids with elaborate side chains which would not satisfy our synthetic and structural requirements for the polyamine and oligoboronic acid libraries. The exception is 3-aminomethylbenzoic acid (3-Amb) which recently became available. However, what was also needed were building blocks that complement the many long and flexible ones already in use. To this end, we prepared two long and rigid biphenyl amino acids (1,4Amp and 3,3Amp, Figure 4.3), both as their FMOC derivatives for polyamide elongation, and in their *N*-acylated form required for the termination synthesis and decoding.

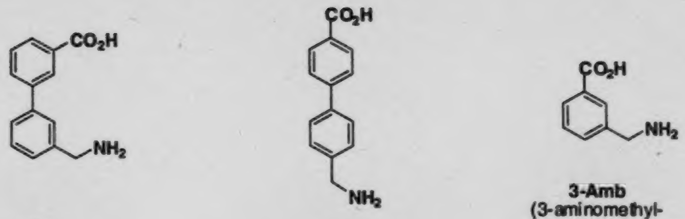

3,3Amp
(3-[3'-aminomethyl-phenyl]benzoic acid)

1,4Amp
(1-[4'-aminomethyl-phenyl]benzoic acid)

3-Amb
(3-aminomethyl-benzoic acid)

Figure 4.3: New building blocks.

The synthesis of the biphenyl amino acids was achieved through the Suzuki coupling of the two corresponding phenyl units: a bromo-acid, protected as a *t*-butyl ester, and amino-protected boronic acid. Although a carboxylphenyl boronic acid is less expensive than the amino-boronic acid, attaching the *t*-butyl ester protective group to this substrate proved too difficult. Therefore, in making the 3,3Amp derivatives, the bromo-ester **88** was prepared from acid **87** using carbonyl diimidazole (CDI) and *t*-butanol (Scheme 4.6).[130] The commercially available aminoboronic acid **89** was protected as a trifluoroacetamide **90** and then coupled cleanly with **88** using Suzuki conditions reported by Buchwald and co-workers[131] to afford the protected biphenyl amino acid **91**. Conversion to the FMOC derivative **94** involved liberation of the amine using potassium carbonate to give **93**, then attaching the FMOC group using FMOC-Cl, and finally removing the *t*-butyl with TFA. The synthesis of the *N*-butyryl derivative **95** was done in a similar fashion with the exception of reacting the free amine in **93** with butyric anhydride. (Isolation of the free amino acid from **93** by treatment with TFA was possible, but poor solubility made it difficult to work with).

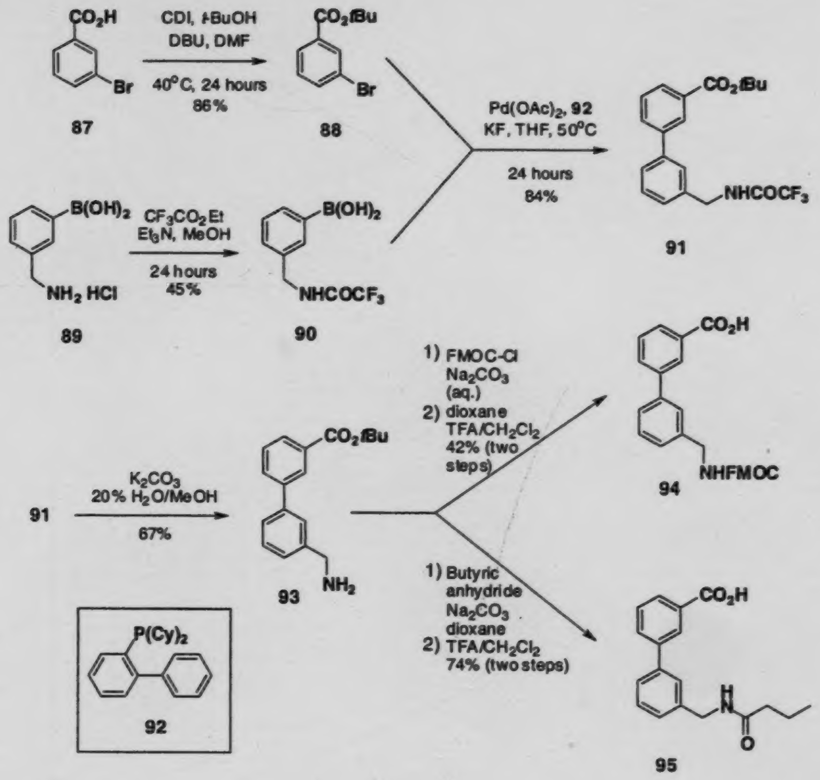

CO$_2$H
Br
87
CDI, t-BuOH
DBU, DMF
40°C, 24 hours
86%
CO$_2t$Bu
Br
88
Pd(OAc)$_2$, 92
KF, THF, 50°C
24 hours
84%
CO$_2t$Bu
NHCOCF$_3$
91
B(OH)$_2$
NH$_2$ HCl
89
CF$_3$CO$_2$Et
Et$_3$N, MeOH
24 hours
45%
B(OH)$_2$
NHCOCF$_3$
90
91
K$_2$CO$_3$
20% H$_2$O/MeOH
67%
CO$_2t$Bu
NH$_2$
93
1) FMOC-Cl
Na$_2$CO$_3$
(aq.)
2) dioxane
TFA/CH$_2$Cl$_2$
42% (two steps)
CO$_2$H
NHFMOC
94
1) Butyric anhydride
Na$_2$CO$_3$
dioxane
2) TFA/CH$_2$Cl$_2$
74% (two steps)
CO$_2$H
H
N
O
95
P(Cy)$_2$
92

Scheme 4.6

The synthesis of FMOC and *N*-acyl derivatives of 1,4Amp were achieved in a similar manner as the 3,3Amp derivatives except using the *para* isomers of the phenyl coupling units, **96** and **98**, as starting materials in the Suzuki coupling reaction (Scheme 4.7). The protected amino acid **100** was eventually obtained and converted into the FMOC protected amino acid **102** and the *N*-acetyl derivative **103**. In this case, the *N*-acetyl derivative was prepared in order to distinguish the 1,4Amp residue from its isomer, 3.3Amp, during the LCMS decoding of the partially terminated sequences.

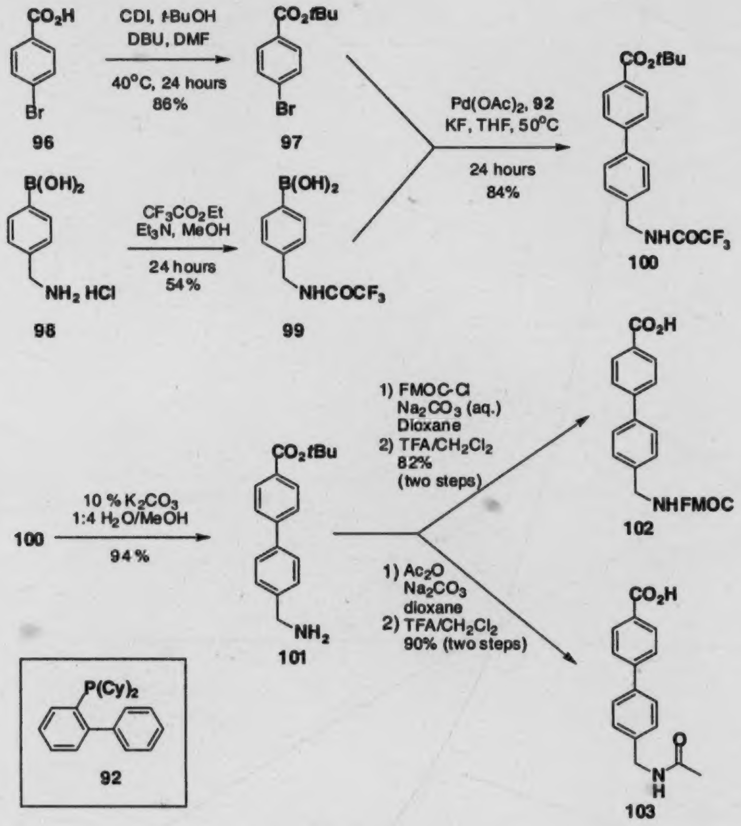
CO₂H
Br
96
CDI, t-BuOH
DBU, DMF
40°C, 24 hours
86%
CO₂tBu
Br
97
B(OH)₂
NH₂ HCl
98
CF₃CO₂Et
Et₃N, MeOH
24 hours
54%
B(OH)₂
NHCOCF₃
99
Pd(OAc)₂, 92
KF, THF, 50°C
24 hours
84%
CO₂tBu
NHCOCF₃
100
100
10 % K₂CO₃
1:4 H₂O/MeOH
94 %
CO₂tBu
NH₂
101
1) FMOC-Cl
Na₂CO₃ (aq.)
Dioxane
2) TFA/CH₂Cl₂
82%
(two steps)
CO₂H
NHFMOC
102
1) Ac₂O
Na₂CO₃
dioxane
2) TFA/CH₂Cl₂
90% (two steps)
CO₂H
O
N
H
103
P(Cy)₂
92

Scheme 4.7

Although the FMOC protected 3-aminomethylbenzoic acid (3-Amb) is commercially available (**104**), the free amino acid, which is often used to make the *N*-acyl derivative is not. Instead, a one pot procedure was employed whereby the FMOC protective group was removed from **104** by KF, and the resulting amine was acylated *in situ* by butyric anhydride to furnish **105** (Scheme 4.8).[132]

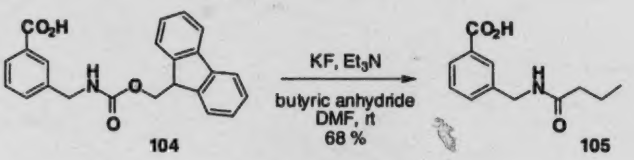
CO₂H
H
N
O
O
104
KF, Et₃N
butyric anhydride
DMF, rt
68 %
CO₂H
H
N
O
105

Scheme 4.8

4.4: Split-pool synthesis of polyamines and oligoboronic acids on TentaGel® resin.

4.4.1: Polyamine library synthesis.

With a new set of 17 building blocks in hand, we were ready to prepare a more advanced 289-membered tetramine library and a 4913-membered pentamine library on TentaGel® support. As with the polystyrene-supported library, a partial termination synthesis was employed in the initial building of the polyamides using a 9:1 mixture of FMOC protected amino acid and the corresponding *N*-acyl derivative (Scheme 4.9, shown for a pentamine library). The exhaustive amide reduction was done using either the iodine-based work-up method adapted for the TentaGel® resin or with piperidine.

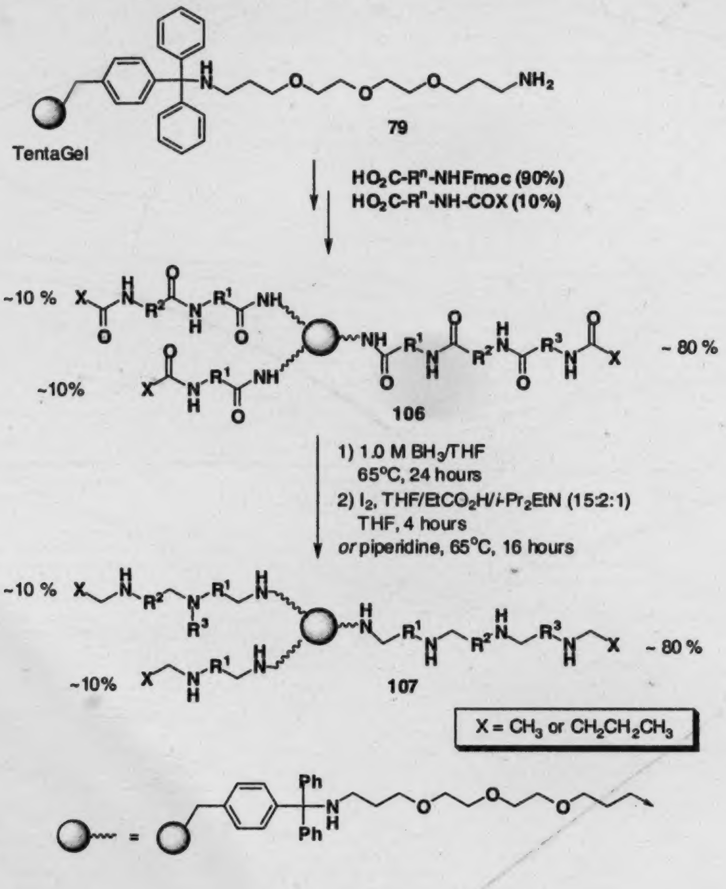
TentaGel
79
HO2C-Rn-NHFmoc (90%)
HO2C-Rn-NH-COX (10%)
~10 %
~10%
~ 80 %
106
1) 1.0 M BH3/THF
65°C, 24 hours
2) I2, THF/EtCO2H/i-Pr2EtN (15:2:1)
THF, 4 hours
or piperidine, 65°C, 16 hours
~10 %
~10%
~ 80 %
107
X = CH3 or CH2CH2CH3
Ph
Ph

Scheme 4.9

4.4.2: Polyamine library decoding on 90-150 μm beads.

A challenge in switching to TentaGel® supported libraries from polystyrene is the reduced loading of the standard sized, 90-150 μm beads and its consequence on the LCMS decoding. The polystyrene beads previously used began with loading values close to 1.0 mmol/g or approximately 240 to 330 picomoles of compound on a single bead. Such quantities are well within the detection limits of the ESMS detector on our LCMS instrument. On the other hand, the TentaGel® beads can have loadings between 0.1 and 0.3 mmol/g or about 24 to 100 picomoles of material per bead. Furthermore, the terminated sequences needed to decode the library are present in no more than one tenth of the full sequence, meaning that the ESMS detector needs to detect quantities as low as 2.4 picomoles. This value approaches the detection limit of the mass spectrometer and, therefore, greater efforts must be made to gain more sensitivity from the instrument. Fortunately, the LCMS decoding conditions used with the polystyrene library left a lot of room for reoptimization.

The initial attention was focused on the 0.1 % TFA used in the eluent to ensure that all polyamines elute as their ammonium salts. TFA is known to suppress ionization of the analyte within the mass spectrometer by forming strong ion pairs in the gas phase that are not detected by the mass analyzer.[133] With the polystyrene libraries, the large amounts of compound on a single bead were sufficient to compensate for the ionization suppression and, therefore, the TFA counterion was not a serious problem during decoding. However, with the TentaGel® pentamine library, very little signal was observed by LCMS from a single bead when using TFA in the eluent. To show that the resin does at least contains the library, a few milligrams (i.e. thousands of beads) were cleaved and its contents analysed by LCMS. The result was a series of intense mass signals arising from the terminated sequences and a larger number of weaker signals with higher masses produced by the full sequences. Following this confirmation, the first measure taken to improve instrument senstivity towards single beads was replacing TFA with 1 % formic acid. Lowering the flow rate of the HPLC also improves analyte ionization in the spectrometer's spray chamber and thus increases the signal strength.[134]

To allow a lower flow rate without compromising chromatographic resolution, an HPLC column with a narrower internal diameter was used (2.1 mm instead of 4.6 mm). Single beads were then analysed with these new conditions, and although some beads were decoded, the LC signals were still weak and the decoding efficiency was too poor to be useful. Furthermore, many of the LC signals were co-eluting very early in the chromatogram ($R_f < 1$ min.). Ideally, some chromatographic separation is desired as it further aids in the library decoding by allowing the comparison of retention times of terminated sequences. The use of 1 % acetic acid in the method gave little improvement where formic acid failed.

Derivatization of the supported pentamines **107** by reaction with phenylisocyanate was tried next hoping that the oligourea derivatives **108** would improve the signal intensity and chromatographic resolution (Scheme 4.10). Although the resolution was improved with 1 % formic acid in the eluent, the LCMS traces contained a heavy amount of noise especially when single beads were reacted individually with small volumes of phenylisocyanate solution.

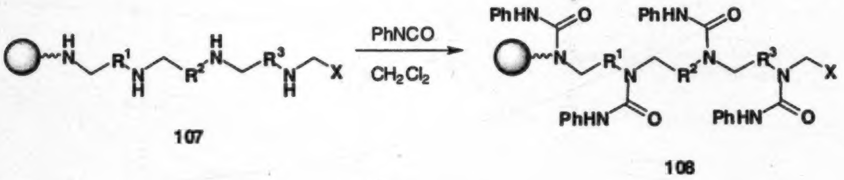

Scheme 4.10

Rather than eluting the polyamines as their salts, it was decided to examine them as free bases by using high pH conditions. (These conditions required using a chromatographic column resistant to high pH). When single beads were analyzed with 0.02 M ammonium hydroxide in the eluent, the intensity of the signals was much greater compared to the acidic conditions, however, the resolution was extremely poor, giving very broad peaks. Fortunately, polyacetylation of the secondary amines with acetic anhydride prior to cleavage from the bead greatly improved the resolution giving nice, sharp and intense peaks under high pH conditions. These beads were reliably decoded from single resin beads taken from both the tetramine and pentamine libraries. Polyacetylation of the entire resin-bound library prior to single bead isolation tended to give better decoding efficiencies (approximately 100%) and cleaner LC traces than when single beads are individually polyacetylated. An example of a tetracetylated library member is shown in Figure 4.4 for the pentamine sequence βAla^{Ac}-3,3Amp^{Ac}-1,4Amp^{Ac} (the superscripted Ac denotes an acetylated polyamine residue). The top of the figure represents the total ion current (TIC) chromatogram while the bottom is the overall electrospray mass spectrum of the acetylated polyamine eluting in the middle of the chromatogram. It was quite common to have the full sequences show a doubly charged ion in the mass spectrum ([M+2H]/2) along with some fragmentation signals. In this particular example, chromatographic resolution helped uncover the mass of the first terminated sequence which was buried underneath the doubly charged ion of the full sequence in the mass spectrum.

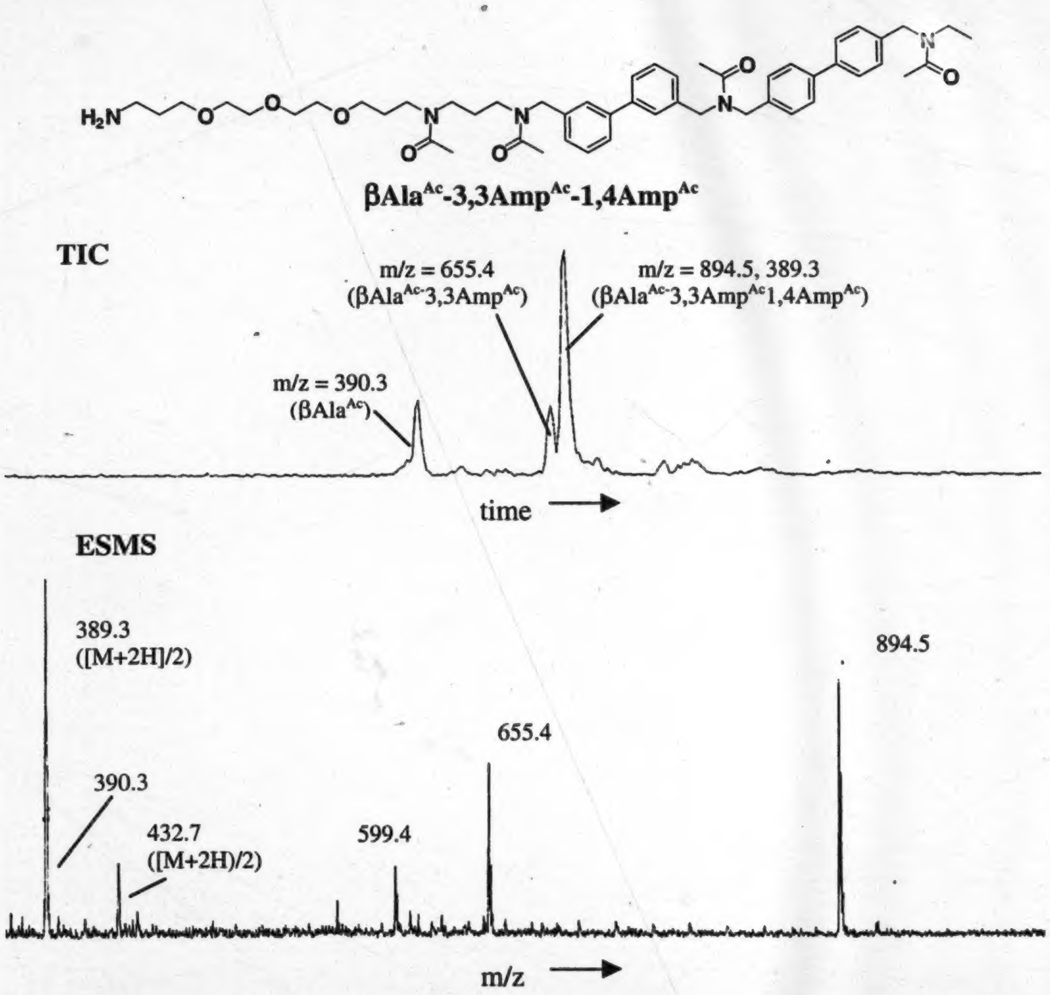

Figure 4.4: Sample decoding from a 90-150 μm TentaGel® resin bead expressing the sequence βAla^{Ac}-3,3Amp^{Ac}-1,4Amp^{Ac}. (LC signals elute between 5.9 and 8.0 minutes). Note: the mass signal of 432.7 and 599.4 are fragments of the full sequence.

4.4.3: Polyamine library decoding on 250-300 μm beads.

Although the 90-150 μm, standard sized beads were eventually decoded, it was rather inconvenient to polyacetylate the polyamines on individual beads. Furthermore, with an oligoboronic acid library, we would not be able to derivatize each compound the same way prior to every LCMS analysis. Therefore, we turned to larger 250-300 μm beads which have a much larger capacity, up to 2 nanomoles of material, compared to the standard sized beads which have only about 50 picomoles. This increased capacity, of course, will ease the decoding of polyamine and oligoboronic acid libraries without the need for derivatization.

With these beads only a tetramine library was synthesized. The amide reductions were carried out using both the iodine method and the piperidine method as work-ups. The decoding was performed on underivatized beads using the same LCMS conditions that were employed with the polystyrene library; that is, 0.1 % TFA in the eluent of acetonitrile and water. In general, it was found that tetramine beads produced via the piperidine work-up gave higher quality LCMS traces. Although the iodine method did provide some good quality traces, there were many that contained unidentifiable signals including some with the previously mentioned MH+28 and/or MH+24 signals. In addition, the iodine tended to stain the beads very slightly after the work-up resulting in an intense background fluorescence when viewed under an epi-fluorescent microscope. This strong background can be problematic when screening the library against fluorescently tagged targets. The decoding efficiency for tetramines from both the iodine and piperidine methods was about 80 % for both. Occasionally, beads would be encountered that gave absolutely no signal. In these cases there may have been nothing on the bead to begin with, or a problem may have occurred in the sample handling or injection (example: insolubility in methanol, incomplete cleavage from the bead, etc). In many LC traces some PEG polymer (MH+44*n*) eluted after the tetramine sequences presumably from the breakdown of the resin matrix.

4.4.4: Triboronic acid library synthesis and decoding.

With the ability to decode underivatized polyamine libraries, we were now able to produce split-pool oligoboronic acid libraries on TentaGel® resin beads. The boronation was done in the usual manner with benzyl bromide **40** to give library **110** from the tetramines **109** (Scheme 4.11). When the reaction was done on tetramines generated via the iodine promoted work-up, the single bead LCMS analyses showed a larger number of impure oligoboronic acid sequences containing unidentifiable signals, with and without boron atoms. On the other hand, when using the tetramine libraries from the piperidine work-up, the LCMS traces were much cleaner and, thus, easier to decode. It was found that the boronation reaction needed at least two days to ensure complete alkylation of all sequences in the library. The dehydration observed in the mass spectrometer almost always followed the pattern of one and two water molecules lost from the diboronic acid terminating sequence, and three molecules lost from the full triboronic acid. Only with the residue 1,4Amp^B was no dehydration observed, presumably due to its extreme rigidity which prevents the boronic acids from reaching each other and forming boronic anhydrides.

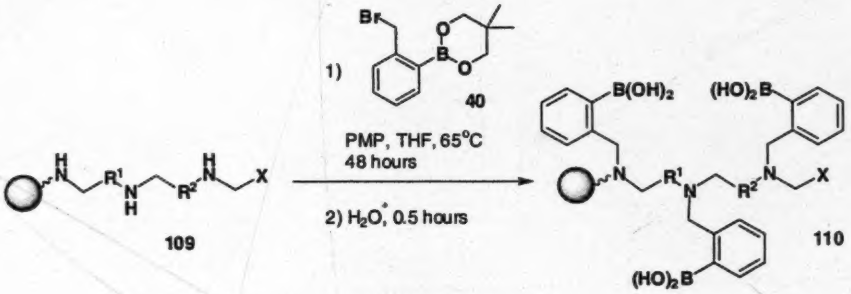

Scheme 4.11

An example of an LCMS decoding of a triboronic acid is depicted in Figure 4.5 for the sequence 8Aoc^B-12Ado^B. In some LCMS analyses of other triboronic acids a small amount of underboronation was observed, but 8Aoc^B-12Ado^B seems fully boronated. There is an LC signal that corresponds to masses of 850.7 and 840.6, but the identity of this signal is not known and seems to be unique to this sequence. In general, the purity of most triboronic acids resemble that shown in the LC trace in Figure 4.4. There are a few, of course, that are higher quality and others that are somewhat poorer compared to 8Aoc^B-12Ado^B, and then there are some beads that provide no LC signal at all. As with the tetramine library approximately 80% of the beads were unambiguously decoded.

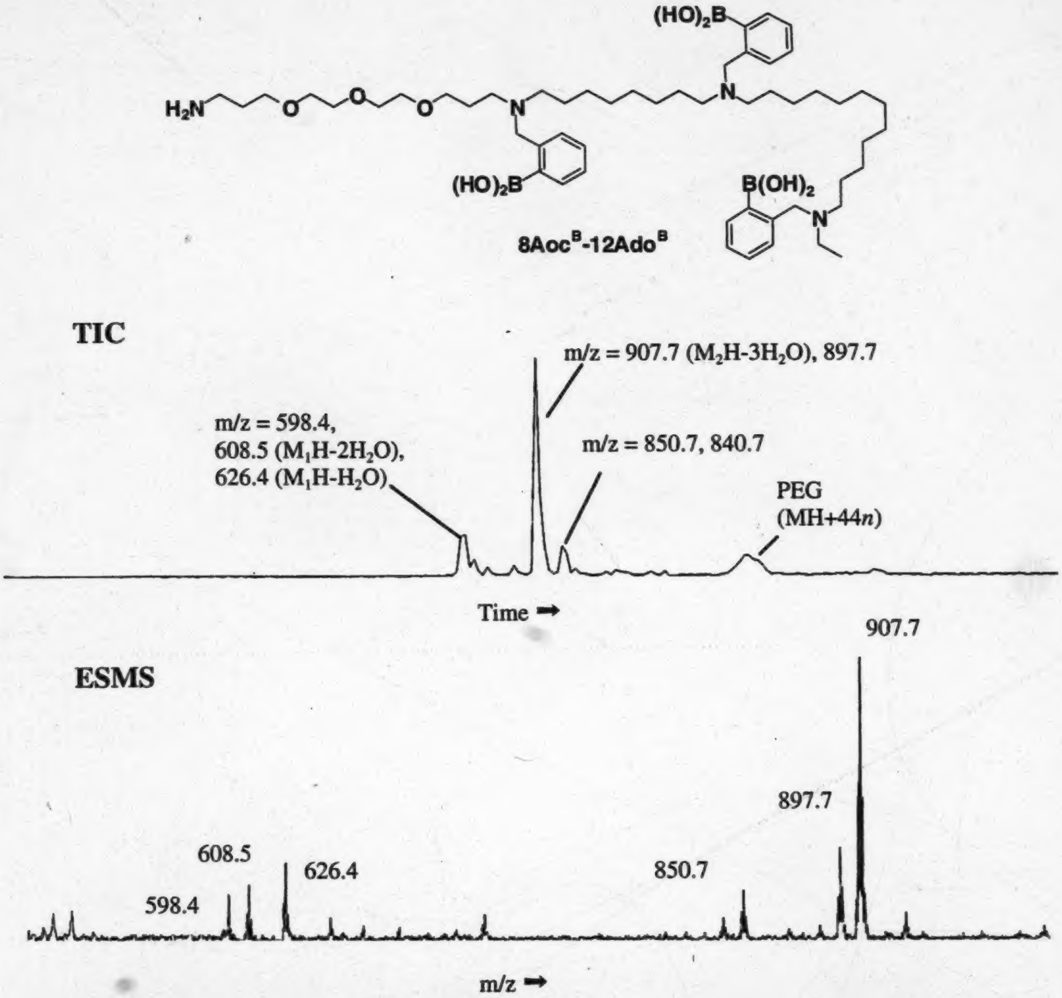

Figure 4.5: Single bead decoding of 8Aoc^B-12Ado^B from a 250 - 300 µm TentaGel® bead. (M$_1$H denotes the diboronic acid terminating sequence of 8Aoc^B, M$_2$H the full triboronic acid 8Aoc^B-12Ado^B ; LC peaks elute between 6.5 and 7.4 minutes).

Figure 4.5 reveals an example of reoccurring and very peculiar signals observed in many LCMS analyses of triboronic acids. These signals have a mass of 10 units less than the mass of both the full sequence and the diboronic acid terminating sequence. In many cases, as with 8Aoc^R-12Ado^R, this mysterious compound, MH-10, co-elutes in the LC trace with MH suggesting that it forms in the mass spectrometer from a complex fragmentation process of MH. In other cases, MH-10 elutes slightly behind MH indicating that the compound is formed before it reaches the spectrometer, perhaps even during the boronation reaction, and elutes through the column independently. Occasionally a signal that corresponds to MH-28 is detected co-eluting with MH-10, suggesting that the compound is actually the result of MH losing a 28 mass unit fragment (e.g., C_2H_4, B-OH) which then gains a water molecule. Unfortunately detailed studies have not been conducted into the electrospray mass spectrometry of boronic acids, and so the events that lead to the MH-10 and MH-28 compounds are not completely understood. Nonetheless, these signals are always minor relative to the desired triboronic acids.

Continued analysis of random beads from the triboronic acid library revealed a disturbing problem with linear sequences ending with the residue γAbu^B. As shown in Figure 4.6 for the sequence 8Aoc^B-γAbu^B, rather than finding the expected LCMS trace we obtained one that shows the decomposition of the full sequence into smaller fragments. The expected signals appear at 608 and 626 for the terminated diboronic acid, 8Aoc^B ($M_1H - 2H_2O$ and $M_1H - H_2O$ respectively) and 795 for the full triboronic acid ($M_2H - 3H_2O$). What is also observed, in greater intensity, were two signals 14 mass units less than the M_1H peaks (594 and 612 or $M_1H - nH_2O - 14$) and a signal which seems be the overalkylated product of these signals at 710.

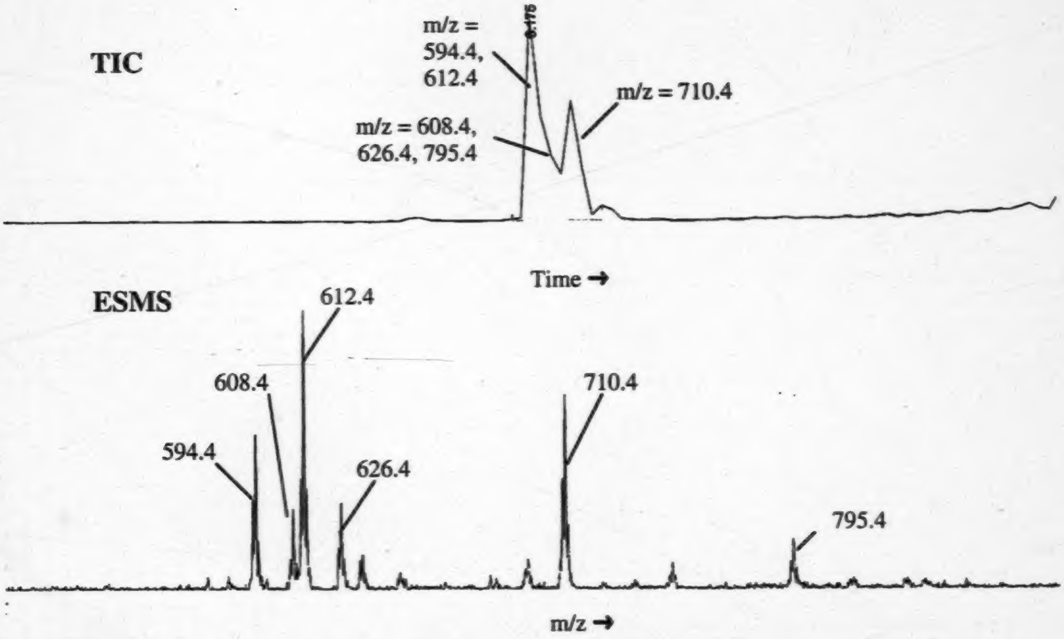

Figure 4.6: LCMS of fragmented 8Aoc^B-γAbu^B (LC peaks elute between 6.1 and 6.5 minutes; see text for further details).

A similar series of decomposition signals were observed in a tribenzylated library **111** that was obtained via benzylation of **109** (Scheme 4.12).

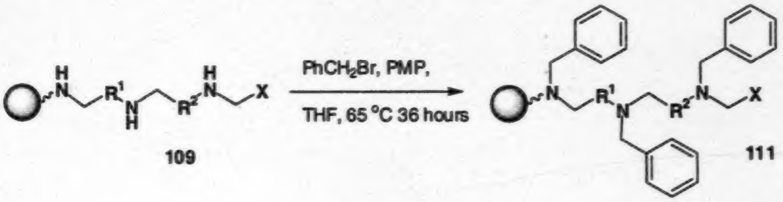

Scheme 4.12

Again, the culprit seems to be the γAbu residue at the end of straight chain sequences. For instance, in the sequence 8Aoc^{Bn}-γAbu^{Bn} (the superscripted Bn denotes a benzylated polyamine residue), the expected the masses were 556 for the terminated dibenzylated triamine, 8Aoc^{Bn} (M_1H) and then the fully benzylated tetramine at 717 (M_2H). These signals were indeed obtained but in small amounts. Instead, the major signals were from a mass at 646, which corresponds to the overbenzylation of M_1H (M_1H + Bn), and at 632 which is more puzzling since it 14 mass units less than M_1H + Bn.

Since the fragments elute independently they are likely generated outside of the mass spectrometer, perhaps during the alkylation step. It seems reasonable to propose that the nitrogen on the γAbu$^{B/Bn}$ residues in **112** and **115** (Scheme 4.13) acts as a nucleophile and attacks that carbon adjacent to the nitrogen on the 8Aoc$^{B/Bn}$ forming a pyrrolidine fragment **113** from the γAbu$^{B/Bn}$. In the case of boronic acid **112**, the 8Aoc nitrogen is more prone to displacement due to coordination with the boron. The resulting fragment **114** can subsequently become alkylated by the benzyl bromide **40** or stay as a secondary amine possibly coordinated to the boron. In either case, the fragments require the loss of an additional 14 mass units to give the observed masses in the mass spectrum, yet the identity of these 14 units presently unknown. It maybe from a methylene group or perhaps the boronic acids condense with methanol, but a more thorough investigation is needed to determine the exact identity of the products. With the benzylated amine **115**, it is possible that the γAbu nitrogen is quarternized by overalkylation by the benzylbromide enhancing its potential as a leaving group. Indeed, overalkylation of the M_1H and M_2H is observed in the mass spectrum, indicating that quarternization is common. The resulting **116** after cleavage of **113** again must loose 14 mass units to give the mass at 632.

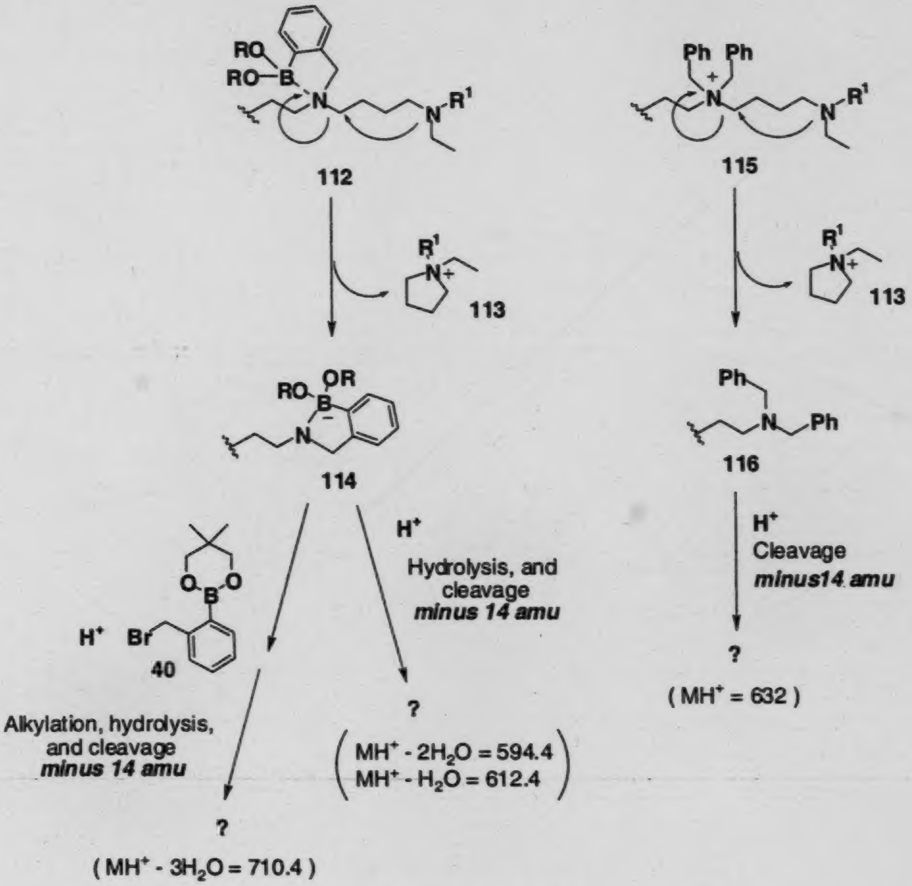
112
113
114
H⁺
Hydrolysis, and cleavage
minus 14 amu
?
MH⁺ - 2H₂O = 594.4
MH⁺ - H₂O = 612.4
H⁺
40
Alkylation, hydrolysis, and cleavage
minus 14 amu
?
(MH⁺ - 3H₂O = 710.4)
115
113
116
H⁺
Cleavage
minus14 amu
?
(MH⁺ = 632)

Scheme 4.13

4.5: Conclusions.

The synthesis of split-pool libraries of polyamines and oligoboronic acid was achieved on hydrophilic TentaGel® resin allowing for their on-bead screening against water soluble biological molecules. These libraries were made possible by an alternative TentaGel®-trityl linkage that employs a methylene bridge between the trityl linker and the PEG spacer. This resin has shown to be capable of withstanding the conditions of the exhaustive amide reduction and the subsequent work-up. In general, it was found that the piperidine work-up of the borane-amine adducts afforded polyamines of higher purity than the iodine protocol as discovered by the synthesis and analysis of individual compounds. For this reason, piperidine has become the preferred method for the work-up of the TentaGel® supported libraries.

The decoding by LCMS of the partially terminated libraries was considerably more challenging than the previously synthesized polystyrene supported libraries due to the lower loading levels on TentaGel® supports. For this reason the libraries were prepared on both standard, 90-150 μm beads and the larger, 250-300 μm beads which express more compound per bead than the standard sized ones. The polyamines on the standard beads were eventually decoded after polyacetylating the polyamines and then eluting them through the HPLC column using basic rather that acidic eluent conditions. However, polyamines and oligoboronic libraries on the macrobeads were decoded without any derivatization.

The analysis of some of the oligoboronic acid library members revealed some peculiar by-products that may be forming in the boronation reaction with **32**. A small, yet ubiquitous signal that is ten mass units less than the signal of the desired oligoboronic acid sequences was commonly observed in the random decoding of library beads. In addition, an apparent decomposition reaction was observed involving linear oligoboronic acids containing a γAbu^{B} residue at the end of the sequence. It appears that this undesired side reaction arises from the cyclization of the γAbu^{B} residue upon itself resulting in the cleavage of the entire sequence. Thus, in future library syntheses, the γAbu building block will need to be avoided. Despite these small impurities and side reactions, a large proportion of the beads are adequately functionalized and their sequences decodeable, thus it was decided to go ahead and attempt to screen the library against oligosaccharides.

Chapter Five:

Screening of TentaGel® supported polyamine and oligoboronic acid libraries.

5.1: Targets for polyamine libraries.

Up until now, the only on-bead library screening assays performed were between a polystyrene-supported tetramine library against a series of trisulfonated, diazo dyes and a short peptide labeled with a coloured dye (Chapter Three). These targets were well suited for the early libraries since they were organic soluble, allowing them to be used in solvents that swell polystyrene resin, and they were naturally coloured which made visualizing them on the resin beads very easy. In the aftermath of these experiments, the next obvious challenge was to screen biologically relevant targets, and for this purpose the TentaGel® supported libraries, described in Chapter Four, were prepared for screening under aqueous conditions. Targets that are suitable for TentaGel® supported polyamines are ones that are polyanionic in nature, with well defined structures that allows the formation of selective ion pairing interactions. Potential targets include RNA and DNA,[56, 64-67] which can bind to the polyamines through their phosphate backbones, and possibly through hydrogen bonding to the base pairs within the oligonucleotide. In addition, proteins with a high number of anionic residues may bind with high affinity to various members of a polyamine library. One class of such proteins includes membrane ion channels which are already known to bind natural polyamines like spermidine and some acylpolyamine neurotoxins.[52, 71]

Oligosaccharides that possess a high degree of negative-charge can also make targets for a polyamine library. One particular example is heparin, a sulfated glycosaminoglycan well known for its anticoagulant activity.[135, 136] The structure of the polysaccharide is based on a carbohydrate backbone consisting of alternating 1,4-linked uronic acids (10 % D-glucuronic and 90 % L-iduronic) and glucosamine residues that combine together to give a polysaccharide chain with a high degree of structural variability (Figure 5.1). The molecular weight ranges between 5 and 40 kDa, with an average of approximately 15 kDa. Heparin's average negative charge is approximately –75, giving it the highest negative charge density of any known biological macromolecule.

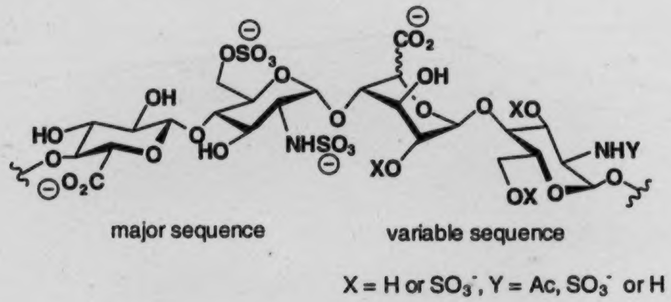

Figure 5.1: Repeating units in heparin.

Heparin inhibits blood coagulation by binding to and activating antithrombin III (AT III), a serine protease inhibitor that regulates the coagulation process. Once activated, AT III forms tight complexes with several blood coagulation factors resulting in their inhibition.[135, 136]

Although heparin, oligonucleotides and proteins are interesting targets, the biggest challenge in screening them against a split-pool library of ligands is detecting their binding to an active resin bead. Perhaps the most direct way of visualizing the binding event is to have the target labeled with a coloured or fluorescent reporter molecule. This method works well with simple, short sequences of biomolecules, as was demonstrated with the hemogloblin peptide in Chapter Three. Unfortunately, the synthesis and purification of even these molecules can be complicated. For instance, a labeled heparin unit would need to be prepared via a laborious multi-step synthesis starting from its monosaccharide building blocks and then sulfated at the very end with the label already installed to avoid isolation and reactivity problems with the sulfates. For other molecules, particularly RNA, the amounts obtained maybe too low to be useful for the multiple trails required for an on-bead screening assay. Conjugating full sized proteins is another possibility, but controlling the reaction site on the protein is difficult in most cases.

What would be more desirable is a screening assay for resin-bound libraries that does not require any manipulation of the target itself. This, in principle, would allow the screening of a larger number of biomolecules that otherwise would be very difficult to conjugate with a label. To this end, we examined screening our TentaGel® polyamine libraries against smaller biomolecules that have not been conjugated with a reporter compound. Of interest to us were D-glucosamine-2,3,6-trisulfate (GATS), a known component of the AT III binding unit of heparin,[136, 137] and inositol-1,4,5-triphosphate (IP_3), a so-called second messenger involved in cellular signal transduction.[138] One can envision that active polyamines towards these targets can potentially make good inhibitors for biological applications.

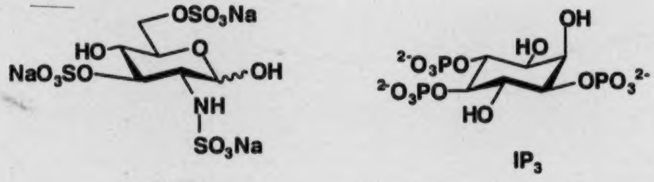

GATS

IP_3

Figure 5.2: Small polyanionic targets for TentaGel® bound polyamines.

5.2: Competitive assays for on-bead polyamine screening.

Our earlier studies on screening trisulfonated dyes against the polystyrene-supported tetramine libraries, described in Chapter Three, led us to the idea of introducing an additional polyanionic species to the screening mixture that can displace the dye from the resin beads. In a screening application, an anionic dye would have to bind nonselectively to all resin-bound polyamines, and then a target would selectively displace the dye from certain beads carrying active library members for that particular target. In other words, the active beads are now clear while the inactive ones remain coloured. Analogous competitive assays are used in solution studies,[139] but to our knowledge there are no reports of its application in on-bead assays. (Note: a recent report by Anslyn and co-workers described the rational design of a dual cationic-boronic acid based heparin receptor which employed the use of a competitive dye in monitoring the binding.)[140]

A nonselective dye would preferably possess only one anionic functional group so that the binding to the polyamine library is nonselective, and would need to be used in excess, relative to the polyamines, in order to ensure an even colour distribution of all beads. Some dye candidates that were eventually examined are depicted below (Figure 5.3).

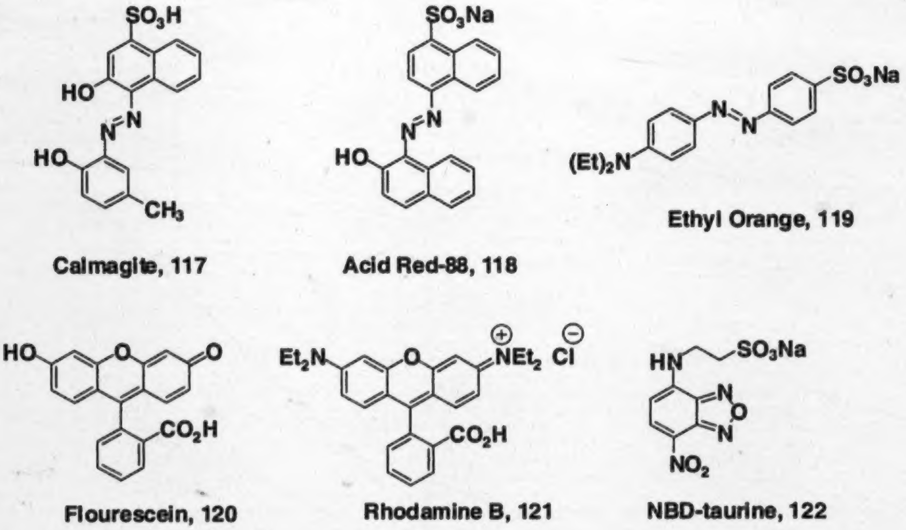

Calmagite, 117

Acid Red-88, 118

Ethyl Orange, 119

Flourescein, 120

Rhodamine B, 121

NBD-taurine, 122

Figure 5.3: Dyes used in displacement assays.

Upon suspending underivatized TentaGel® resin in an aqueous solution of dyes **117** to **121** (or almost any other commercially available dye for that matter) it was quickly discovered that the dyes bound very tightly and indiscriminately to the PS-PEG resin matrix.[141] To prevent this nonspecific background binding, a mixed organic-aqueous solvent system was required, usually a 1:1 mixture of water and DMF or a 2:1 mixture of water and isopropanol. The only exception are fluorescent dyes containing the nitrobenzodioazole (NBD) heterocycle such as NBD-taurine **122**, which in most cases, can be used in complete aqueous conditions.[142]

Between the azo dyes, ethyl orange (**119**) seemed to be more practical than the others since it was easiest to observe under a microscope when staining a resin bead (with the other dyes the beads appeared transparent when observed under the light of the microscope), and it was also less prone to binding to the resin matrix. With ethyl orange, the tetramine library was suspended in 1:1 water and DMF at pH 5.5 (MES) containing 10^{-4} M of the dye followed by the addition of 10^{-2} M of GATS. Although the resin was somewhat lighter in colour compared to the control (that is, without the GATS), no clear colour differences were observed among the beads, which meant that differences in selectivity could not be detected. Upon the addition of a large excess of GATS all the beads became clear. Therefore, the challenge seemed to be balancing the complete staining of the resin using a minimum amount of dye and then adding enough of the target to selectively displace it without saturating the beads and causing all of the dye to be displaced.

The use of fluorescent dyes (**120** to **122**) was then attempted, hoping that their bright fluorescence observed under an epi-fluorescent microscope would help to visualize the subtle colour differences in the beads indicative of some selective binding. Of the group of fluorescent dyes, fluorescein (**120**) and NBD-taurine (**122**) were the easiest to observe over the background fluorescence of the resin beads. Employing the proper fluorescent excitation and emission filters in the microscope (see section 7.17 in Chapter Seven), the beads fluoresced a light blue colour when swollen alone in water. Bound to **120** or **122** they appear fluorescent green. With rhodamine B (**121**), the dye failed to bind to the polyamine libraries as it was easily washed off with repeated rinsed with isopropanol. It also required a different fluorescence filter which did not provide any dramatic colour difference between the unbound and bound resin beads. However, a problem was encountered when attempting to screen GATS and IP_3 against TentaGel® supported tetramines that can potentially jeopardize the use of dyes **120** and **122** in a competitive assay. It was found that with prolonged excitation of the stained beads, their fluorescence intensity decreased, that is becaome bleached, going from green to blue. This fluorescence bleaching of inactive beads is problematic since it will lead to a high number of false positives.

Thus, with these exploratory studies, it appears that further development is required for a competitive assay for on-bead screening. What is still needed is a dye that evenly stains the resin, giving it a colour that is very easily distinguishable from the background colour of the bead, and then is easily displaced by small concentrations of the target. Also, limitations of our polyamine libraries themselves may make it difficult to observe selective dye displacement especially when the libraries are relatively small. A larger library (10^4 to 10^6 members) should increase the probability of having a highly potent member that can be clearly observed among the other members. Unfortunately, split-pool library as small as ours, may not include such a member.

5.3: Indirect screening methods for oligosaccharide binding.

Although the development of a competitive assay for our polyamine libraries has failed thus far, the possibility of using one for the oligoboronic acids was examined. The inspiration for this idea was prompted by recent reports of the use Alizarin Red S (ARS) as a competitive indicator in the solution-phase assays of boronic acid-based glucose and fructose chemosensors.[16, 48, 139] In an aqueous solution ARS appears purple and non-fluorescent, but in the presence of a boronic acid forms an orange-coloured, fluorescent boronate complex **123** (Scheme 5.1). Complex **123** reverts back to free ARS by the addition of a saccharide which competes with ARS for the boronic acid. The outcome is a change in colour and fluorescence as the boronic acid binds to the saccharide.

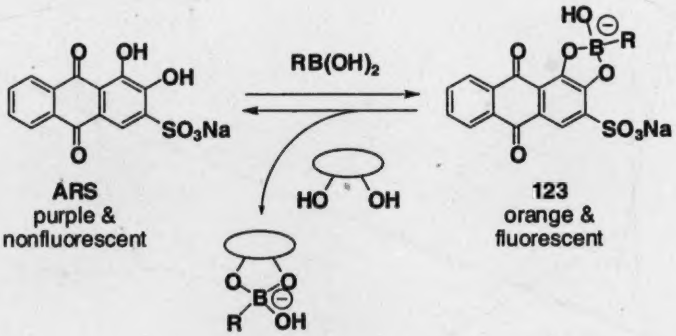

Scheme 5.1

When the ARS dye was mixed with the resin-supported oligoboronic acid library in 2:1 water/isopropanol, it was observed that the beads immediately became orange but changed colour only marginally even after adding very large concentrations (approximately 1 M) of fructose. Therefore, due to the inability to affect a dramatic colour and fluorescence change with more dilute concentrations of saccharide, it was decided that, for the time being, this type of competitive assay is best left to applications in solution-phase assays.

Another idea was to employ a well-established qualitative test for reducing sugars called the Benedict's test. This test involves the reduction of $CuSO_4$ by the sugar under basic conditions to form Cu_2O which appears as a rusty-coloured precipitate. The disadvantage of this technique is that biological oligosaccharides exist as glycosides in Nature, and so lack the reducing end that is required to react with the Benedict's solution. Yet there may still be some applications with the GATS heparin unit in the screening against the polyamines. While in solution the Benedict's test does provide the rusty precipitate with GATS indicative of a positive test, but when the monosaccharide was bound to the polyamine beads, the precipitate was difficult to observe. This difficulty maybe due to its rather light colour, but more likely because the amount of GATS bound to the bead was too small for accurate detection by this method.

The use of a boronic acid-containing dye was also examined. One such dye is the commercially available dansyl derivative **124**. It was hoped that the boronic acid would form a boronate ester with the free diols on the saccharide-receptor complex on the bead. However, dye **124** was notorious at binding to the PS-PEG matrix and could not be washed off with any organic solvent.

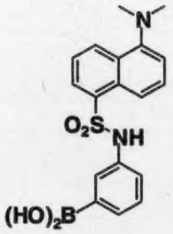

124

5.4: Screening of fluorescein labeled Lewis-b tetrasaccharide.

It became clear that developing an indirect assay for oligosaccharide binding to resin beads was not leading to any desired results. Thus, the only option remaining was to employ labeled targets. While fluorescently labeled oligosaccharides are commercially available, in many cases only a small percent of the sample is labeled (1 to 5 %) making it difficult to observe against the background fluorescence of the beads. Furthermore, many labeled biological macromolecules are sold in very small quantities and are extremely expensive. For these reasons, these commercial products were avoided. Fortunately, fluorescently labeled oligosaccharides had been previously synthesized in our department and some were kindly provided to us by Professor Ole Hindsgaul. To begin, we chose the labeled derivatives of Lewis-b (Le^b) tetrasaccharide, **125** and **126**, as ideal targets for the triboronic acid library.

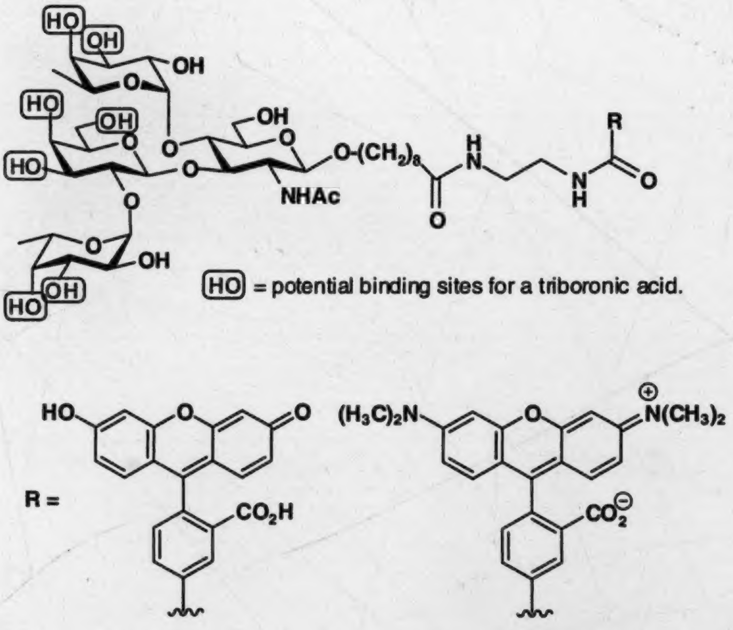

HO = potential binding sites for a triboronic acid.

Fluorescein, **125**

Tetramethylrhodamine (TMR), **126**

Figure 5.4: Labeled Le^b used for the screening of the triboronic acid library.

One disadvantage of this tetrasaccharide is that there are no saccharide units that can isomerize between pyranose and furanose forms, and according to the studies by Eggert and Norrild with monosaccharides, the furanose form is required in order to form a tight complex with a boronic acid-based receptor.[17, 19] However, it was hoped that the lack of isomerizing units can be overcome by an enhanced cooperative binding effect involving all three boronic acids on the receptor and the *cis* diols on the two fucose units and the 3,4,6-triol on the galactose, resulting in the formation of three boronate esters (see Figure 5.4). Cooperative effects have been observed with boronic acid-based receptors in the past,[22, 27] but only in allosteric systems and dentrimeric models developed in the laboratories of Shinkai. However, simpler receptors containing more than two boronic acids that also use a cooperative mechanism have yet to be reported. Therefore, it remains unclear at this stage whether binding can be enhanced with three boronic acids against a saccharide that cannot isomerize.

Among **125** and **126**, the fluorescein-labeled tetrasaccharide was chosen due to the relative ease in which it can be seen with the epi-fluorescent microscope against the background of the resin beads (*vide supra*). The TMR label on **126**, on the other hand, was more difficult to observe over the background. Fluorescence bleaching by the microscope was reduced by limiting the excitation time of the beads. With both labels, it was found that complete aqueous conditions can be used, without organic additives, as no nonselective binding resulted when the labeled tetrasaccharides were exposed to underivatized TentaGel® beads.

For screening against the TentaGel® bound triboronic acid library (obtained via a triamine library that was prepared using the piperidine-based work-up), approximately 20 to 45 mg of the resin was suspended in a 10^{-5} M solution of **125** in 0.01 M phosphate buffer at pH 7.4, and then shaken for 16 hours. Interestingly, when the suspension was observed with the microscope, approximately 6 to 12% of the beads appeared fluorescent green indicating the binding of the tetrasaccharide to a group of active resin-bound triboronic acids. The solution after the screening, however, remained fluorescent indicating that not all of the target was taken up by the library. When the green beads were isolated (quickly before they became quenched) and decoded by LCMS it was found that many of the sequences contained combinations of βAla^B, εAhx^B, and 8Aoc^B

residues, along with a smaller number of Nva^{B}. In addition, a significant number of sequences which had a linear residue followed by γAbu^{B} unit were discovered. Unfortunately, these were the very sequences that were fragmenting into pieces during the alkylation of the tetramines towards the preparation of the triboronic acid library (see Chapter Four for a discussion of this side reaction). It almost seemed as though the products of the fragmentation reaction were selective for the tetrasaccharide!

In order to investigate the validity of these 'hits,' the fluorescein labeled Le^{b} was screened against the tribenzylated (**121**) and triacetylated (**127**) tetramine libraries under the same conditions used with the triboronic acids (Figure 5.5).

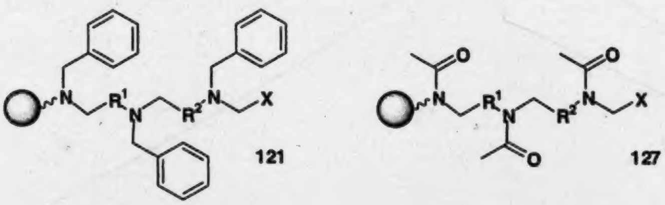

Figure 5.5: "Controls" tested against Le^{b}-NBD (**125**).

Against the triacetylated library, about 5% of the beads appeared green, albeit less intense than with the triboronic acids. Decoding of these beads gave a more or less random mixture of sequences with no consensus, but interestingly many of them had a small amount of under acetylation and thus contained some free amine sites. With the tribenzylated library, between 5 to 10% of the beads were very intensely fluorescent, and when decoded, revealed themselves to support almost exclusively the fragmented sequences ending with the γAbu^{Bn} residue. Since neither the triacetylated nor tribenzylated libraries were ever expected to bind to the tetrasaccharide, one began to expect the fluorescein label itself was acting as a binding target for the libraries. With this possibility, another test was performed, this time against fluorescein alone. In order to stay as close as possible to the labeled target **125**, the fluorescein analogue **129** was prepared without the Le^{b}, but containing the alkyl chain to mimic the spacer between the dye and the tetrasaccharide. Its preparation involved the coupling of *n*-hexylamine to isomers of fluorescein-hexanoic acid **128** via its *N*-hydroxysuccinimidyl ester (Scheme 5.2).

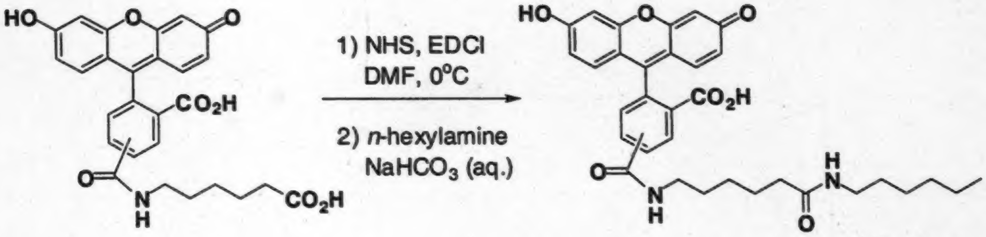

128 **129**

Scheme 5.2

Upon mixing **129** with the triboronic acid library, the solution became decolourized and approximately 30 to 40% of the beads were varying shades of green with 10% being suspiciously very intense. These intense beads were isolated and decoded, and the results were very similar to those obtained when the library was screened against the labeled tetrasaccharide **125**; that is, a high number of linear residues, the residue Nva^{B}, and many fragmented γAbu^{B} containing sequences. In conclusion, it appeared that the library was binding the fluorescein label and not the Le^{b} tetrasaccharide. The reason for this binding maybe the presence of the carboxylate functionality on the dye which can attract the fragmented γAbu^{B} sequences since this fragment likely exists as a positively charged quarternary ammonium ion according to its mass spectrum. The unique attraction by the dye towards the other residues, particularly Nva^{B}, however, cannot be adequately explained without further extensive experiments.

5.5: Synthesis and screening of NBD-labeled Lewis-b.

5.5.1: Synthesis of labeled Lewis-b.

Since fluorescein was clearly not inert to the resin-supported libraries an alternative label was needed. To this end, we attempted to employ the more hydrophobic NBD dye. Conjugation of Le^{b} with NBD was achieved starting from the 8-methoxycarbonyloctanol glycoside of Le^{b} **130**, generously provided to us once again by Professor Ole Hindsgaul. The tetrasaccharide was converted cleanly to the amino-amide upon heating with neat ethylenediamine, providing the required amine functionality for coupling to the *N*-hydroxysuccinimidyl ester of the NBD derivative **131** (Scheme 5.3).[143] The final Le^b NBD conjugate **132** was obtained as a fluffy yellow solid after preparative thin layer chromatography and lyophilization.

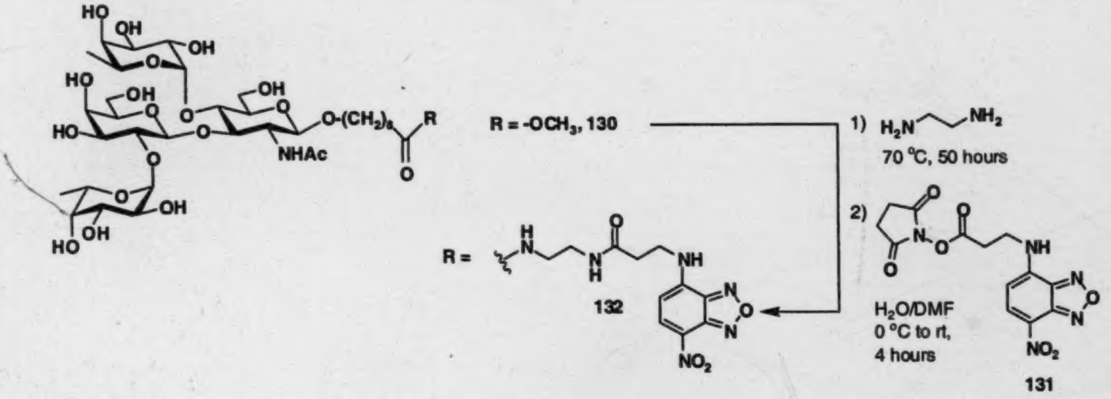
HO
OH
OH
HO
OH
OH
HO
O
O
O
O
O-(CH2)8
R
NHAc
O
OH
OH
HO
R = -OCH3, 130
1) H2N NH2
70 °C, 50 hours
2)
H2O/DMF
0 °C to rt,
4 hours
131
R =
H
N
H
O
NH
132
NO2

Scheme 5.3

A control NBD conjugate, without the tetrasaccharide, was also prepared in order to test the PS-PEG matrix and the resin bound triboronic acids for nonselective binding. The conjugate **135** was obtained starting from methyloctanoate (**133**) which was transformed into the amino-amide **134** by treatment with ethylenediamine before subjection to NBD-chloride for an aromatic nucleophilic substitution reaction (Scheme 5.4).

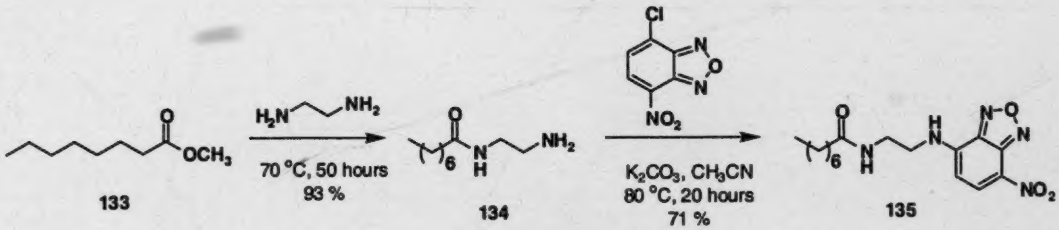
OCH3
133
H2N NH2
70 °C, 50 hours
93 %
6
NH2
134
Cl
NO2
K2CO3, CH3CN
80 °C, 20 hours
71 %
6
NO2
135

Scheme 5.4

5.5.2: Screening against the triboronic acid library.

Upon mixing the control conjugate **135** with underivatized TentaGel® resin in 0.01 M HEPES buffer at pH 7.4 in water, the beads immediately became yellow in colour and intensely fluorescent. This surprising, indiscriminate binding to the resin matrix by the dye, was fortunately suppressed by the addition of an equal volume of isopropanol.

With the Le^b NBD conjugate **132**, a 10^{-5} M solution in 0.01 M HEPES (pH 7.4) in 1:1 isopropanol/water was mixed with approximately 15 mg of the triboronic acid library. However, after 12 hours of swirling none of the beads appeared fluorescent green; instead all beads remained dark blue under the microscope. Increasing the concentration of **132** to 1.2×10^{-3} M, the highest that could be obtained, did not result in any detectable binding to any of the beads. Interestingly, it was eventually discovered that with the Le^b-NBD conjugate, the need for isopropanol was not necessary as no matrix binding was observed when the NBD was attached to the tetrasaccharide. However, binding to the resin supported triboronic acids was never observed even under completely aqueous conditions. It was thought that increasing the pH to 10 may result in some boronate complexation between the library and conjugate **132** through the formation of hydroxyboronate ions (see Chapter One) instead of the aminoboronate. Unfortunately, no green fluorescent beads were ever observed under all circumstances, which probably meant that the library was inactive towards the Le^b.

5.5.3: Conclusions on the screening of Lewis-b

The lack of active triboronic acids in the screening against Le^b is most likely due to the absence of a pyranose-furanose isomerizing saccharide unit in the tetrasaccharide. Indeed, solution phase results in the literature between boronic acid-based receptors and methyl glycosides gave lower binding affinities compared to the reducing sugars.[144] Unfortunately, the desired cooperative binding effect involving the three boronic acids on the saccharide-receptor library was not enough to overcome the inability for Lewis-b to isomerize. If any binding had occurred on the beads, the affinity would have been too low to detect simply with the naked eye under a low-powered microscope. This difficulty was compounded by the background fluorescence from the resin beads themselves, and by the fluorescence quenching of the fluorescent labels. However, as with the tetramine library , the library size may have been a limitation, whereby its small size may have resulted in the exclusion of a potentially active Le^b receptor. The small library reflects the limitations of the triboronic acid library synthesis which still suffers from a lack of true diversity, even with 17-building blocks, since each are employed only twice in two amide coupling reactions. The diversity was further hampered, in part, by the loss of many library members ending with the γAbu^B unit. In addition, half of the library is redundant; each sequence starting from one direction from the resin linker (R^1-R^2) has a counterpart in the opposite direction (R^2-R^1). The role of the resin matrix, as well as the effects of a fluorescent label on the tetrasaccharide binding are also not fully understood. Results so far have taught us that the binding of the fluorescein label to the library, as well as the chronic binding of the labels to the resin matrix, cannot be ignored during the on-bead screening.

In the end, it appears that on-bead screening of a labeled oligosaccharide to resin-bound boronic acid-based receptors is far from straight forward. Many factors such as the quality of the library and detecting the binding to the beads require more attention. Furthermore, it appears more clear that a furanose form of a saccharide with a free anomeric hydroxyl is required for tight binding, which means screening labeled glycosides, which do not satisfy that criteria, may be an improper strategy with the current approach.

Chapter Six:

Solid-phase synthesis and solution-phase evaluation of triboronic acid-based saccharide receptors.

6.1: Introduction.

Failure to observe the binding of the Lewis-b conjugate 132 to the TentaGel® supported triboronic acid library prompted a number of questions:

1) Is it possible to observe the binding on the resin beads, or is the binding affinity too weak between the boronic acid and the oligosaccharide such that detection by simple observation with the naked eye is impossible? The affinities reported by Shinkai *et al.* for their saccharide receptors ranged between 10^3 and 10^2 M^{-1}. For our chosen target, Lewis-b, which is more complicated than those tested by Shinkai, we anticipated the stability constants would be in this range only if cooperative binding between all three boronic acids occurred. In other words, can binding affinities in this range be observed on the resin beads using a fluorescently labeled target? Further complicating the on-bead assay was the chronic background fluorescence emitted from the beads themselves, and the tendency for the fluorescent probe to undergo photobleaching during the screening process.

2) Is there any advantage in having three boronic acid units in an oligosaccharide receptor in the first place? Two boronic acids units are commonly employed in selective monosaccharide receptors, but as mentioned in the previous Chapter, little is known about the effects of having more than two units. In the screening of Lewis-b, it was hoped that the formation of three, strong boronate esters between the triboronic acid and three monosaccharide units on the tetrasaccharide would afford a high enough binding affinity to observe on the resin, despite the absence of any monosacharide unit capable of isomerizing between pyranose and furanose forms. However, the lack of observable

binding may indicate that the extra boronic acid is not helpful, but in fact only complicates the synthesis of the receptor.

3) What are the structural requirements of the saccharide itself towards binding to a boronic acid under aqueous conditions? In Chapter One it was mentioned that a single arylboronic acid has an inherent affinity for fructose over other monosaccharides, and that there is a preference for fructose to be in its furanose form while complexed to the boronic acid. Diboronic acids, such as Shinkai's receptors **12** and **20**, bind preferentially to glucose, and again the monosaccharide exists in its furanose form when bound to the receptors. Thus, the ability to isomerize from pyranose to furanose seems important for boronic acid recognition. This isomerization, or mutarotation, occurs when there exists free hydroxyls both at the anomeric center and at the C-4 of an aldohexose (example, glucose) or C-5 of a ketohexose (example, fructose). This means that glycosides, which are substituted at the anomeric center, will likely make weak binders with Shinkai's 2-*N,N*-dialkylmethylaminophenyl boronic acid system. Unfortunately, oligosaccharides in Nature are glycosides, linked to either a protein (glycoprotein) or a lipid (glycolipid). However, it may still be possible to design a boronic acid containing receptor that can tightly bind to geometrically favorable *cis*-diols of saccharides that cannot isomerize. Obviously, such a receptor will greatly expand the utility of boronic acids in saccharide recognition rather than limiting them to a few select targets.

6.2: Triboronic acid-based receptors.

6.2.1: Receptor design.

In order to answer some of these questions, a series of individual triboronic acids were designed and synthesized to evaluate their binding to a group of saccharides. Rather than screening these receptors on resin beads it was decided to move entirely into solution to avoid the problems associated with the on-bead assays. In addition, solution assays will allow the determination of stability constants and thus provide a quantitative assessment of each receptor. Their general structure (**136**) is depicted in Scheme 6.1.

The main difference between these receptors and those made in the split-pool library is the incorporation of an anthracene sensing unit which can detect the binding of the saccharide to the boronic acid by the PET mechanism described in Chapter One.[23] Each receptor could be synthesized individually on trityl-polystyrene resin using what is essentially an amide reduction/alkylation sequence via diamide **138** and tetramine **137**. The long diamine spacer was included in order to move the substrate away from the bulky trityl linker during the solid-phase synthesis and to prevent the terminal amine from interfering with the binding of a boronic acid. The spacer is PEG-like in nature in hopes of increasing the solubility of the receptors in aqueous buffer.

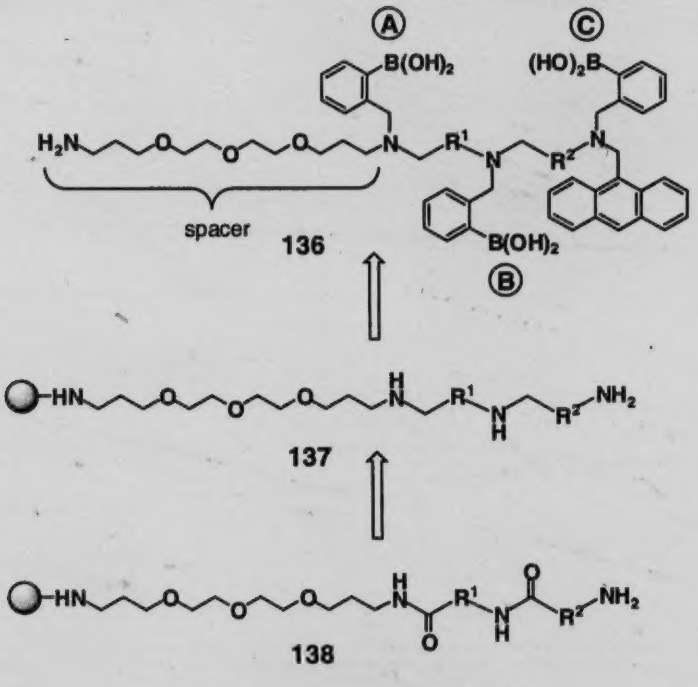

Scheme 6.1

It was realized that with three boronic acid units on the receptors, a saccharide will have the option of binding either all three boronic acids or only two of them. If three boronates are formed then the binding will be indicated by the fluorescence enhancement of the anthracene moiety at the end of the receptor. If only two boronates are formed then the fluorescence enhancement will depend on which boronic acids bind the saccharide and whether it is adjacent to the anthracene sensor. For this reason, the "library" of receptors was divided into two "sublibraries" to help distinguish whether the saccharide complexes the receptor with three boronate interactions or with only two. If only two are formed, then sublibraries should also inform us whether the binding occurs between boronic acids **A** and **B** or between **B** and **C** (Figure 6.1).

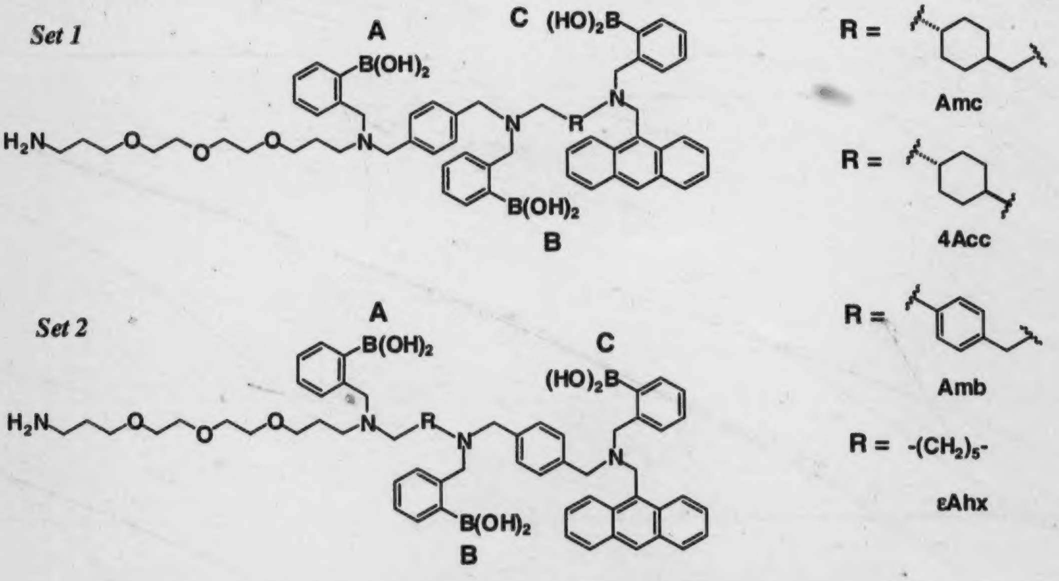

Figure 6.1: "Sublibraries" of triboronic acid-based receptors.

In one sublibrary (Set 1) the first residue between boronic acid units **A** and **B** was fixed as an Amb^B unit while the second residue between **B** and **C** (that is, -CH_2-R) was varied, being either Amc^B, 4Acc^B, Amb^B, or εAhx^B. In the other sublibrary (Set 2), the first residue was varied and the second was held constant at Amb^B (of course, only one Amb^B-Amb^B-Anth^B needs to be made in one set). If the binding occurs between the furthest two boronic acids, **A** and **C**, or to all three of them, due to the combination of R and Amb^B, then both Set 1 and 2 would appear similarly active. On the other hand, if a saccharide binds only to boronic acids **B** and **C** because of a preference for a specific R then the receptor in Set 1 (Amb^B-CH_2-R-Anth^B) would would appear more active than the "reverse" receptor in Set 2 (CH_2-R-Amb^B-Anth^B). Similarly, if the binding is between boronic acids **B** and **C** because of a preference for Amb^B than the receptors in Set 2 would appear more active than those in Set 1. In cases where there appears to be diboronate binding due to the effects of a single residue, then the truncated diboronic acid receptor containing only that particular residue will need to be synthesized in order to confirm that only two boronic acids are involved in the binding. It will be assumed that the most active receptors are 1:1 complexes near the anthracene unit since the higher number of boronate esters from one receptor to a single saccharide should result in tighter binding compared to complexes with multiple saccharides binding separately to each boronic acid on a single receptor.

6.2.2: Receptor synthesis.

The main challenge in the synthesis of these receptors was the inclusion of the anthracene sensing unit at the terminus of the tetramine backbone. The initial approach (Scheme 6.2) involved first the reductive amination of 9-anthracenylaldehyde onto the terminal amine of diamide **138** to give the intermediate **139**, and then reduction to tetramine **140**. However, upon subjecting **139** to borane-THF followed by either the iodine or piperidine based work-ups, very little of the desired tetramine was obtained. (This chemical incompatibility between the anthracenyl unit and the borane treatment was discovered by Dr. Duane Stones of our laboratories during the synthesis of a few model compounds).

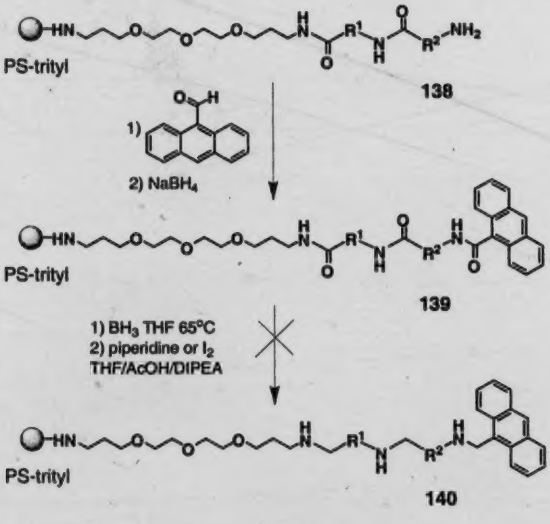

Scheme 6.2

The alternative strategy was to install the anthracene unit after the reduction which unfortunately complicated the synthesis by adding a number of additional steps (Scheme 6.3). (The receptors in Set 2 were prepared by the author, while Dr. D. Stones prepared those in Set 1).

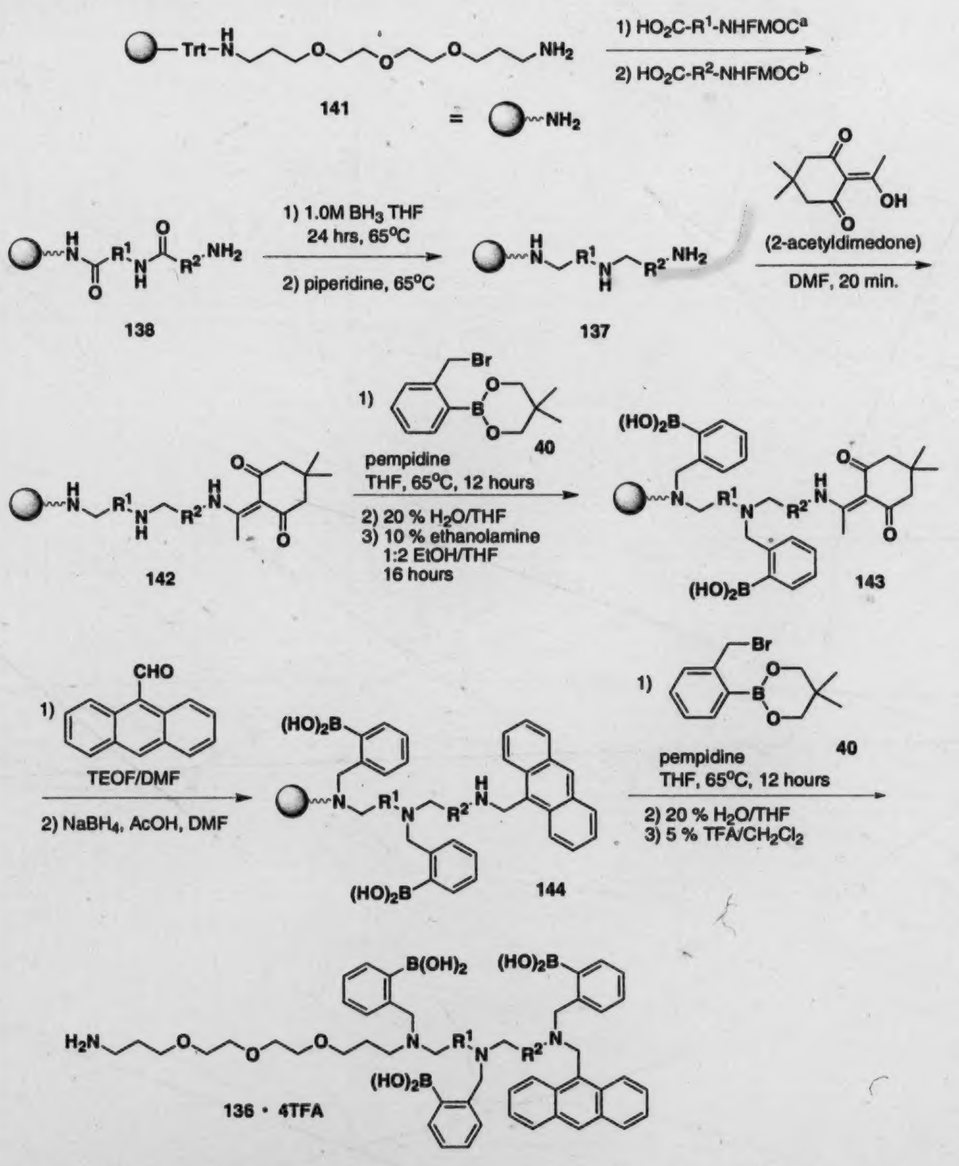

Trt
141
1) HO$_2$C-R^1-NHFMOC^a
2) HO$_2$C-R^2-NHFMOC^b
138
1) 1.0M BH$_3$ THF
24 hrs, 65°C
2) piperidine, 65°C
137
(2-acetyldimedone)
DMF, 20 min.
142
1)
40
pempidine
THF, 65°C, 12 hours
2) 20 % H$_2$O/THF
3) 10 % ethanolamine
1:2 EtOH/THF
16 hours
143
1)
TEOF/DMF
2) NaBH$_4$, AcOH, DMF
144
1)
40
pempidine
THF, 65°C, 12 hours
2) 20 % H$_2$O/THF
3) 5 % TFA/CH$_2$Cl$_2$
136 • 4TFA

[a] i)HBTU, HOBt and HO-R^1-NHFMOC (2 eq. each), *i*-Pr$_2$EtN (4 eq.), DMF, 2 hours; ii) 1:4 piperidine/DMF, 0.5 hours; iii) repeat i) with HO-R^2-NHFMOC; iv) 1:4 piperidine/DMF, 0.5 hours.

Scheme 6.3

The trityl-polystyrene linked diamine resin **141** was prepared in a similar fashion from trityl chloride resin as described for the TentaGel® resin **79** (see Scheme 4.2). However, due to the higher loading polystyrene resin, a small amount of resin crosslinking (~11%) could not be avoided even when using a large excess of the diamine relative to the polystyrenyl trityl chloride. From **141**, FMOC-protected amino acids were coupled using the standard protocol with HBTU/HOBt, then treated with piperidine to liberate the terminal amine. The resulting diamide, **138**, was reduced to the polyamine **137** employing the piperidine-based work-up procedure to cleave the borane-amine intermediates. The iodine promoted work-up was avoided due to suspicions from previous work (Chapter Four) that it maybe harmful to PEG spacers.

Before incorporating the anthracene unit, the first two arylboronic acids were attached to the secondary amines. This was achieved first by protecting the primary amine as a Dde derivative **142** by treatment with 2-acetyldimedone. Although this protection step should be selective for primary amines,[77, 107] it appeared by LCUV/MS analysis that a small amount of the secondary amines reacted as well. Fortunately, the over-reaction of 2-acetyldimedone was minimized by the use of 1.5 equivalents for no more than 20 minutes. With **142** in hand, the secondary amines were alkylated with benzyl bromide **40** over 24 hours. The resin-bound boronate esters were then hydrolysed to the corresponding acids and the Dde protective group removed to provide the primary amine in **143**. Strangely, the use of 2% hydrazine in DMF, the standard protocol to remove the Dde group, resulted in many unidentifiable signals in the LCUV/MS traces. Therefore, deprotection was instead achieved by treating the resin with 10 % ethanolamine in 1:2 ethanol/THF for 16 hours.[145]

To attach the anthracene sensing unit onto **143** to give **144**, a two-step reductive amination procedure was employed, whereby the imine was preformed by treatment of the free amine with 9-anthracenylaldehyde. After rinsing away the excess aldehyde, the imine was reduced with sodium borohydride in the presence of acetic acid.

Reductive amination of intermediate **144** with 2-formylphenylboronic acid was attempted on some substrates in order to afford **136**, but the reaction could never be driven to completion. Thus, the final boronic acid unit was also attached by a second alkylation with **40**. However, prolonged treatment of **144** with boronate **40** led to small amounts of overalkylation in some cases, but fortunately this was minimized by limiting the reaction time to no more than 12 hours. After hydrolysis of the boronate ester, the receptor **136** was cleaved from the resin to give the tetrakis(trifluoroacetate) salt as a yellow oil in >99% overall crude yield based on the initial, commercial loading of the resin. The high yields maybe due to difficulty in removing all or the residual TFA and/or an inaccurate loading provided by the supplier of the polystyrene resin.

In addition to synthesizing the triboronic acid saccharide receptors, a diboronic acid, with only the Amb unit, was also prepared (by the author). This receptor (Amb^{B}-Anth^{B}), will provide additional insights into the possible involvement of three boronic acids over two, by comparing its binding affinities with the other receptors. The synthesis of Amb^{B}-Anth^{B} was performed in a similar fashion as illustrated in Scheme 6.3 with the exception, of course, of coupling only the FMOC derivative of 2-aminomethylbenzoic acid to resin **141**.

All reactions shown in Scheme 6.3 were evaluated by cleaving small amounts of resin (~ 5 mg) after every step and performing an LCUV/MS analysis of cleaved contents. In some cases, such as with the polyamines, NMR spectra were obtained. Unfortunately, NMR analysis of the final boronic acids proved very difficult due to equilibrating mixtures of boronic anhydrides resulting in highly complicated spectra. This phenomenon was often observed in NMR spectra of any cleaved compound containing more than one 2-(*N,N*-dialkylmethylamino)phenylboronic acid and no conditions were ever found to give cleaner spectra (e.g., D_2O as solvent, using NaOD/D_2O, etc). Therefore, LCUV/MS was much more useful in analyzing the identity and purity of oligoboronic acids, and thus was the primary method for characterizing them along with high resolution ESMS.

The purities and MS signals of the receptors are given in Table 6.1 (see the Appendix for ESMS spectra and LCMS/UV data). It should be noted that HPLC purities using UV detection are generally more reliable than with MS detection, due to the difficulty in ionizing oligoboronic acids in the mass spectrometer. The difference in the ionization between the oligoboronic acids and small amounts of impurities in the sample frequently made the impurities appear in higher quantities than they are in reality. A diode array UV detector was employed to analyze the receptors at different wavelengths in order to obtain a more representative assessment of the purity. The wavelength at 370 nm, which is the excitation wavelength of anthracene, was chosen to detect the presence of any anthracene containing impurities. A relatively pure HPLC trace at this wavelength ensures us that it is mainly the desired receptor that will be monitored during titrations with the saccharides and not any unwanted anthracene derivatives. This criterion is in fact essential in guaranteeing the validity of the subsequent binding measurements.

The purity of the receptors appears to depend on whether the Amb^B residue was positioned beside the spacer (Set 1) or at the end of the sequence adjacent to the anthracene (Set 2). When Amb^B was at the end the purities were generally good according to LCUV, especially considering that a linear sequence of 10 to 11 steps were carried out without any purification of intermediates (Table 6.1). These purity values were somewhat expected since the chemistry was initially optimized (by Dr. D. Stones) with the Amb at the terminus. However, when the Amb^B was next to the spacer, the purities depended on the nature of the second residue beside the anthracene. As a result, the receptors in Set 1 required further purification by semi-preparative HPLC. Common impurities had were indentified were small amounts of overalkylation from the final alkylation step, as well as *bis*-anthracenylation in some cases. Note that the contamination by the diamine spacer in each sample is not represented in the HPLC purities given in the table. Thus the values are artificially higher without taking into account the diamine. However, this diamine is not expected to affect the relative binding affinities among receptors.

Table 6.1: ESMS and HPLC purities of receptors **136.**

Receptor[a,b]	ESMS (*m/z*)	Purity by LCUV
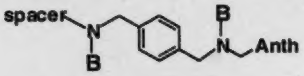 (Amb^{B}Anth^{B})[d]	780.4 (MH-H_2O) 770.4 752.4 (MH-2H_2O)	82 % (254 nm) 75 % (210 nm) 92 % (370 nm)
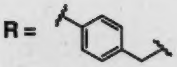 (Amb^{B}Amb^{B}Anth^{B})	997.5 (MH-3H_2O) 987.5 807.5[c]	75 % (254 nm) 59 % (210 nm) 92 % (370 nm)
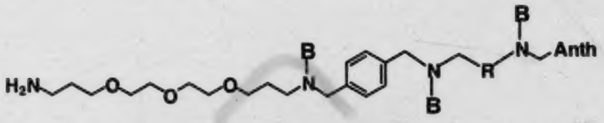 Amb^{B}-CH_2-R-Anth^{B} (Set 1)		
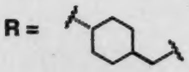 (Amb^{B}Amc^{B}Anth^{B})	1003.6 (MH-3H_2O) 913.6	67 % (254 nm) 54 % (210 nm) 73 % (370 nm)
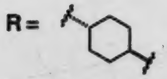 (Amb^{B}4Acc^{B}Anth^{B})	969.5 (MH-3H_2O-20)[e]	54 % (254 nm) 42 % (210 nm) 58 % (370 nm)

Table 6.1: Continued.

R = -$(CH_2)_5$-	977.6 (MH-$3H_2O$)	56 % (254 nm)
(Amb^{B}εAhx^{B}Anth^B)	967.5	50 % (210 nm)
	787.4^c	67 % (370 nm)

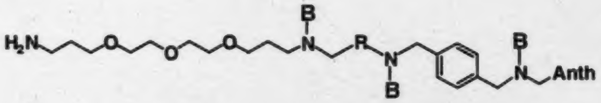

CH_2-R-Amb^B-Anth^B (Set 2)

R = 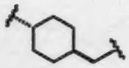	1003.6 (MH-$3H_2O$)	76 % (254 nm)
(Amc^{B}Amb^{B}Anth^B)	913.6	59 % (210 nm)
	813.5^C	88 % (370 nm)
R = 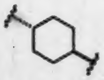	989.6 (MH-$3H_2O$)	75 % (254 nm)
	979.6	70 % (210 nm)
(4Acc^{B}Amb^{B}Anth^B)	749.5^C	91 % (370 nm)
R = -$(CH_2)_5$-	977.5 (MH-$3H_2O$)	56 % (254 nm)
(εAhx^{B}Amb^{B}Anth^B)	967.6	48 % (210 nm)
	787.5^C	71 % (370 nm)

---

[a] Analysed as their tetrakis(trifluoroacetate) salts. [b] "B" Denotes a 2-methylenephenylboronic acid unit; "Anth" denotes the anthrecene unit.

[c] Loss of the anthracenyl group by MS fragmentation.

[d] Spacer = $H_2N(CH_2)_3O\ (CH_2)_2O(CH_2)_2O(CH_2)_3NH$-

[e] Analyzed at 80 V instead of 120 V like the rest.

The masses of each oligoboronic acid, by electrospray, is also given in Table 6.1. As usual, only the mass of the anhydride was detected. With the triboronic acids, some fragmentation of the anthracenyl (MH-xH$_2$O-190) was observed. In addition, a minor signal with 10 amu's less than the mass of the triboronic anhydride was found co-eluting with all triboronic acids in both MS and UV traces (see Chapter Four for a discussion of the MH-10 signal).

6.3: Disaccharide targets.

In order to assess the possible advantages of three boronic acids in a saccharide receptor, different disaccharides were chosen as model targets over simpler monosaccharides. Lactulose and melibiose were selected as it was predicted that their ability to isomerize from pyranose to furanose forms might aid in binding (Scheme 6.4). Turanose was also chosen, and although it can isomerize, the 1-3 linkage between the monosaccharide units restricts the amount of isomerization that occurs. In addition, there is no 2,3-*cis* diol in the fructose unit which was shown to be important in binding to boronic acids.[17, 19] Lactose was also tested on some of the receptors since it possesses the free anomeric hydroxyl yet cannot isomerize due to the 1-4 linkage between the galactose and the glucose units. Finally, the disaccharide trehalose was used as a negative control since, being a glycoside, it should not be expected to bind to any of the receptor.

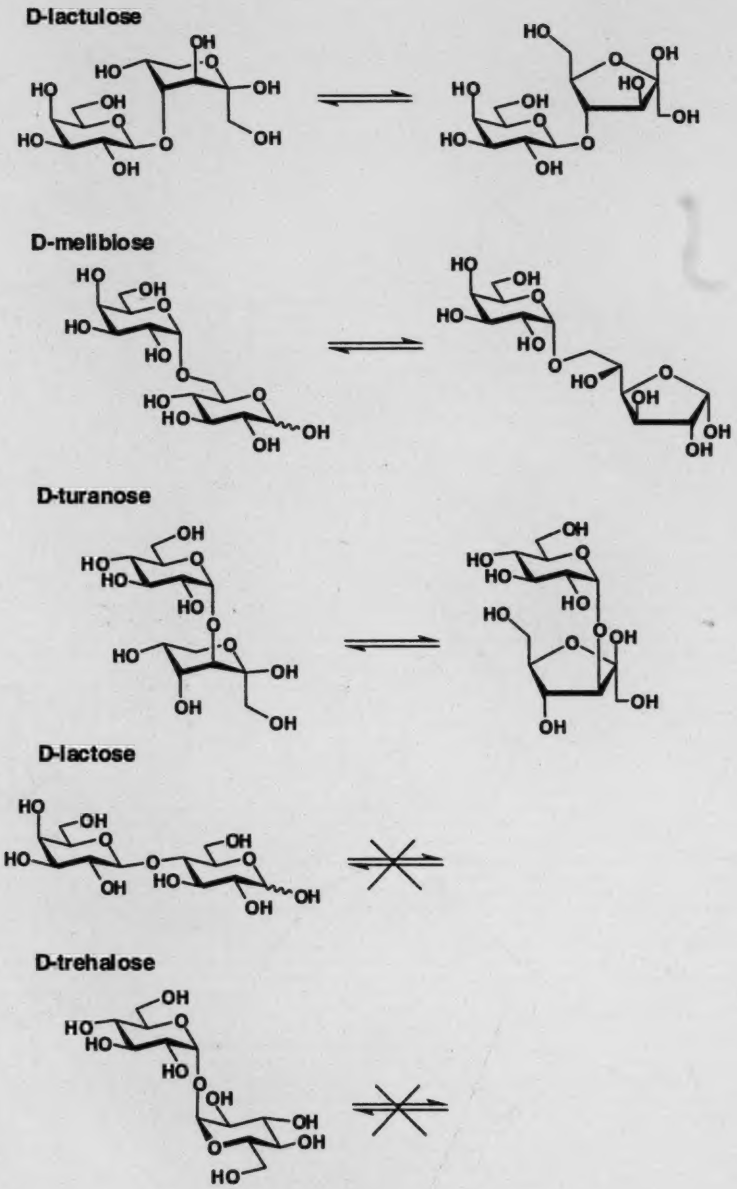
D-lactulose
D-melibiose
D-turanose
D-lactose
D-trehalose

Scheme 6.4

6.4: Measurement of binding affinities.

The stability constants for each receptor was determined by monitoring its increase in fluorescence intensity upon aliquot additions of a 1.0 M solution of each disaccharide.[22, 146] All titrations were performed in 0.01 M phosphate buffer at pH 7.8 in a 1:1 mixture of water and methanol (the methanol was added to fully solubilize the receptor). Figure 6.2 illustrates an example of the fluorescence enhancement of Amb^B-4Acc^B-Anth^B upon addition of lactulose.

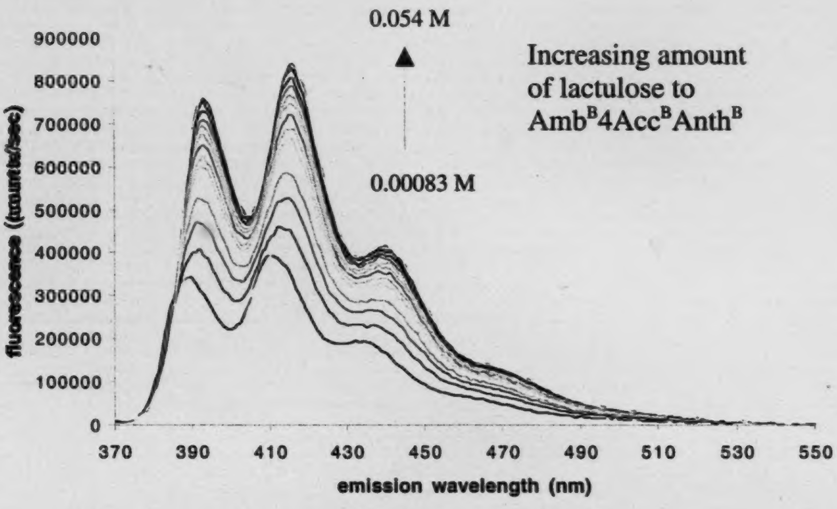

Figure 6.2: Fluorescence enhancement of a receptor upon titration with disaccharide. Concentration of receptor: 2.60×10^{-6} M in 1:1 water/methanol with 0.01 M phosphate buffer (pH 7.8). Excitation: 370 nm.

The fluorescence enhancement at 423 nm was measured to create a titration curve from which the stability constant (K_a) was determined using a modified Benesi-Hildebrand equation (Eq. 2), which assumes a 1:1 stoichiometry in the formation of a saccharide-oligoboronate complex.[147-149]

$$\frac{1}{(I-I_o)} = \frac{1}{K_a \bullet (I_{max}-I_o) \bullet [S]} + \frac{1}{(I_{max}-I_o)} \qquad \text{Eq. 2}$$

In this equation, I is the fluorescence intensity upon addition of saccharide, S; I_o is the flourescence intensity when $[S] = 0$; I_{max} is the maximum intensity that is reached; and K_a is the stability constant. The stability constant is obtained by plotting $1/(I - I_o)$ versus 1/[S], which should give a straight line, and then dividing the intercept by the slope. Figure 6.3 shows common titration curves, represented by the receptor 4Acc^{B}-Amb^{B}-Anth^{B}, obtained from each disaccharide. (All titration curves are shown in the Appendix section). For some titrations, after adding the first few microliters of a 1.0 M disaccharide solution to the receptor, the fluorescence intensity mysteriously dropped before increasing upon further additions to give the recognizable titration curve. In these cases, which were common for very weak binders, the curve was extrapolated to I_o and then plotted according to Eq. 2. All titrations were done at least twice and an average was taken.

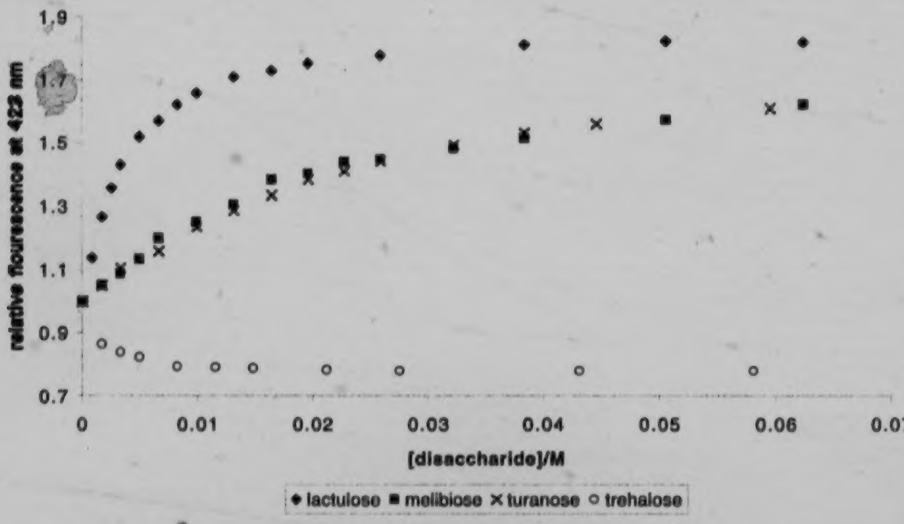

Figure 6.3: Titration curves of 4Acc^{B}Amb^{B}Anth^{B} with disaccharides. Concentration of receptor: 2.60×10^{-6} M. Excitation: 370 nm, emission: 423 nm.

Table 6.2 gives the stability constants between each receptor and the model disaccharides. One cautionary note: the minor impurites in some of the crude samples may have affected the stability constants by possibly competing for the saccharide, or even quenching the fluorescence of the anthracene sensor. Thus the values that are shown can only be used to determine significant trends in receptor affinity rather than taken as absolute. The general trends in the stability constants are clear when comparing between the disaccharides. Lactulose was found to have the greatest binding strength to all receptors with affinities between 50 and 100 times greater than those of melibiose and turanose. However, as expected, trehalose consistently gave no increase in fluorescence intensity. In addition, lactose was examined against Amb^{B}-Amb^{B}-Anth^{B} and showed no binding to the receptor. These results provide further support for the requirement of an isomerizing reducing end in the saccharide in order to form a complex with a boronic acid in aqueous solution.

Table 6.2: Stability constants (M^{-1}) between receptors 136 and disaccharides

	Melibiose	Lactulose	Turanose	Trehalose
	K_a $(I_{max}/I_O)^a$	K_a $(I_{max}/I_O)^a$	K_a $(I_{max}/I_O)^a$	
Amb^{B}-Anth^{B}	16 (1.5)	221 (1.6)	6.9 (1.4)	-
Amb^{B}-Amb^{B}-Anth^{B}	6.8 (1.7)	126 (1.6)	13 (1.5)	-
Set 1				
Amb^{B}-εAhx^{B}-Anth^{B}	58 (3.4)	433 (3.8)	149 (4.0)	-
Amb^{B}-Amc^{B}-Anth^{B}	6.0 (2.1)	387 (2.3)	3.8 (2.2)	-
Amb^{B}-4Acc^{B}-Anth^{B}	4.6 (2.5)	214 (3.2)	7.8 (2.4)	-
Set 2				
εAhx^{B}-Amb^{B}-Anth^{B}	12 (1.5)	138 (1.5)	15 (1.7)	-
Amc^{B}-Amb^{B}-Anth^{B}	11 (2.0)	201 (1.6)	14 (1.6)	-
4Acc^{B}-Amb^{B}-Anth^{B}	23 (2.0)	187 (1.8)	18 (1.6)	-

[a] I_{max}/I_O taken from Eq. 1 and from the titration curves.

As discussed earlier, a number of scenarios are conceivable that would suggest the participation of more than one boronic acid binding to the disaccharides. If a particular triboronic acid sequence binds with all three of its boronic acid units, then it is expected that the affinity will be greater than compared to the diboronic acid receptor, Amb^B-Anth^B. Importantly, this triboronic acid sequence will also record greater binding affinities in both Set 1 and Set 2 (that is, for both R^1-R^2 and the corresponding reverse sequence R^2-R^1) compared to any diboronate binding. Cooperative binding between only the two distal boronic acids (**A** and **C** in Figure 6.1) may also give higher stability constants in both sets. However, according to the values given in Table 6.2, neither of these cases seems to occur, at least with these particular receptors and disaccharides. With turanose, there is a slight increase, relative to Amb^B-Anth^B, in the affinities in the Set 1 and Set 2 receptors, but the increase is small and probably within experimental error. Furthermore, the magnitude of the increases for the turanose titrations are different within both sets. In the case of Amb^B-Amb^B-Anth^B with lactulose, and to some extent melibiose, the third residue actually appears to reduce the binding affinity compared to Amb^B-Anth^B. This apparent reduction maybe due to the disaccharide "dividing its time" between the two Amb^B units, one of which is not detected by the sensor.

Another scenario is where it is solely the nature of the residue next to the anthracene sensing unit that is responsible for the fluorescence enhancement. In this case the binding affinities in the two sets of receptors will be different. The analyses with the εAhx^B containing receptors seems to best illustrate this scenario. Against melibiose, the Set 1 receptor, Amb^B-εAhx^B-Anth^B, exhibits an approximately 5 to 10-fold greater affinity for this disaccharide compared to all other receptors. Against lactulose, Amb^B-εAhx^B-Anth^B is the strongest binder by approximately 2-fold. Perhaps the most impressive of all is an almost 10-fold greater stability between Amb^B-εAhx^B-Anth^B and turanose relative to the other receptors titrated against this disaccharide including εAhx^B-Amb^B-Anth^B. This high affinity towards turanose is particularly interesting given that the disaccharide has no 2,3-*cis* diol when the fructose unit is in its furanose form. In addition, the receptor Amb^B-Amc^B-Anth^B, displayed significant affinity for lactulose with a K_a value second only to Amb^B-εAhx^B-Anth^B. However, the corresponding receptors in

Set 2, εAhx^{B}-Amb^{B}-Anth^{B}, and εAhx^{B} -Amb^{B}-Anth^{B}, did not show the same increase in binding strength; with εAhx^{B}-Amb^{B}-Anth^{B}, for instance, the stability is actually lower than the diboronic acid receptor.

This difference between the two sets seems to suggest at this point that the model saccharides that were examined are binding to boronic acids surrounding the εAhx and Amc residues next to the anthracene, and are causing the binding enhancement without the Amb unit at the other end (Figure 6.4). It is assumed that these greater stability constants would employ at least two boronic acid units possibly leaving the other unit on the Amb residue to bind as a monoboronic acid saccharide receptor. Indeed, the lower stability constants observed through most of Set 2 against each disaccharide may suggest that only the single boronic acid adjacent to the anthracene sensing moiety (i.e. unit **C**) is binding to the disaccharide. Alternatively, it maybe that the Amb^{B} residue by itself binds as a diboronate, but when adjacent to another residue which binds more strongly, a competition for the disaccharide ensues that results in a reduced affinity observed for the Amb^{B} residue. Thus, the other two boronic acids linked to the other residue and away from the anthracene senosr are binding to the disaccharide as a stronger diboronate complex that is independent of the Amb.

Set 1

Set 2

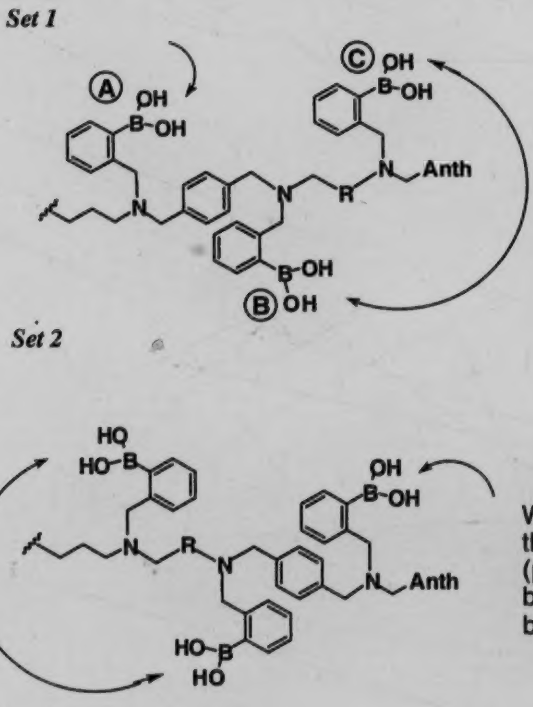

Enhanced binding to diboronic acid unit detected by adjacent anthracene

Weaker binding observed throughout most of Set 2; (possibly competing for the middle boronic acid to make a diboronate binding).

Figure 6.4: Suspected binding profile of triboronic acid saccharide receptors.

6.5: Recent Studies.

In order to verify the proposal above, more studies needed to be done to determine conclusively if diboronate formation is the main contributor to the saccharide recognition particularly when εAhx and Amc are involved. To this end, the diboronic acids Amc^{B}-Anth^{B} and εAhx^{B}-Anth^{B} were recently synthesized without the Amb^{B} unit and evaluated for their binding against lactulose (Figure 6.5. This work was performed by Dr. D. Stones). Indeed, it was found that their stability constants (K_a = 519 M^{-1} for both) were almost 2.5 times greater than Amb^{B}-Anth^{B} against the same disaccharide, which seems to reflect the greater affinities observed in Set 1 in Table 6.2. The slight increase in the stability constants with Amc^{B}-Anth^{B} and εAhx^{B}-Amb^{B} compared to their respective Set 1 triboronic acids maybe attributed to the lack of competitive binding to an adjacent boronic acid. Nevertheless, these recent results provide further evidence that only two boronic acids are being used in the binding to the model disaccharides and the nature of the residue in between the boronic acids has a definite effect on the binding strength.

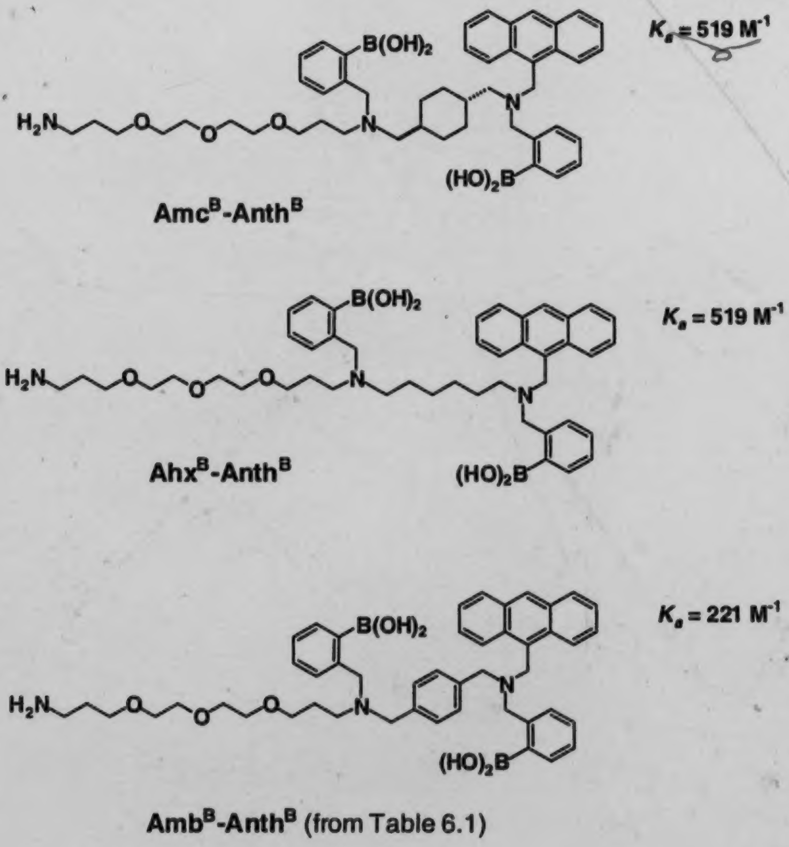
K_a = 519 M^{-1}
B(OH)$_2$
H$_2$N
N
(HO)$_2$B
Amc^B-Anth^B
K_a = 519 M^{-1}
B(OH)$_2$
H$_2$N
N
(HO)$_2$B
Ahx^B-Anth^B
K_a = 221 M^{-1}
B(OH)$_2$
H$_2$N
N
(HO)$_2$B
Amb^B-Anth^B (from Table 6.1)

Figure 6.5: Diboronic acids recently prepared and tested against lactulose.

However, in each case it is unknown at the present time which portion of the disaccharide unit interacts with the receptor, that is, whether it is the monosaccharide unit at the reducing end or the entire disaccharide. With lactulose in particular, a titration between a receptor with fructose monosaccharide will help to determine if there were any interactions with both the galactose and fructose units in the lactulose . If the stability constants are the same, then the binding to lactulose is occurring solely at the fructose unit of the disaccharide; if the binding is much less, then likely the galactose unit is required to form an additional boronate interaction. However, if the binding with fructose monosaccharide is higher than with lactulose, then it maybe due to the galactose unit actually hindering the boronate interaction by steric repulsion.

6.6: Assay against blood group B trisaccharides.

It was envisioned that a triboronic acid would be an ideal receptor towards trisaccharide targets that possess enough hydroxyl groups to potentially form three boronate esters. To this end, two trisaccharides were examined (Figure 6.6): blood group B trisaccharide and 3-fucosyllactose, both obtained commercially. Due to the expense of these trisaccharides only the triboronic acid, Amb^{B}Amb^{B}Anth^{B}, was tested and only single point fluorescence measures were taken rather than a full titration. In addition, the diboronic acid Amb^{B}Anth^{B} was tested for comparison.

With both trisaccharides, small aliquots of the oligosaccharide at 1.2×10^{-3} M and then 2.4×10^{-3} M concentrations were added to a 2.60×10^{-7} M solution of the triboronic acid in the 1:1 methanol/water mixture with 0.01 M phosphate buffer (pH 7.8). The fluorescence was monitored for any increase in intensity after each addition. Unfortunately, no increase was observed in both cases with Amb^{B}Amb^{B}Anth^{B} or Amb^{B}Anth^{B} indicating the lack of any strong binding to the trisaccharides. It should be mentioned that 3-fucosyllactose is unable to isomerize to the furanose from at the reducing end due to the 1-4 linkage to the glucose unit. Furthermore, the 1-3 linkage on the galactose unit at the reducing end of blood group B trisaccharide will sevrely limit the amount of isomerization that can occur in this case. These results, with both oligosaccharides, seem to provide preliminary evidence, at least with the triboronic acid Amb^{B}Amb^{B}Anth^{B}, that increasing the number *cis*-diols on a saccharide does not necessarily compensate for its inability to isomerize between pyranose and furanose forms. Therefore, what was obsesrved in these experiments also might the explain the difficulty that was faced in attempting to observe saccharide binding to resin supported triboronic acids described in Chapter Five.

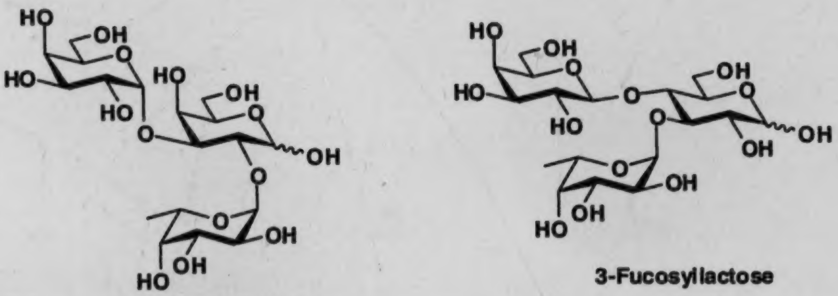

Blood Group B Trisaccharide

3-Fucosyllactose

Figure 6.6: Trisaccharide targets for $\mathrm{Amb^BAmb^BAnth^B}$

6.7: Conclusions and future prospects.

6.7.1: Conclusions to triboronic acid saccharide receptors.

The triboronic acids that were synthesized were used to determine whether more than two boronic acid units on a single saccharide receptor would enhance the binding affinity towards disaccharides and more complex oligosaccharides. The positive effect of three boronic acids in a particular receptor would have been ideally indicated by roughly equal and relatively large stability constants in both Set 1 and 2 (i.e. $\mathrm{R^1\text{-}R^2}$-Anth and $\mathrm{R^2\text{-}R^1}$-Anth) of our small parallel library. Using this criteria, our preliminary results involving a series of model disaccharides found that the presence of three boronic acids does not greatly improve the affinity. Likewise, there appeared to be no sequence that showed any significant communication between the furthest two boronic acid units (**A** and **C**) without the middle unit (**B**). Furthermore, the triboronic acid $\mathrm{Amb^B\text{-}Amb^B\text{-}Anth^B}$ gave no detectable fluorescence increase against two trisaccharides that were tested, indicating that even increasing the number of vicinal *cis*-diols does not necessarily lead to a higher binding affinity with a triboronic acid.

However, individual residues in certain triboronic acid sequences resulted in greater affinity for particular disaccharides as was indicated by the larger stability constants in one set compared to the other set. For instance, within Set 1, the $\mathrm{Amb^B\text{-}\varepsilon Ahx^B\text{-}Anth^B}$ receptor in its assay with each disaccharide (except trehalose), and $\mathrm{Amb^B\text{-}Amc^B\text{-}Anth^B}$ with lactulose, were highly active compared to their counterparts in Set 2.

The strong binding observed from these receptors maybe due to the εAhx^B and Amc^B residues acting without the Amb^B residue. Indeed the evaluation of the diboronic acids εAhx^B-Anth^B and Amc^B-Anth^B against lactulose resulted in stability constants comparable to their respective triboronic acids in Set 2, showing that the Amb^B unit is not necessary for the binding to occur.

Finally, these results, combined with data in the literature,[14, 17, 19, 24] indicate that the strongest binding between a boronic acid and a saccharide occurs when a saccharide is capable of isomerizing between its pyranose and furanose forms, and contains a set of easily accessible hydroxyls, such as a vicinal *cis*-diol. The furanose form apparently provides a special geometrical arrangement of hydroxyl groups that favour the formation of a tight boronate complex (see structures **13** and **20b** in Chapter One). However, the requirement for pyranose-furanose isomerization for tight binding, unfortunately limits the type of oligosaccharides that boronic acid can bind in Nature.

However, the strong binding observed between Amb^B-εAhx^B-Anth^B and turanose is interesting because this disaccharide has no 2,3-*cis*-diol on the fructose due to substitution at 3-OH, one of its important hydroxyl groups for binding while in its furnanose form. This leads to the question of whether the binding is actually occurring with the fructose unit still as a pyranose ring which possesses a 4,5-*cis* diol. This high binding affinity needs to be further verified by evaluating the stability constant between turanose and the diboronic acid εAhx^B-Anth^B.

6.7.2: Future research into combinatorial approaches to boronic acid-based saccharide receptors.

If diboronic acids alone can potentially be employed against various saccharides, it seems reasonable to explore a library of such compounds. Indeed, the results that have already been obtained from both the tri- and diboronic acids studied in this Chapter provide some potential leads towards some new saccharide receptors. In fact, long aliphatic chains, such as that in the εAhx containing boronic acids, have been previously demonstrated by other laboratories to be beneficial in some designed receptors.[146, 150] However, more elaborate spacers, such as rigid groups like Amc and 4Acc, have not been investigated due to the difficulty others have had in their synthesis. In addition, no investigation has been reported in the literature examining the effects of increasing the Lewis acidity of the boronic acid by the incorporation of electron withdrawing substituents on the phenylboronic acid unit. It is possible that increasing the boron's Lewis acidity will create a stronger coordination between a diol and the orthodialkylmethylaminoboronic acid. (Preliminary data gathered by Dr. Stones has shown that cyano substituents *para* to the boronic acid on the phenyl ring in Amc^B-Anth^B does seem to have a positive effect on the binding affinity towards lactulose). Thus by modifying both the spacer and the electronic properties of the boronic acid, it maybe possible to discover receptors that can bind glycosides in their pyranose forms thereby increasing the potential of targeting more complex oligosaccharides.

A library of diboronic acids (**145** in Figure 6.7) that can investigate both the Lewis acidity of the boronic acid and the structure of the spacer can be prepared in a parallel fashion using the solid-phase synthesis depicted in Scheme 6.3. The anthracene sensing unit can be employed for detecting the saccharide binding, but in order to facilitate any high-throughput screening, and potentially expand library diversity, a competitive assay can be used with a dye such as Alizarin Red S. As discussed in Chapter 5, these dyes change colour as they are displaced from the boronic acid by a saccharide.[48, 49, 139] This may allow an assay whereby the saccharide binding can be monitored by simply observing the colour change of the dye. Fortunately, competitive binding assays of this type work best in the solution phase. Removing the anthracene unit would also simplify the preparation of the receptors, since its use in the triboronic acids required an undesired lengthening of the synthesis. Furthermore, efforts are on the way in our laboratories for synthesizing substituted boronic acids with electron withdrawing substituents (examples: cyano and nitro groups) with enhanced Lewis acidity (work by Dr. Xiaosong Lu, a post-doctoral associate). These electronically modulated boronic acids can be incorporated into the libraries assuming that they will increase the affinity to a diol.

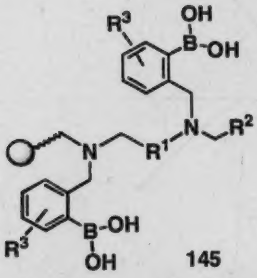

145

R^1 = diversity element originating from an amino acid.
R^2 = anthracenyl, or another diversity element.
R^3 = electron withdrawing group to enhance the Lewis acidity of the boronic acid.

Figure 6.7: Potential future library of diboronic acids.

Combining our experience with ion pairing and boronic acids, another parallel library of receptors can be prepared that is selective towards ionic saccharides such as uronic acids and sialic acid.[43, 151] The design of such a library is illustrated in Figure 6.8. Synthetically, it can be prepared by a route analogous to that shown in Scheme 6.3, but instead the terminal amine is either left free (**147**) or is converted to a guanidinium (**146**). Under neutral, aqueous conditions the amine and the guanidinium are cationic and can therefore bind to the carboxylate of the saccharide, while the boronic acid can bind to its diols. As with the diboronic acid library, a high-throughput screening strategy can be envisioned by using Alizarin Red S or a similar dye. The sialic acid, in particular, is an interesting target since it has been demonstrated by Shinkai *et al.*[151] to bind to a receptor in a cooperative fashion via boronate formation and ion pairing, even though it cannot isomerize to a furanose form. Many complex oligosaccharides feature sialic acid as an important unit, and thus a receptor for this monosaccharide would be useful in applications for identifying the unit in newly discovered glycosylated biomolecules.

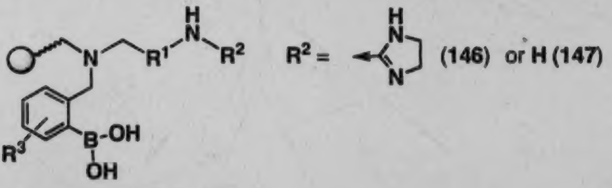

Figure 6.8: Potential receptors for uronic acids and sialic acid.

The synthesis of a large, structurally diverse, split-pool library of saccharide receptors will require a different strategy than that used previously. As mentioned earlier, it is now believed that a mixed binding approach is a more suitable route. This approach can best be achieved by incorporating boronic acid units into a peptide in where the boronic acids bind to the diols, while the peptide binds using the binding modes employed in lectins. As previously demonstrated, peptide libraries alone can afford selective receptors for simple monosaccharides,[41] and therefore, perhaps by adding a boronic acid, both the affinity and the selectivity may improve. Furthermore, this peptide-boronic acid may even be applicable to more complex oligosaccharides. One approach is depicted in Scheme 6.5 towards the receptor **150**, and involves the trisubstituted boronic acid **148** as the key building block. Attachment to the resin by alkylation and then release of the protective group gives **149** from where a peptide can be assembled and eventually terminated with another aryl boronic acid to afford the receptor **150**. The peptides in the library can be simple α-amino acids with side chains that are known to bind to saccharides in lectins. This simpler synthesis of library **150** may also provide library members that are more pure than the oligoboronic acid library prepared via the polyamines. Encoding of the split-pool library can be achieved using the same partial termination synthesis strategy employed for the oligoboronic acid libraries. Alternatively, another encoding method can be used, such as radio frequency[44] or optical encoding[45] tags which allow unrestricted diversity as opposed to mass spectrometric methods. It is envisioned that by using labeled oligosaccharides, similar to Le^b-NDB, an on-bead assay can be performed using these new libraries. A solution phase screening approach can also be employed if the on-bead assay remains troublesome.

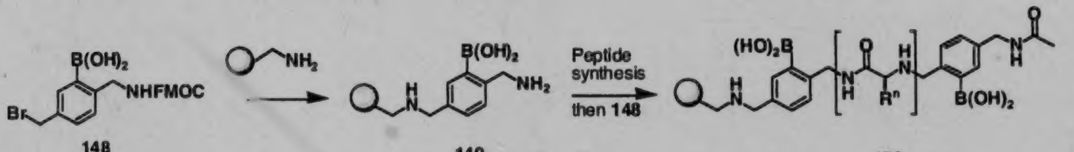

148 **149** **150**

Scheme 6.5

Chapter Seven:

Thesis conclusions.

This thesis described the progress towards the goal of creating a split-pool library of boronic acid-based receptors for complex oligosaccharides that can operate under physiological conditions. It began by developing a polyamine scaffold on solid support resin onto which the boronic acids could be attached. The polyamine was prepared via the exhaustive amide reduction of a resin bound polyamide which in turn was assembled by simple FMOC peptide synthesis. In order to encode the split-pool library a partial termination synthesis of the polyamide library was employed which allowed the identity of each bead supported compound to be determined by LCMS analysis. Once the polyamine scaffold was obtained and the boronic acids were attached, various strategies were explored for screening the oligoboronic acids against oligosaccharides until it was finally decided to employ NBD-labeled glycosides. However, upon screening the resin supported split-pool library, it was discovered that oligosaccharide binding was too weak to be observed using the chosen screening method.

Although the ultimate goal of this project gave somewhat disappointing results, much was discovered en route to the oligoboronic acid libraries. Namely, a method for exhaustively reducing resin bound polyamides with borane that employed a more efficient and relatively mild work-up protocol on the intermediate borane-amine adducts. This work-up procedure uses iodine in a buffered medium to cleave adducts and is mild enough to be used on acid sensitive resin linkers, namely the trityl linker. In addition, it is quick and can be done at room temperature making it amenable to high-throughput synthesis. This iodine-promoted work-up was used to synthesize natural acylpolyamine neurotoxins and a branched analogue that would have difficult to make by other existing methods. It was also demonstrated in the synthesis of a split-pool library of 189 tetramines on polystyrene resin. From this tetramine library a group of selective ligands for polyanionic compounds were discovered in a series of on-bead assays. One of the disadvantages of the iodine protocol, unfortunately, is that it is restricted to amino-trityl polystyrene resins, as other polystyrene bound linkers were found incompatible. On very elaborate polyamide substrates, the resulting polyamine is slightly less pure when the iodine based method was used in the work-up compared to using piperidine exchange protocol. Furthermore, polyamides bound to PS-PEG resins give inferior quality polyamines using the iodine protocol compared to piperidine. However, a TentaGel® resin bound trityl linker was developed that was capable of withstanding prolonged exposure to borane, thus enabling the synthesis of resin supported polyamines that still have potential for being screened against biological targets in an on-bead assay.

Further contributions to the field of combinatorial chemistry in this work can be found in the applications of LCMS in the decoding of nonpeptidic, split-pool libraries supported on both polystyrene and PS-PEG resins. It proved to be fast and, for the most part, an efficient method for decoding partially terminated oligomeric sequences. It has the additional advantage in that the purity of the library can be evaluated simultaneously while decoding. Perhaps the most serious disadvantage is the limits it imposes on the choice of building blocks due to conflicting masses that cannot be distinguished in the mass spectrometer. These limits restricted the size of the libraries that were made.

No active polyamines or oligoboronic acids from our split-pool libraries were discovered yet against any biological targets. For the polyamines, part of the problem was finding a proper method for screening the bead supported libraries, as no method currently exists for detecting the binding of a non-labeled polyanionic target (with the exception of a dye) on a bead expressing an active library member. For the time being, employing labeled targets may be the best option. With the triboronic acids, it may have been that the binding affinities were too low to observe on the resin beads. This lack of observable binding may have reflected the strict structural requirements necessary in a saccharide in order for them to bind boronic acids; that is, the need to have a free reducing end that is capable of converting between pyranose and furanose forms and the presence of a geometrically favorable vicinal *cis*-diol. However, with lessons learned in a smaller, parallel library of triboronic acids and the set of diboronic acids that were prepared, a new generation of boronic acid based saccharide receptors are in the planning that can potentially overcome these hurdles. Therefore, with continuous work in this laboratory, and others around the world, a solution to the elusive goal of small molecule binding to oligosaccharides under physiological conditions, may one day be found…

Chapter Eight:
Experimental.

8.1: General procedures.

Most FMOC-protected amino acids and *N*-acetyl amino acids were purchased from Novabiochem (La Jolla, California) or Advanced Chemtech (Louisville, Kentucky). Those FMOC amino acids not commercially available were prepared using the procedure of Lapatsanis *et al.*[109] Polystyrene resins (90-150 μm) were purchased from Rapp-Polymere (Tübingen, Germany) or Novabiochem, whereas TentaGel® resins (90-150 μm and 250-300 μm) were purchased from Rapp-Polymere exclusively. THF was dried by distillation over sodium/benzophenone; CH_2Cl_2, pyridine, and triethylamine over calcium hydride. Anhydrous DMF and NMP were obtained commercially from Aldrich (Oakville, Ontario) and stored at 4°C to minimize decomposition to dimethylamine and carbon dioxide. HPLC-grade solvents (acetonitrile, and methanol) were obtained from Caledon (Edmonton, Alberta) and used without further purification. HPLC-grade deionized water was obtained by passage of distilled water through a Millipore Simplicity water purification system. Borane-tetrahydrofuran complex (1.0 M) was obtained from Aldrich in 100 mL bottles and stored at 4°C. Peptide coupling reagents, HBTU and HOBt-H_2O, were purchased from Novabiochem and used without further purification. All other reagents were acquired commercially and used directly and used as received.

All glassware used in reactions (expect those done in water) were flamed dried under high vacuum (< 1 Torr), cooled to room temperature and then backfilled with nitrogen or argon. Evacuation and backfill cycles on the glassware were done at least three times until it was finally kept in an argon or nitrogen atmosphere. Heating of round bottom flasks during reactions was done in a silicone oil bath. Flash chromatography was performed through silica gel (230-400 mesh) purchased from Silicycle (Quebec City, Quebec). Thin layer chromatography was done on 0.25 mm Merck precoated silica plates (60F-254) and were visualized under shortwave ultraviolet light (254 nm), or by staining with 5% phosphomolybdic acid in ethanol or 1 mg/mL ninhydrin in ethanol (for amines) followed by heating over a heat gun. When not indicated, the reaction can be assumed to have been done at room temperature (~ 25°C).

Solid-phase reactions that could be done at room temperature were performed in sealed polypropylene filter vessels (BioRad) and vortexed on a platform shaker, or shaken on a mechanical shaker. Upon completion of the reaction, the resin was filtered directly inside the filter vessel and then rinsed repeatedly with solvent with vigorous vortexing in between rinses. Solid-phase reaction which required heating, were moisture or air sensitive, or done on a large scale (≥ 2 g of resin) were performed in a flamed dried, round bottom flask, and then transferred to a polypropylene filter vessel where the resin was rinsed. In cases where the resin stuck to the sides of the round bottom flasks, silanization of the glassware with 10% trimethylsilylchloride in toluene for 16 hours sometimes helped to alleviate this problem. However, silanized glassware cannot be flamed dried since it destroys the effect of silanization. Parallel reactions in some cases were performed using a Argonaut Quest semi-automated synthesizer. Loadings of resins were based on the initial loadings provided by the commercial supplier unless stated otherwise. Yields of products cleaved off the resin are crude yields unless stated otherwise.

NMR spectra were acquired on Varian INOVA 300, 400 and 500 spectrometers, or a Bruker WH-300 (75.5 MHz ^{13}C NMR only) in deuterated solvents referenced to the residual protonated form of the solvent. (Specific solvents are indicated for each compound). Coupling constants (*J*-values) are expressed in Hertz (Hz) and are considered precise to within ±0.5 Hz. Multiplicities are given the following abbreviations: s = singlet, d = doublet, t = triplet, and q = quartet. The carbon resonance of the trifluoroacetate counter ion in the polyamines are only observed in the ^{13}C NMR spectra when the sample is very concentrated. Methylene carbons in long aliphatic chains frequently overlap in the ^{13}C NMR spectra due to close chemical equivalence, and therefore, are not all observed. Trifluoroacetate salts obtained after TFA cleavage of resin bound substrates were often obtained as crude oils and thus gave poor elemental analyses. Oligoboronic acids cleaved from the resin gave very complex NMR spectra due to the formation of equilibrating boronic anhydrides. On aryl boronic acids, the carbon bonded to the boron is not observed in the ^{13}C NMR spectra due to slow relaxation.

LCMS analyses were performed on a Hewlett-Packard/Agilent 1100 MSD using an atmospheric pressure ionization (API) spray chamber. LC and MS conditions for each LCMS/UV analysis are described separately for each compound or library. High resolution electrospray mass spectra were acquired on a Micromass ZabSpec TOF. Infrared spectra were obtained NicPlan microscope coupled to a Nicolet-Magna-IR™ 750 spectrophotometer. Melting points were obtained on a Gallenkamp melting point apparatus and are uncorrected. Fluorescence titrations were performed on a Photon Technology International (PTI) fluorometer.

8.2: General procedure for the synthesis of polyamides on aminotrityl resin.

The resin is weighed into a polypropylene filter vessel and rinsed three times with DMF. A 0.5 M solution of FMOC-amino acid (2 equivalents with respect to the loading of the resin) in DMF is then added to the resin (In some cases, NMP is used in place of DMF for solubility reasons). The suspension is vortexed for 2 to 5 minutes before the addition of a 0.3 M DMF solution of HBTU and HOBt-H_2O (2 equivalents). After an additional 2 to 5 minutes of vortexing, DIPEA (4 equivalents) is added. The suspension is then vortexed for 2 hours, drained and rinsed five times with DMF. Ninhydrin[152] and bromophenol blue assays on the resin should be negative. The FMOC protective group is removed by treating the resin two times with 20% piperidine in DMF – first for 5 minutes then for 30 minutes. The resin is then rinsed five times with DMF. Both the amino acid coupling and the FMOC removal are repeated until the final amino acid is attached. To terminate the polyamide sequence with an acetyl group, the FMOC is first removed from the peptide for the final time. The resin is then swelled in DMF and Et_3N (0.4 mL per gram of resin) is added. The suspension is vortexed for 2 to 5 minutes before the addition of acetic anhydride (1.0 mL per gram of resin). After 1 hour of vortexing the resin is drained and rinsed with DMF (3×), methanol (3×), and dichloromethane (5×). It is then dried under high vacuum for >12 hours.

8.3: General procedure for the exhaustive amide reduction of polystyrene-bound polyamides.

To the resin-bound polyamide, weighed inside a flamed-dried, round bottom flask equipped with a condenser and a stir bar, is added the 1.0 M BH_3/THF solution (10 equivalents per amide) while under argon atmosphere. The suspension is then heated to 65 °C with gently stirring until the reaction is complete (typically 1 to 3 days). (Note: an argon atmosphere or a good nitrogen flow through the flask and condenser is required to ensure a successful reaction). Upon cooling to room temperature the suspension is quickly transferred into a polypropylene filter vessel via a pipette using dry THF to rinse the flask. After rinsing the resin with THF (5×), cleavage of the borane-amine adducts is done using either of two methods: 1) Iodine: To every 100 mg of resin is added 0.5 mL of dry THF, 0.14 mL of DIPEA, and then 0.28 mL of acetic acid in this order with vigorous vortexing in between each addition. This is followed by the careful addition (exothermic!) of iodine (5 equivalents per borane-amine adduct) in 0.5 mL of THF. The final ratio of THF:DIPEA:acetic acid should be approximately 7:1:2. The vessel is then vortexed for 4 hours at room temperature. Afterwards the resin is filtered and rinsed with THF (3×), 1:3 Et_3N/DMF (3×), methanol (3×), and dichloromethane (5×) and dried under high vacuum for >12 hours. A clean reaction will usually be indicated by the resin returning to its original pale colour prior to reduction. 2) Exchange with piperidine: The resin is rinsed with piperidine (3×), and then using approximately 2 – 3 mL of piperidine per 100 mg of resin, is transferred into a round bottom flask with a pipette and heated to 65°C for 16 hours. The suspension is then cooled and transferred into a new polypropylene vessel and rinsed with THF (3×), methanol (3×) and dichloromethane (5×) before it is dried under high vaccum for >12 hours.

8.4: Typical cleavage of solid-supported polyamide/polyamines from trityl linkers.

The resin is weighed into a round bottom flask and stirred in a 5% TFA/CH_2Cl_2 solution (15 - 20 mL per gram of resin) for 15 minutes to 1 hour depending on the amount of resin. The contents are then filtered through glass wool and the resin rinsed thoroughly with 5% TFA/dichloromethane (3×) followed by methanol (5×). The filtrate is evaporated and dried under high vacuum for >12 hours. In some cases, after filtering the resin, the filtrate is concentrated to a small volume (< 1 mL) and then flooded with diethyl ether to precipitate the product. The precipitate can then be isolated by filtration or centrifugation and dried under high vacuum.

On a small scale (< 5 mg), for LCMS analysis, the resin is placed inside a vial with teflon lined cap and then suspended in 1 mL of 5% TFA in dichloromethane for 10 to 15 minutes until it is filtered and evaporated.

8.5: Synthesis of polyamines on polystyrene resin.

1,3-diaminopropane trityl resin (45).

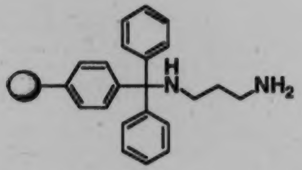

1,3-Diaminopropane (8.0 mL, 96 mmol) was dissolved in 4 mL of dry dichloromethane inside a 100 mL polypropylene filter vessel. Trityl chloride resin (0.987 g, 0.937 mmol, 0.95 mmol/g substitution according to the commercial source) was then added to the solution in 4 portions over one hour with vortexing in between additions. After vortexing for an additional hour, 2 mL of methanol was added followed by another 20 minutes of vortexing. The resin was then filtered and rinsed with methanol (3×), 1:4 Et_3N/DMF, (3×) methanol, and dichloromethane (5×) and dried under high-vacuum over for >12 hours to give 1,3-diaminopropane trityl resin **45** (1.024 g). A ninhydrin assay[152] gave a positive result (dark blue beads). Assumed complete conversion (theoretical loading: 0.92 mmol/g).

1,3-diaminopropane trityl resin linked *N*-acetyl-L-alanine-*N*-L-phenylalanine (21).

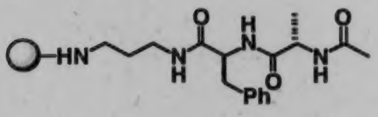

29

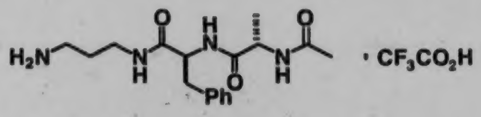

29'

Triamide **29** was synthesized as described in the general procedure for a polyamide. A portion of the resin was cleaved to give the trifluoroacetate salt **29'** which was checked by NMR and ESMS. Crude yield: 95%. ^{1}H NMR (300 MHz, CD_3OD) δ 7.35 - 7.18 (m, 5H), 4.46 (dd, *J* = 8.7 Hz, 6.3 Hz, 1H), 4.14 (apparent q, *J* =7.2 Hz, 1H), 3.24 (t, *J* = 8.4 Hz, 2H), 3.16 (dd, *J* =13.8 Hz, 6.3 Hz, 1H), 3.00 (dd, *J* =13.8 Hz, 8.7 Hz, 1H), 2.83 (dt, *J* = 3.3 Hz, 7.2 Hz, 2H), 1.96 (s, 3H), 1.77 (quintet. *J* = 6.8 Hz, 2H), 1.22 (d, *J* = 7.2 Hz, 3H). ^{13}C APT NMR (75.5 MHz, CD_3OD) δ 175.3 (C), 174.1 (C), 173.9 (C), 138.4 (C), 130.2 (CH), 129.5 (CH), 127.9 (CH), 56.3 (CH), 51.2 (CH), 38.1 (CH_2), 38.0 (CH_2), 36.9 (CH_2), 28.5 (CH_2), 22.5 (CH_3), 17.3 (CH_3). ESMS *m/z* 335.5 (MH^+).

12-Amino-(4*S*)-methyl-(7*S*)-benzyl-3,6,9-triazaundecane tetrakis-(trifluoroacetic acid) salt (LL-31).

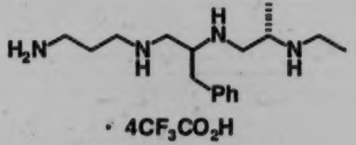

Resin-bound triamide **29** (0.351 g, 0.259 mmol, 0.74 mmol/g) was reduced over 24 hours and then treated with iodine as described in the general procedure to give the supported tetramine **30**. A portion of the tetramine (0.174 g, 0.134 mmol, 0.77 mmol/g) was cleaved to provide 95 mg (crude yield: 95%) of **LL-31** as a yellow oil. Purity by HPLC: 82%. HPLC conditions – column: Zorbax XDB-C8 (4.6 × 50 mm, 3.5 μm); eluent: 10% acetonitrile (0.1% TFA) and 90% water (0.1% TFA) to 20 % acetonitrile over 15 minutes

at 0.700 mL/min; column temperature: 20°C; detection: UV detection at 250 nm. ^{1}H NMR (300 MHz, CD_3OD) δ 7.38 - 7.18 (m, 5H), 3.24 - 2.84 (m, 12H), 2.79 (dd, *J* = 4.2, 13.5 Hz, 1H), 2.63 (dd, *J* = 7.8, 13.5 Hz, 1H) , 2.20 - 2.00 (m, 2H), 1.31 (t, *J* = 7.3 Hz, 3H), 1.27 (d, *J* = 6.8 Hz, 3H). ^{13}C APT NMR (75.5 MHz, CD_3OD) δ 138.5 (C), 130.3 (CH), 129.9 (CH), 127.9 (CH), 58.2 (CH), 54.9 (CH), 52.2 (CH_2), 49.2 (CH_2), 45.9 (CH_2), 41.3 (CH_2), 39.5 (CH_2), 37.8 (CH_2), 25.2 (CH_2), 14.8 (CH_3), 11.5 (CH_3). ESMS *m/z* 315.5 (MNa^+), 293.5 (MH^+), 147.6 ((M+2H)/2). HRMS-ESMS for $C_{17}H_{33}N_4$ (MH^+) calcd. 293.270522, obsd. 293.271472. IR (methanol cast) 3001 (N-H stretches), 1675, 1202, 1131, 799, 721. $[\alpha]_D$ = (+) 1.46° (c = 76.8 mg/mL in methanol).

12-Amino-(4*R*)-methyl-(7*R*)-benzyl-3,6,9-triazaundecane tetrakis-(trifluoroacetic acid) salt (DD-31).

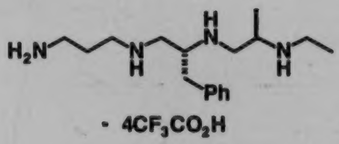

Procedure followed was the same as for **LL-31**. Crude yield: 92%. Purity by HPLC (same conditions as for **LL-21**): 86%. ^{1}H NMR (300 MHz, CD_3OD) δ 7.40 - 7.20 (m, 5H), 3.22 - 2.84 (m, 12H), 2.80 (dd, *J* = 4.2, 13.5 Hz, 1H), 2.63 (dd, *J* = 7.8, 13.5 Hz, 1H), 2.18 – 2.00 (m, 2H), 1.31 (t, *J* = 7.2 Hz, 3H), 1.28 (d, *J* = 6.6 Hz, 3H). ^{13}C APT NMR (75.5 MHz, CD_3OD) δ 138.5 (C), 130.3 (CH), 130.0 (CH), 128.0 (CH), 58.2 (CH), 54.9 (CH), 52.0 (CH_2), 49.2 (CH_2), 45.9 (CH_2), 41.3 (CH_2), 39.3 (CH_2), 37.8 (CH_2), 25.2 (CH_2), 14.8 (CH_3), 11.5 (CH_3). ESMS *m/z* 315.5 (MNa^+), 293.5 (MH^+). HRMS-ESMS for $C_{17}H_{33}N_4$ (MH^+) calcd. 293.270522, obsd. 293.270779. IR (methanol cast) 3006 (N-H stretches), 1673 cm^{-1}. $[\alpha]_D$ = (-) 14.7° (c = 24.3 mg/mL in methanol).

12-Amino-(4*S*)-methyl-(7*R*)-benzyl-3,6,9-triazaundecane tetrakis-(trifluoroacetic acid) salt (LD-31).

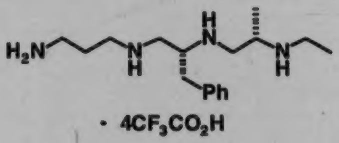

Procedure followed was the same as for **LL-31**. Crude yield: >99%. Purity by HPLC (same conditions as for **LL-31**): 78%. ^{1}H NMR (300 MHz, CD_3OD) δ 7.40 - 7.20 (m, 5H), 3.24 - 2.82 (m, 12H), 2.65 (dd, *J* = 7.2, 7.2 Hz, 1H), 2.61 (dd, *J* = 7.8, 7.8 Hz, 1H), 2.14 – 2.00 (m, 2H), 1.30 (t, *J* = 7.5 Hz, 3H), 1.29 (d, *J* = 7.2 Hz, 3H). ^{13}C APT NMR (75.5 MHz, CD_3OD) δ 138.5 (C), 130.7 (CH), 130.0 (CH), 128.0 (CH), 58.4 (CH), 54.9 (CH), 52.0 (CH_2), 50.7 (CH_2), 45.9 (CH_2), 40.6 (CH_2), 39.2 (CH_2), 37.8 (CH_2), 25.2 (CH_2), 14.5 (CH_3), 11.6 (CH_3). ESMS *m/z* 315.5 (MNa^+), 293.5 (MH^+). IR (methanol cast) 3006 (N-H stretches), 1675 cm^{-1}. HRMS-ESMS for $C_{17}H_{33}N_4$ (MH^+) calcd. 293.270522, obsd. 293.270182. $[\alpha]_D$ = (+) 1.45° (c = 25.2 mg/mL in methanol).

12-Amino-(4*R*)-methyl-(7*S*)-benzyl-3,6,9-triazaundecane tetrakis-(trifluoroacetic acid) salt (DL-31).

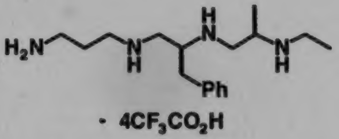

Procedure followed was the same as for **LL-23**. Crude yield: 95%. Purity by HPLC (same conditions as for **LL-31**): 80%. ^{1}H NMR (300 MHz, CD_3OD) δ 7.40 - 7.20 (m, 5H), 3.24 - 2.82 (m, 12H), 2.65 (dd, *J* = 8.4, 9.9 Hz, 1H), 2.60 (dd, *J* = 8.4, 8.4 Hz, 1H), 2.14 – 2.00 (m, 2H), 1.30 (t, *J* = 7.5 Hz, 3H), 1.29 (d, *J* = 6.6 Hz, 3H). ^{13}C APT NMR (75.5 MHz, CD_3OD) δ 138.5 (C), 130.3 (CH), 130.0 (CH), 128.0 (CH), 58.4 (CH), 55.0 (CH), 52.0 (CH_2), 50.7 (CH_2), 46.0 (CH_2), 40.6 (CH_2), 39.3 (CH_2), 37.8 (CH_2), 25.2 (CH_2), 14.5 (CH_3), 11.8 (CH_3). ESMS *m/z* 315.5 (MNa^+), 293.5 (MH^+). HRMS-ESMS for $C_{17}H_{33}N_4$ (MH^+) calcd. 293.270522, obsd. 293.270825. IR (methanol cast) 3006 (N-H stretches), 1674 cm^{-1}. $[\alpha]_D$ = (-) 1.17° (c = 28.3 mg/mL in methanol).

N^{3,6,9}- triacetyl-12-amino-(4*R*)-methyl-(7*S*)-benzyl-3,6,9-triazaundecane trifluoroacetate (32).

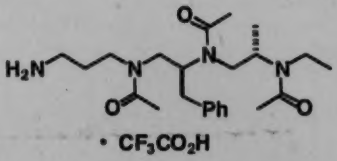

The supported tetramine **30** (86 mg, 0.072 mmol, 0.84 mmol/g) was swelled in 1.0 mL of DMF. Et_3N (0.21 mL) was added and the resin vortexed for one minute before the addition acetic anhydride (0.34 mL). The suspension was vortexed for 16 hours and then rinsed with DMF (3×), methanol (3×) and dichloromethane (5×) and dried under high vacuum for >12 hours to give the resin-bound tetramine triacetate (0.130 g). A portion of the resin (26.4 mg, 0.020 mmol, 0.76 mmol/g) was cleaved from the support with 5 % TFA/CH_2Cl_2 as described above to afford 11 mg (>99% crude yield) of the tetramine triacetate trifluoroacetate salt **32**. Purity by HPLC (same conditions as for **LL-31**): 82 %. ^{1}H NMR (300 MHz, CD_3OD) δ mixture of 9 amide rotomers. IR (methanol cast) 2984.34 (N-H stretches), 1677, 1617. HRMS-ESMS for $C_{23}H_{39}N_4O_3$ (MH^+) calcd. 419.302217, obsd. 419.301333.

1,6-diaminohexane trityl resin (37).

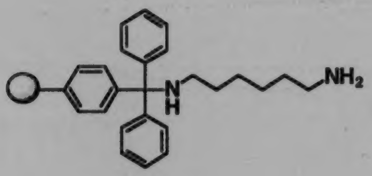

To 1,6-diaminohexane (11.16 g, 95 mmol) in 25 mL of dichloromethane (turbid solution), stirring inside a dry round bottom flask under argon, was added trityl chloride polystyrene resin (2.02 g, 1.9 mmol, 0.95 mmol/g) portionwise over an hour. Additional dichloromethane was used to rinse the resin from the sides of the flask. The suspension was stirred for an additional hour before adding 5 mL of methanol. After a further 20 minutes of vortexing, the stirred was drained and the resin rinsed with methanol (3×), 1:4 Et_3N/DMF (3×), methanol (3×), and dichloromethane (5×) and then dried under vacuum overnight to give resin **37** (2.11g, theoretical loading, assuming complete coupling, is 0.88 mmol/g).

Trityl-polystyrene bound $H_2N(CH_2)_6$NH-Gly-εAhx-βAla-Ac (38).

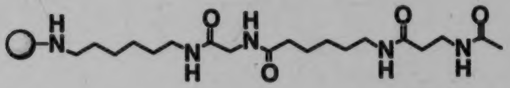

38

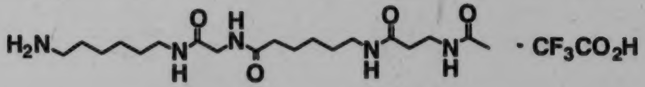

38'

The resin-bound tetramide was prepared starting from resin **37** and using the general amide coupling procedure described in the general section using HO-Gly-FMOC, HO-εAhx-FMOC, and HO-βAla-Ac. A portion of the resin (78 mg, 0.076 mmol) was cleaved in 1.0 mL of 5 % TFA in dichloromethane to give the trifluoroacetate salt **38'** (24 mg, 62 %) which was checked by ESMS and ^{1}H NMR. ^{1}H NMR (500 MHz, CD_3OD) δ 3.78 (s, 2H), 3.40 (t, *J* = 7.0 Hz, 2H), 3.20 (t, *J* = 7.0 Hz, 2H), 3.16 (t, *J* = 7.0 Hz, 2H), 2.91 (t, *J* = 7.5 Hz, 2H), 2.36 (t, *J* = 7.0 Hz, 2H), 2.27 (t, *J* = 7.5 Hz, 2H), 1.91 (s, 3H), 1.70 – 1.60 (m, 4H), 1.52 (sextet, *J* = 6.5 Hz, 4H), 1.42 – 1.33 (m, 6 H). ESMS *m/z* 400.2 (MH^+).

Trifluoroacetate salt of pentamine (39).

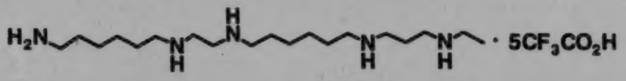

The resin-bound peptide **38** was reduced with 1.0 M BH_3/THF over 48 hours as described in the general section using the iodine promoted work-up to give the bound pentamine **35**. Cleavage of **35** (0.179 g, 0.181 mmol at 1.03 mmol/g) with 10 mL of 5% TFA in dichloromethane for 1 hour afforded the crude product **39** as dark oil (0.119 g, 71%). The oil was purified by precipitation of a concentrated methanol solution with diethyl ether giving a brown solid (74 mg, 44%). HPLC conditions – column: Zorbax SB-C8 (2.1 × 50 mm, 3.5 μm); eluent: 5 to 85% acetonitrile (0.1% TFA) in water (0.1% TFA) over 5 minutes at 0.5 mL/min then maintained at 85% for another 7 minutes; column temperature: 25°C; MS conditions – Capillary voltage (positive mode): 3200 V; mass scanning range: 100 – 800 amu; fragmentor voltage: 80 V; drying gas temperature: 350°C; gas flow 10L/min; nebulizer pressure: 40 psig. ^{1}H NMR (500 MHz, CD_3OD) δ 3.41 (s, 4H), 3.13 – 2.00 (m, 14H), 2.92 (m ,2H), 2.12 – 2.07 (m, 2H), 1.76 – 1.66 (m, 8H), 1.45 (m, 8H), 1.31 (t, *J* = 7.3 Hz, 3H). ^{13}C APT NMR (125 MHz, DMSO-d_6) δ 158.7 (quartet, $\underline{C}OCF_3$), 116.8 (quartet, $CO\underline{C}F_3$), 46.8 (CH_2), 46.5 (CH_2), 43.8 (CH_2), 42.5 (CH_2), 418 (CH_2), 38.6 (CH_2, two overlapping signals), 26.7 (CH_2), 25.5 (CH_2), 25.4 (CH_2), 25.3 (CH_2), 25.3 (CH_2), 25.3 (CH_2), 22.3 (CH_2), 10.7 (CH_3) (note: a number of CH_2 from the aliphatic chain overlap due to close chemical equivalence). IR (microscope): 3050 (N-H stretches), 2944, 2868, 1667, 1475, 1423, 1198, 1134, 834, 799, 721 cm^{-1}. HRMS-ESMS for $C_{19}H_{46}N_5$ (MH^+) calcd. 344.37477, obsd. 344.37449.

Trityl-polystyrene bound $H_2N(CH_2)_6NH$-Amc-LVal-4Amb-Ac (42).

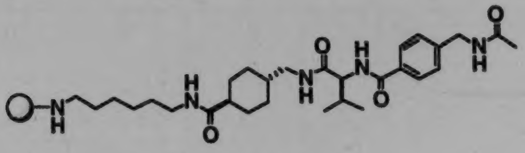

42

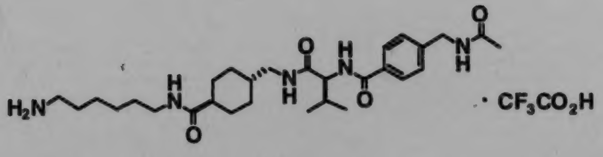

42'

The resin-bound tetramide **42** was prepared using the general amide coupling procedure described above using Amc-FMOC, LVal-FMOC and 4Amb-Ac. A portion of the resin was cleaved with 5% TFA in dichloromethane to give the trifluoroacetate salt **42'** which was checked by ESMS and ^{1}H NMR. ^{1}H NMR (300 MHz, CD_3OD) δ 7.80 (d, J = 8.4 Hz, 2H), 7.38 (d, J = 8.4 Hz, 2H), 4.41 (s, 2H), 4.27 (d, J = 8.1 Hz, 2H), 3.20 - 2.96 (m, 4H), 2.90 (t, J = 7.5 Hz, 2H), 2.22 - 2.04 (m, 2H), 2.00 (s, 3H), 1.90 - 1.30 (m, 16H), 1.01 (d, J = 6.6 Hz, 3H), 1.00 (d, J = 6.9 Hz, 3H). ESMS *m/z* 530.3 (MH^+).

Trifluoroacetate salt of pentamine 43.

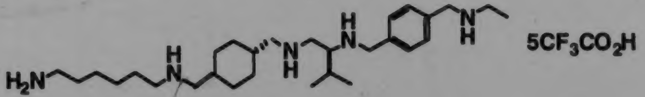

The reduction of **42** with BH_3 was done over a period of 48 hours using both the iodine- and the piperidine promoted work-ups as described in the general section. Obtained in both cases was the resin bound pentamine **36** which was cleaved to provide **43**. Iodine procedure - Crude yield: 69% as a brown oil. Purity by HPLC: 78% by UV (210 nm), 72% by MS. Piperidine procedure - Crude yield: 65% as a colourless oil. Purity by HPLC: 89% by UV (210 nm), 89% by MS. HPLC/MS conditions were same as for pentamine **39** except for UV detection at 210 nm.. ^{1}H NMR (500 MHz, CD_3OD) δ 7.65

(d, *J* = 8.2 Hz, 2H), 7.55 (d, *J* = 7.9 Hz, 2H), 4.44 (d, *J* = 13.1 Hz, 1H), 4.35 (d, *J* = 13.1 Hz, 1H), 4.22 (s, 2H), 3.62 – 3.60 (m, 2H), 3.47 (dd, *J* = 3.0, 14.5 Hz, 1H), 3.41 (dd, *J* = 7.5, 14.5 Hz, 2H), 3.09 (q, *J* = 7.5 Hz, 2H), 3.04 – 2.90 (m, 6H), 2.86 (d, *J* = 7.0 Hz, 2H), 2.42 (m, 1H), 1.97 – 1.82 (m, 4H), 1.80 – 1.62 (m, 6H), 1.45 – 1.42 (m, 4H), 1.32 (t, *J* = 7.0 Hz, 3H), 1.12 (d, *J* = 7.0 Hz, 3H), 1.12 – 1.04 (m, 2H), 1.05 (d, *J* = 7.0 Hz, 3H). ^{13}C APT NMR (75.5 MHz, CD_3OD) δ 162.2 (q, $\underline{C}OCF_3$), 134.2 (CH), 133.6 (CH), 132.2 (C), 132.1 (C), 117.8 (q, $CO\underline{C}F_3$), 61.9 (CH), 55.7 (CH_2), 54.6 (CH_2), 51.3 (CH_2), 50.2 (CH_2), 49.4 (CH_2), 47.4 (CH_2), 43.8 (CH_2), 40.5 (CH_2), 36.1 (CH), 36.0 (CH), 30.8 (CH_2), 30.4 (CH_2), 28.1 (CH_2), 28.3 (CH), 27.0 (CH_2), 26.9 (CH_2), 26.8 (CH_2), 18.8 (CH_3), 16.0 (CH_3), 11.3 (CH_3). IR (methanol cast): 2942 (broad), 1675, 1203, 1135, 836, 800, 722 cm^{-1}. HRMS-ESMS for $C_{29}H_{56}N_5$ (MH^+) calcd 474.453572, found 474.454339.

8.6: Synthesis of PhTX-433 analogue.

Trityl polystyrene bound $H_2N(CH_2)_3NH$-L-Ala-γAbu (46).

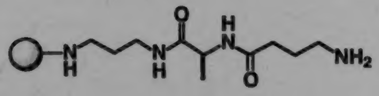

46

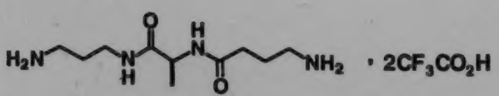

46'

Resin-bound diamide **46** was prepared using the general amide coupling procedure described above starting from 1,3-diaminopropane trityl resin (**16**) and using HO-LAla-FMOC and then HO-γAbu-FMOC. A portion of the resin was cleaved 5% TFA in dichloromethane to give the di(trifluoroacetate) salt **46'** which was checked by ESMS and ^{1}H NMR. ^{1}H NMR (300 MHz, CD_3OD) δ 4.22 (q, *J* = 7.2 Hz, 1H), 3.30 (t, *J* = 7.0 Hz, 2H), 2.97 (t, *J* = 7.0 Hz, 2H), 2.94 (t, *J* = 7.0 Hz, 2H), 2.37 (t, *J* = 7.1 Hz, 2H), 1.92 (quintet, *J* = 7.2 Hz, 2H), 1.84 (quintet, *J* = 7.2 Hz, 2H), 1.35 (d, *J* = 7.2 Hz, 3H). ESMS *m/z* 231.1 (MH^+).

Trityl-polystyrene bound 1,12-diamino-(7*S*)-methyl-5,8-diazadedacane (47).

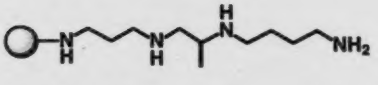

47

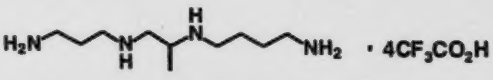

47'

Reduction of the resin bound diamide **46** was achieved using the general borane reduction/iodine work-up protocol described above to give **47**. Approximately 40 mg was cleaved from the resin using 5% TFA/dichloromethane to give the tetrakis(trifluoroacetate) salt **47'**. ^{1}H NMR (300 MHz, CD_3OD) δ 3.71 (apparent heptet, 1H), 3.48 (dd, *J* = 5.9 Hz, 13.4 Hz, 1H), 3.31 (dd, *J* = 5.9 Hz, 13.4 Hz, 1H), 3.24 – 2.94 (m, 8H), 2.12 (quintet, *J* = 7.8 Hz, 2H), 1.90 – 1.65 (m, 4H), 1.46 (d, *J* = 6.9 Hz, 3H). ^{13}C NMR (75.5 MHz, CD_3OD) δ 163.2 ($\underline{C}OCF_3$), 52.9 (CH), 50.8 (CH_2), 46.9 (CH_2), 45.9 (CH_2), 39.9 (CH_2), 37.9 (CH_2), 25.5 (CH_2), 24.3 (CH_2), 15.0 (CH_3). ESMS-HRMS for $C_{10}H_{27}N_4$ (MH^+) calcd. 203.223572, obsd. 203.223107.

Trityl-polystyrene bound BOC protected tetramine (48).

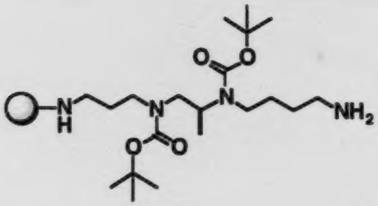

The resin-bound tetramine **47** (138 mg, 0.091 mmol at 0.66 mmol/g) was rinsed three times with DMF. 2-acetyldimedone (33 mg, 0.18 mmol) in 1.0 mL DMF was then added to the resin. The suspension was vortexed for 2 hours before it was drained and rinsed with DMF (3×) and dichloromethane (5×). The resin was resuspended in 1.0 mL of dichloromethane, and to this was added DIPEA (65 μL, 0.36 mmol). After vortexing for 1 minute, a concentrated solution of $(BOC)_2O$ (159 mg, 0.728 mmol) in 0.5 mL dichloromethane was added. The suspension was vortexed for 14 hours before it was filtered and rinsed with dichloromethane (3×) and DMF (5×). This was followed by two treatments of 1.5 mL of a 2% $H_2NNH_2 \cdot H_2O$ solution in DMF for 10 minutes and then 30 minutes to afford **48** which was used directly in the next step (below).

PhTX-433 analogue (PhTX-43'3•3TFA).

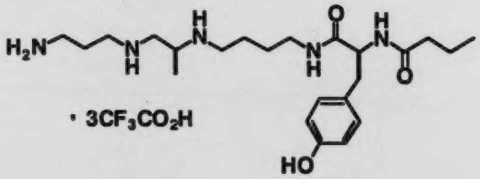

To the resin-bound BOC protected tetramine **48** was coupled to Tyr(O*t*Bu)-FMOC and then butyric anhydride, using the peptide coupling protocol described above, and then dried under high vacuum for >12 hours. The resin (96 mg, 0.049 mmol at 0.51 mmol/g) was weighed into a 25 mL round bottom flask and suspended in 4 mL of a solution containing 95 % TFA, 2.5 % TIPS and 2.5 % water. The suspension was stirred for 2 hours and then filtered through glass wool. The filtrate was concentrated to an oil and then redissolved in a small amount of methanol. This solution was then flooded with diethyl ether and cooled to 4°C to precipitate the product. The clear supernatant was removed and the precipitation procedure repeated. The precipitate was then dried under high vacuum for 16 hours to afford a yellow solid that was **PhTX-43'3•3TFA** in 75% yield (29 mg) from the diamide **47** in 88% purity as determined by HPLC. (Conditions – column: Zorbax SB-C18, 4.6 × 150 mm, 5 μm; gradient: 10% acetoniltrile (0.1% TFA) and 90% water (0.1% TFA) for 20 minutes at 1.5 mL/min; UV detection: 274 nm; column temperature: 2°C). ^{1}H NMR (300 MHz, CD_3OD) δ 7.04 (d, *J* = 8.1 Hz, 2H), 6.70 (d, *J* = 8.4 Hz, 2H), 4.40 (dd, *J* = 6.9 Hz, 8.5 Hz, 1H), 3.62 – 3.50 (m, 1H), 3.28 – 2.96 (m, 10H), 2.97 (dd, *J* = 6.6 Hz, 13.8 Hz, 1H), 2.80 (dd, *J* = 8.7 Hz, 13.8 Hz, 1H), 2.16 (t, *J* = 7.2 Hz, 2H), 2.12 – 1.98 (m, 2H), 1.70 – 1.46 (m, 6H), 1.42 (d, *J* = 6.6 Hz, 3H), 0.84 (t, *J* = 7.5 Hz, 3H). ^{13}C APT NMR (75.5 MHz, CD_3OD) δ 176.1 (C), 174.1 (C), 163.2 (q, $\underline{C}OCF_3$), 157.3 (C), 131.3 (CH), 129.1 (C), 118.1 (q, $CO\underline{C}F_3$), 116.2 (CH), 56.8 (CH), 52.7 (CH), 50.6 (CH_2), 46.9 (CH_2), 46.2 (CH_2), 39.2 (CH_2), 38.7 (CH_2), 38.2 (CH_2), 37.8

(CH_2), 27.2 (CH_2), 25.5 (CH_2), 24.5 (CH_2), 20.2 (CH_2), 15.1 (CH_3), 13.9 (CH_3). HRMS-ESMS for $C_{23}H_{42}N_5O_3$ (MH^+) calcd. 436.328766, obsd. 436.329035.

8.7: Polyamine library synthesis and decoding on polystyrene resin.

1,2-diaminodedacane trityl polystyrene resin (50).

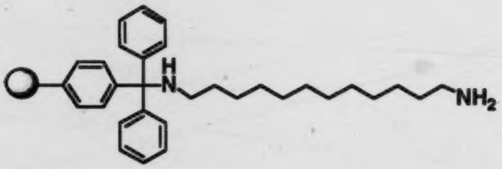

The resin was prepared in the same manner as 1,6-diaminohexane trityl resin (**37**) using 1,12-diaminodedacane (12.54 g, 62.58 mmol) in 60 mL of dry CH_2Cl_2 (turbid solution) and chlorotrityl polystyrene resin (1.07 mmol/g according to the commercial supplier, 1.950 g, 2.086 mmol). Obtained 1.469 g of resin **50** (Theoretical loading is 0.91 mmol/g.)

Partial termination synthesis of the triamide library.

The synthesis of the split-pool triamide library was done using a semi-parallel automated synthesizer. The resin was split 14 portions (102 mg, 0.093 mmol each) into 5 mL reaction vessels and rinsed with dichloromethane (3×) and then NMP (3×). To each vessel was added 0.7 mL of an NMP solution containing 0.51 M of the FMOC amino acid (0.36 mmol) and 0.057 M of the *N*-acyl amino acid (0.04 mmol). The suspensions were mixed for 5 minutes before the addition of 1.2 mL of an NMP solution containing 0.30 M HBTU (0.36 mmol) and 0.30 M HOBt•H_2O (0.36 mmol). After mixing for 1 minute the DIPEA (0.12 mL 0.7 mmol) was added. The suspensions were then mixed for 2 hours before they were drained and rinsed with NMP (3×) and dichloromethane (5×). Ninhydrin[152] assays of all 14 portions were negative indicating no free amines. The resins were then resuspended in dichloromethane, and mixed thoroughly into a single polypropylene reaction vessel. The pooled resin was then dried under high vacuum for 16 hours. The average loading, using the average molecular mass of all amino acids that had been coupled, was calculated to be 0.69 mmol/g. The resin was again split 14 portions (100 mg 0.069 mmol) into 5 mL reaction vessels. The FMOC protective groups were removed by two treatments with 1:4 piperidine in NMP (5 minutes, then 30 minutes), and then resin was rinsed with NMP (5×). A similar amide coupling procedure as described above was employed except using 0.55 mL of a 0.50 M solution of the *N*-acyl amino acids (0.28 mmol) in NMP, 0.92 mL of an NMP solution containing 0.30 M HBTU (0.28 mmol) and 0.30 M HOBt•H_2O (0.28 mmol), and then DIPEA (96 μL, 0.55 mmol). Ninhydrin assays from each vessel were negative. The resin portions were then mixed using the method described above to give the encoded, split-pool library of triamides. The average loading was calculated to be 0.72 mmol/g.

Preparation of the tetramide library (51).

The tetramide library (**51**) was synthesized in a similar manner as described for the triamide library, except involving a second amide coupling with a 9:1 mixture of FMOC amino acid and *N*-acyl amino acid before complete sequence termination with the *N*-acyl amino acid. Average loading: 0.62 mmol/g.

Preparation of the tetramine library.

To the tripeptide library (397.6 mg, approx. 0.286 mmol), weighed into a 25 mL round bottom flask equipped with a condenser and stir bar, was added 1.0 M BH_3/THF (8.6 mL, 8.6 mmol) while under nitrogen atmosphere. The suspension was slowly stirred for 2 days at 65°C. It was then transferred into a 10 mL polypropylene reaction vessel and rinsed with THF (4×). 1 mL of THF was added followed by 0.28 mL of DIPEA, 0.56 mL acetic acid and a 1 mL solution of I_2 (1.11 g, 4.29 mmol) in THF. The suspension was vortexed for four hours until it was filtered and rinsed with THF (4×), 1:3 Et_3N/DMF (4×), methanol (4×), and dichloromethane (5×) and then dried over 16 hours under high vaccumm to give the triamine library. Average loading: 0.74 mmol/g.

Preparation of the pentamine library (52).

The reduction of the tetramides **50** towards the pentamine library was done in a similar manner as with the tripeptide library except the reaction was over 3 days. Average loading: 0.64 mmol/g.

Single bead resin cleavage and LCMS analysis.

The dried beads were spread out on glass Petri dish and observed under a microscope. The beads were picked up using the tip of a 25 μL glass microsyringe containing 5 to 7.5 μL of 5% TFA in dichloromethane, and then transferred into a 200 μL glass conical microvial. The TFA solution was injected into the microvial which concomitantly removed the bead from the syringe tip into the microvial with the solution. The microvial was then placed inside an 2 mL volume autosampler vial which was then capped. After 15 minutes the cap was removed from the autosampler vial to allow the TFA solution to evaporate. Methanol (5.0 - 7.5 μL) was added to the conical microvial and the solution injected into an LCMS. The identity of each polyamine sequence was determined by the mass differences between the partially terminated sequences and the full sequence that eluted through the LC column. LC conditions - column: Zorbax SB-C8 4.6×50 mm, 3.5 μm; eluent: 15 to 85% acetonitrile (0.1% TFA) in water (0.1% TFA) over 5 minutes then maintained at 85% for 7 minutes at 0.7 mL/min; MSD conditions - capillary voltage: 3200 V (positive mode); fragmentor voltage: 120 V; mass scanning range: 250 – 900 amu; nebulizer pressure: 40 psig; gas temperature: 350°C; drying gas flow: 10.0 L/min.

8.8: Library screening against trisulfonated dyes.

Screening of the tetramine library against trisulfonated dyes.

Approximately 3 mg of resin bound tetramine (~ 13000 beads) was added to 400 μL of a 0.050 M solution of MES-TRIS (pH 7.0 in water) in 1:9 water/DMF ('solution A') inside a 2.5 cm diameter, 0.8 cm deep glass Petri dish. Resin clumps were broken up either physically or by vigorous swirling of the dish. 12.8 μL of a 1.25×10^{-3} M solution of the dye in 'solution A' was then quickly added to the swirling suspension to make a final dye concentration of 3.75×10^{-5} M. For screening in the presence of spermidine, 12.8 μL of a 1.05×10^{-2} M solution of spermidine in 'solution A' was first added and, after 10 minutes of swirling, was followed by the addition of 12.8 μL of a 1.25×10^{-3} M solution of the dye in 'solution A'. The final concentration of spermidine was 3.16×10^{-4} M. In both cases the suspension was swirled for 1 hour during which time the dye solution turned clear. While under a microscope, the darkest beads were isolated with a thin glass capillary and transferred onto another Petri dish where they were washed with 1:9 water/DMF with no buffer (5×) and dichloromethane (5×) with the capillary. The beads were then transferred into a conical microvial and analysed by LCMS using the method described above. Screenings at pH 5.5 were done the same way as outlined above except in a solution of 0.025 M MES buffer (pH 5.5 in water) in 1:9 water/DMF ('solution B').

8.9: Synthesis of triamine-amides, and determination of binding constants.

Triamine amide 8Aoc^R-8Aoc^R (62).

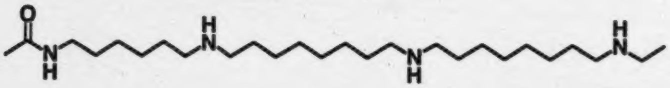

From 1,6-diaminohexane polystyrene-trityl resin **37** the triamide **60** was prepared using the standard amide coupling protocol described in the general section with the amino acid derivatives HO-8Aoc-FMOC and HO-8Aoc-Ac. Resin **60** (0.418 g, 0.314 mmol, 0.75mmol/g) was then treated with 1.0 M BH_3 in THF (11.5 mL, 11.5 mmol) as described above. After 2 days at 65°C the resin was filtered, rinsed with THF and then treated with I_2 (1.280 g, 4.955 mmol) in a 7/2/1 mixture of THF, acetic acid and DIPEA for four hours according to the general procedure. It was then rinsed with THF (4×), 1:3 Et_3N/DMF (4×), methanol (4×), and dichloromethane (5×) to give the supported tetramine. The resin was resuspended in 2 mL of dichloromethane, and to this was added DIPEA (0.26 mL, 1.5 mmol) followed by $(BOC)_2O$ (0.69 mL, 3.0 mmol). The suspension then was vortexed for 24 hours before it was rinsed with dichloromethane (5×). The BOC protected tetramine **61** was subsequently cleaved from the resin by repeated treatments with 1% TFA in dichloromethane (3 mL each time, 10 times all together). After each treatment, the resin was filtered and the filtrate collected as a separate fraction containing 2 mL of 10% pyridine in methanol. The fractions were checked by LCMS and those containing pure compound were combined and evaporated. The residue was then dissolved in 2 mL of pyridine and cooled to 0°C before the addition of Ac_2O (50 μL, 0.53 mmol). After stirring for 5 hours at room temperature the reaction was concentrated and then suspended in 50 mL of water. The product was extracted into ether (3×30 mL) and washed with water (2×20 mL), brine (20 mL) and dried over anhydrous Na_2SO_4. Flash column chromatography through silica gel using 5% methanol in dichloromethane yielded the BOC-protected triamine-amide. Exposure to 1:1 TFA/dichloromethane for one hour followed by evaporation yielded the final product **62** as a clear oil (42 mg, 19% yield based on theoretical loading of resin-bound triamide **60**). ^1H NMR (500 MHz, 20 % D_2O in DMSO-d_6) δ 2.98 (t, J = 7.0 Hz, 2H), 2.84 (q, J = 7.5, 2H), 2.82 – 2.79 (m, 10H), 1.78 (s, 3H), 1.51 (broad s, 8H), 1.35 (quintet, J = 7.0 Hz, 2H), 1.30 – 1.80 (m, 22H), 1.13 (t, J = 7.5Hz, 3H). ^{13}C APT NMR (125 MHz, CD_3OD) δ 173.2 (CO), 49.0 (CH_2), 49.0 (CH_2), 48.5 (CH_2), 44.1 (CH_2), 40.2 (CH_2), 30.8 (CH_2), 30.2 (CH_2), 30.0 (CH_2), 27.5 (CH_2), 27.4 (CH_2), 27.4 (CH_2), 27.3 (CH_2), 27.3 (CH_2), 27.2 (CH_2), 22.7 (CH_3), 11.6 (CH_3); note the large amount of overlap of the aliphatic CH_2 signals in the ^{13}C NMR spectrum. IR (methanol cast) 3300, 2937, 1674 cm^{-1}. HRMS-ESMS for $C_{26}H_{57}N_4O$ (MH^+) calcd. 441.453238 obsd. 441.453572.

Triamine amide 2Acc^{R}-εAhx^{R} (66).

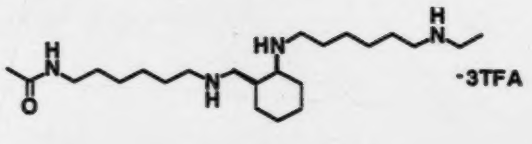

The synthesis of the resin supported triamide **63**, using HO-2Acc-FMOC and HO-εAhx-Ac, and the exhaustive amide reduction with the iodine procedure was done as described in the general section. However, after the iodine-promoted work-up significant amounts of triaminoborohydride **64** were detected by LCMS of the cleaved product. Full conversion to triamine **65** was achieved after vortexing the resin (0.410 g, 0.332 mmol) in 8 mL of THF containing 1.0 mL of ethylene glycol and 0.5 mL of DIPEA for 16 hours followed by rinsing with THF (3×), methanol (3×), and dichloromethane (5×). The entire amount of this resin was subsequently BOC protected, cleaved from the resin, acetylated and finally deprotected using the same procedure described in the synthesis of triamine-amide **60**. Obtained **66** (45 mg, 15 % yield based on theoretical loading of resin-bound triamide **63**) as a clear oil ^{1}H NMR (500 MHz, 20 % D$_2$O in DMSO-d$_6$) δ 3.20 (m, 1H), 3.11 (t, *J* = 12.5 Hz, 1H), 2.98 (t, *J* = 7.0 Hz, 2H,), 2.95 - 2.78 (m, 10H), 2.33 (m, 1H), 1.78 (s, 3H), 1.75 - 1.60 (m, 3H), 1.60 – 1.55 (m, 6H), 1.43 – 1.34 (m, 6H), 1.27 (broad s, 9H), 1.31 (t, *J* = 7.5 Hz, 3H). ^{13}C APT NMR (125 MHz, CD$_3$OD) δ 173.1 (C), 163.2 (q, $\underline{C}$OCF$_3$), 118.1 (q, CO$\underline{C}$F$_3$), 60.3, (CH), 47.0 (CH$_2$), 48.3 (CH$_2$), 47.1 (CH$_2$), 45.7 (CH$_2$), 44.1 (CH$_2$), 40.2 (CH$_2$), 35.4 (CH), 30.2 (CH$_2$), 27.4 (CH$_2$), 27.2 (CH$_2$), 27.2 (CH$_2$), 27.2 (CH$_2$), 27.1 (CH$_2$), 27.0 (CH$_2$), 26.8 (CH$_2$), 25.4 (CH$_2$), 24.8 (CH$_2$), 22.7 (CH$_3$), 20.8 (CH$_2$), 11.6 (CH$_3$). IR (methanol cast) 3425, 2943, 2865, 1676 cm^{-1} HRMS-ESMS for C$_{23}$H$_{49}$N$_4$O (MH$^+$) calcd. 397.390638 obsd. 397.390081.

NMR titration of dyes 59 and 58 with triamine amides 62 and 66.

To a 2.56×10^{-3} M solution of triamine-amide in 0.6 mL of 20% D$_2$O/DMSO-d$_6$ inside an NMR tube, was added increasing amounts of dye (c = 0.066 M), dissolved the same solvent mixture. Initially small increments of the dye were added (2.4 μL, 0.1 equivalents) but as the change in chemical shift became smaller, larger volumes (12 μL, 0.8 equivalents) were added. For **62** the methylene protons at 1.226 ppm were monitored. For **66** the methylenes at 1.271 ppm were observed. The K_a's were determined using the curve fitting software developed by Christopher A. Hunter (http://www.shef.ac.uk/uni/projects/smc/software.html).

Job Plot of dye 58 and triamine amide 62.

Equimolar solutions (c = 0.132 M) of **62** and **58** were prepared in 20 % D_2O/DMSO-d_6. In separate NMR tubes, varying proportions of each solution were prepared maintaining a total volume of 20 μL. They were then diluted to 0.7 mL and the change in the chemical shift of the dye proton at 7.445 ppm was monitored.

8.10: Dye extractions.

Trityl-polystyrene bound 2Acc^R-εAhx^R (67).

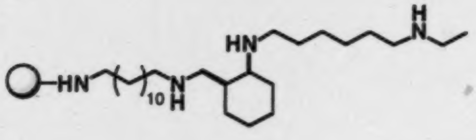

67

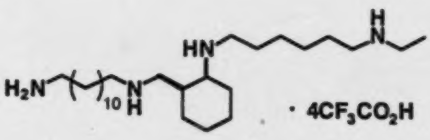

67'

The synthesis of the resin supported triamide precursor to **67** and the exhaustive amide reduction with the iodine procedure was done as described in the general section. The only exception was the additional work-up with ethylene glycol that was described for the synthesis of **66**. A portion of the resin (95 mg at 0.74 mmol/g, 0.0705 mmol) was cleaved with 5% TFA in dichloromethane for one hour and then filtered through glass wool. The resin was washed with methanol and the filtrate evaporated giving a yellow oil (40 mg crude, 63%) corresponding to the tetrakis(trifluoroacetate) salt **67'**. ^{1}H NMR (500 MHz, CD_3OD) δ 3.35 (m, 1H), 3.15 - 2.96 (m, 6H), 2.98 (m, 2H) 2.91 (m, 4H), 2.55 (m, 1H), 1.94 - 1.30 (m, 36H), 1.29 (t, *J* = 7.5 Hz, 3H). ^{13}C APT NMR (125 MHz, CD_3OD) δ 162.6 (q, $\underline{C}OCF_3$), 118.2 (q, $CO\underline{C}F_3$), 60.3 (CH), 50.1 (CH_2), 48.3 (CH_2), 47.1

(CH_2), 45.7 (CH_2), 44.1 (CH_2), 40.9 (CH_2), 35.4 (CH), 30.7 (CH_2), 30.7 (CH_2), 30.6 (CH_2), 30.6 (CH_2), 30.5 (CH_2), 30.3 (CH_2), 30.2 (CH_2), 28.7 (CH_2), 27.7 (CH_2), 27.5 (CH_2), 27.1 (CH_2), 26.8 (CH_2), 25.4 (CH_2), 24.4 (CH_2), 24.5 (CH_2), 11.6 (CH_3). IR (methanol cast) 3300 - 2700, 2931, 1677 cm^{-1}. HRMS-ESMS for $C_{27}H_{59}N_4O$ (MH$^+$), calcd. 439.473973 obsd. 439.473684.

Trityl-polystyrene bound 8Aoc^R-8Aoc^R (68).

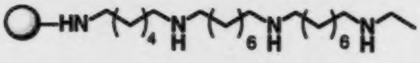
68

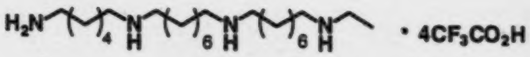
68'

The synthesis of the resin supported triamide precursor to **67** and the exhaustive amide reduction with the iodine procedure was done as described in the general section. A portion of the resin (175 mg at 0.92 mmol/g, 0.16 mmol) was cleaved with 5% TFA in dichloromethane for one hour and then filtered through glass wool. The resin was washed with methanol and the filterate evaporated giving a yellow oil (111 mg crude, 80%) corresponding to the tetrakis(trifluoroacetate) salt **68'**. ^{1}H NMR (500 MHz, CD_3OD) δ 3.04 (q, J = 7.5 Hz, 2H), 3.02 – 2.95 (m, 9H), 2.92 (t, J = 8.0 Hz, 2H), 1.75 – 1.62 (m, 12H), 1.45 – 1.42 (m, 8H), 1.42 – 1.35 (m, 12H), 1.29 (t, J = 7.0 Hz, 3H). ^{13}C APT NMR (125 MHz, CD_3OD) δ 162.9 (q, $\underline{C}OCF_3$), 118.2 (q, $CO\underline{C}F_3$), 49.0 (CH_2 broad peak with a shoulder; likely more than one signal), 48.9 (CH_2), 48.5 (CH_2), 44.1 (CH_2), 40.6 (CH_2), 30.0 (CH_2), 28.0 (CH_2), 27.5 (CH_2), 27.4 (CH_2), 27.3 (CH_2), 27.1 (CH_2), 27.0 (CH_2), 11.6 (CH_3); note the large number of overlapping aliphatic CH_2 signals. IR (methanol cast) 3300 - 2700, 2931, 1677 cm^{-1}. HRMS-ESMS for $C_{27}H_{59}N_4O$ (MH$^+$), calcd. 439.473973 obsd. 439.473684.

Staining of resin-bound tetramines with a 1:1 mixture of 58 and 59.

Tetramine resin **67** or **68** (12 mg, 0.0087 mmol) was vortexed for 1 hour in 3 mL of "solution A" containing 0.0017 M of **59** and 0.0017 M of **58**. The suspension was then drained and the filtrate collected and analysed by HPLC. The dark red-coloured resin was rinsed four times with 10% water in DMF to remove any unbound dye. Displacement of the dyes from the resin was achieved by washes with $PhSO_3Na$ in DMF starting with a 0.1 M solution (3×) followed by a 0.5 M solution (4×). During each of the $PhSO_3Na$ washings, the solution turned from clear to red. The rinses were collected as separate fractions and then analysed by HPLC. LC column: Zorbax SB-C18 4.6×150 mm, 3.5 μm; eluent: 5 to 20% acetonitrile over 10 minutes in 25 mM phosphate buffer (pH 7.0) then maintained at 20% for 4 minutes at 0.8 mL/min; UV detection at 507 nm.

8.11: Synthesis of biphenyl amino acids.

3-trifluoroacetyl(aminomethyl)phenylboronic acid (90).

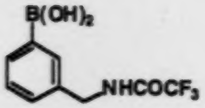

3-aminomethylphenylboronic acid hydrochloride **89** (1.063 g, 5.67 mmol; obtained from CombiBlocks, San Diego) was weighed into a dry 25 mL round bottom flask. The flask was flushed with nitrogen gas before 12 mL of methanol was added to dissolve the boronic acid. This was followed by the addition of triethylamine (0.79 mL, 5.67 mmol) and then ethyl trifluoroacetate (1.3 mL, 11.3 mmol). The reaction was then stirred at room temperature for 24 hours. The methanol was then evaporated and the residue dissolved in 70 mL of ethyl acetate which was subsequently was washed with 2×20 mL of water. The combined aqueous washes were then back-extracted with 2×20 mL of ethyl acetate. The organic extractions were combined, washed with brine, dried over anhydrous $MgSO_4$ and then evaporated leaving **90** as a light brown solid (0.640 g, 45%). The product was used in its crude form in the subsequent reaction. ^1H NMR (300 MHz, 1% D_2O in CD_3OD) δ 7.67 (m, 2H), 7.32 (m, 2H), 4.44 (s, 2H). ^{13}C APT NMR (75.5 MHz, 1% D_2O in CD_3OD) δ 159.0 (q, $\underline{C}OCF_3$), 137.4 (C), 134.3 (CH), 134.2 (CH), 130.6 (CH), 128.9 (CH), 117.6 (q, CF_3), 44.4 (CH_2). IR (microscope): 3292, 3102, 2938, 1704, 1352, 1180 cm^{-1}. HRMS-ESMS for $C_9H_9F_3BNO_3Na$ (MNa^+), calcd 270.05198 obsd. 270.05172.

4-trifluoroacetyl(aminomethyl)phenylboronic acid (98).

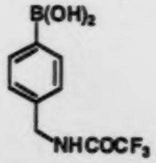

The preparation of **98** from 4-aminomethylphenylboronic acid hydrochloride (obtained from CombiBlocks, San Diego) was done as described with compound **90**. Yield 54%. ^{1}H NMR (300 MHz, 1% D_2O in CD_3OD) δ 7.70 (d, *J* = 5.4 Hz, 2H), 7.23 (d, *J* = 6.0 Hz, 2H), 4.43 (s, 2H). ^{13}C APT NMR (75.5 MHz, 1% D_2O in CD_3OD) δ 159.1 (q, $\underline{C}OCF_3$), 140.4 (C), 135,2 (CH), 127.7 (CH), 117.6 (q, $CO\underline{C}F_3$), 44.2 (CH_2). IR (microscope): 3283, 3099, 2960, 1703, 1187, 1114 cm^{-1}. HRMS-ESMS for $C_9H_9F_3BNO_3Na$ (MNa^+), calcd 270.05198 obsd. 270.05172.

3-(3'-trifluoracetylaminomethylphenyl)benzoic *t*-butyl ester (91).

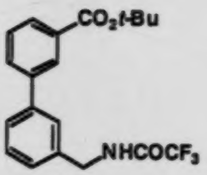

The coupling reaction was done according to the procedure developed by Buchwald *et al.*[131] The trifluoroacetimide protected 3-(aminomethyl)phenyl boronic acid **90**, (0.497 g, 2.01 mmol), $Pd(OAc)_2$ (19 mg, 0.084 mmol), ligand **92** (59 mg, 0.17 mmol) and KF (0.390 g, 6.71 mmol) were weighed into a dry 25 mL round bottom flask. The flask was evacuated and backfilled with N_2 three times until it was kept under a N_2 atmosphere. THF (5 mL) was then added followed by the 3-bromobenzene *t*-butyl ester **88**[130] (0.32 mL, 1.00 mmol). The solution was heated to 50°C for 24 hours, cooled to room temperature, and then diluted with 120 mL of diethyl ether and washed with 50 mL 1 N NaOH(aq). The NaOH(aq) wash was back-extracted with 30 mL of diethyl ether. The ether solutions were combined, washed with brine, dried over anhydrous $MgSO_4$ and then evaporated. The crude material was purified by silica gel flash chromatography using 20 % ethyl acetate in hexanes to give **91** as a yellow oil (0.538 g, 84% yield). ^{1}H NMR (300 MHz, $CDCl_3$) δ 8.16 (d, J = 1.6 Hz, 1H), 7.96 (dd, J = 1.2, 7.7 Hz, 1H), 7.70 (dd, J = 1.2, 7.8 Hz, 1H), 7.56 (dd, J = 1.2, 7.7 Hz, 1H), 7.52 – 7.40 (m, 3H), 7.29 (d, J = 7.6 Hz, 1H), 6.73 (broad s), 4.58 (d, *J* = 5.7 Hz, 2H), 1.60 (s, 9H). ^{13}C APT NMR (75.5 MHz, $CDCl_3$) δ 165.8 (C), 157.5 (q, $\underline{C}OCF_3$), 140.8 (C), 140.5 (C), 136.8 (C), 132.4 (C), 131.0 (CH), 129.3 (CH), 128.7 (CH), 128.4 (CH), 127.9 (CH), 127.7 (CH), 127.1 (CH), 126.7 (CH), 115.9 (q, $CO\underline{C}F_3$), 81.3 (C), 43.7 (CH_2), 28.0 (CH_3). IR (CH_2Cl_2 cast): 3314, 3095, 1712, 1553, 1163, 755 cm^{-1}. HRMS-EIMS for $C_{20}H_{20}F_3NO_3$ (M^+), calcd 379.13953 obsd. 379.13919.

3-(3'-aminomethylphenyl)benzoic acid trifluoroacetate salt (93).

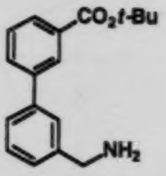

To trifluoroacetimide protected 3-(3'-aminomethylphenyl)benzoic *t*-butyl ester **91** (480 mg, 1.27 mmol) was added 10 mL of 10% K_2CO_3 in 3:2 methanol-water solution. An additional 6 mL of methanol was necessary to help dissolve the starting material. The reaction was stirred at room temperature for 48 hours and then concentrated. The residue was dissolved in 40 mL of ethyl acetate and then washed with 3×15 mL of water. The combined aqueous washes were then back-extracted with 2×20 mL of ethyl acetate. The ethyl acetate extracts were combined and washed with brine, dried over anhydrous Na_2SO_4 and then evaporated to give the titled compound (**93**) as a yellow oil (239 mg, 67%). The compound was used in the next reaction without further purification. ^{1}H NMR (400 MHz, $CDCl_3$) δ 8.16 (s, 1H), 7.91 (d, *J* = 7.7 Hz, 1H), 7.70 (d, *J* = 7.7 Hz,

1H), 7.55 (s, 1H), 7.49 – 7.30 (m, 4H), 3.94 (s, 2H), 1.57 (s, 9H). ^{13}C APT NMR (125 MHz, $CDCl_3$) δ 165.7 (CO), 142.9 (C), 141.0 (C), 140.6 (C), 132.4 (C), 131.0 (CH), 129.1 (CH), 128.6 (CH), 128.2 (CH), 127.9 (CH), 126.4 (CH), 126.0 (CH), 125.8 (CH), 81.3 (C), 46.1 (CH_2), 28.2 (CH_3). IR ($CHCl_3$ cast): 3500, 2976, 1711, 1368, 1314, 1255, 1162, 1117, 754 cm^{-1}. HRMS-EIMS for $C_{18}H_{21}NO_2$ (M^+), calcd 283.12723 obsd. 283.15753.

3-(3'-*N*-FMOC-aminomethylphenyl)benzoic acid (94).

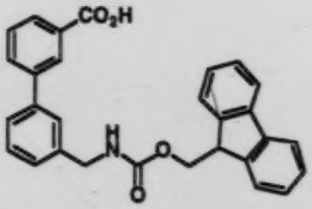

To 3-(3'-aminomethylphenyl)benzoic *t*-butyl ester **93** (154 mg, 0.543 mmol) was added 4 mL of dioxane and 0.85 M Na_2CO_3(aq) (0.60 mL, 0.54 mmol). The suspension was completely dissolved by an additional 1 mL of dioxane and 1 mL of water. The solution was then cooled to 0°C before adding FMOC-Cl (140 mg, 0.543 mmol) in 1 mL of dioxane. It was then stirred at room temperature for 4 hours and then diluted with 50 mL diethyl ether. The mixture was then washed with 2×10 mL of water. The aqueous layers were combined and back-extracted with 10 mL of diethyl ether. The combined organic phases were then washed with brine, dried over anhydrous Na_2SO_4 and concentrated to a yellow oil. Flash chromatography through silica gel with 20% ethyl acetate in hexanes afforded the *t*-butyl ester of 3-(3'-FMOC-aminomethylphenyl)benzoic acid as a clear oil (182 mg, 74%). The ester was directly exposed to 1:1 TFA and dichloromethane for 1 hour at room temperature before concentrated to a small volume. Diethyl ether was added forming a white precipitate that was collected by filtration and dried under high vacuum to give **94** (102 mg, 58% from the *t*-butyl ester, or 42% from free amine **93**). Melting point: 198 – 200°C. ^{1}H NMR (400 MHz, DMSO-d_6) δ 8.16 (broad s, 1H), 7.96 – 7.80 (m, 4H), 7.66 (d, J = 9.5 Hz, 2H), 7.60 – 7.52 (m, 3H), 7.42 (t, J = 9.0 Hz, 1H), 7.36 (t, J = 9.0 Hz, 2H), 7.28 – 7.22 (m, 3H), 4.32 (d, J = 9.0 Hz, 2H), 4.25 (d, J = 7.5 Hz, 2H), 4.20 (t, *J* = 8.5 Hz, 1H). ^{13}C APT NMR (125 MHz, DMSO-d_6) δ 167.0 (CO), 156.1 (CO), 143.6 (C), 140.5 (C), 140.4 (C), 140.3 (C), 139.1 (C), 131.3 (C), 130.9 (CH), 129.1 (CH), 128.9 (CH), 128.1 (CH), 127.4 (CH), 127.1 (CH), 126.8 (CH), 126.5 (CH), 125.4 (CH), 125.1 (CH), 124.9 (CH), 119.9 (CH), 65.3 (CH_2), 46.7 (CH), 43.7 (CH_2). IR (microscope): 3314, 3000 – 2500, 1693, 1267, 756, 737 cm^{-1}. HRMS-ESMS calcd. for $C_{29}H_{23}NO_4Na$ (MNa^+) 472.152478, obsd. 472.152722.

3-(3'-*N*-butryl-aminomethylphenyl)benzoic acid (95).

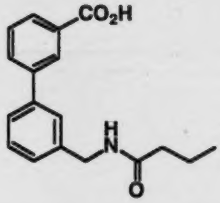

To 3-(3'-aminomethylphenyl)benzoic *t*-butyl ester **93** (85 mg, 0.30 mmol) was added 1mL of dioxane and 0.85M Na_2CO_3(aq) (0.35 mL, 0.30 mmol). A small amount of dioxane (<1 mL) was added to help in the dissolution of the starting material. The solution was cooled to 0 °C before adding butyric anhydride (0.049 mL, 0.30 mmol). It was then allowed to stir at room temperature for 2 hours and then diluted with 25 mL of diethyl ether. The mixture was washed with 2×10 mL of water. The aqueous layers were then combined and back-extracted with 2×10 mL of diethyl ether. The combined organic phases were washed with brine, dried over anhydrous Na_2SO_4 and concentrated to a clear oil (86 mg, 81%). The *t*-butyl ester was then removed with 1 mL of 1:1 TFA in dichloromethane for 1 hour. Evaporation of the solution and drying under high vacuum gave 3-(3'-*N*-butyryl-aminomethylphenyl)benzoic acid (**95**) as an off-white solid (66mg, 91% from the *t*-butyl ester, or 74% from the free amine **93**). Melting point: 135 – 137°C. ^1H NMR (500 MHz, DMSO-d_6) δ 8.34 (t, *J* = 6.0 Hz, 1H), 8.16 (broad s, 1H), 7.93 (d, *J* = 8.0 Hz, 1H), 7.88 (d, *J* = 8.0 Hz, 1H), 7.60 (t, *J* = 7.5 Hz, 1H), 7.56 (m, 2H), 7.43 (t, *J* = 8.0 Hz, 1H), 7.24 (d, *J* = 8.0 Hz, 1H), 4.34 (d, *J* = 5.5, 2H), 2.12 (t, *J* = 7.3 Hz, 2H), 1.55 (sextet, *J* = 7.3 Hz, 2H), 0.85 (t, *J* = 7.3 Hz, 3H). ^{13}C APT NMR (125 MHz, DMSO-d_6) δ 171.8 (CO), 166.9 (CO), 140.5 (C), 140.3 (C), 139.0 (C), 131.3 (C), 130.8 (CH), 129.1

(CH), 128.9 (CH), 128.1 (CH), 127.1 (CH), 126.6 (CH), 125.4 (CH), 125.0 (CH), 41.9 (CH_2), 37.3 (CH_2), 18.7 (CH_2), 13.6 (CH_3). IR (microscope): 3304, 2964. 1687, 1641, 693, 753 cm^{-1}. HRMS-EIMS (*m/z*) calcd. for $C_{18}H_{19}NO_3$ 297.1351 (M^+) obsd. 297.13649.

Protected 4-(4'-aminomethylphenyl)benzoic *t*-butyl ester (100).

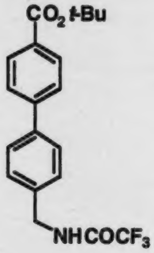

The procedure followed was the same as for the synthesis of **91**. For this reaction, employed the trifluoroacetamide protected 4-(aminomethyl)phenyl boronic acid **99** (0.502 g, 2.03 mmol), $Pd(OAc)_2$ (19 mg, 0.084 mmol), ligand **92** (59 mg, 0.17 mmol), KF (0.393 g, 6.76 mmol) and 4-bromophenyl *t*-butyl ester **97** (0.33 mL, 1.7 mmol) to obtain **100** as a yellow oil after silica gel flash chromatography with 20% ethyl acetate in hexane (0.54 g, 84%). ^{1}H NMR (300 MHz, $CDCl_3$) δ 7.98 (d, *J* = 8.2 Hz, 2H), 7.54 (2 overlapping d's, *J* = 8.1 Hz, 4H), 7.34 (d, *J* = 8.0 Hz, 2H), 7.20 – 7.00 (broad s, 1H), 4.54 (d, *J* = 5.9 Hz, 2H), 1.58 (s, 9H). ^{13}C APT NMR (75.5 MHz, $CDCl_3$) δ 165.7 (C), 157.4 (q, $\underline{C}OCF_3$), 144.3 (C), 140.1 (C), 135.9 (C), 131.0 (C), 130.0 (CH), 128.5 (CH), 127.8 (CH), 126.8 (CH), 116.0 (q, $CO\underline{C}F_3$), 81.2 (C), 43.5 (CH_2), 28.2 (CH_3). IR (CH_2Cl_2 cast): 3290, 3103, 2982, 1715, 1608, 1181 cm^{-1}. HRMS-EIMS calcd. for $C_{20}H_{20}F_3NO_3$ (M^+) 379.13953, obsd. 379.13981.

4-(4'-aminomethylphenyl)benzoic acid trifluoroacetate salt (101).

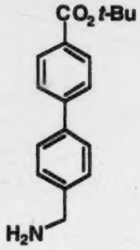

To the trifluoroacetamide protected 4-(4'-aminomethylphenyl)benzoic *t*-butyl ester **100** (479 mg, 1.28 mmol) was added 10 mL of a 10% K_2CO_3 in 2:1 methanol-water solution. An additional 3 mL of methanol was necessary to help dissolve the starting material. The reaction was stirred at room temperature for 28 hours and then concentrated. The residue was dissolved in 40 mL of ethyl acetate and then washed with 3×15 mL of water. The aqueous layers were combined and then back-extracted with 2×20 mL of ethyl acetate. The combined ethyl acetate extracts were washed with brine, dried over anhydrous Na_2SO_4 and then evaporated to give the free amine product as a yellow oil (344 mg, 96 %). The product was used without further purification in the next step. ^{1}H NMR (300 MHz, CD_3OD) δ 8.00 (d, J = 8.7 Hz, 2H), 7.67 (d, J = 8.7 Hz, 2H), 7.64 (d, J = 8.4 Hz, 2H), 7.43 (d, J = 8.7 Hz, 2H), 3.83 (s, 2H), 1.60 (s, 9H). ^{13}C APT NMR (125 MHz, CD_3OD) δ 167.3 (CO), 146.4 (C), 143.7 (C), 139.8 (C), 131.8 (C), 130.9 (CH), 129.1 (CH), 128.3 (CH), 127.8 (CH), 82.3 (C), 46.3 (CH), 28.5 (CH_3). IR (microscope): 3357, 3357, 3052, 2982, 1704, 1607, 1300, 1121, 774 cm^{-1}. HRMS-ESMS (*m/z*) calcd. for $C_{18}H_{22}NO_2$ 284.16466 (MH^+) obsd. 284.16451.

4-(4'-*N*-FMOC-aminomethylphenyl)benzoic acid (102).

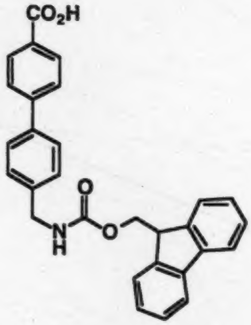

Compound **102** was prepared via a similar procedure described for **104**. To 4-(4'-aminomethylphenyl)benzoic *t*-butyl ester (**101**) (300 mg, 1.06 mmol) was added 2 mL of dioxane and 0.85 M Na_2CO_3(aq) (1.2 mL, 1.1 mmol). The suspension was completely dissolved by additional 5 mL of dioxane. The solution was cooled to 0°C before adding FMOC-Cl (274 mg, 1.06 mmol) in 2 mL of dioxane. After stirring at room temperature for 4 hours the reaction was diluted with 100 mL of diethyl ether was and washed with 2×20 mL of water. The combined aqueous phases were back-extracted with 20 mL of diethyl ether. The combined organic phases were washed with brine, dried over anhydrous Na_2SO_4 and concentrated to a yellow oil. Silica gel flash chromatography with 33% ethyl acetate and hexanes afforded the *t*-butyl ester of 4-(4'-FMOC-aminomethylphenyl)benzoic acid as a clear oil (0.473 g, 88% yield). The ester was removed by the same procedure described for compound **104** to provide the free acid **102** (0.397 g, 94% yield from the ester, 82% from the free amine **101**). Melting point: 243 – 244°C. ^{1}H NMR (500 MHz, DMSO-d_6) δ 8.01 (d, *J* = 8.0 Hz, 2H), 7.88 (d, *J* = 7.0 Hz, 2H), 7.78 (d, *J* = 8.5 Hz, 2H), 7.70 (d, *J* = 8.0 Hz, 2H), 7.68 (d, *J* = 8.5 Hz, 2H), 7.41 (t, *J* = 7.5 Hz, 2H), 7.34 – 7.30 (m, 4H), 4.36 (d, *J* = 7.0 Hz, 2H), 4.23 (m, 3H). ^{13}C APT NMR (125 MHz, DMSO-d_6) δ 166.9 (CO), 156.2 (CO), 143.9 (C), 143.7 (C), 140.6 (C), 139.8 (C), 137.3 (C), 129.6 (CH), 129.3 (C), 127.5 (CH), 127.4 (CH), 126.9 (CH), 126.7 (CH), 126.5 (CH), 125.0 (CH), 120.0 (CH), 65.3 (CH_2), 46.8 (CH), 43.4 (CH_2). FTIR (microscope): 3311, 3000 – 2500, 1680, 1608, 1525, 1254, 773, 735. HRMS-ESMS for $C_{29}H_{23}NO_4Na$ (MNa^+) calcd. 472.152478, obsd. 472.152459.

4-(4'-acetylaminomethylphenyl)benzoic acid (103).

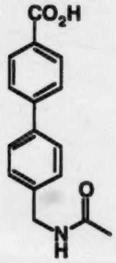

Preparation of the titled compound was done using a similar procedure as described for **95** except using acetic anhydride instead of butyric anhydride. For this reaction, used free amine **101** (209 mg, 0.740 mmol), acetic anhydride (0.074 mL, 0.78 mmol), in 0.85M Na_2CO_3(aq) (0.92 mL, 0.78 mmol) and 3mL of dioxane. The *t*-butyl ester was then removed by TFA treatment to give **103** as a white powder (179 mg, 90 % from **101**). Melting point: 290 –295°C (decomposed). ^{1}H NMR (500 MHz, DMSO-d_6) δ 8.37 (t, *J* = 5.0 Hz, 1H), 8.00 (d, *J* = 8.0 Hz, 2H), 7.77 (d, *J* = 8.5 Hz, 2H), 7.68 (d, *J* = 8.0 Hz, 2H), 7.36 (d, *J* = 8.0 Hz, 2H), 4.29 (d, *J* = 5.5 Hz, 2H), 1.88 (s, 3H). ^{13}C APT NMR (125 MHz, DMSO-d_6) δ 168.9 (CO), 166.9 (CO), 143.9 (C), 139.7 (C), 137.3 (C), 129.7 (CH), 129.3 (C), 127.8 (CH), 129.7 (CH), 126.4 (CH), 41.8 (CH_2), 22.6 (CH_3). FTIR (microscope): 3342, 2933, 1678, 1606, 1549, 775 cm^{-1}. HRMS-EIMS for $C_{16}H_{15}NO_3$ calcd. 269.10519 (M^+) obsd. 269.10478.

8.12: Synthesis of trityl-TentaGel® resin (described for 250-300 μm beads).

The procedure below is described for 250-300 μm but is also applicable for standard 90-150 μm beads.

Preparation of Grignard reagent (76).

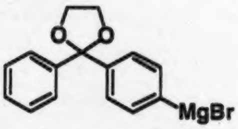

Magnesium turnings (0.328 g, 13.5 mmol) were weighed into a flamed dried 50 mL, 3-necked round bottom flask fitted with an addition funnel and condenser, and containing a small iodine crystal and stir bar. 4-bromobenzophenone ethylene acetal[153] (4.14 g, 13.6 mmol) was then added into the addition funnel. The reaction apparatus was then evacuated and backfilled with argon three times until it finally was kept under an atmosphere of argon gas. 2 mL of dry THF was added to the magnesium and 15 mL to the bromide in the addition funnel. About 2 mL of the bromide solution was added to the magnesium and within a few minutes of stirring, the Grignard reaction was initiated. The remaining bromide was added to the flask slow enough to maintain a gentle reaction. After the addition was complete the reaction was heated to reflux for 1.5 hours. It was then cooled and used directly in the subsequent reaction described below.

TentaGel® MB (250-300 μm) bound benzophenone bound resin (77).

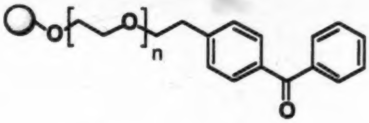

TentaGel® MB Br resin was dried before the reaction by storage under high vacuum (< 1 Torr) over drierite/KOH for 2 days. The resin (2.50 g, 0.675 mmol at 0.27 mmol/g according to elemental analysis on bromine) and CuBr•DMS (0.278 g, 1.35 mmol) were weighed into a flamed dried 250 mL, 3-necked round bottom flask fitted with a condenser. (Note: no stir bar was used as it was found to damage this type of resin while stirring). The flask was evacuated and backfilled with argon three times and then maintained under an argon atmosphere. 35 mL of dry THF was then added followed by 4 mL of HMPA. Using an air tight syringe, the Grignard solution prepared in the above reaction was transferred to the flask. The flask was then kept for 5 days at 70 °C with occasional swirling.[154] The reaction was then cooled to room temperature and quenched by the slow addition of 10 mL of saturated $NH_4Cl(aq)$. The suspension was transferred into a large 100 mL glass filter vessel and rinsed with saturated $NH_4Cl(aq)$ (3×), water (3×), methanol (3×), and dichloromethane (5×). The resin was resuspended in 10 mL dichloromethane before adding 1 mL of $HClO_4$ (70% in water) which turned the resin green in colour. The suspension was shaken for 24 hours until it was drained and rinsed with dichloromethane (3×), 1:3 Et_3N/DMF (3×), methanol (3×), and dichloromethane (5×). The resin was then dried under high vacuum over drierite/KOH for 16 hours to give resin **77**. Elemental analysis on bromine gave 0.001% Br or 1.25×10^{-4} mmol/g Br. IR (microscope): 1654 cm^{-1} (C=O stretch).

TentaGel® MB trityl alcohol (78).

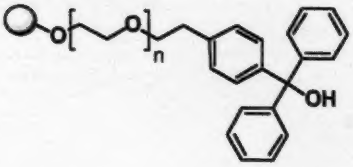

The reaction was found to work best when freshly prepared phenylmagnesium bromide was used. Resin **77** was weighed (2.38 g, 0.64 mmol at approximately 0.27 mmol/g) into a flame-dried 100 mL round bottom flask and placed under an atmosphere of argon gas. 20 mL of dry THF was added to the resin followed by 1 M phenylmagnesium bromide solution in THF (7 mL, 7 mmol). The reaction flask was gently shaken on a mini-vortexer with a clamp loosely holding the neck of the flask. After 24 hours of shaking at room temperature, the reaction was quenched with 10 mL of 0.5 M HCl (aq), transferred into a 100 mL glass filter vessel and then rinsed with water (3×), 5% $NaHCO_3$(aq) (3×), water (3×), THF (3×), methanol (3×), and dichloromethane (5×). The resin was then dried under high vacuum over drierite/KOH for 16 hours affording resin **78**. IR (microscope): 3511 cm^{-1} (OH stretch) and the loss of carbonyl stretch at 1654 cm^{-1}.

TentaGel® MB bound 1-trityl-4,7,10-trioxa-1,13-tridecanediamine resin (79).

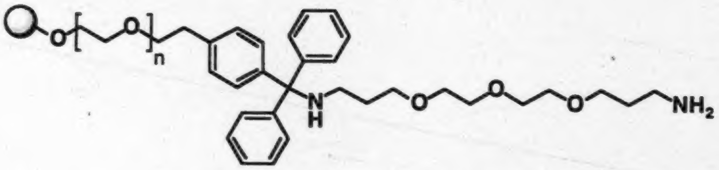

To resin **78** (2.3 g), inside a glass filter vessel, was added 10 mL of 10 % thionyl chloride in dichloromethane. The vessel was sealed and shaken for 45 minutes at room temperature and then drained. The same thionyl chloride treatment was repeated two more times until it was finally drained and rinsed with dry chloromethane (5×) to give the trityl chloride. Dichloromethane was then added to resuspend the resin. This suspension was added over one hour, via a pipette, into a solution of 4,7,10-trioxa-1,13-tridecanediamine (10 mL) in dichloromethane (10 mL) inside a dry 250 mL round bottom flask shaking on a mini-vortexer. After the addition was complete, the flask was shaken for an additional 16 hours until it was quenched with 2 mL of methanol. The resin was transferred to a 100 mL polypropylene filter vessel and rinsed with methanol (3×), 1:3 Et_3N/DMF (3×), methanol (3×), dichloromethane (5×) and then dried under high vacuum over drierite/KOH for 48 hours to give resin **79**. Elemental analysis on nitrogen: 0.4148% or 0.148 mmol/g (60% yield based on theoretical commercial loading; 0.246 mmol/g).

8.13: Exhaustive amide reduction on TentaGel® bound polyamides.

Tetramine 84.

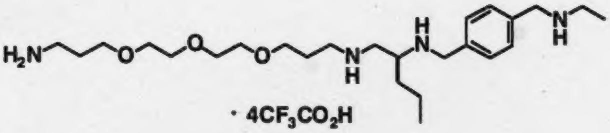

TentaGel® MB bound triamide **82** was synthesized on resin **79** using the general amide coupling protocol described in the general section using the amino acid derivatives HO-LNva-FMOC and HO-4Amb-Ac. Resin **82** was weighed (0.418 g, 0.0502 mmol) into a flame-dried 25 mL round bottom flask, without a stir bar. The flask was fitted with a condenser before everything was placed under argon atmosphere. 1.0 M borane-THF complex was then added (6.0 mL, 6.0 mmol) to the resin. The suspension was heated to 65 °C for 30 hours until it was cooled and transferred into a 25 mL polypropylene filter vessel and rinsed extensively with dry THF. The resin was then resuspended in 2 mL of THF before adding 0.27 mL DIPEA. After vortexing for one minute, 0.53 mL of $EtCO_2H$ was added. The suspension was vortexed for 1 minute before the slow addition of a THF solution of iodine (1.2 g in 2 mL). The final ratio of THF/$EtCO_2H$/DIPEA should be 12:2:1. After vortexing for 4 hours, the resin was drained and then rinsed with THF (3×), 1:3 Et_3N/DMF (3×), methanol (3×), and dichloromethane (5×). The resin was then dried under high vacuum over drierite/KOH for 48 hours to give **83**. On a separate batch of resin on the same scale, another amide reduction was performed except a piperidine-promoted work-up was done according to the procedure in given in the general section. In both reactions the resins were cleaved with 5% TFA in dichloromethane to give the polyamine **84** as the tetrakis(trifluoroacetate) salt. Iodine procedure - crude yield: 42%. Purity by LCMS/UV – 65% at 210 nm; 59% by MS. Piperidine procedure - crude yield: 47%. HPLC purity: 90% by UV (210 nm), 84% by MS. HPLC conditions – column: Zorbax SB-C8 (2.1 × 50 mm, 3.5 μm); eluent: 5 to 85% acetonitrile (0.1% TFA) in water (0.1% TFA) over 5 minutes at 0.7 mL/min then maintained at 85% for another 7 minutes; column temperature: 25°C; MS conditions – Capillary voltage (positive mode): 3200 V; mass scanning range: 100 – 900 amu; fragmentor voltage: 80 V; drying gas temperature: 350°C; gas flow 10L/min; nebulizer pressure: 40 psig. ^{1}H NMR (500 MHz, CD_3OD) δ 7.64 (d, *J* = 8.0 Hz, 2H), 7.55 (d, *J* = 8.5 Hz, 2H), 4.39 (d, *J* = 13 Hz, 1H), 4.27 (d, *J* = 13 Hz. 1H), 4.22 (s, 2H), 3.68 – 3.58 (m, 13H), 3.50 (dd, *J* = 6.5, 14 Hz, 1H), 3.45 (dd, *J* = 4.5, 14 Hz, 1H), 3.25 (dd, *J* = 7.5, 12.5 Hz, 1H), 3.20 (dd, *J* = 7.0, 12.5 Hz, 1H), 3.10 (q, *J* = 7.3 Hz, 2H), 3.07 (t, *J* = 6.6 Hz, 2H), 2.01 (q, *J* = 6.9 Hz, 2H), 1.91 (quintet, *J* = 5.8 Hz, 2H), 1.94 – 1.88 (m, 1H), 1.82 – 1.74 (m, 1H), 1.53 – 1.42 (m, 2H), 1.32 (t, *J* = 7.3 Hz, 3H), 1.04 (t, *J* = 7.2 Hz, 3H). ^{13}C APT NMR (125 MHz, CD_3OD) δ 134.3 (C), 134.0 (C), 131.8 (CH), 131.5 (CH), 71.3 (CH_2), 71.3 (CH_2), 71.2 (CH_2), 71.1 (CH_2), 70.1 (CH_2), 69.2 (CH_2), 57.0 (CH), 51.4 (CH_2), 49.8 (CH_2), 49.0 (CH_2), 48.2 (CH_2), 43.9 (CH_2), 39.8 (CH_2), 32.1 (CH_2), 28.3 (CH_2), 27.4 (CH_2), 19.6 (CH_2), 14.1 (CH_3), 11.5 (CH_3). IR (methanol cast): 3400 – 2500, 1675, 1202, 1134 cm^{-1}. HRMS-ESMS for $C_{25}H_{49}N_4O$ (MH^+), calcd. 453.37992 obsd. 453.37982.

Triboronic acid 86.

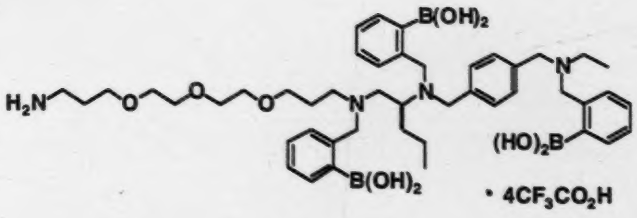

TentaGel® bound tetramine **83** was weighed (0.35 g, 0.042 mmol at 0.12 mmol/g) into a dry 25 mL round bottom flask without a stir bar. A condenser was fitted to the round bottom and together they underwent three evacuation and argon backfill cycles until they were maintained under an argon atmosphere. The resin was then swelled in 8.5 mL of dry THF before the addition of 1,2,2,5,5-pentamethylpiperidine (PMP) (0.23 mL, 1.26 mmol) followed by 2-(bromomethyl)phenylboronate ester **40**[22] (0.26 mL at 1.39 g/mL, 1.26 mmol). The reaction was heated to 65 °C for 48 hours until it was cooled and transferred into a 25 mL polypropylene filter vessel using THF. The resin was rinsed with THF (3×), water (1 minute and then 30 minutes), THF (3×), methanol (3×) and dichloromethane (3×). It was then dried under high vacuum over drierite/KOH for 16 hours to give the resin bound triboronic acid **85**. Cleavage of the resin (0.332 g) with 5 % TFA in dichloromethane gave the titled compound **86** (29 mg, crude yield: 58%) Purity by HPLC - 59% by MS, 75% by UV (210 nm) HPLC/MS conditions are the same as for polyamine **84** described above. ^{1}H NMR (500 MHz, 1% D_2O in CD_3OD or $NaOD/D_2O$) complex mixture of boronic anhydrides. ESMS *m/z* 801.5 (MH^+), 401.3 ($[M+2H^+]/2$). HRMS-ESMS calcd. for $C_{46}H_{64}B_3N_4O_6$ ($MH - 3H_2O$) 801.510502, obsd. 801.510837.

8.14: Synthesis and decoding of split-pool polyamine and oligoboronic acid library on TentaGel® resin.

Syntheses of tetramide/triamide libraries on standard sized (90-150 μm) beads.

Resin **79** (0.24 mmol/g, standard sized) was split 17 portions into 5 mL polypropylene filter vessels (17×114 mg, 0.027 mmol each). The resin was rinsed with dichloromethane (3×) and NMP (3×) before the addition of 0.44 mL of an NMP solution containing 0.27 M of the FMOC amino acid (0.120 mmol) and 0.030 M of the corresponding *N*-acylamino acid (0.013 mmol). The suspensions were vortexed for 5 minutes, before adding to each vessel 0.44 mL of an NMP solution containing 0.30 M HBTU and 0.30 M HOBt•H_2O (0.13 mmol each). After another 1 minute of further vortexing, DIPEA (50 μL, 0.27 mmol) was added to the suspensions. The suspensions were then vortexed for 2 hours before they were filtered and rinsed with DMF (4×) and dichloromethane (4×). The resins were then suspended in dichloromethane and mixed together thoroughly into a large 100 mL polypropylene filter vessel and dried under high vacuum for 16 hours. The resin was then split again (17×112 mg, 0.0256 mmol each) and rinsed with dichloromethane and NMP. The FMOC protective group was removed by two treatments with 1:4 piperidine/NMP (5 minutes, then 30 minutes). After rinsing the resins with NMP (5×), they were coupled to their respective amino acid derivatives exactly as described above. They were then rinsed and mixed the same way as described earlier. A portion of the resin was removed and stored as a triamide library. The final coupling was done on 17 portions of the resin (17 × 89 mg, 0.021 mmol each), after FMOC removal with 1:4 piperidine, using 0.34 mL of 0.30 M solutions of the *N*-acyl amino acids (0.10 mmol), 0.34 mL of 0.30 M solution of HBTU and HOBt•H_2O (0.10 mmol each), and DIPEA (36 μL, 0.20 mmol). After two hours the resins were rinsed, mixed and dried as before to give the tetramide library **106**.

TentaGel® supported pentamine library.

The reduction of the tetramide library was done as described for compound **84** using the modified iodine-promoted work-up with 0.3 g/mL iodine in a 12:2:1 mixture of THF, propionic acid and DIPEA to give the pentamine library **107**.

Polyacetylation and LCMS decoding of the pentamine library.

Polyacetylation on a milligram scale of resin (10 mg) was achieved by first suspending the resin in 0.5 mL of DMF. DIPEA (22 μL) was added, followed by acetic anhydride (50 μL). The suspension was vortexed for 22 hours and then rinsed with DMF (4×) methanol (4×), and dichloromethane (5×). Single beads were isolated as described in Section 7.7 and then analysed by LCMS. LC conditions – column: Zorbax Extend-C18 2.1×50 mm, 5.0 μm; eluent: (solution A: 0.020 M NH_4OH in 80% acetonitrile in water; solution B: 0.020 M NH_4OH in water) 10% solution A in solution B up to 85% solution A over 4 minutes then maintained at 85% for another 11 minutes at 0.5 mL/min; MSD conditions – capillary voltage: 3200 V (positive mode); fragmentor voltage: 80 V; mass scanning range: 350 – 1000 amu; nebulizer pressure: 40 psig; gas temperature: 350°C; drying gas flow: 10 L/min).

For the polyacetylation of single beads, the bead was isolated into a conical microvial, as outlined in Section 7.7, and covered with 5 μL of a solution containing 10% acetic anhydride and 5% triethylamine in dichloromethane. The microvial was placed inside the autosampler vial which was then capped tightly and stored at 4°C for 24 hours. The cap was then removed from the vial to allow the solution to evaporate. The bead in the microvial was then exposed to 5 μL of 5% TFA in dichloromethane for 15 minutes. The cleaved contents were dissolved in 7.5 μL of methanol and analysed by LCMS as described in the previous paragraph.

Triamide library syntheses on macrobead (250 – 300 μm) TentaGel® resin.

The synthesis of the triamide library supported on Macrobead TentaGel® resin was done in a similar fashion as other polyamide libraries. Briefly, resin **79** (0.14 mmol/g, macrobeads) was split 17 portions (17×130 mg, 0.0182 mmol). Each resin was suspended in 0.30 mL NMP. The resins were then treated sequentially with 0.30 mL of an NMP solution containing 0.27 M of the FMOC amino acid (0.081 mmol) and 0.030 M of the corresponding *N*-acylamino acid (0.01 mmol), along with 0.30 mL of an NMP solution containing 0.30 M HBTU and 0.30 M HOBt•H_2O (0.091 mmol each) and then DIPEA (32 μL, 0.182 mmol). After 2 hours of vortexing, the resins were filtered, rinsed and then mixed together. In the final amide coupling the resin was split 17 portions (17×130 mg, 0.17 mmol each), deprotected with 1:4 piperidine in DMF, and then suspended in 0.30 mL NMP. The resins were then treated with 0.29 mL of a 0.30 M NMP solution of the *N*-acyl amino acid derivative (0.086 mmol), 0.29 mL of a 0.30 M NMP solution of HBTU and HOBt•H_2O (0.086 mmol each) and then DIPEA (30 μL, 0.17 mmol). The resin was vortexed for 2 hours, rinsed, combined and then dried to give the triamide library.

TentaGel® supported tetramine library.

The reduction of the triamide library was done as described for compound **84** using both the modified iodine-promoted work-up and the piperidine based work-up to give the tetramine library. Single beads were isolated and decoded in the same manner and LCMS conditions as the polystyrene bound polyamines described in Section 7.7.

TentaGel® supported triboronic acid library.

Alkylation of the tetramine library with **40** was done as described for triboronic acid **86** to give the triboronic acid library. Single beads were isolated and decoded in the same manner and LCMS conditions as the polystyrene bound polyamines described in Section 7.7.

8.15: Synthesis and screening of anthracenyl-triboronic acids

Trityl-polystyrene bound 4,7,10-trioxa-1,13-tridecanediamine resin (141).

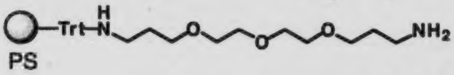

Resin **141** was prepared in a similar fashion as described for resin **79**. Briefly, polystyrene supported trityl chloride resin (5 g at 1.38mmol/g, 6.9 mmol) was added portionwise, over an hour, to a stirring solution of 4,7,10-trioxa-1,13-tridecanediamine (60.8 g, 276 mmol) in dichloromethane (60 mL). After additional stirring over 16 hours 10 mL of methanol was added. Resin was then rinsed with methanol, triethylamine/DMF (1:4), methanol and then dichloromethane (4× each) before it was dried under high vacuum for 16 hours. Theoretical loading was calculated to be 1.10 mmol/g

Preparation of resin-bound diamino-diamides (138).

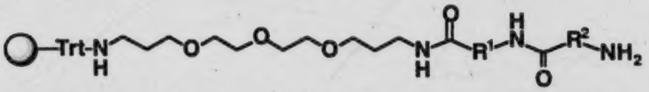

The diamino-diamides **138** were all prepared starting from 0.90 g (1.0 mmol) of resin **142** using the general procedure for the synthesis of polyamides on aminotrityl resin described in Section 7.2. Employed as the FMOC-amino acid building blocks: HO-Amb-FMOC, HO-Amc-FMOC, HO-4Acc-FMOC, and HO-εAhx-FMOC.

Conversion to tetramines (137)

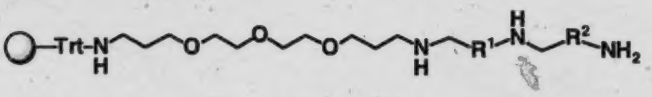

The reduction of **138** was done on 0.28 mmol of resin using 1.0 M BH_3/THF (8.4 mL, 8.4 mmol) at 65°C for 24 hours followed by the piperidine (8 mL) based work-up as described in Section 7.3. After the resins were dried a portion was cleaved (70 mg) with 5 % TFA in dichloromethane to yield in each case a colourless oil after evaporation. Each product was analysed by NMR. Results for individual tetramines are shown below. (Note that a small amount of the free diamine spacer, about 10 –15 %, is present in each NMR spectrum).

εAhx^{R}Amb^R

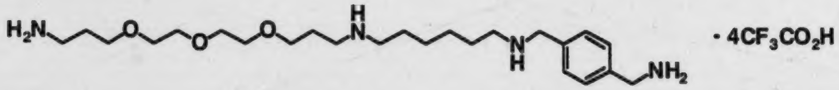

Crude yield:>99 % (clear oil). ^{1}H NMR (500 MHz, CD_3OD) δ 7.57 (d, *J* = 8.3 Hz, 2H), 7.54 (d, *J* = 8.3 Hz, 2H), 4.22 (s, 2H), 4.15 (s, 2H), 3.65 – 3.58 (m, 12H), 3.11 (t, *J* = 7.5 Hz, 2H), 3.07 – 3.05 (m, 4H), 3.00 (t, *J* = 8.0 Hz, 2H), 1.95 (quintet, *J* = 7.5 Hz, 2H), 1.92 (quintet, *J* = 5.5 Hz, 2H), 1.76 – 1.65 (m, 4H), 1.43 (m, 2H). ^{13}C APT NMR (125 MHz, CD_3OD) δ 162.1 (q, $\underline{C}OCF_3$), 135.9 (C), 133.6 (C), 131.6 (CH), 130.7 (CH), 117.8 (q, $CO\underline{C}F_3$), 71.3, (CH_2), 71.3 (CH_2), 71.2 (CH_2), 71.2 (CH_2), 70.0 (CH_2), 69.5 (CH_2), 51.9 (CH_2), 48.9 (CH_2), 48.7 (CH_2), 47.3 (CH_2), 43.9 (CH_2), 39.7 (CH_2), 28.4 (CH_2), 27.4 (CH_2), 27.2 (CH_2), 27.1 (CH_2), 27.1 (CH_2), 27.0 (CH_2). HRMS-ESMS calcd for $C_{24}H_{47}O_3N_4$ (MH^+) 439.364817, obsd. 439.365024.

Amb^{R}Amb^R

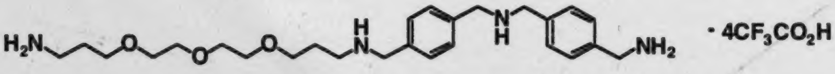

Crude yield: 55 % (clear oil). ^{1}H NMR (500 MHz, CD_3OD) δ 7.58 – 7.55 (m, 8H), 4.29 (s, 4H), 4.25 (s, 2H), 4.15 (s, 2H), 3.65 – 3.58 (m, 12H), 3.18 (t, *J* = 7.5 Hz, 2H), 3.05 (t, *J* = 7.0 Hz, 2H), 1.99 (quintet, *J* = 6.5 Hz, 2H), 1.91 (quintet, *J* = 6.0 Hz, 2H). ^{13}C APT

NMR (125 MHz, CD_3OD) δ 162.3 (q, $\underline{C}OCF_3$), 135.9 (C), 134.1 (C), 133.8 (C), 133.3 (C), 131.8 (CH), 131.8 (CH), 131.6 (CH), 130.7 (CH), 117.8 (q, $CO\underline{C}F_3$) 71.3, (CH_2), 71.3 (CH_2), 71.2 (CH_2), 71.2 (CH_2), 70.0 (CH_2), 69.6 (CH_2), 51.8 (CH_2), 51.7 (CH_2), 47.2 (CH_2), 43.9 (CH_2), 39.6 (CH_2), 28.4 (CH_2), 27.2 (CH_2). HRMS-ESMS calcd for $C_{26}H_{43}O_3N_4$ (MH^+) 459.333517, obsd. 459.333224.

4Acc^{R}Amb^R

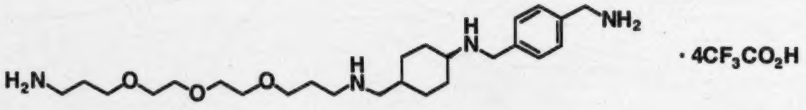

Crude yield:>99 % (clear oil). ^1H NMR (500 MHz, CD_3OD) δ 7.60 (d, J = 8.0 Hz, 2H), 7.54 (d, J = 8.3 Hz, 2H), 4.27 (s, 2H), 4.15 (s, 2H), 3.65 – 3.59 (m, 12H), 3.75 (m, 1H), 3.15 (t, J = 7.5 Hz, 2H), 3.08 – 3.06 (m, 4H), 2.06 (m, 1H), 2.00 – 1.95 (m, 4H), 1.92 (quintet, J = 6.0 Hz, 2H), 1.82 – 1.71 (m, 6H). ^{13}C APT NMR (125 MHz, CD_3OD) δ 162.3 (q, $\underline{C}OCF_3$), 135.8 (C), 133.6 (C), 131.7 (CH), 130.7 (CH), 117.8 (q, $CO\underline{C}F_3$), 71.3, (CH_2), 71.3 (CH_2), 71.2 (CH_2), 71.2 (CH_2), 70.0 (CH_2), 69.5 (CH_2), 57.0 (CH), 51.2 (CH_2), 48.0 (CH_2), 43.9 (CH_2), 39.7 (CH_2), 39.6 (CH_2), 32.3 (CH), 28.3 (CH_2), 27.2 (CH_2), 26.3 (CH_2), 25.4 (CH_2) HRMS-ESMS calcd for $C_{25}H_{47}O_3N_4$ (MH^+) 451.364817, obsd. 451.364868.

Amc^{R}Amb^R

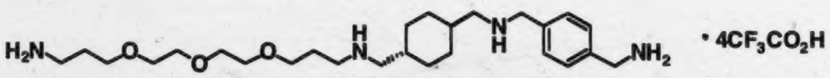

Crude yield: >99 % (clear oil). ^1H NMR (500 MHz, CD_3OD) δ 7.58 (d, J = 8.3 Hz, 2H), 7.53 (d, J = 8.3 Hz, 2H), 4.23 (s, 2H), 4.15 (s, 2H), 3.65 – 3.58 (m, 12H), 3.11 (t, J = 7.5 Hz, 2H), 3.07 (t, J = 7.0 Hz, 2H), 2.91 (d, J = 7 Hz, 2H), 2.88 (d, J = 7.0 Hz, 2H), 1.96 (quintet, J = 8.0 Hz, 2H), 1.94 – 1.88 (m, 6H), 1.70 – 1.60 (m, 2H), 1.10 – 1.06 (m, 6H). ^{13}C APT NMR (125 MHz, CD_3OD) δ 162.3 (q, $\underline{C}OCF_3$), 135.9 (C), 133.3 (C), 131.8

(CH), 130.7 (CH), 117.8 (q, $CO\underline{C}F_3$), 71.3, (CH_2), 71.3 (CH_2), 71.2 (CH_2), 71.2 (CH_2), 70.0 (CH_2), 69.6 (CH_2), 54.6 (CH_2), 54.3 (CH_2), 52.4 (CH_2), 48.0 (CH_2), 43.9 (CH_2), 39.7 (CH_2), 36.0 (CH), 36.0 (CH), 30.7 (CH_2), 30.6 (CH_2), 28.4 (CH_2), 27.1 (CH_2). HRMS-ESMS calcd for $C_{26}H_{49}O_3N_4$ (MH^+) 465.380467, obsd. 465.380724.

Amino-diboronic acid (143).

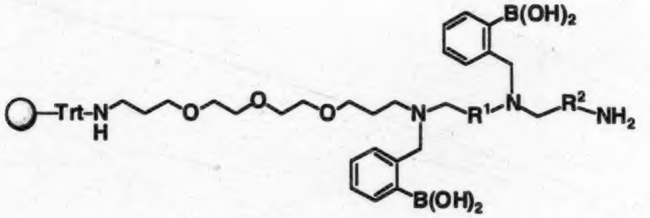

In a typical procedure, resin-supported tetramine **137** (0.22 mmol) was initially swelled in 1.5 mL DMF before the addition of a 0.35 M solution of 2-acetyldimedone (0.95 mL, 0.33 mmol) in DMF to the vortexing suspension. After 20 minutes of vortexing, the suspension was filtered and rinsed with DMF (4×) and dichloromethane (4×). The resin was then dried under high vacuum for >12 hours to afford the Dde protected tetramine **142**. It was then weighed (0.19 mmol) into a dry 25 mL round bottom flask and swelled in 5 mL THF. PMP (0.68 mL, 3.8 mmol) was then added followed by benzyl bromide **40** (0.78 mL, 3.8 mmol). The suspension was heated to 65 °C for 24 hours and then filtered and rinsed with THF (3×), 20 % H_2O in THF (2×: 1 minute, 30 minutes), THF (3×), methanol (3×) and then THF (5×) to provide the Dde protected diboronic acid. Removal of the Dde protective group was initiated by first rinsing the resin with 5 mL of 10 % ethanolamine in 1:2 ethanol in THF (2×, 1 minute each). It was then vortexed in the same ethanolamine solution for 24 hours before it was filtered and rinsed with THF (4×), methanol (4×) and dichloromethane (5×) and dried under high vacuum for > 24 hours to provide the resin bound diboronic acid **143**.

An opportunity to cleave resin bound Amb^{B}Dde (91 mg at 0.75 mmol/g, 0.069 mmol) was taken for analysis by NMR and HRMS-ESMS.

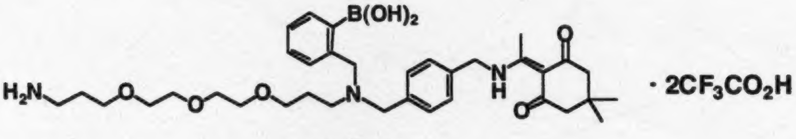

Amb^{B}Dde

Crude yield:>99 % (pale yellow oil containing 15 % of the free diamine spacer). ^{1}H NMR (500 MHz, CD_3OD) δ 7.87 (d, J = 6.3 Hz, 1H), 7.57 (d, J = 8.2 Hz, 2H), 7.53 – 7.45 (m, 5H), 4.79 (s, 2H), 4.48 (s, 2H), 4.70 – 4.40 (broad s overlapping with signal at 4.48 ppm, 2H), 3.60 – 3.54 (m, 8H), 3.50 – 3.48 (m, 2H), 3.60 – 3.40 (m, 2H), 3.21 (t, J = 7.5 Hz, 2H), 3.02 (t, J = 7.0 Hz, 2H), 2.58 (s, 2H), 2.38 (s, 4H), 1.95 – 1.88 (broad s overlapping with signal at 1.88, 2H), 1.88 (quintet, J = 6.0 Hz, 2H), 1.02 (s, 6H). ^{13}C APT NMR (125 MHz, CD_3OD) δ 175.9 (CO), 162.2 (q, $\underline{C}OCF_3$), 139.7 (C), 137.5 (CH), 135.8 (C), 133.7 (CH), 133.0 (CH), 132.1 (CH), 130.6 (C), 130.5 (CH), 129.5 (CH), 71.4 (CH_2), 71.3 (CH_2), 71.2 (CH_2), 71.1 (CH_2), 69.9 (CH_2), 69.9 (CH_2), 60.8 (CH_2), 58.5 (CH_2), 53.5 (CH_2), 52.5 (CH_2), 47.9 (CH_2), 39.5 (CH_2), 31.2 (CH_2), 28.5 (CH_3), 28.4 (CH_2), 25.2 (CH_2), 18.9 (CH_3), 0.60 (CH_3). One quarternary C(sp^2) is missing along with the C(sp^2) bonded to the boron. ESMS *m/z* 602.3 (MH-2H_2O), 620.4 (MH-H_2O), 638.4 (MH^-). HRMS-ESMS calcd for $C_{35}H_{53}BNO_7$ (MH^+) 638.397657, obsd. 638.397533.

Anthracenyl-diboronic acid (145).

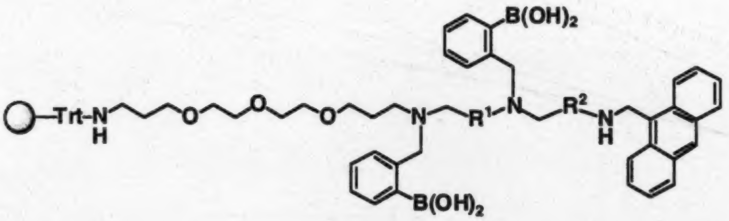

In a typical procedure, the Dde protected diboronic acid **144** (0.09 mmol) was rinsed with dry DMF (3×) in a polypropylene filter vessel under argon atmosphere. 0.5 mL triethylorthoformate (TEOF) was added followed by a 0.89 M solution of 9-anthracenyl aldehyde (1.1 mL, 0.90 mmol) in DMF. The dark brown suspension was vortexed for 4 hours before it was filtered and rinsed with dry DMF (5×) under argon. The resin was then suspended in 0.5 mL of DMF before the addition of $NaBH_4$ (34 mg, 0.90 mmol) dissolved in 1 mL of DMF. After vortexing for 1 minute acetic acid (0.054 mL, 0.90 mmol) was added slowly causing the suspension to fizz. The suspension was then vortexed for 16 hours and rinsed with DMF (3×), methanol (3×), and dichloromethane (5×) and dried under high vacuum to give the resin bound anthracenyl diboronic acid **144**.

Anthracenyl-triboronic acid tetrakis(trifluoroacetate) (136).

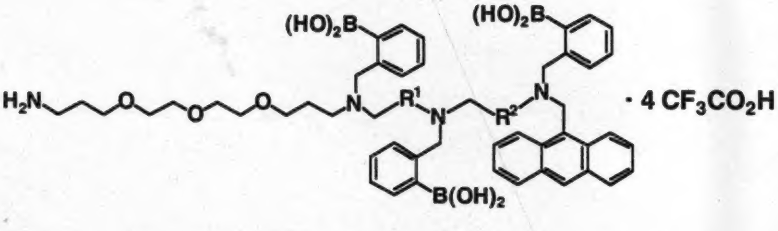

The final alkylation was done in a similar fashion as for diboronic acid **143**. Briefly, resin **144** (0.064 mmol), was refluxed in 2 mL of THF with PMP (0.058 mL, 0.32 mmol) and boronate **40** (0.066 mL, 0.32 mmol) for 10 hours. Afterwards boronate ester was hydrolysed to the acid and the resin rinsed as described above. After drying under high vacuum the entire resin was cleaved with 5 % TFA in dichloromethane to give, after evaporation, a yellow oil which was the triboronic acid **136** as its tetrakis-(trifluoroacetate) salt, all in >99 % yield. NMR of the triboronic acids gave complex mixtures of anhyd-rides. Analysis by LCMS/UV was done using the same LC and MSD conditions described for tetramine **84** with the exception of a fragmentor voltage of 120 V (see Appendix for copies of LCUV/MS traces).

Amb^{B}Anth^{B}. Purity by HPLC/UV: 82 % (254 nm), 75 % (210 nm), 92 % (370 nm). ESMS (*m/z*) 780.4 (MH-3H_2O), 770.4, 752.4. HRMS-ESMS calcd for $C_{47}H_{58}B_2O_7N_3$ (MH-H_2O) 798.446087, obsd. 798.446128.

Ahx^{B}Amb^{B}Anth^B. Purity by HPLC/UV: 82 % (254 nm), 75 % (210 nm), 71 % (370 nm). ESMS (*m*/*z*) 977.5 (MH-3H$_2$O), 967.6, 787.5. HRMS-ESMS calcd for $C_{62}H_{74}B_3O_6N_4$ (MH-3H$_2$O) 977.573103 obsd. 977.573073.

Amb^{B}Amb^{B}Anth^B. Purity by HPLC/UV: 75 % (254 nm), 59 % (210 nm), 92 % (370 nm). ESMS (*m*/*z*) 997.5 (MH-3H$_2$O), 987.5, 807.5. HRMS-ESMS calcd for $C_{62}H_{68}B_3O_6N_4$ (MH-3H$_2$O) 997.541802 obsd. 997.541211.

4Acc^{B}Amb^{B}Anth^B. Purity by HPLC/UV: 75 % (254 nm), 70 % (210 nm), 91 % (370 nm). ESMS (*m*/*z*) 989.6 (MH-3H$_2$O), 979.6, 749.5. HRMS-ESMS calcd for $C_{61}H_{72}B_3O_6N_4$ (MH-3H$_2$O) 989.573103 obsd. 989.573733.

Amc^{B}Amb^{B}Anth^B. Purity by HPLC/UV: 76 % (254 nm), 59 % (210 nm), 88 % (370 nm). ESMS (*m*/*z*) 1003.6 (MH-3H$_2$O), 993.6., 813.5. HRMS-ESMS calcd for $C_{62}H_{74}B_3O_6N_4$ (MH-3H$_2$O) 1003.588753 obsd. 1003.588169.

Fluorescence titration and determination of stability constants

Solutions of 2.60×10^{-6} M concentration of the triboronic acid receptors **136** were prepared in 0.010 M phosphate buffer (pH 7.8) in 1:1 water/methanol. 3.0 mL of each solution was added to a quartz cuvette and titrated with a 1.0 M solution of the saccharide dissolved in the 1:1 water/methanol buffer mixture. The fluorescence emission spectrum (excitation wavelength: 370 nm) was taken after each addition of the saccharide solution. Titration curves were constructed by plotting the relative fluorescence intensity at 423 nm versus concentration of the saccharide in the cuvette. The stability constants, K_a were determined using the Benesi-Hildebrand equation by plotting $1/(I-I_o)$ versus 1/[saccharide] and obtaining the ratio between the intercept and the slope.[147-149]

8.16: Acylation of amino acids.

The procedure followed was adapted from Bodanszky and Bodanszky.[110] In our hands, the free amino acid was dissolved in 1 equivalent of 1N NaOH(aq) and then cooled in an ice-water bath. An additional 0.25 equivalents of 1N NaOH(aq) were then added followed by 0.25 equivalents of the acid anhydride. After the solution became homogeneous, the additions of 1N NaOH(aq) and the anhydride are repeated four more times until a total of 1.25 equivalents of each were added. In some cases additional 1N NaOH(aq) was needed after each portion to ensure alkalinity. The reactions were monitored by thin layer chromatography (TLC) using, as an eluent, 4:1:1 *n*-butanol/water/acetic acid, and ninhydrin to visualize the plates. Stirring of the solution at room temperature was continued over 16 hours, or when judged complete by TLC. It was then re-cooled in an ice-water bath and acidified to pH 2 with concentrated HCl(aq). Product isolation depended on the particular derivative and are described below individually.

N-acetyl-L-norvaline (HO-LNva-Ac).[155]

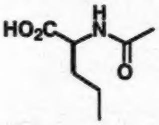

Product was isolated upon saturation of the reaction mixture with solid NaCl and the formation of an oily suspension. The suspension was extracted into ethyl acetate which was was dried over anhydrous $MgSO_4$ and concentrated to give a white solid (35% yield). ^{1}H NMR (300 MHz, CD_3OD) δ 4.34 (dd, *J* = 5.1, 9.0 Hz, 1H), 1.97 (s, 3H), 1.85 – 1.58 (m, 2H), 1.48 – 1.32 (m, 2H), 0.94 (t, *J* = 7.3Hz, 3H). ^{13}C APT NMR (75.5 MHz, CD_3OD) δ 175.6 (CO), 173.2 (CO), 53.4 (CH), 34.6 (CH_2), 22.2 (CH_3), 20.0 (CH_2), 13.8 (CH_3).

N-butyryl-D-norvaline (HO-DNva-COPr)

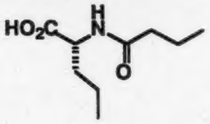

Product was obtained as an oily suspension after acidification and then isolation as described for HO-LNva-Ac. Excess butyric acid was removed by heating the sample to 45°C at < 1 Torr for 16 hours giving a clear viscous oil. (90% yield). ^{1}H NMR (300 MHz, CD_3OD) δ 4.35 (dd, *J* = 5.0, 9.1Hz, 1H), 2.21 (t, *J* = 7.1 Hz, 2H), 1.86 – 1.58 (m, 2H), 1.63 (t, *J* = 7.4 Hz, 2H), 1.48 – 1.30 (m, 2H), 0.94 (overlapping t's, *J* = 7.3Hz, 6H). ^{13}C APT NMR (75.5 MHz, CD_3OD) δ 176.2 (CO), 175.7 (CO), 53.3 (CH), 38.6 (CH_2), 34.7 (CH_2), 20.3 (CH_2), 20.1 (CH_2), 13.9 (CH_3), 13.9 (CH_3). IR (methanol cast): 3305, 2963, 3050 – 2700 (broad), 1721, 1622, 1545 1205 cm^{-1}. HRMS-EIMS (*m/z*) calcd. for $C_9H_{17}O_3N$ (M^+) 187.12085, obsd. 187.12127.

8-(*N*-acetylamino)octanoic acid(HO-8Aoc-Ac), $HO_2C(CH_2)_7NHCOCH_3$

Acidification of the reaction mixture yielded a precipitate which was filtered, washed with cold water and then dried over KOH/drierite under high vacuum giving a fluffy white solid. (95% yield). Melting point: 122 - 124°C. ^{1}H NMR (300 MHz, CD_3OD) δ 3.13 (t, *J* = 6.9 Hz, 2H), 2.27 (t, *J* = 7.3 Hz, 2H), 1.91 (s, 3H), 1.59 (quintet, *J* = 7.1 Hz, 2H), 1.48 (quintet, *J* = 6.9 Hz, 2H), 1.34 (broad s, 6H). ^{13}C APT NMR (75.5 MHz, CD_3OD) δ 177.6 (CO), 173.1 (CO), 40.5 (CH_2), 34.9 (CH_2), 30.3 (CH_2), 30.1 (CH_2), 30.0 (CH_2), 27.8 (CH_2), 26.0 (CH_2), 22.5 (CH_3). IR (microscope): 3349, 2929, 2522 (broad), 1705, 1611, 1556 cm^{-1}. HRMS-EIMS (*m/z*) calcd. for $C_{10}H_{19}O_3N$ (M^+) 201.13649, obsd. 201.13664.

4-(*N*-acetylaminomethyl)benzoic acid (HO-4Amb-Ac).[156]

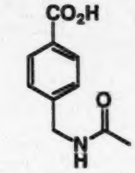

Acidification yielded a precipitate which was filtered, washed with cold water and then dried over KOH/drierite under high vacuum giving a fluffy white solid (79% yield). Spectral data matched that in the literature.[156] ^{1}H NMR (300 MHz, CD_3OD) δ 7.97 (d, *J* = 8.4 Hz, 2H), 7.37 (d, *J* = 8.6 Hz, 2H), 4.41 (s, 2H), 2.00 (s, 3H). ^{13}C APT NMR (75.5 MHz, CD_3OD) δ 173.3 (CO), 169.6 (CO), 145.4 (C), 131.0 (CH), 130.8 (C), 128.4 (CH), 43.8 (CH_2), 22.5 (CH_3).

N-butyryl-D-phenylalanine (HO-DPhe-CO*n*Pr)

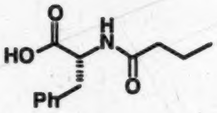

Product was initially obtained as an oil after extraction into ethyl acetate and concentration. This oil crystallized upon addition of diethyl ether (31% yield). Melting point: 111-114°C. ^{1}H NMR (300 MHz, CD_3OD) δ 7.10 – 7.30 (m, 5H), 4.65 (dd, *J* = 4.9, 9.2 Hz, 1H), 3.21 (dd, *J* = 4.9, 13.8 Hz, 1H), 2.93 (dd, *J* = 9.3, 13.9 Hz, 1H), 2.12 (t, *J* = 7.4 Hz, 2H), 1.52 (sextet, *J* = 7.4 Hz, 2H), 0.82 (t, *J* = 7.4 Hz, 3H). ^{13}C APT NMR (75.5 MHz, CD_3OD) δ 175.8 (CO), 175.3 (CO), 138.7 (C), 130.3 (CH), 129.3 (CH), 127.7 (CH), 55.2 (CH), 38.7 (CH_2), 38.5 (CH_2), 20.2 (CH_2), 13.9 (CH_3). IR (microscope): 3342, 3068, 3033, 2960 – 2455, 1703, 1624, 1551, 1268, 1238, 1223 cm^{-1}. HRMS-EIMS (*m/z*) calcd. for $C_{13}H_{17}O_3N$ (M^+) 235.12085, obsd. 235.12090.

2-(*N*-acetylamino)cyclohexane carboxylic acid (HO-2Acc-Ac).

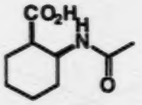

The product was obtained as a white solid after acidification followed by addition of solid NaCl and then extraction into ethyl acetate as described for HO-LNva-Ac (67% yield). Melting point: 154 - 156°C. ^{1}H NMR (300 MHz, CD_3OD) δ 4.19 (dt, *J* = 4.1, 8.0 Hz, 1H), 2.73 (dt, *J* = 4.2, 7.7 Hz 1H), 1.93 (s, 3H), 2.00 – 1.90 (m ,1H), 1.90 – 1.75 (m, 1H), 1.75 – 1.38 (m, 6H). ^{13}C APT NMR (75.5 MHz, CD_3OD) δ 177.0 (CO), 172.6 (CO), 48.9 (CH), 45.4 (CH), 30.5 (CH_2), 26.5 (CH_2), 24.2 (CH_2), 23.7 (CH_2), 22.6 (CH_3). IR (microscope): 3320, 2926, 2493 (broad), 1688, 1613, 1551, 1277 cm^{-1}. HRMS-EIMS (*m/z*) calcd. for $C_9H_{15}O_3N$ (M^+) 185.10519, obsd. 185.10528.

4-(*N*-butyrylamino)cyclohexane carboxylic acid (HO-4Acc-COPr)

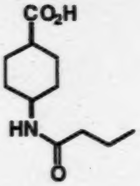

Product was obtained as a white solid upon acidification, washing with water and then drying as described for HO-8Aoc-Ac (65% yield). Melting point: 143 - 144°C. ^{1}H NMR (300 MHz, CD_3OD) δ 3.76 (m, 1H), 2.50 – 2.46 (m , 1H), 2.13 (t, *J* = 7.1 Hz, 2H), 2.01 – 1.93 (m, 2H), 1.74 – 1.48 (m, 6H), 1.60 (quintet, *J* = 7.4 Hz, 2H), 0.92 (t, *J* = 7.4 Hz, 3H). ^{13}C APT NMR (75.5 MHz, CD_3OD) δ 178.7 (CO), 175.4 (CO), 47.9 (CH), 40.9 (CH), 38.9 (CH_2), 30.2 (CH_2), 26.3 (CH_2), 20.5 (CH_2), 13.9 (CH_3). IR (microscope): 3276, 2954, 1724, 1599, 1567, 1201 cm^{-1}. HRMS-EIMS (*m/z*) calcd. for $C_{11}H_{19}O_3N$ (M^+) 213.13649, obsd. 213.13685.

12-(*N*-acetylamino)dodecanoic acid(HO-12Ado-Ac), $HO_2C(CH_2)_{11}NHCOCH_3$

This reaction was done using methanol as a co-solvent due to the poor solubility of the amino acid in water. The amount of methanol was equal to the volume of 1 equivalent of 1 N NaOH (aq). Product was obtained as a white solid upon acidification, washing with water and then drying as described for HO-8Aoc-Ac (14 % yield). Melting point: 111 – 114°C. ^{1}H NMR (300MHz, CD_3OD) δ 3.13 (t, *J* = 7.0 Hz, 2H), 2.66 (t, *J* = 7.5 Hz, 2H), 1.91 (s, 3H), 1.65 – 1.50 (m, 2H), 1.50 – 1.40 (m, 2H), 1.30 (broad s, 14H). ^{13}C APT NMR (75.5 MHz, DMSO-d_6) δ 174.5 (CO), 168.8 (CO), 38.4 (CH_2), 33.7 (CH_2), 29.1 (CH_2), 29.0 (CH_2), 29.0 (CH_2), 28.9 (CH_2), 28.8 (CH_2), 28.6 (CH_2), 26.4 (CH_2), 22.6 (CH_3). IR (microscope): 3347, 2917, 2520 (broad), 1704, 1602, 1557 cm^{-1}. HRMS-EIMS (*m/z*) calcd. for $C_{14}H_{27}O_3N$ (M^+) 257.19910, obsd. 257.19926.

4-(*N*-acetylaminomethyl)cyclohexane carboxylic acid (HO-Amc-Ac)

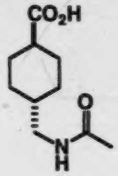

Product was obtained as a white solid upon acidification, washing with water and then drying as described for HO-8Aoc-Ac (38% yield). Melting point: 156 - 158°C. ^{1}H NMR (300 MHz, CD_3OD) δ 3.00 (d, *J* = 6.8 Hz, 1H), 2.20 (tt, *J* = 3.6, 12.0 Hz, 1H), 1.98 (dd, *J* = 3.4, 13.7 Hz, 2H), 1.92 (s, 3H), 1.81 (dd, *J* = 3.2, 13.6 Hz, 2H), 1.52 – 1.38 (m , 1H), 1.38 (dq, *J* = 3.4, 12.4 Hz, 2H), 0.98 (dq, *J* = 3.5, 12.9 Hz, 2H). ^{13}C APT NMR (75.5 MHz, CD_3OD) δ 179.8 (CO), 173.3 (CO), 46.5 (CH_2), 44.4 (CH), 38.6 (CH), 30.9 (CH_2), 29.8 (CH_2), 22.3 (CH_3). IR (microscope): 3342, 2932, 1703, 1598, 1562 cm^{-1}. HRMS-EIMS (*m/z*) calcd. for $C_{10}H_{17}O_3N$ (M^+) 199.12085, obsd. 199.12058.

6-*N*-acetylaminohexanoic acid (HO-6Ahx-Ac), $HO_2C(CH_2)_5NHCOCH_3$

Product was obtained as a white fluffy solid upon acidification, washing with water and then drying as described for HO-8Aoc-Ac (95% yield). Melting point: 101 - 103°C. ^{1}H NMR (400 MHz, D_2O) δ 3.24 (t, *J* = 6.8 Hz, 2H), 2.46 (t, *J* = 7.2 Hz, 2H), 2.04 (s, 3H), 1.69 (quintet, *J* = 7.6 Hz, 2H), 1.61 (quintet, *J* = 7.2 Hz, 2H), 1.42 (quintet, *J* = 7.2 Hz, 2H). ^{13}C APT NMR (75.5 MHz, CD_3OD) δ 177.8 (CO), 173.2 (CO). 40.3 (CH_2), 34.8 (CH_2), 30.0 (CH_2), 27.5 (CH_2), 25.7 (CH_2), 22.5 (CH_3). IR (microscope): 3350, 2942, 3098 – 2574 (broad), 1703, 1603, 1559 cm^{-1}. HRMS-EIMS (*m/z*) calcd. for $C_8H_{15}O_3N$ (M^+) 173.10519, obsd. 173.10526.

4-γ-*N*-acetylaminobutyric acid (HO-γAbu-Ac), $HO_2C(CH_2)_3NHCOCH_3$

After the reaction was judged complete by TLC it was acidified by the addition of concentrated HCl(aq). The addition of solid NaCl failed to precipitate the product. Therefore, the mixture was evaporated and the residue extracted into 20% methanol in dichloromethane while filtrating to remove the NaCl. The extraction solvent was then evaporated yielding a colorless oil (20% yield). ^{1}H NMR (300 MHz, D_2O) δ 3.21 (t, *J* = 6.9 Hz, 2H), 2.43 (t, *J* = 7.2 Hz, 2H), 1.98 (s, 3H), 1.82 (quintet, *J* = 6.9 Hz, 2H). ^{13}C APT NMR (75.5 MHz, CD_3OD) δ 175.0 (CO), 174. 9 (CO), 40.7 (CH_2), 31.8 (CH_2), 25.1 (CH_2), 21.4 (CH_3). IR (methanol cast): 3245, 2953, 1735, 1625, 1549, 1093 cm^{-1}. HRMS-EIMS (*m/z*) calcd. for $C_6H_{11}O_3N$ (M^+) 145.07389, obsd. 145.07389.

3-(*N*-butyrylaminomethyl)benzoic acid (HO-3Amb-Ac, 105)

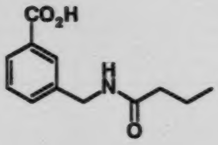

Acylation of 3-(*N*-FMOC-aminomethyl)benzoic acid (**104**) was done according to the procedure by Li *et al.*[132] To a mixture of **104** (0.446 g, 1.19 mmol) and KF (0.277 g, 4.77 mmol) in 7 mL of DMF was added triethylamine (0.50 mL, 3.1 mmol) followed by butyric anhyride (0.22 mL, 1.3 mmol). The solution was stirred at room temperature for 36 hours going from clear to cloudy. 105 mL of ethyl acetate was then added to the flask and washed with 2×30 mL of 5% HCl(aq). The product was then extracted into 10 % $NaHCO_3$(aq) (3×20 mL). The basic solution was acidified to pH 2 with concentrated HCl(aq). Solid NaCl was added producing a cloudy mixture which was extracted into ethyl acetate (3×20 mL), washed with brine, dried over anhydrous Na_2SO_4 and evaporated to give the *N*-butyryl derivative **105** a white solid (0.178 g, 67%). Melting point: 161 - 163°C. ^{1}H NMR (300 MHz, CD_3OD) δ 7.95 (broad s, 1H), 7.89 (bd, *J* = 6.0 Hz, 1H), 7.50 (broad d, *J* = 6.3 Hz, 1H), 7.44 (t, *J* = 8.1 Hz, 1H), 4.41 (s, 2H), 2.22 (t, *J* = 7.5 Hz, 2H), 1.66 (quintet, *J* = 7.2 Hz, 2H), 0.94 (t, *J* = 7.5 Hz, 3H). ^{13}C APT NMR (75.5 MHz, CD_3OD) δ 176.1 (C), 169.6 (C), 140.8 (C), 133.1 (CH), 132.2 (C), 129.7 (CH), 129.6 (CH), 129.5 (CH), 43.7 (CH_2), 39.0 (CH_2), 20.4 (CH_2), 14.0 (CH_3). IR (microscope): 3313, 3100 – 2550, 2960, 1690, 1639, 1544, 1311 cm^{-1}. HRMS-EIMS calcd for $C_{12}H_{15}O_3N$ (M^+) 221.10519, obsd. 221.10542.

8.17: Labeling of Lewis-b with nitrobenzobenzodiazole.

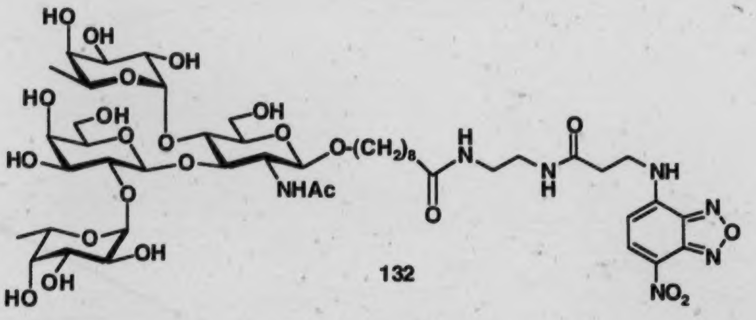

132

The procedure followed,starting from the 8-methoxycarbonyloctanol glycoside of Le^b (supplied by Prof. O. Hindsgaul), was previously described by Zhang *et al.*[143] The labeling reagent employed was 4-(7-nitro-2,1,3-benzooxadiazoyl-4-ylamino)propionic acid (**131**, from Molecular Probes, Eugene, Oregon; λ_{em}(max) = 530 nm, λ_{ex}(max) = 466 nm in methanol). After preparative TLC, using as a eluent chloroform/methanol/water (60:35:6), and lyophilization, a fluffy yellow solid was obtained which was checked by ESMS and ^{1}H NMR. ^{1}H NMR (500 MHz, D_2O) δ 8.45 (broad s, 1H), 6.46 (d, *J* = 9.3 Hz, 1H), 5.14 (d, *J* = 3.7 Hz, 1H), 5.02 (d, *J* = 3.9 Hz, 1H), 4.85 (apparent q, *J* = 6.5 Hz, 1H), 4.67 (d, *J* = 8.0 Hz, 1H), 4.36 (d, *J* = 8.0 Hz, 1H), 4.34 (apparent q, *J* = 7.0 Hz, 1H), 4.11 (dd, *J* = 10.5, 10.5 Hz, 1H), 3.96 (apparent d, *J* = 10.0 Hz, 1H), 3.93 (dd, *J*= 3.0, 10.5 Hz, 1H), 3.87 – 3.67 (m, 12H), 3.62 – 3.56 (m, 2H), 3.53 – 3.51 (m, 1H), 3.49 – 3.42 (m, 2H), 3.34 – 3.29 (m, 2H), 3.29 – 3.24 (m, 2H), 2.72 (t, *J* = 6.5 Hz, 2H), 2.06 (t, *J* = 7.5 Hz, 2H), 2.04 (s, 3H), 1.48 – 1.38 (m, 4H), 1.38 – 1.20 (m, 2H), 1.26 (d, *J* = 6.5 Hz, 6H), 1.20 – 1.10 (m, 6H). HRMS-ESMS calcd for $C_{46}H_{73}O_{24}N_7Na$ ($M+Na^+$) 1130.460467, obsd. 1130.460645. The labeled oligosaccharide was observed in the epi-fluorescent microscope using an Olympus WU cube with excitation band: 330 – 385 nm and emission band: > 420 nm, and a WIB cube with excitation band: 460 – 490 nm and emission band: > 515 nm,

Bibliography.

[1] R. E. Badine, S. L. Bender, *Chem. Rev.* **1997**, *97*, 1359-1472.

[2] P. B. Dervan, R. W. Burli, *Curr. Opin. Chem. Biol.* **1999**, *3*, 688-693.

[3] T. Hermann, *Angew. Chem. Int. Ed.* **2000**, *39*, 1890-1905.

[4] J. Gallego, G. Varani, *Acc. Chem. Res,* **2001**, *34*, 836-843.

[5] A. Varki, *Glycobiology* **1993**, *3*, 97-130.

[6] H. Lis, N. Sharon, *Chem. Rev.* **1998**, *98*, 637-674.

[7] E. E. Simanek, G. J. McGarvey, J. A. Jablonowski, C.-H. Wong, *Chem. Rev.* **1998**, *98*, 833-862.

[8] W. S. Somers, J. Tang, G. D. Shaw, R. T. Camphausen, *Cell* **2000**, *103*, 467-479.

[9] A. Varki, *J. Clin. Invest.* **1997**, *99*, 158-162.

[10] P. Sears, C.-H. Wong, *Angew. Chem. Int. Ed.* **1999**, *38*, 2300-2324.

[11] A. P. Davis, R. S. Wareham, *Angew. Chem. Int. Ed.* **1999**, *38*, 2978-2886.

[12] A. P. Davis, R. S. Wareham, *Angew. Chem. Int. Ed.* **1998**, *37*, 2270.

[13] T. D. James, K. R. A. S. Sandanayake, S. Shinkai, *Angew. Chem. Int. Ed. Engl.* **1996**, *35*, 1911-1922.

[14] T. D. James, S. Shinkai, *Top. Curr. Chem.* **2002**, *218*, 159-200.

[15] J. P. Lorand, J. O. Edwards, *J. Org. Chem.* **1959**, *24*, 769.

[16] G. Springsteen, B. Wang, *Tetrahedron* **2002**, *58*, 5291-5300.

[17] J. C. Norrild, H. Eggert, *J. Chem. Soc. Perkin Trans. 2* **1996**, 2583-2588.

[18] Y. Shiomi, M. Saisho, K. Tsukagoshi, S. Shinkai, *J. Chem. Soc. Perkin Trans. 1* **1993**, 2111-2117.

[19] J. C. Norrild, H. Eggert, *J. Am. Chem. Soc.* **1995**, *117*, 1479-1484.

[20] G. Wulff, *Pure App. Chem.* **1982**, *54*, 3403.

[21] J. C. Norrild, I. Sotofte, *J. Chem. Soc. Perkin Trans. 2* **2001**, 727-732.

[22] T. D. James, K. R. A. S. Sandanayake, R. Iguchi, S. Shinkai, *J. Am. Chem. Soc.* **1995**, *117*, 8982-8987.

[23] A. P. deSilva, H. Q. N. Gunaratne, T. Gunnlaugsson, A. J. M. Huxley, C. P. McCoy, J. T. Rademacher, T. E. Rice, *Chem. Rev.* **1997**, *97*, 1515-1566.

[24] M. Bielecki, H. Eggert, J. C. Norrild, *J. Chem. Soc. Perkin Trans. 2* **1999**, 449-455.

[25] A. Sugasaki, M. Ikeda, M. Takeuchi, S. Shinkai, *Angew. Chem. Int. Ed.* **2000**, *39*, 3839-3842.

[26] A. Sugasaki, M. Ikeda, M. Takeuchi, K. Koumoto, S. Shinkai, *Tetrahedron* **2000**, *56*, 4717-4723.

[27] S. Shinkai, M. Ikeda, A. Sugasaki, M. Takeuchi, *Acc. Chem. Res.* **2001**, *34*, 494-503.

[28] A. Sugasaki, K. Sugiyasu, M. Ikeda, M. Takeuchi, S. Shinkai, *J. Am. Chem. Soc.* **2001**, *123*, 10239-10244.

[29] A. R. Vaino, K. D. Janda, *J. Comb. Chem.* **2000**, *2*, 579-596.

[30] B. Yan, *Comb. Chem. High Thru. Scr.* **1998**, *1*, 215-229.

[31] B. Yan, *Acc. Chem. Res.* **1998**, *31*, 621-630.

[32] M. J. Shapiro, J. S. Gounarides, *Prog. Nucl. Mag. Res. Sp.* **1999**, *35*, 153-200.

[33] C. Spanka, P. Wentworth, K. D. Janda, *Comb. Chem. High Thru. Scr.* **2002**, *5*, 233-240.

[34] P. Wentworth, K. D. Janda, *Chem. Commun.* **1999**, 1917-1924.

[35] D. J. Gravert, K. D. Janda, *Chem. Rev.* **1997**, *97*, 489-509.

[36] D. P. Curran, *Angew. Chem. Int. Ed.* **1998**, *37*, 1175-1196.

[37] D. P. Curran, *Synlett.* **2001**, 1488-1496.

[38] A. Furka, M. Sebestyen, M. Asgedom, G. Dibo, *Int. J. Pept. Prot. Res.* **1991**, *37*, 487.

[39] J. M. Ostresh, G. M. Husar, S. E. Blondelle, B. Dorner, P. A. Weber, R. A. Houghten, *Proc. Natl. Acad. Sci. USA* **1994**, *91*, 11138-11142.

[40] K. S. Lam, M. Lebl, V. Krchnak, *Chem. Rev.* **1997**, *97*, 411-448.

[41] N. Sugimoto, D. Miyoshi, J. Zou, *Chem. Commun.* **2000**, 2295-2296.

[42] E. P. Edman, *Acta Chemica Scand.* **1950**, *4*, 283-293.

[43] S. Patterson, B. D. Smith, R. E. Taylor, *Tetrahedron Lett.* **1998**, *39*, 3111-3114.

[44] K. C. Nicolaou, X. Y. Xiao, Z. Parandoosh, A. Senyei, M. P. Nova, *Angew. Chem. Int. Ed. Engl.* **1995**, *34*, 2289-2291.

[45] K. C. Nicolaou, J. A. Pfefferkorn, H. J. Mitchell, A. J. Roecker, S. Barluenga, G.-Q. Cao, R. L. Affleck, J. E. Lillig, *J. Am. Chem. Soc.* **2000**, *122*, 9954-9967.

[46] W. C. Still, *Acc. Chem. Res.* **1996**, *29*, 155-163.

[47] R. S. Youngquist, G. R. Fuentes, M. P. Lacey, T. Keough, *J. Am. Chem. Soc.* **1995**, *117*, 3900-3906.

[48] S. Arimori, C. J. Ward, T. D. James, *Tetrahedron Lett.* **2002**, *43*, 303-305.

[49] G. Springsteen, B. Wang, *Chem. Commun.* **2001**, 1608-1609.

[50] S. S. Cohen, *A Guide to Polyamines*, Oxford University Press, New York, **1998**.

[51] R. H. Scott, K. G. Sutton, A. C. Dolphin, *Trends in Neuroscience* **1993**, *16*, 155-160.

[52] K. Williams, *Biochem. J.* **1997**, *325*, 289-297.

[53] R. A. Casero, P. M. Woster, *J. Med. Chem.* **2001**, *44*, 1-26.

[54] B. Klenke, S. M., B. M.P., R. Brun, I. H. Gilbert, *J. Med. Chem.* **2001**, *44*, 3440-3452.

[55] H. S. Kim, K. C. Kwon, K. S. Kim, L. C.H., *Bioorg. Med. Chem. Lett.* **2001**, *11*, 3065-3068.

[56] O. Phanstiel, H. L. Price, L. Wang, J. Juusola, M. Kline, S. M. Shah, *J. Org. Chem.* **2000**, *65*, 5590-5599.

[57] T. Ren, G. Zhang, D. Liu, *Tetrahedron Lett.* **2001**, *42*, 1007-1010.

[58] G. F. Graminski, C. L. Carlson, J. R. Ziemer, F. Cai, N. M. J. Vermeulen, S. M. Vanderwerf, M. R. Burns, *Bioorg. Med. Chem. Lett.* **2002**, *12*, 35-40.

[59] M. R. Burns, C. L. Carlson, S. M. Vanderwerf, J. R. Ziemer, R. S. Weeks, F. Cai, H. K. Webb, G. F. Graminski, *J. Med. Chem.* **2001**, *44*, 3632-3644.

[60] R. J. Bergernon, W. R. Weimar, Q. Wu, Y. Feng, J. S. McManis, *J. Med. Chem.* **1996**, *39*, 5257-5266.

[61] M. Delfini, A. L. Segre, F. Conti, R. Barbucci, *J. Chem. Soc. Perkin Trans. 2* **1980**, 900-903.

[62] A. Kanavorioti, E. E. Baird, P. J. Smith, *J. Org. Chem.* **1995**, *60*, 4873-4883.

[63] M. Belting, B. Havsmark, M. Jonsson, S. Persson, L. A. Fransson, *Glycobiology* **1996**, *6*, 121-129.

[64] M. C. Wahl, M. Sundaralingam, *Biopolymers* **1997**, *44*, 45.

[65] D. B. Tippen, M. Sundaralingam, *J. Mol. Biol.* **1997**, *267*, 1171-1185.

[66] H. Deng, V. A. Bloomfield, J. M. Benevides, G. J. Thomas, *Nucleic Acids Res.* **2000**, *28*, 3379-3385.

[67] B. Frydman, W. M. Westler, K. Samejima, *J. Org. Chem.* **1996**, *61*, 2588-2589.

[68] G. J. Quigley, M. M. Teeter, A. Rich, *Proc. Natl. Acad. Sci. USA* **1978**, *75*, 64-68.

[69] S. Schulz, *Angew. Chem. Int. Ed. Engl.* **1997**, *36*, 314-326.

[70] K. Nakanishi, S.-K. Choi, D. Hwang, K. Kerro, M. Orlando, A. G. Kalivretenos, M. Eldefrawi, P. N. R. Usherwood, *Pure Appl. Chem.* **1994**, *66*, 641-678.

[71] K. Nakanishi, X. Huang, H. Jiang, Y. Liu, K. Fang, D. Huang, S.-K. Choi, E. Katz, M. Eldefrawi, *Bioorg. Med. Chem.* **1997**, *5*, 1969-1988.

[72] V. Kuksa, R. Buchan, P. Kong Thoo Lin, *Synthesis* **2000**, 1189-1207.

[73] G. Karigiannis, D. Papaioannou, *Eur. J. Org. Chem.* **2002**, 1841-1863.

[74] G. Byk, M. Frederic, D. Scherman, *Tetrahedron Lett.* **1997**, *38*, 3219-3222.

[75] P. Page, S. Burrage, L. Baldock, M. Bradley, *Bioorg. Med. Chem. Lett.* **1998**, *8*, 1751-1756.

[76] I. R. Marsh, M. Bradley, *Tetrahedron* **1997**, *53*, 17317-17334.

[77] I. A. Nash, B. W. Bycroft, W. C. Chan, *Tetrahedron Lett.* **1996**, *37*, 2625-2628.

[78] E. Jefferson, K. G. Sprankle, E. E. Swayze, *J. Comb. Chem.* **2000**, 2, 100-103.

[79] N. D. Hone, L. J. Payne, *Tetrahedron Lett.* **2000**, *41*, 6149-6152.

[80] D. Jonsson, A. Unden, *Tetrahedron Lett.* **2002**, *43*, 3125-3128.

[81] S. R. Chhabra, A. N. Khan, B. W. Bycroft, *Tetrahedron Lett.* **2000**, *41*, 1099-1102.

[82] G. Karigiannis, P. Mamos, G. Balayiannis, I. Katsoulis, D. Papaioannou, *Tetrahedron Lett.* **1998**, *39*, 5117-5120.

[83] A. Nefzi, J. M. Ostresh, R. A. Houghten, *Tetrahedron* **1999**, *55*, 335-344.

[84] H. C. Brown, P. Heim, *J. Org. Chem.* **1973**, *38*, 912-916.

[85] H. C. Brown, Y. M. Choi, S. Narasimhan, *J. Org. Chem.* **1982**, *47*, 3153-3163.

[86] C. F. Lane, *Aldrichim. Acta* **1973**, *6*, 51.

[87] R. O. Hutchins, K. Learn, B. Nazer, D. Pytlewski, *Org. Prep. Proc. Int.* **1984**, *16*, 335-372.

[88] S. Choi, I. Bruce, A. J. Fairbanks, G. W. J. Fleet, A. H. Jones, R. J. Nash, L. E. Fellows, *Tetrahedron Lett.* **1991**, *32*, 5517-5520.

[89] V. Ferey, P. Vedrenne, L. Toupet, T. Le Gall, C. Mioskowski, *J. Org. Chem.* **1996**, *61*, 7244-7245.

[90] M. A. Schwartz, B. F. Rose, B. Vishnuvajjala, *J. Am. Chem. Soc.* **1973**, *95*, 612-613.

[91] G. M. Dubowchik, R. A. Firestone, *Tetrahedron Lett.* **1996**, *37*, 6465-6468.

[92] A. Nefzi, J. M. Ostresh, J. P. Meyer, R. A. Houghten, *Tetrahedron Lett.* **1997**, *38*, 931-934.

[93] J. M. Van Paasschen, R. A. Geangel, *J. Am. Chem. Soc.* **1972**, *94*, 2680.

[94] D. G. Hall, C. Laplante, S. Manku, J. Nagendran, *J. Org. Chem.* **1999**, *64*, 698-699.

[95] S. Manku, C. Laplante, D. Kopac, T. Chan, D. G. Hall, *J. Org. Chem.* **2001**, *66*, 874-885.

[96] J. E. Douglass, *J. Am. Chem. Soc.* **1964**, *86*, 5431.

[97] W. Mills, L. J. Todd, J. C. Huffman, *Chem. Commun.* **1989**, 900-901.

[98] P. J. Bratt, M. P. Brown, K. P. Seddon, *J. Chem. Soc. Dalton Trans.* **1974**, 2161-2163.

[99] P. Vedrenne, V. LeGuen, L. Toupet, T. LeGall, C. Mioskowski, *J. Am. Chem. Soc.* **1999**, *121*, 1090-1091.

[100] J. R. Appel, J. Johnson, V. L. Narayanan, R. A. Houghten, *Mol. Divers.* **1998**, *4*, 91-102.

[101] S. R. Chhabra, A. N. Khan, B. W. Bycroft, *Tetrahedron Lett.* **2000**, *41*, 1095-1098.

[102] G. B. Quistad, C. C. Reuter, W. S. Skinner, P. A. Dennis, S. Suwanrumpha, E. W. Fu, *Toxicon.* **1991**, *29*, 329-336.

[103] A. Eldefrawi, M. Eldefrawi, K. Konno, N. A. Mansour, K. Nakanishi, E. Oltz, P. N. R. Usherwood, *Proc. Natl. Acad. Sci. USA* **1988**, *85*, 4910-4913.

[104] K. Stromgaard, M. J. Brierley, K. Andersen, F. A. Slok, I. R. Mellor, P. N. R. Usherwood, P. Krogsgaard-Larsen, J. W. Jaroszweski, *J. Med. Chem.* **1999**, *42*, 5224-5234.

[105] M. G. Bixel, M. Krauss, Y. Liu, M. L. Bolognesi, M. Rosini, I. S. Mellor, P. N. R. Usherwood, C. Melchiorre, K. Nakanishi, F. Hucho, *Eur. J. Biochem.* **2000**, *267*, 110-120.

[106] F. Wang, S. Manku, D. G. Hall, *Org. Lett.* **2000**, *2*, 1581-1583.

[107] B. W. Bycroft, W. C. Chan, S. R. Chabra, N. D. Hone, *J. Chem. Soc. Chem. Commun.* **1993**, 778-779.

[108] W. E. Rapp, in *Combinatorial Chemistry: Synthesis and Applications* (Eds.: S. R. Wilson, A. W. Czarnik), Wiley-Interscience, New York, **1997**, pp. 65-94.

[109] L. Lapatsanis, G. Millias, K. Froussios, M. Kolovos, *Synthesis* **1993**, 671.

[110] M. Bodansky, A. Bodansky, *The Practice of Peptide Synthesis*, 2 ed., Springer-Verlag, Berlin, **1994**.

[111] I. Alfonso, B. Dietrich, F. Rebolledo, V. Gotor, J.-M. Lehn, *Helv. Chem. Acta* **2001**, *84*, 280-.

[112] M. W. Hosseini, J.-M. Lehn, *Helv. Chem. Acta* **1986**, *69*, 587-603.

[113] T. Grawe, T. Schrader, P. Finocchiaro, G. Consiglio, S. Fallia, *Org. Lett.* **2001**, *3*, 1567-1600.

[114] S. Manku, D. G. Hall, *Org. Lett.* **2002**, *4*, 31-34.

[115] F. P. Schmidtchen, M. Berger, *Chem. Rev.* **1997**, *97*, 1609-1646.

[116] M. W. Peczuh, A. D. Hamilton, *Chem. Rev.* **2000**, *100*, 2479-2494.

[117] J. A. Aguilar, E. Garciaespana, J. A. Guerrero, S. V. Luis, J. M. Llinares, J. F. Miravet, J. A. Ramirez, C. Soriano, *J. Chem. Soc. Chem. Commun.* **1995**, 2237-2239.

[118] H. Fenniri, M. W. Hosseini, J. M. Lehn, *Helv. Chem. Acta* **1997**, *80*, 786-803.

[119] Y. Kato, M. M. Conn, J. J. Rebek, *J. Am. Chem. Soc.* **1994**, *116*, 3279.

[120] S. E. Schneider, S. N. O'Neil, E. V. Anslyn, *J. Am. Chem. Soc.* **2000**, *122*, 542-543.

[121] K. S. Lam, Z.-G. Zhao, S. Wade, V. Krchnak, M. Lebl, *Drug Dev. Res.* **1994**, *33*, 1994.

[122] S. M. Ngola, P. C. Kearney, S. Mecozzi, K. Russell, D. A. Dougherty, *J. Am. Chem. Soc.* **1999**, *121*, 1192-1201.

[123] This was observed by Dan Kopac of our laboratory during his work.

[124] L. Fielding, *Tetrahedron* **2000**, *56*, 6151-6170.

[125] J. P. Gallivan, D. A. Dougherty, *J. Am. Chem. Soc.* **2000**, *122*, 870-874.

[126] M. Tabet, V. Labroo, P. Sheppard, T. Sasaki, *J. Am. Chem. Soc.* **1993**, *115*, 3866-3868.

[127] M. W. Peczuh, A. D. Hamilton, J. Sanchez-Quesada, J. deMendoza, T. Haack, E. Giralt, *J. Am. Chem. Soc.* **1997**, *119*, 9327-9328.

[128] J. S. Albert, M. S. Goodman, A. D. Hamilton, *J. Am. Chem. Soc.* **1995**, *117*, 1143-1114.

[129] W. Rapp, in *Combinatorial Peptide and Nonpeptide Libraries* (Ed.: G. Jung), VCH, Weimheim, **1996**, p. 425.

[130] S. Ohta, A. Shimabayashi, M. Aono, M. Okamoto, *Synthesis* **1982**, 833-834.

[131] J. P. Wolfe, R. A. Singer, B. H. Yang, S. L. Buchwald, *J. Am. Chem. Soc.* **1999**, *121*, 9550-9561.

[132] W.-R. Li, H.-H. Chou, *Synthesis* **2000**, 84-90.

[133] R. D. Voyksner, in *Electrospray Ionization Mass Spectrometry* (Ed.: R. B. Cole), John Wiley & Sons Inc., New York, **1997**, pp. 323-342.

[134] C. N. McEwan, B. S. Larsen, in *Electrospray Ionization Mass Spectrometry* (Ed.: R. B. Cole), John Wiley & Sons, New York, **1997**, pp. 177-202.

[135] I. Capila, R. J. Linhardt, *Angew. Chem. Int. Ed.* **2002**, *41*, 390-412.

[136] C. A. A. van Boeckel, M. Petitou, *Angew. Chem. Int. Ed. Engl.* **1993**, *32*, 1671-1818.

[137] P. D. J. Grootenhuis, C. A. A. van Boeckel, *J. Am. Chem. Soc.* **1991**, *113*, 2743-2747.

[138] B. V. L. Potter, D. Lampe, *Angew. Chem. Int. Ed. Engl.* **1995**, *34*, 1933-1972.

[139] S. L. Wiskur, H. Ait-Haddou, J. J. Lavigne, E. V. Anslyn, *Acc. Chem. Res.* **2001**, *34*, 963-972.

[140] Z. Zhong, E. V. Anslyn, *J. Am. Chem. Soc.* **2002**, *124*, 9014-9015.

[141] H. Wennemers, W. C. Still, *Tetrahedron Lett.* **1994**, *35*, 6413.

[142] R. Xu, G. Greiveldinger, L. E. Marenus, A. Cooper, J. A. Ellman, *J. Am. Chem. Soc.* **1999**, *121*, 4898-4899.

[143] Y. Zhang, X. Le, N. J. Dovichi, C. A. Compston, M. M. Palcic, P. Diedrich, O. Hindsgaul, *Anal. Biochem.* **1995**, *227*, 368-376.

[144] T. D. James, H. Shinmori, M. Takeuchi, S. Shinkai, *Chem. Commun.* **1996**, 705-706.

[145] J.-C. Truffert, O. Lorthioir, U. Asseline, N. T. Thuong, A. Brack, *Tetrahedron Lett.* **1994**, *35*, 2353-2356.

[146] S. Arimori, M. L. Bell, C. S. Oh, K. Frimat, T. D. James, *J. Chem. Soc. Perkin Trans. 1* **2002**, 803-808.

[147] F. Diederich, K. Dick, D. Griebel, *J. Am. Chem. Soc.* **1986**, *108*, 2273-2286.

[148] K. A. Conners, *Binding constants. The measurement of molecular complex stability*, John Wiley and Sons, New York, **1987**.

[149] S. Fery-Forgues, M.-T. Le Bris, J.-P. Guette, B. Valeur, *J. Phys. Chem.* **1988**, *92*, 6233-6237.

[150] K. R. A. S. Sandanayake, T. D. James, S. Shinkai, *Chem. Lett.* **1995**, 503-504.

[151] M. Yamamoto, M. Takeuchi, S. Shinkai, *Tetrahedron* **1998**, *54*, 3125-3140.

[152] E. Kaiser, R. L. Colscott, C. D. Bossinger, P. I. Cook, *Anal. Biochem.* **1970**, *34*, 595-598.

[153] K. Matsuda, G. Ulrich, H. Iwamura, *J. Chem. Soc. Perkin Trans. 2* **1998**, 1581-1588.

[154] Three days is sufficent on 90 um beads.

[155] T. Shiraiwa, H. Yoshida, M. Tsuda, H. Kurokawa, *Bull. Chem. Soc. Jpn.* **1987**, *60*, 947.

[156] P. Chand, *et al.*, *J. Med. Chem.* **1997**, *40*, 4030-4052.

[157] http://www.shef.ac.uk/uni/projects/smc/software.html

Appendix: Selected NMR spectra and LCUV/MS data.

Table of Contents

A.1: ^{1}H and ^{13}C NMR spectra, and HPLC chromatograms of reported polyamines. 229

^{1}H NMR of LL-**31** 230

^{13}C APT NMR of LL-**31** 231

HPLC traces of diastereomers of **31** 232

^{1}H NMR of **43** (after work-up with piperidine) 233

^{1}H NMR of **43** (after work-up with iodine) 234

^{13}C APT NMR of **43** 235

^{1}H NMR of **39** 236

^{13}C APT NMR of **39** 237

^{1}H NMR of **PhTX43'3** 238

^{13}C APT NMR of **PhTX43'3** 239

^{1}H NMR of **84** 240

^{13}C APT NMR of **84** 241

A.2: ^{1}H and ^{13}C NMR spectra of diphenylamino acids and their intermediates 242

^{1}H NMR of **102** 243

^{13}C APT NMR of **102** 244

^{1}H NMR of **103** 245

^{13}C APT NMR of **103** 246

^{1}H NMR of **94** 247

^{1}H NMR expansion of **94** 248

^{13}C APT NMR of **94** 249

^{1}H NMR of **95** 250

^{13}C APT NMR of **95** 251

A.3: Examples of polyamines and triboronic acids decoded by LCMS. 252

A.3.1. Polyamines from polystyrene resin. 252

Amc^{R}-Amc^{R}-DPhe^{R} 252

DNva^{R}-LPhe^{R}-εAhx^{R} 253

2Acc^{R}-εAhx^{R} 254

8Aoc^{R}-8Aoc^{R} 255

A.3.2. Acetylated polyamines from TentaGel® resin. 256

4Acc^{Ac}-8Aoc^{Ac}-LPhe^{Ac} 256

LPhe^{Ac}-1,4Amp^{Ac}-2Acc^{Ac} 257

3,3Amp^{Ac}-3,3Amp^{Ac}-DNva^{Ac} 258

A.3.3. Tetramines from TentaGel® resin. 259

1,4Amp^{R}-Amc^{R} 259

εAhx^{R}-DNva^{R} 260

8Aoc^{R}-Amc^{R} 261

A.3.4. Triboronic acids from TentaGel® resin. 262

1,4Amp^{B}-3Amb^{B} 262

4Amb^{B}-LNva^{B} 263

12Ado^{B}-3Amb^{B} 264

Amc^{B}-12Ado^{B} 265

A.4. LC and NMR analyses of anthracenyl triboronic acids, 136 266

LC and ESMS of Amb^{B}-Amb^{B}-Anth^{B} 266

LC and ESMS of εAhx^{B}-Amb^{B}-Anth^{B} 267

LC and ESMS of 4Acc^{B}-Amb^{B}-Anth^{B} 268

LC and ESMS of Amc^{B}-Amb^{B}-Anth^{B} 269

LC of Amb^{B}-Anth^{B} 270

ESMS of Amb^{B}-Anth^{B} 271

^{1}H NMR of Amb^{B}Dde 272

^{13}C APT NMR of Amb^{B}Dde 273

A.5. Fluorescence titrations of 136 with disaccharides 274

Set 1 and Amb^{B}-Amb^{B}-Anth^{B} vs lactulose 275

Set 2 and Amb^{B}-Anth^{B} vs lactulose 276

Set 1 and Amb^{B}-Amb^{B}-Anth^{B} vs melibiose 277

Set 2 and Amb^{B}-Anth^{B} vs melibiose 278

Set 1 and Amb^{B}-Amb^{B}-Anth^{B} vs turanose 279

Set 2 and Amb^{B}-Anth^{B} vs turanose 280

A.1: ^{1}H and ^{13}C NMR spectra, and HPLC chromatograms of reported polyamines.

300 MHz, CD_3OD

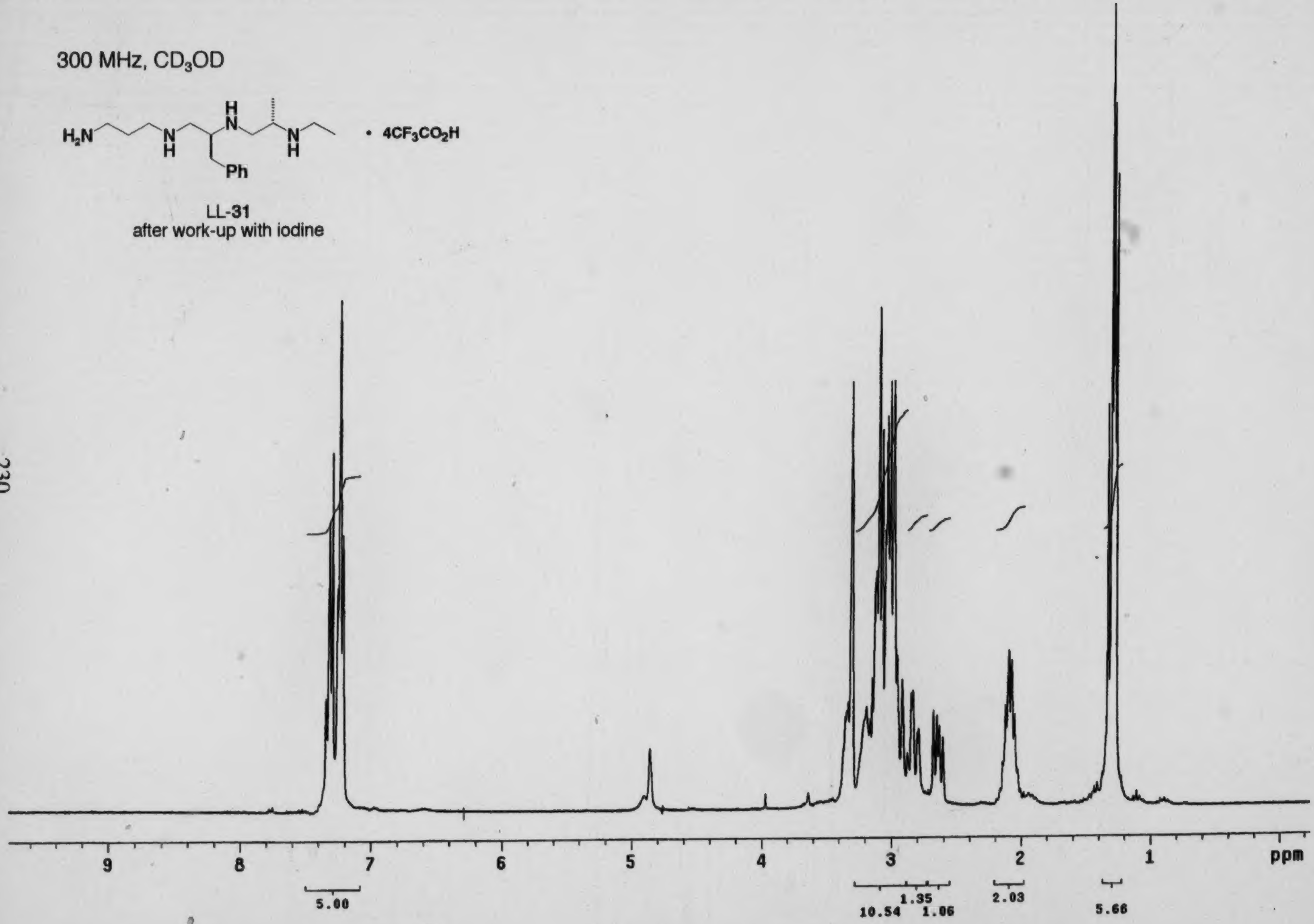

LL-**31**
after work-up with iodine

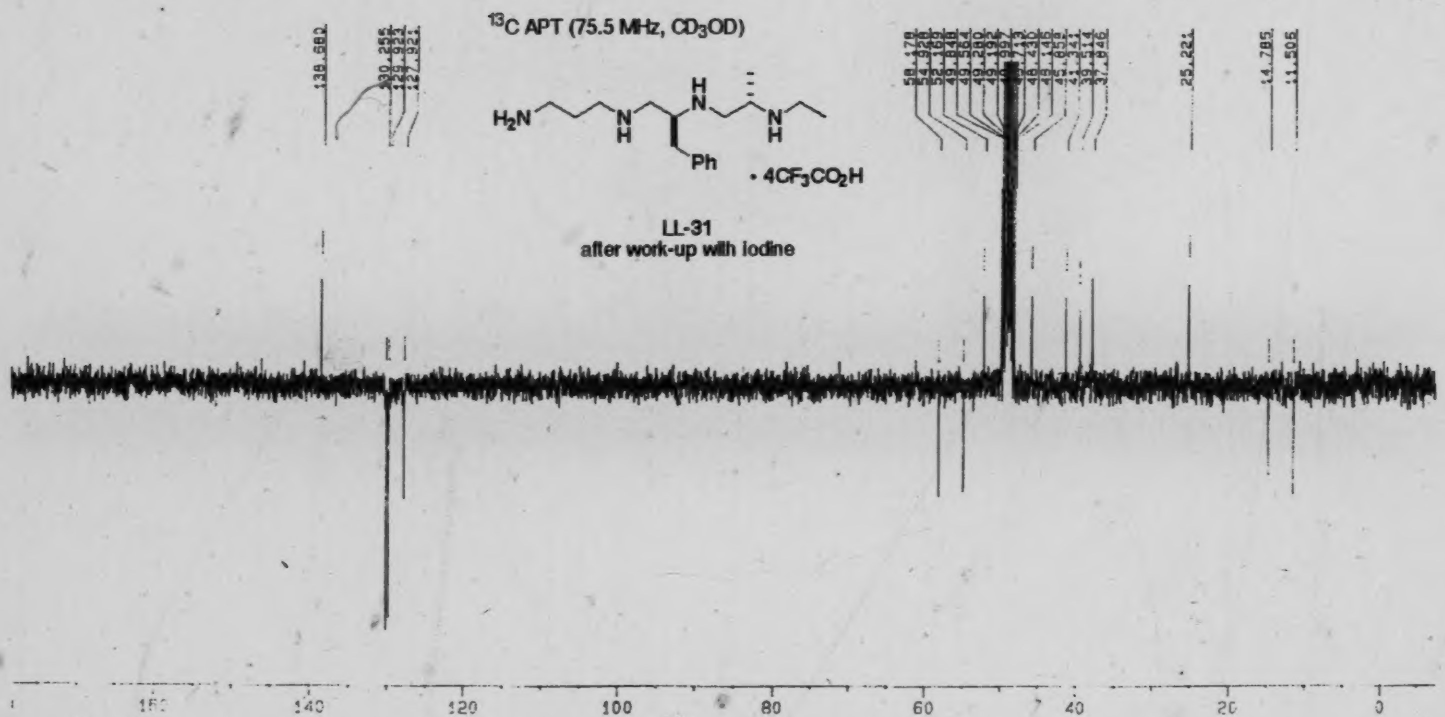^{13}C APT (75.5 MHz, CD$_3$OD)
H$_2$N
N
H
H
N
N
H
Ph
• 4CF$_3$CO$_2$H
LL-31
after work-up with iodine
138.680
130.255
129.923
127.921
58.178
54.928
52.169
49.848
49.564
49.280
41.341
39.514
37.846
25.221
14.785
11.505
160
140
120
100
80
60
40
20
0
ppm

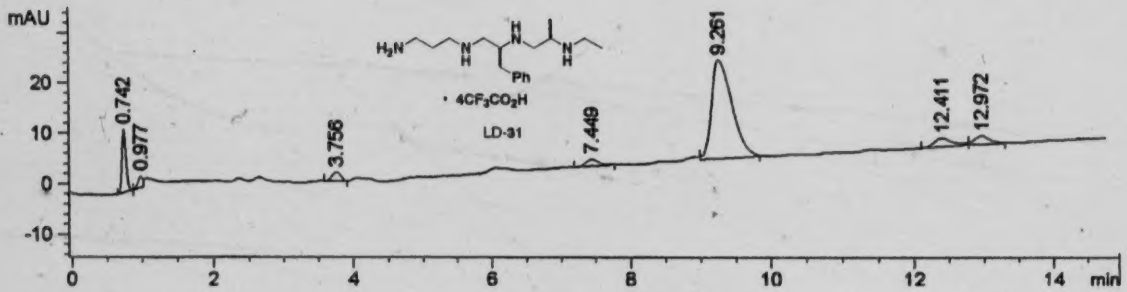
mAU
20
10
0
-10
0
2
4
6
8
10
12
14
min
0.742
0.977
3.756
7.449
9.261
12.411
12.972
H2N
N H
Ph
· 4CF3CO2H
LD-31

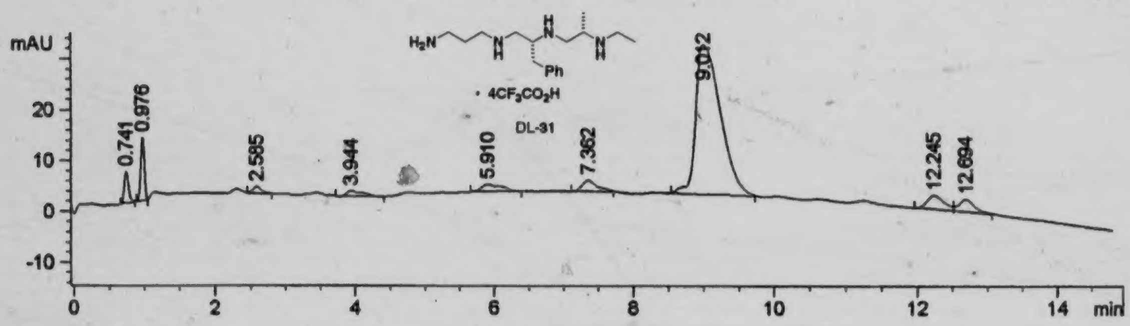
mAU
20
10
0
-10
0
2
4
6
8
10
12
14
min
0.741
0.976
2.585
3.944
5.910
7.362
9.012
12.245
12.694
H2N
N H
Ph
· 4CF3CO2H
DL-31

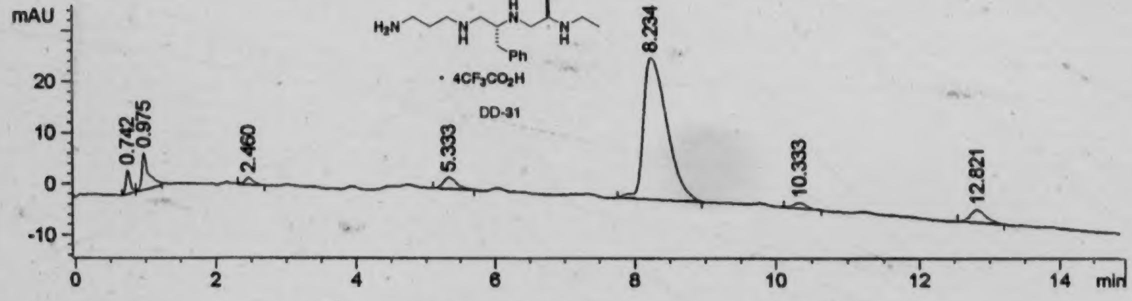
mAU
20
10
0
-10
0
2
4
6
8
10
12
14
min
0.742
0.975
2.460
5.333
8.234
10.333
12.821
H2N
N H
Ph
· 4CF3CO2H
DD-31

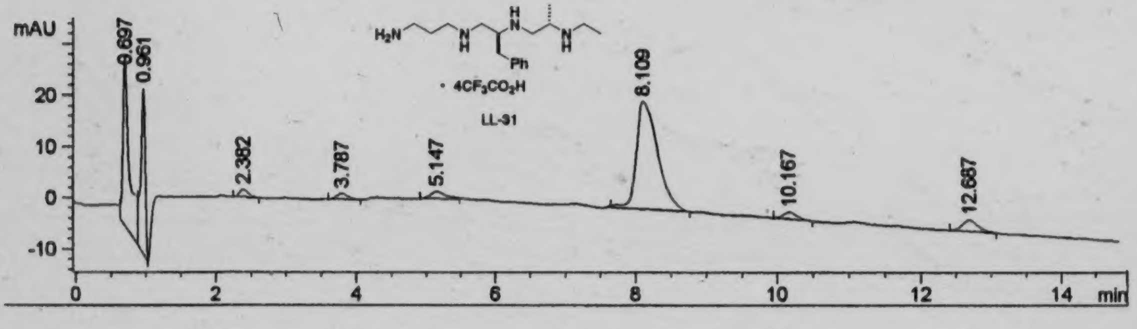
mAU
20
10
0
-10
0
2
4
6
8
10
12
14
min
0.697
0.961
2.382
3.787
5.147
8.109
10.167
12.687
H2N
N H
Ph
· 4CF3CO2H
LL-31

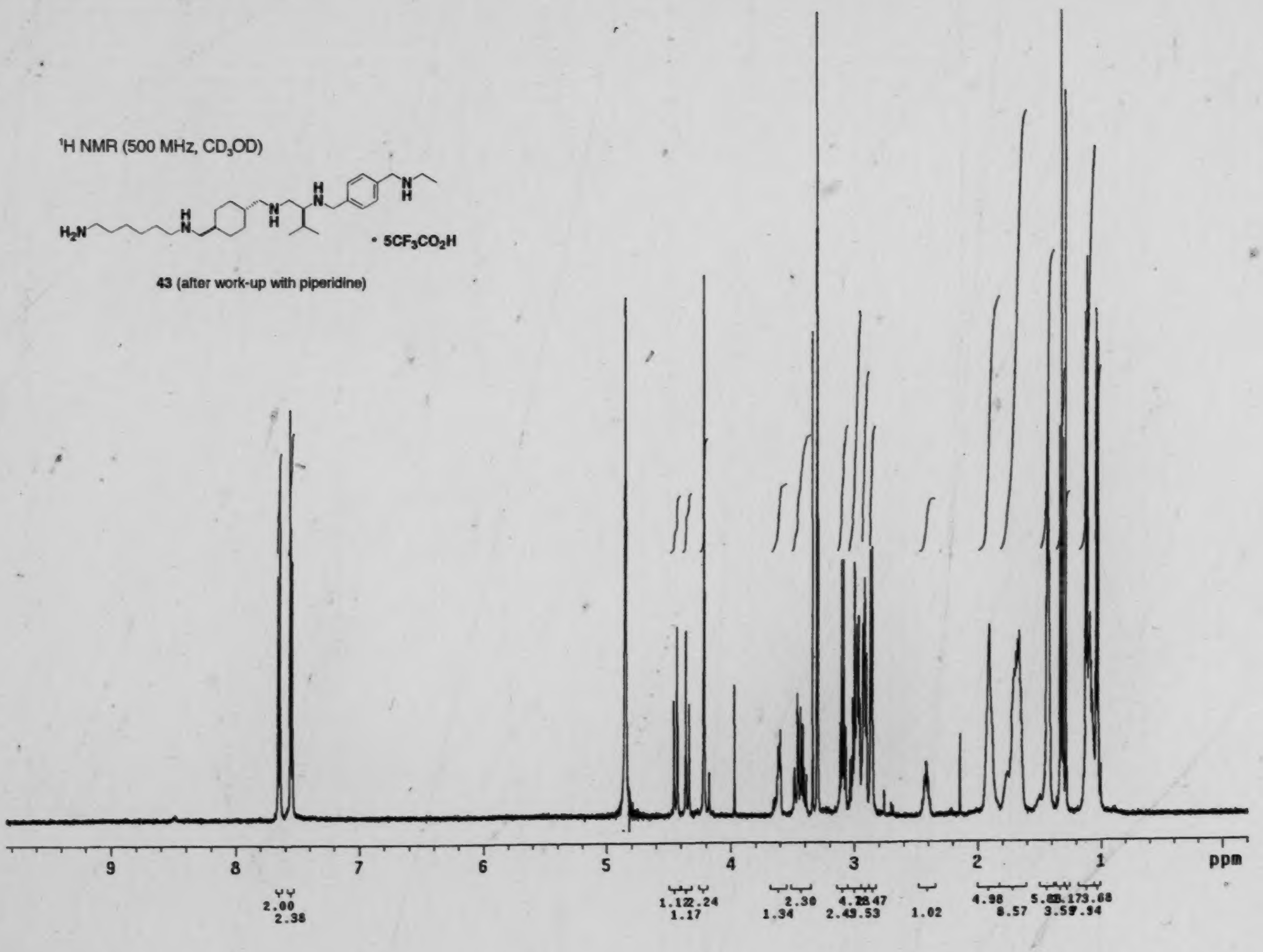

¹H NMR (500 MHz, CD₃OD)

43 (after work-up with piperidine)

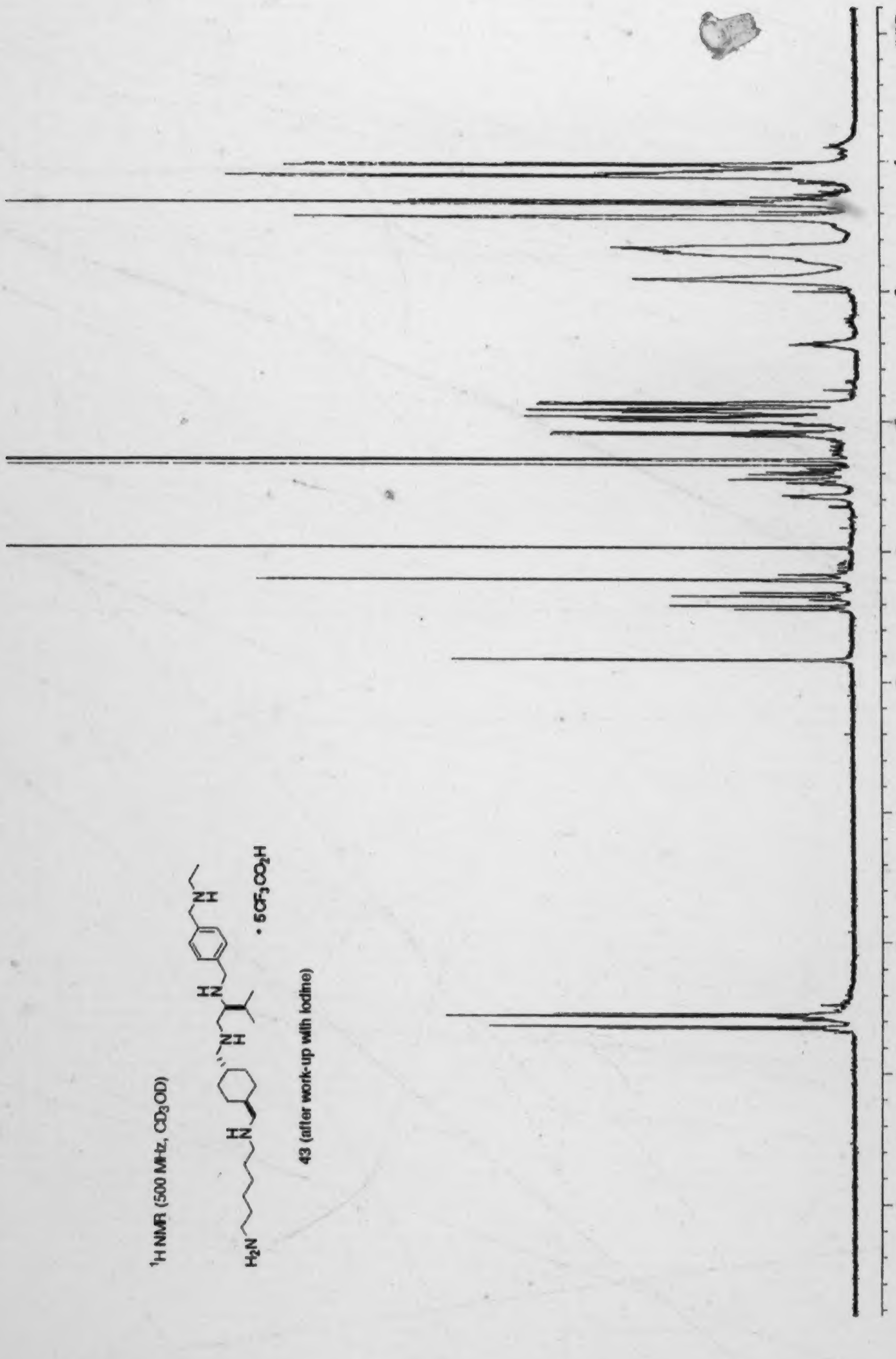

^{1}H NMR (500 MHz, CD_3OD)

43 (after work-up with iodine)

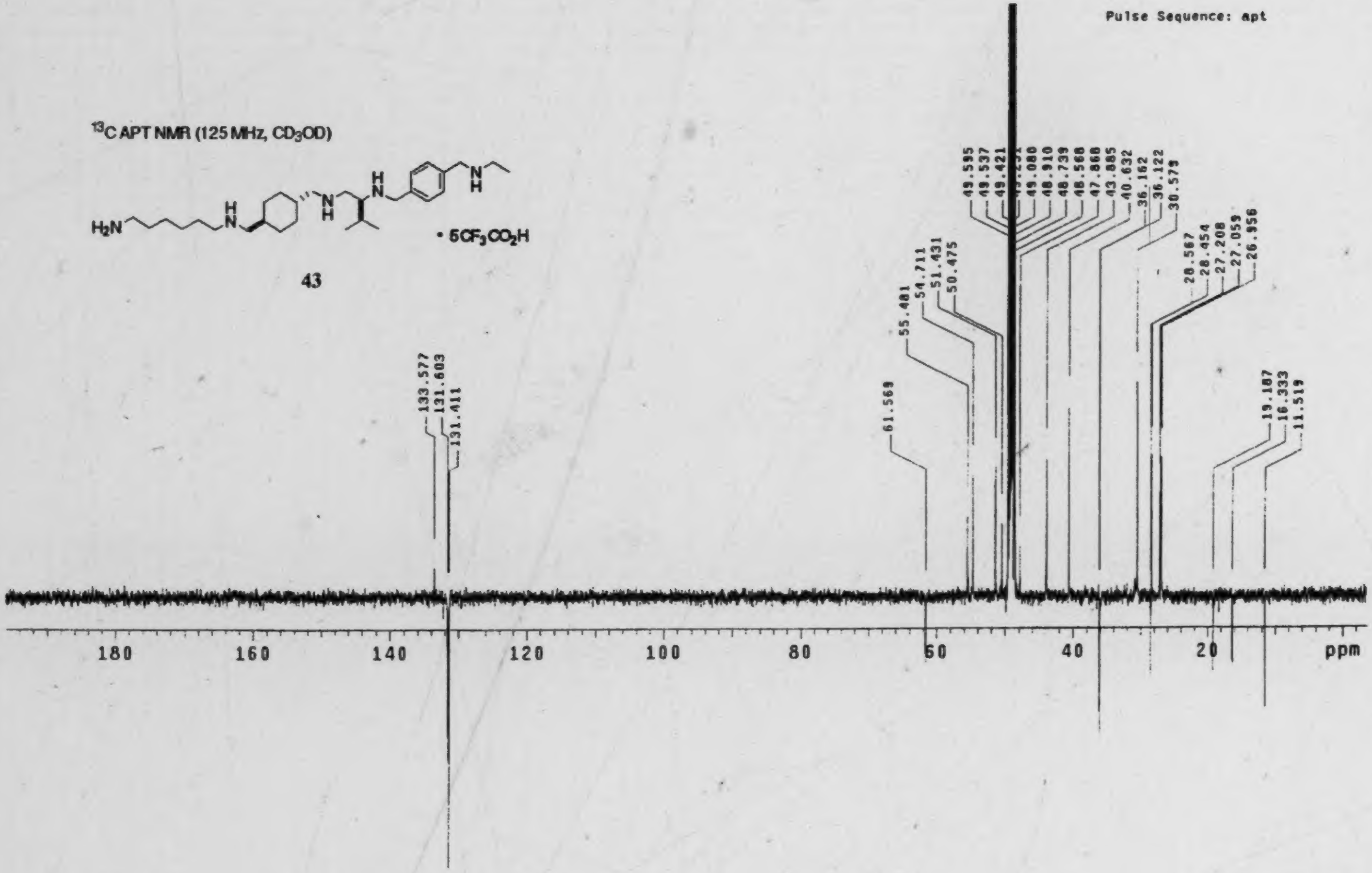

^{13}C APT NMR (125 MHz, CD_3OD)

$\cdot$ 5CF_3CO_2H

43

¹H NMR (500 MHz, CD_3OD)

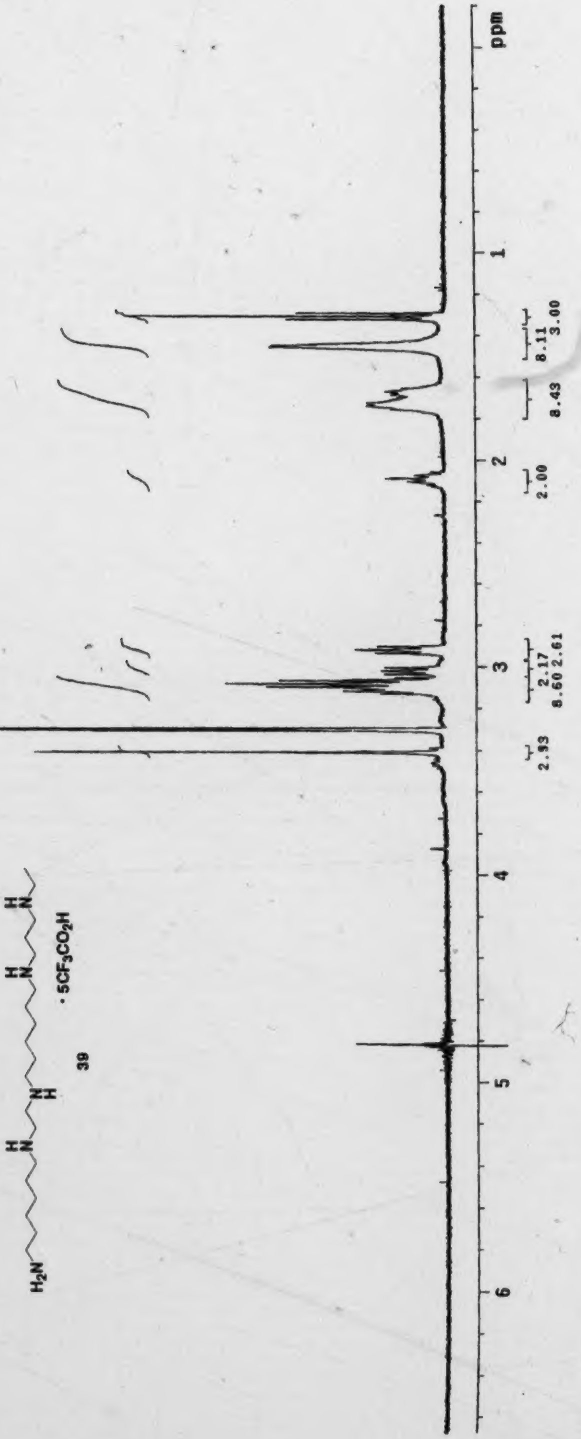

39

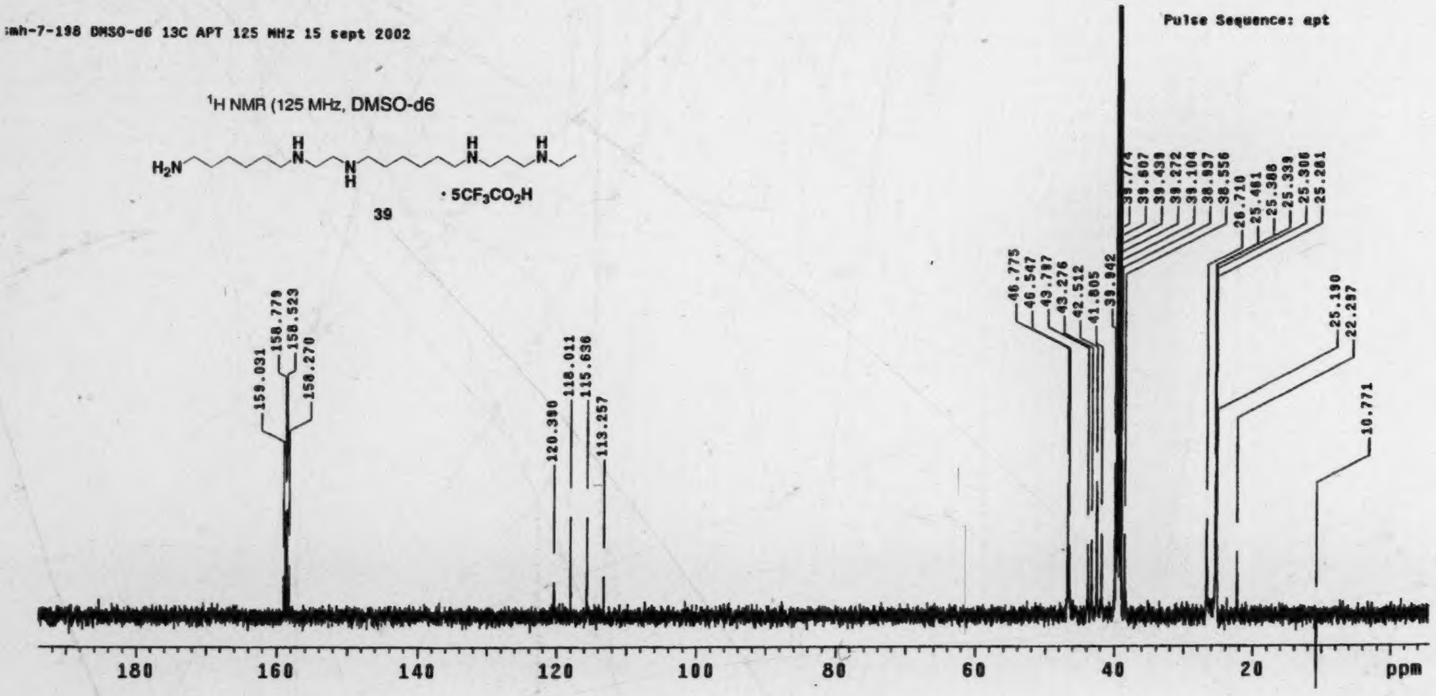

:mh-7-198 DMSO-d6 13C APT 125 MHz 15 sept 2002
Pulse Sequence: apt
^{1}H NMR (125 MHz, DMSO-d6
H2N
H
N
· 5CF3CO2H
159.031
158.779
158.523
158.270
120.390
118.011
115.636
113.257
46.775
46.547
43.787
43.276
42.512
41.805
39.942
39.774
39.607
39.439
39.272
39.104
38.937
38.556
26.710
25.481
25.388
25.339
25.306
25.281
25.190
22.287
10.771
180
160
140
120
100
80
60
40
20
ppm

39

^{1}H NMR (300 MHz, CD$_3$OD)

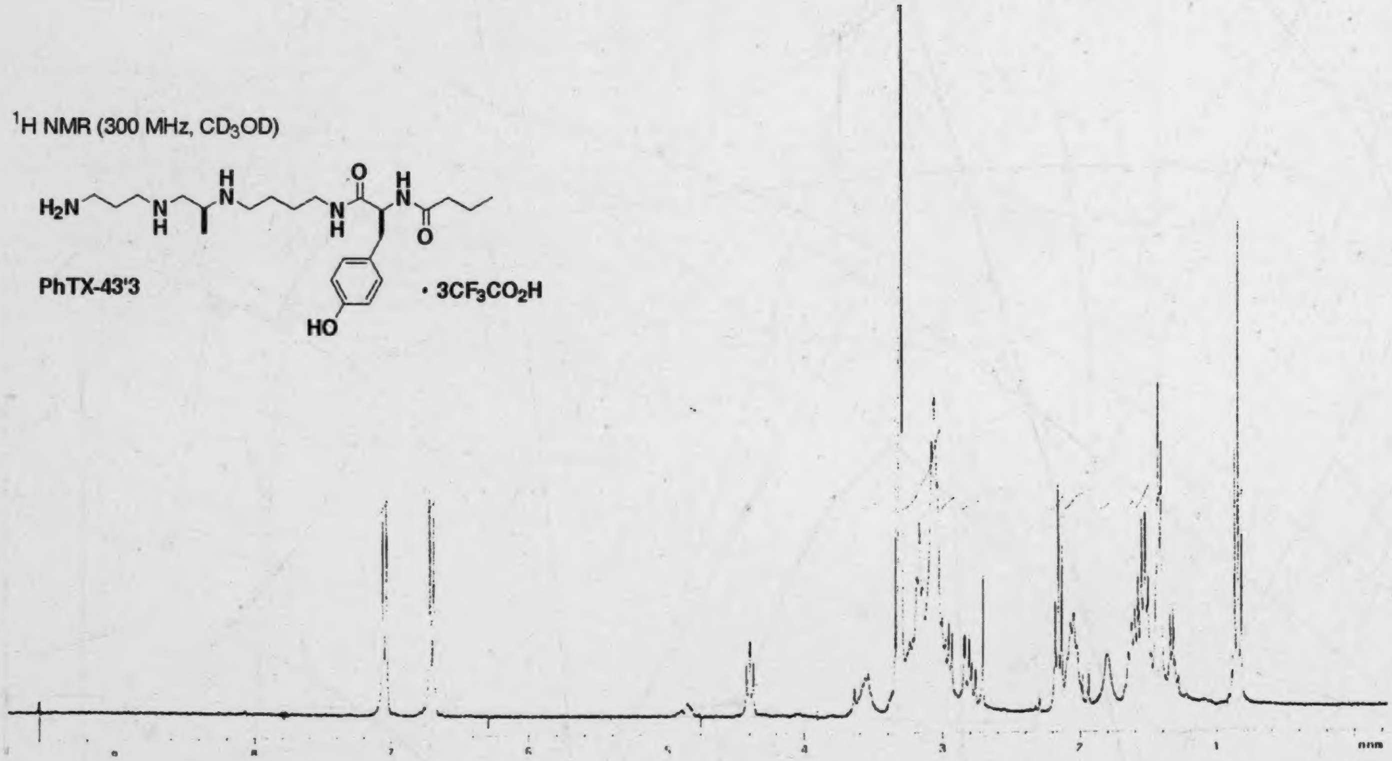

PhTX-43'3

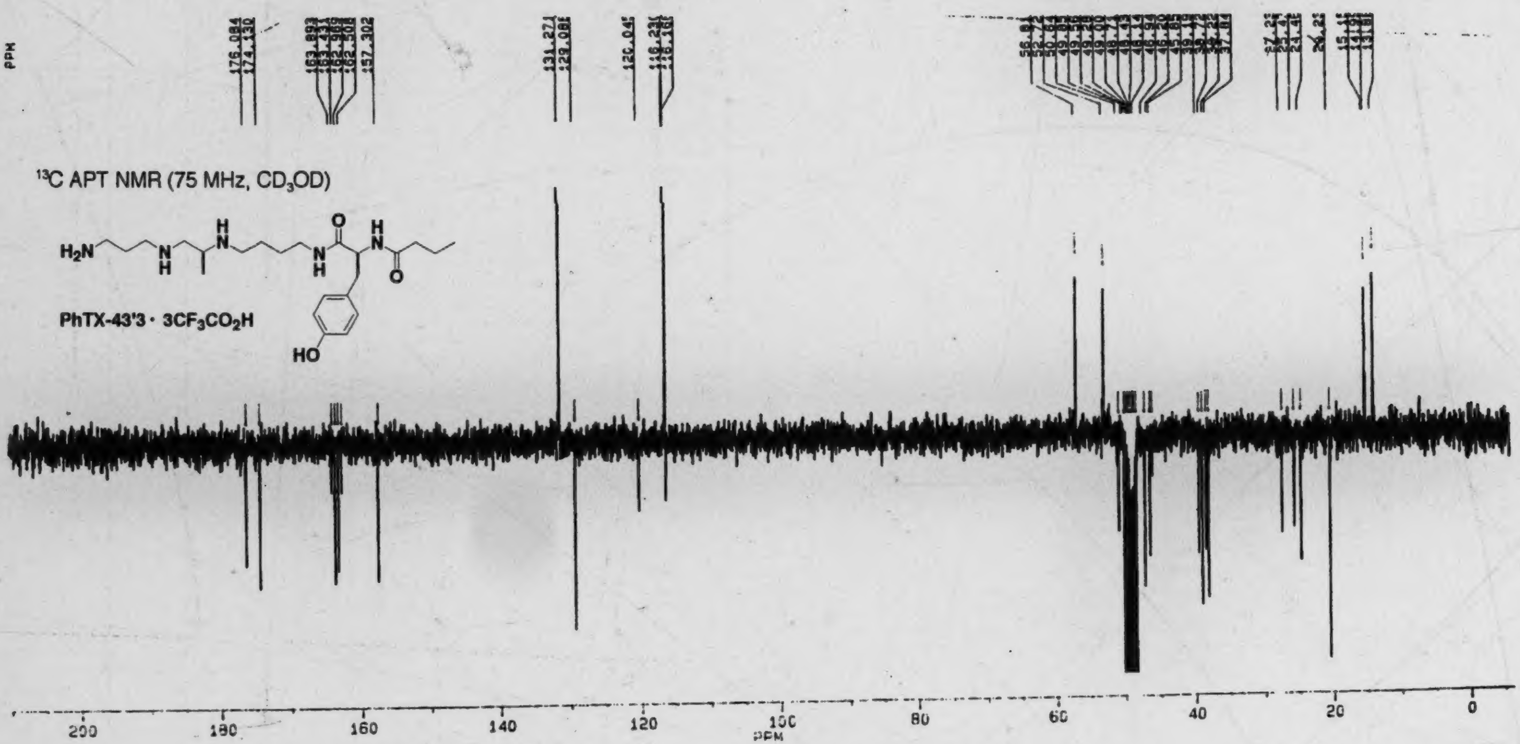

^{13}C APT NMR (75 MHz, CD_3OD)

PhTX-43'3 · $3CF_3CO_2H$

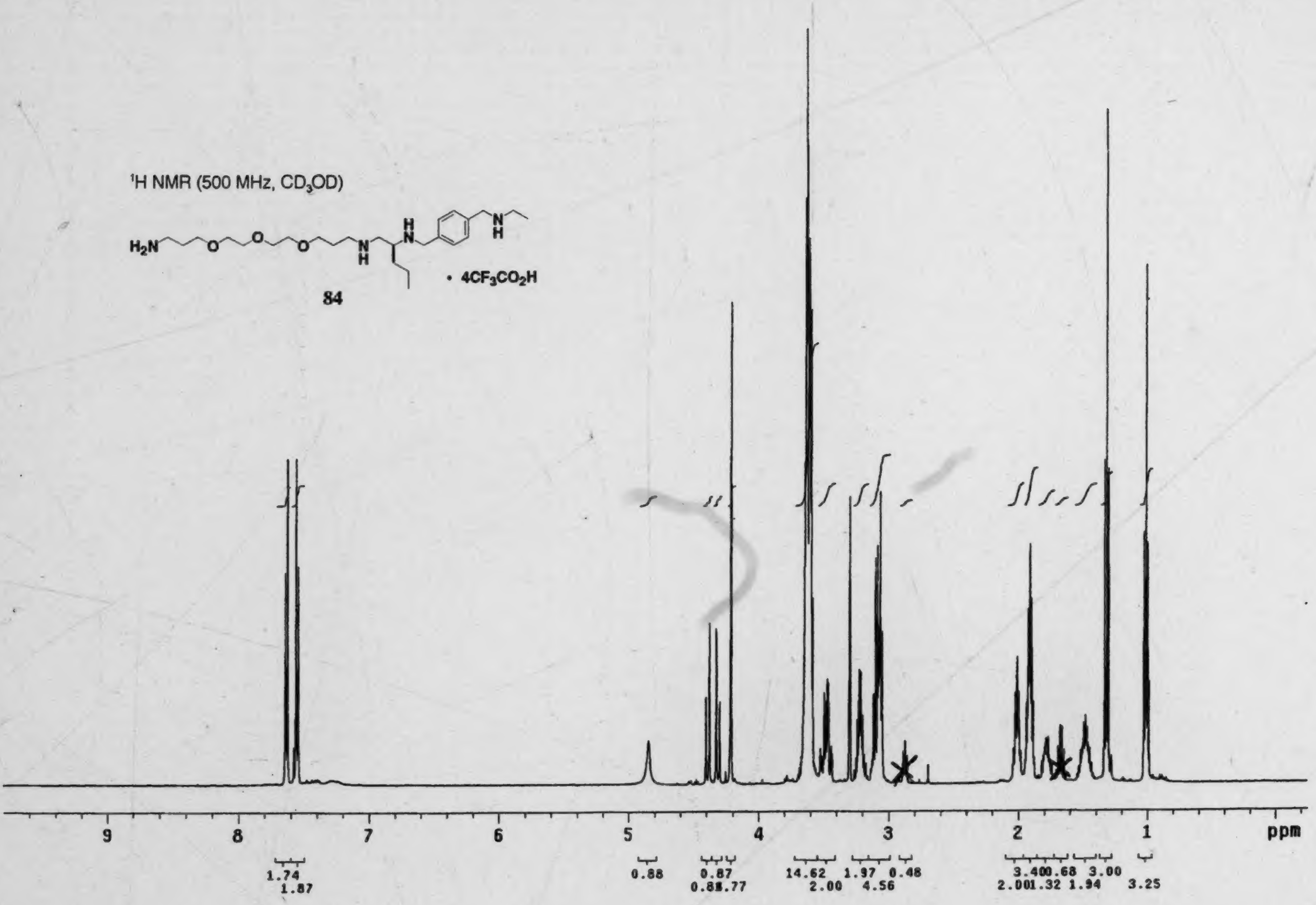
^{1}H NMR (500 MHz, CD$_3$OD)
H$_2$N
O
O
O
N
H
H
N
N
H
• 4CF$_3$CO$_2$H
84
9
8
7
6
5
4
3
2
1
ppm
1.74
1.87
0.88
0.87
0.88
0.77
14.62
2.00
1.97
4.56
0.48
3.40
2.00
0.68
1.32
3.00
1.94
3.25

^{13}C APT NMR (125 MHz, CD_3OD)

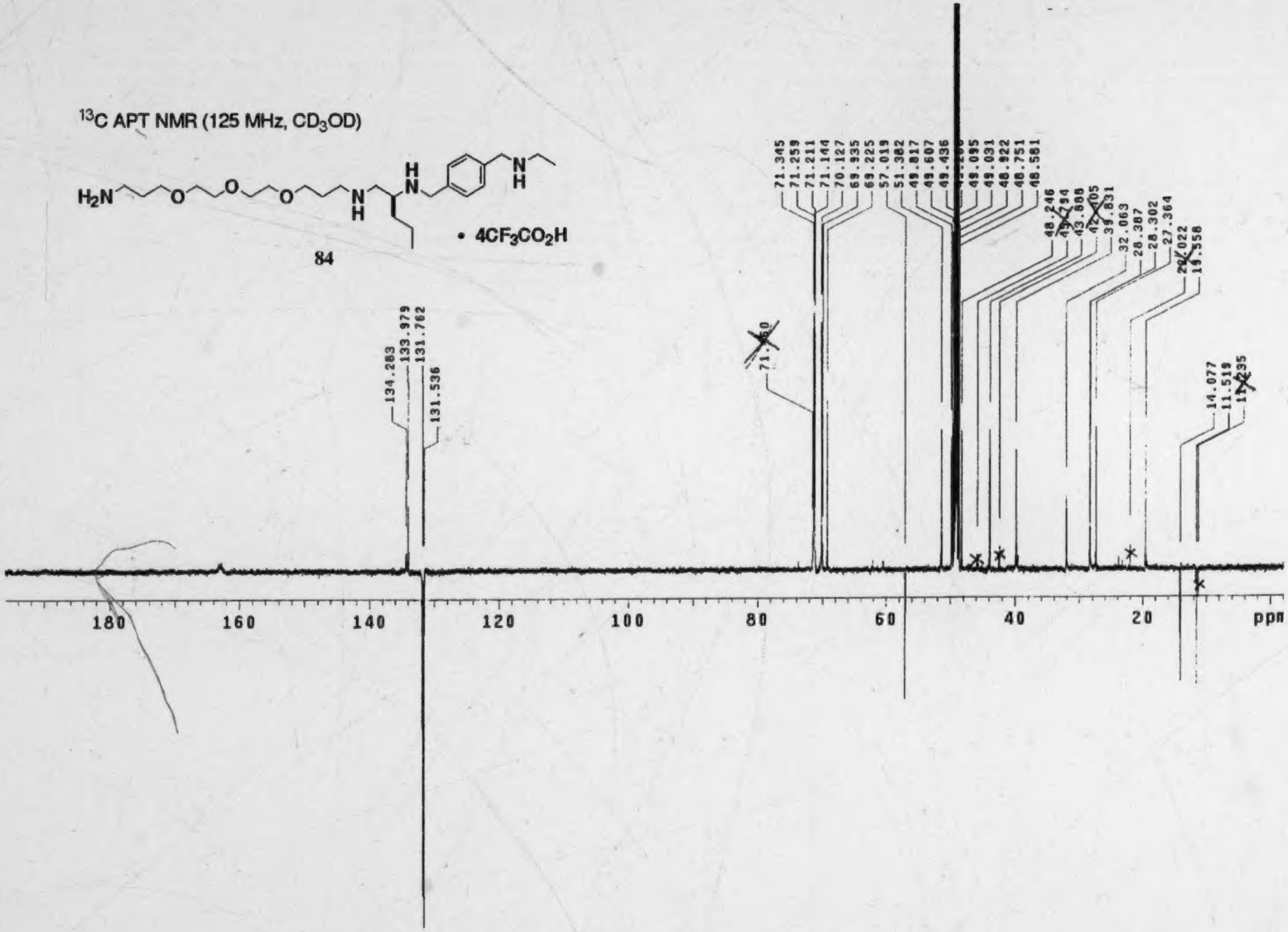

84

A.2: ^{1}H and ^{13}C NMR spectra of diphenylamino acids and their intermediates.

^{1}N NMR (500 MHz, DMSO-d_6)

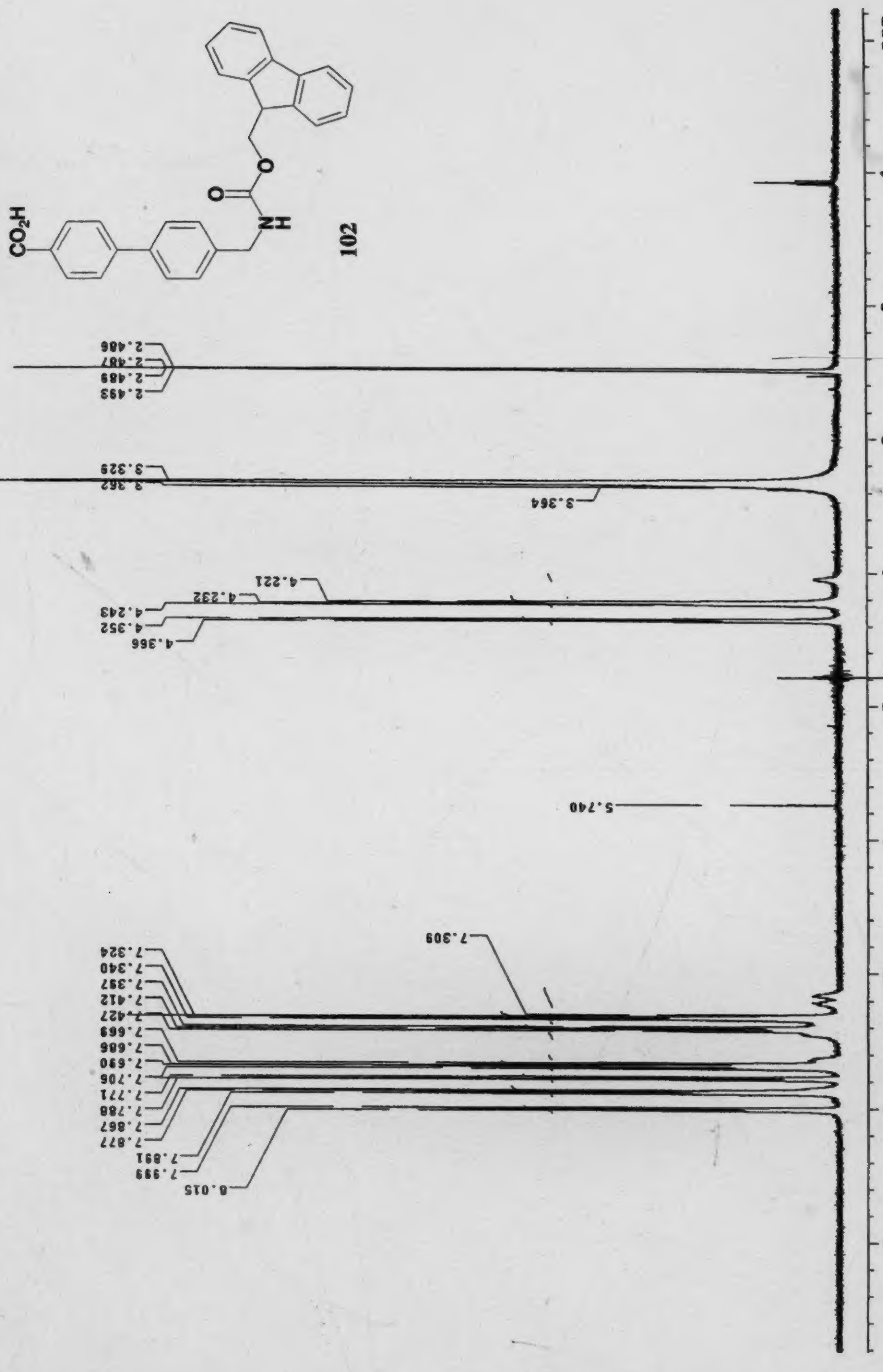

102

^{13}C APT NMR
(125 MHz, DMSO-d_6)

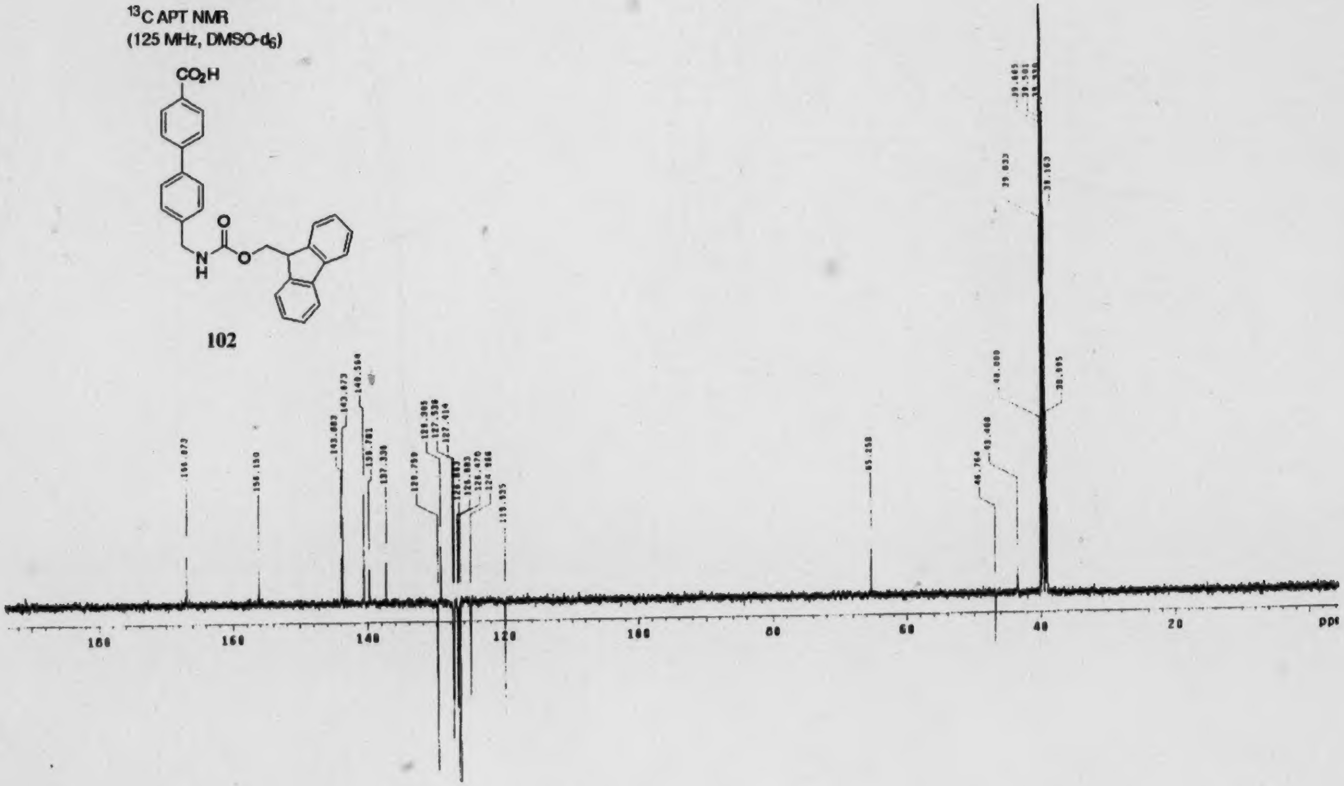

102

^{1}H NMR (500 MHz, DMSO-d_6)

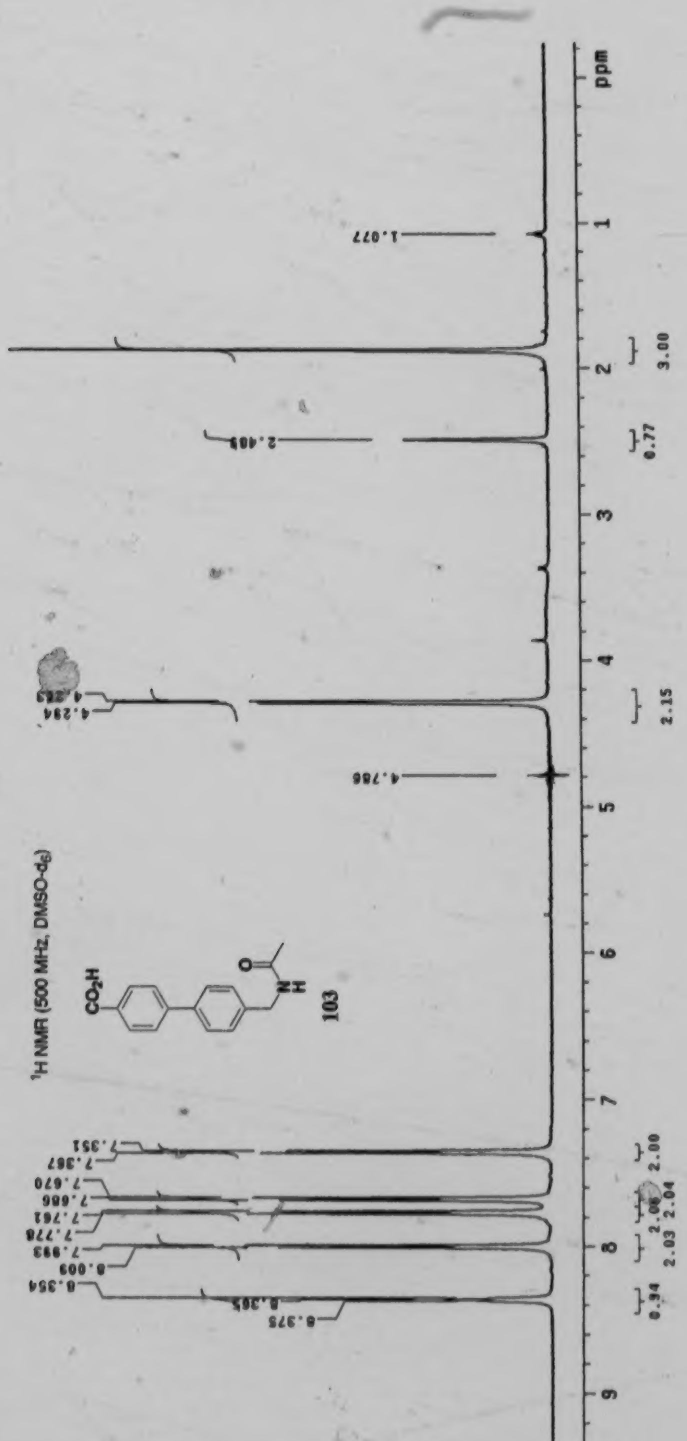

103

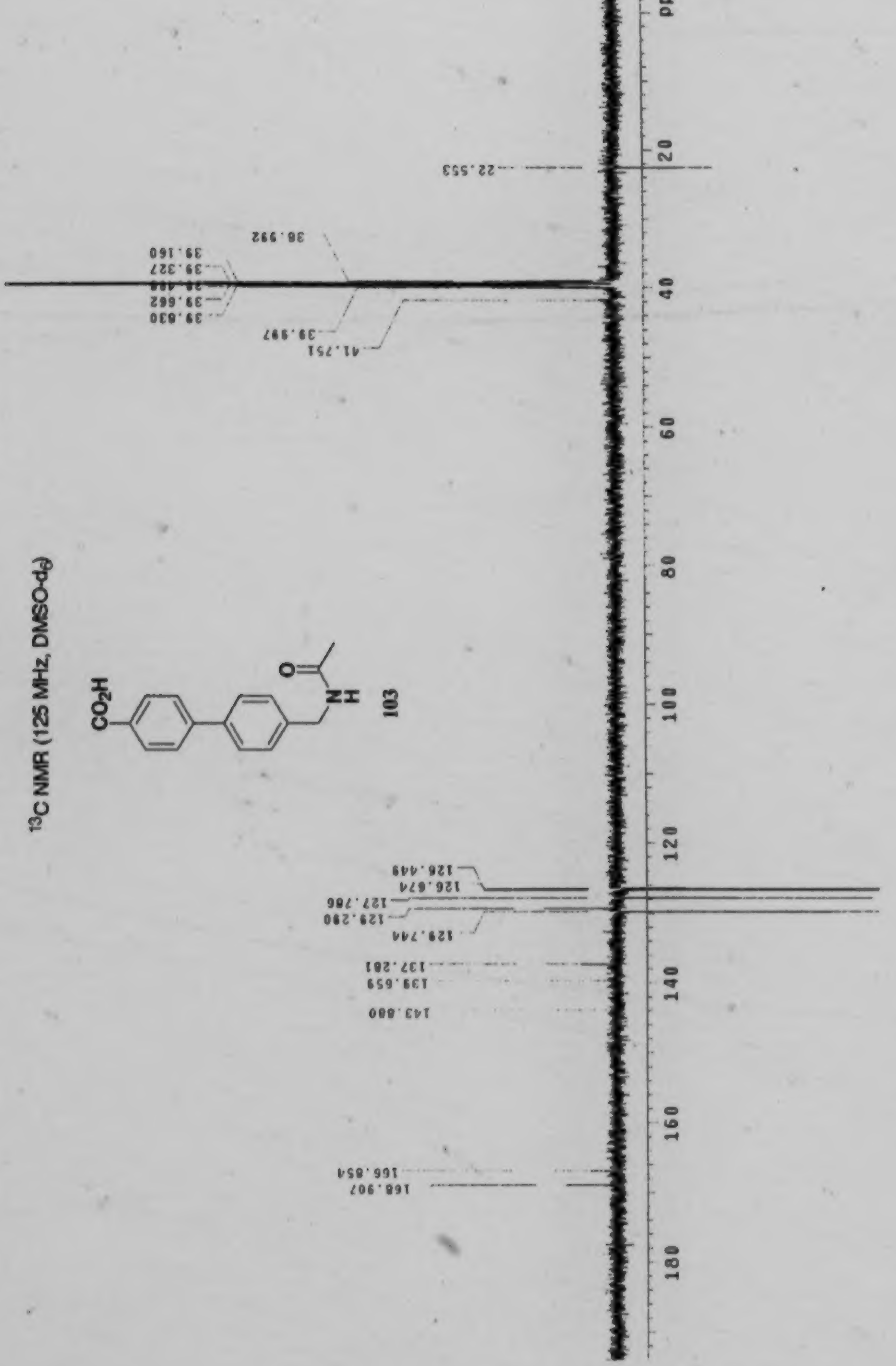

^{13}C NMR (125 MHz, DMSO-d_6)

103

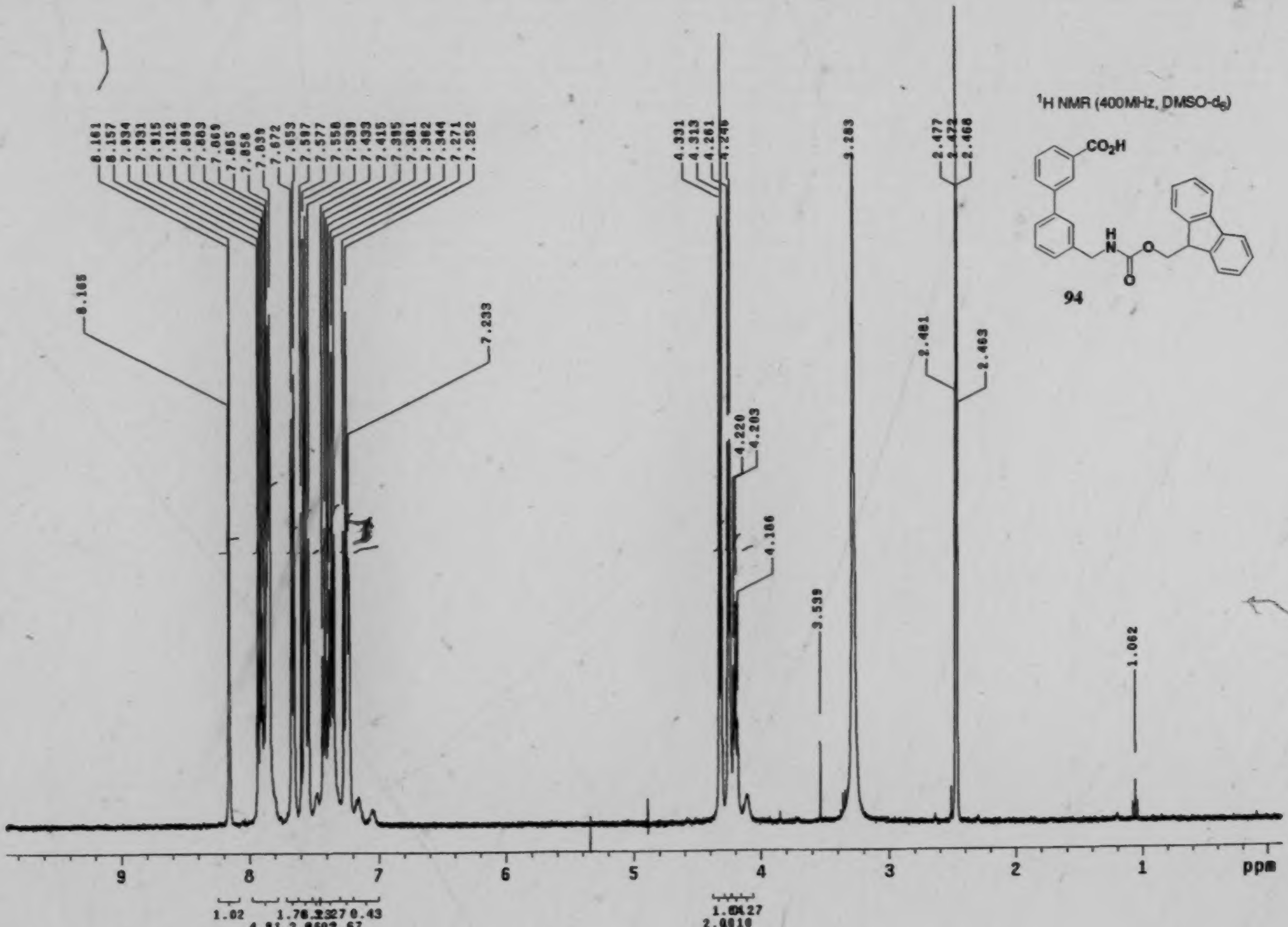
1H NMR (400MHz, DMSO-d6)
CO2H
H
N
O
O
8.161
8.157
7.934
7.931
7.915
7.912
7.899
7.883
7.869
7.865
7.858
7.839
7.672
7.653
7.597
7.577
7.558
7.539
7.433
7.415
7.395
7.381
7.362
7.344
7.271
7.252
8.165
7.233
4.331
4.313
4.261
4.246
4.220
4.203
4.186
3.539
3.283
2.477
2.472
2.468
2.481
2.463
1.062
9
8
7
6
5
4
3
2
1
ppm
1.02
4.81
1.76
2.23
2.27
0.43
2.85
2.67
1.04
1.27
2.08
1.10

94

¹H NMR - expansion
(400MHz, DMSO-d_6)

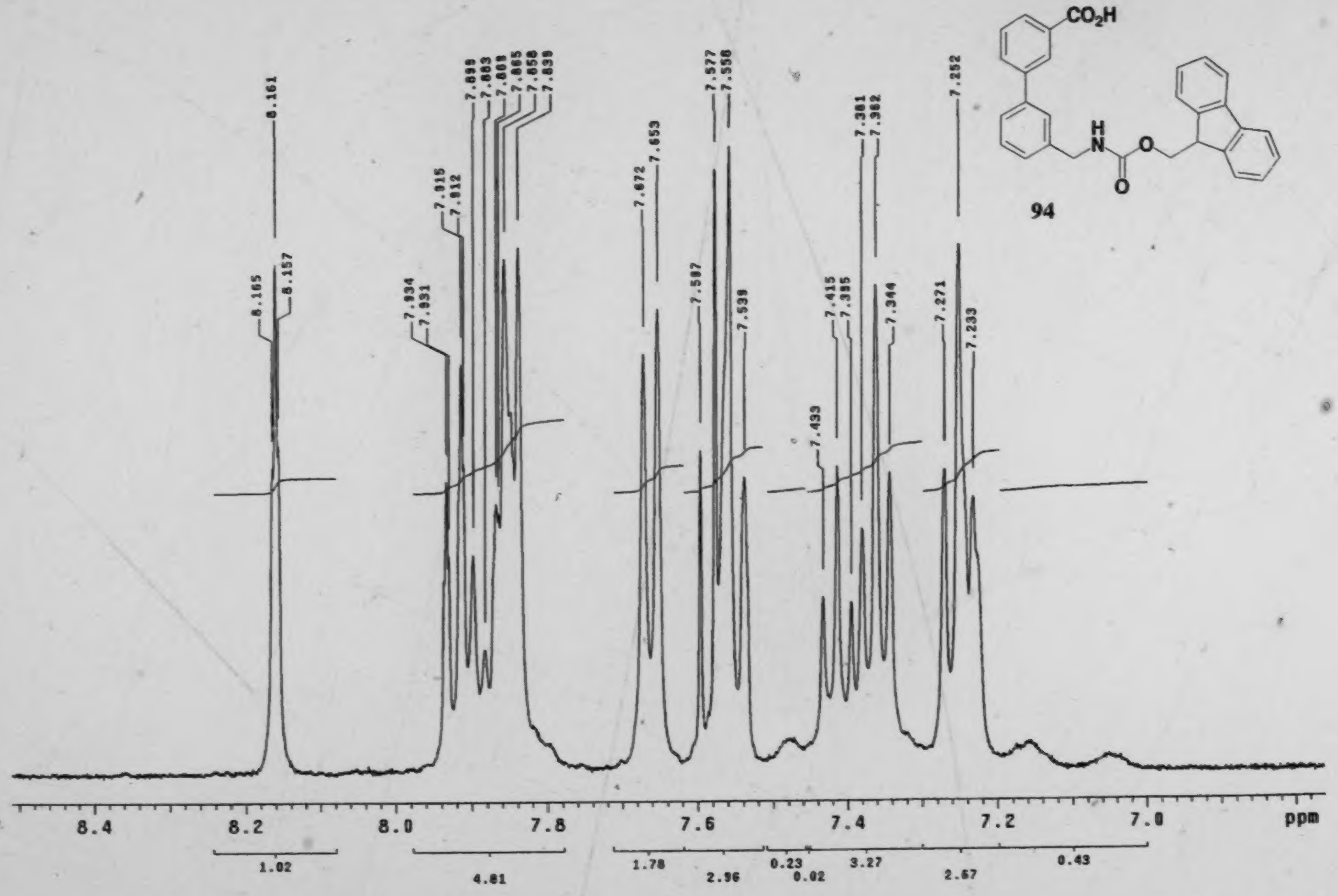

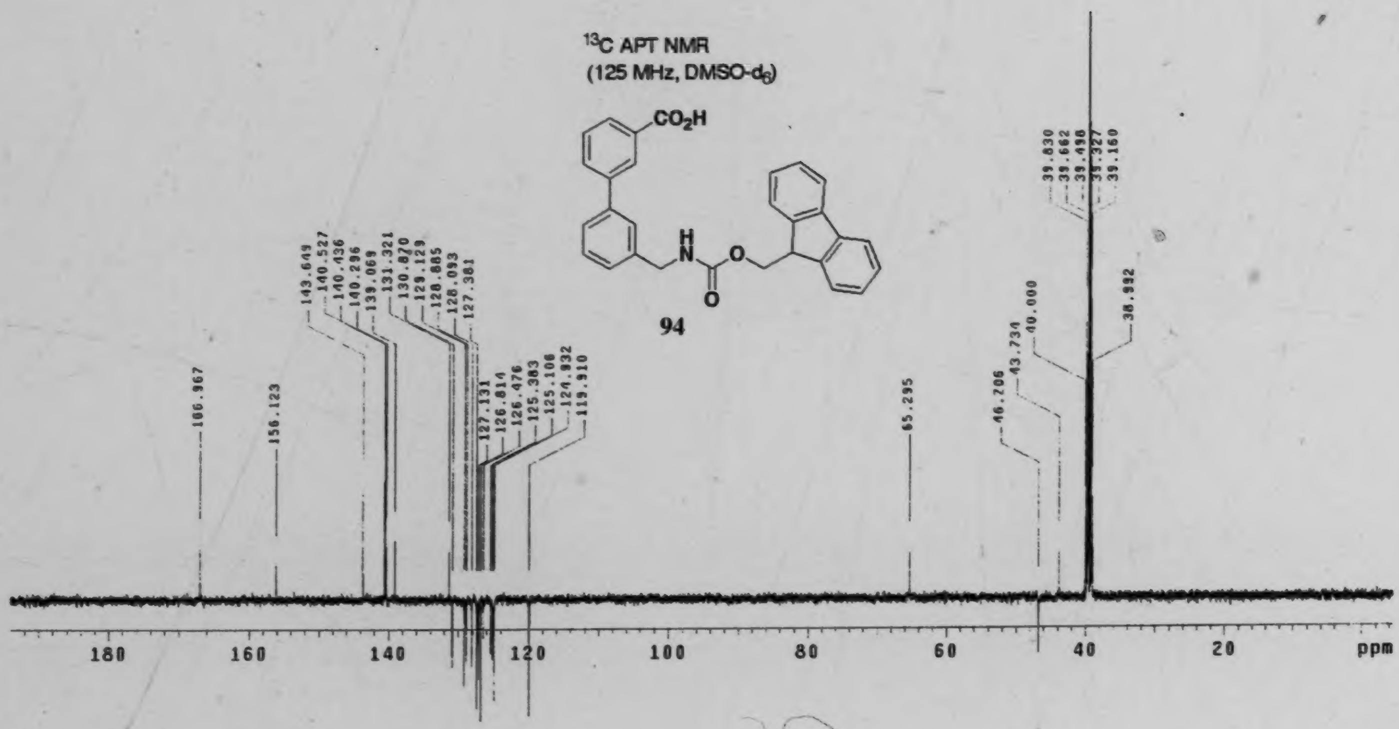
13C APT NMR
(125 MHz, DMSO-d6)
CO2H
H
N
O
O
166.967
156.123
143.649
140.527
140.436
140.296
139.069
131.321
130.820
129.129
128.885
128.093
127.381
127.131
126.814
126.476
125.383
125.106
124.832
119.910
65.295
46.206
43.734
40.000
39.830
39.662
39.498
39.327
39.160
38.992
180
160
140
120
100
80
60
40
20
ppm

94

^{1}H NMR
(500 MHz, DMSO-d_6)

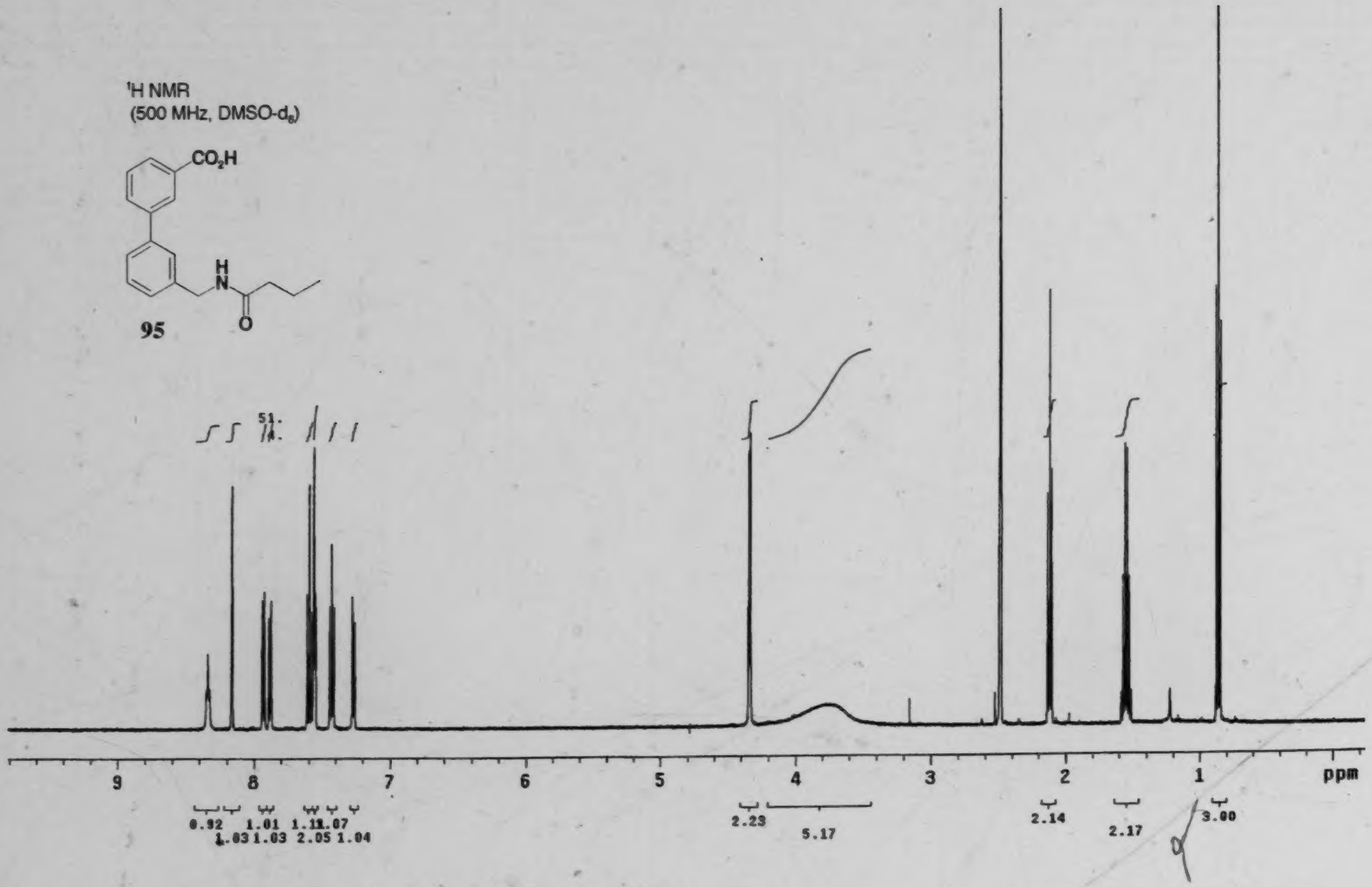

95

^{13}C APT NMR
(125 MHz, DMSO-d_6)

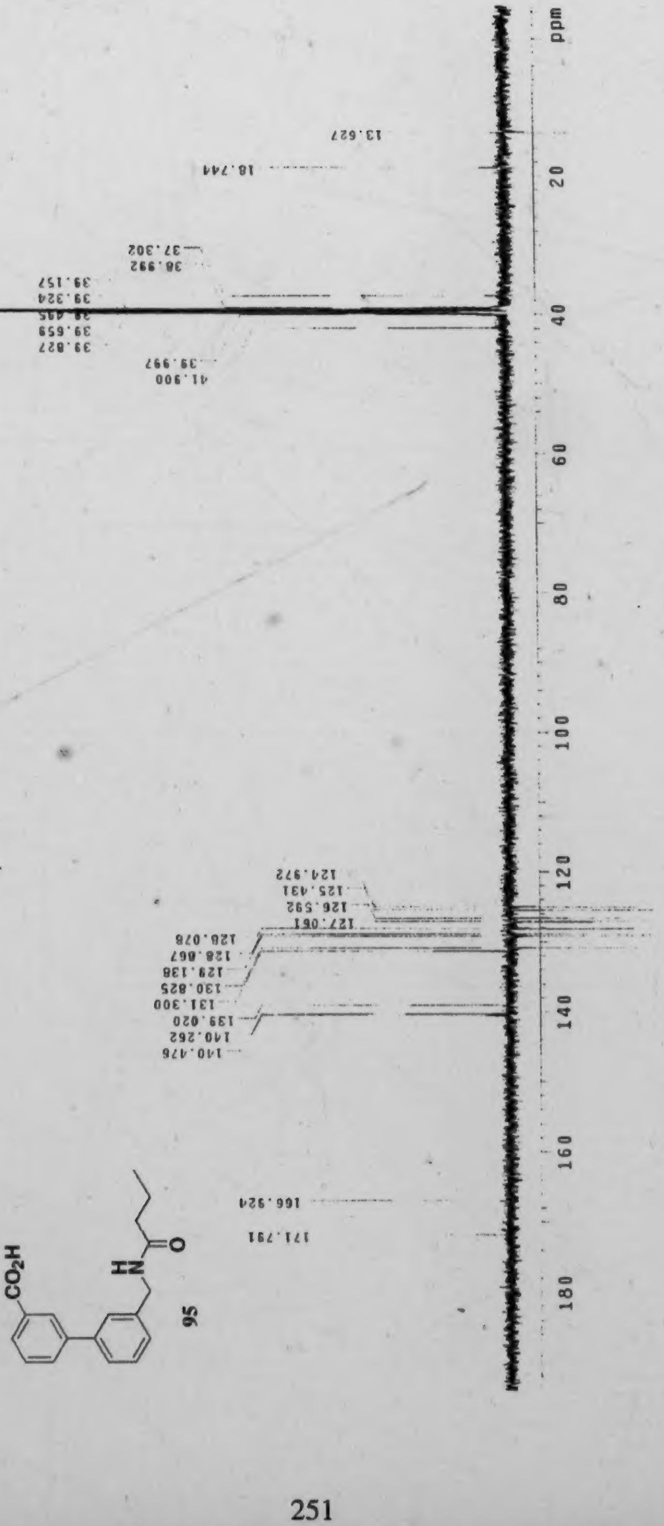

95

A.3: Examples of polyamines and triboronic acids decoded by LCMS.

A.3.1. Polyamines from polystyrene resin.

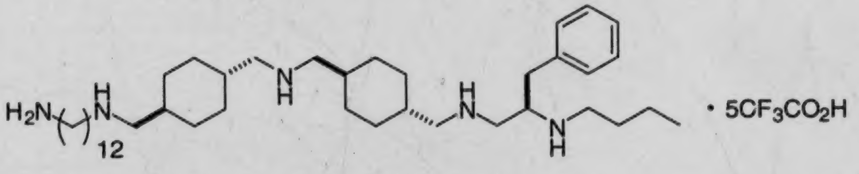
H2N
12
H
N
H
N
H
N
H
N
H
• 5CF3CO2H

Amc^R-Amc^R-DPhe^R*n*Bu

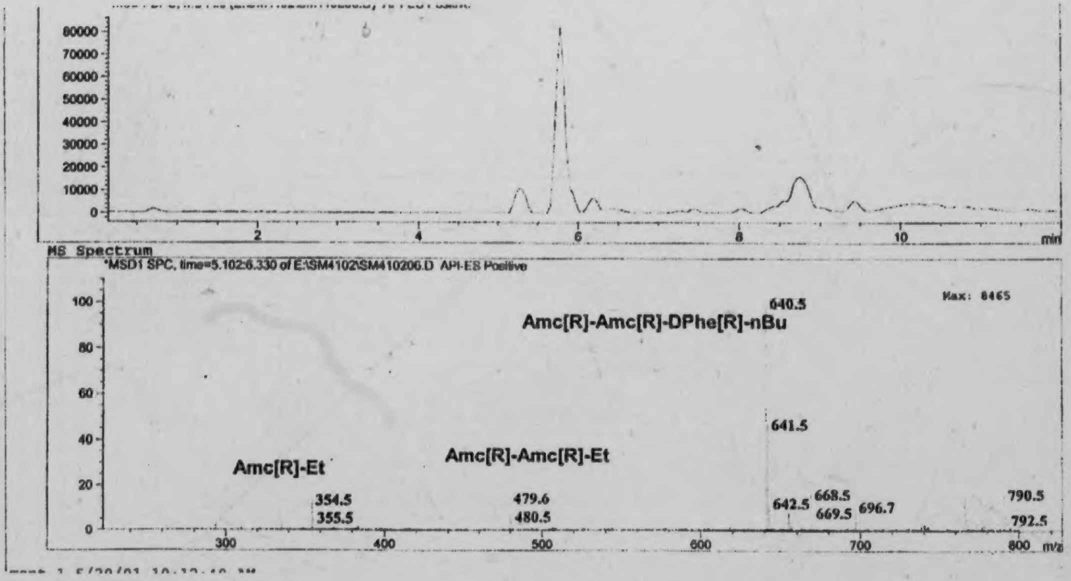

Mass spectrum shown is of LC peaks eluting between 5.1 and 6.3 minutes.

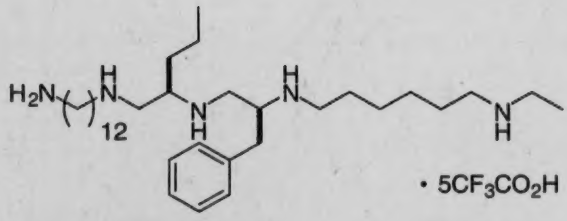

DNva^{R}-LPhe^{R}-εAhx^{R}-Et

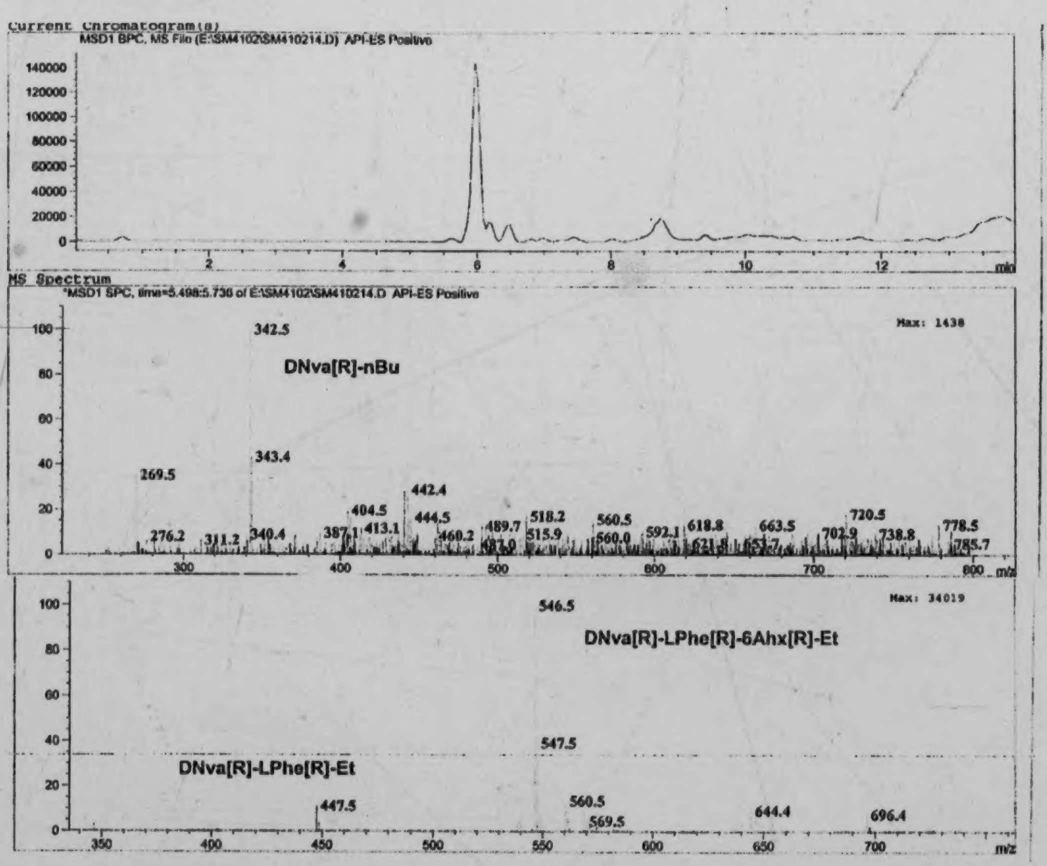

Mass spectra shown are of LC peaks eluting between 5.5 and 5.8 minutes, which gives the first encoding sequence, and between 5.8 and 6.3 minutes, which shows the second encoding sequence and the full sequence.

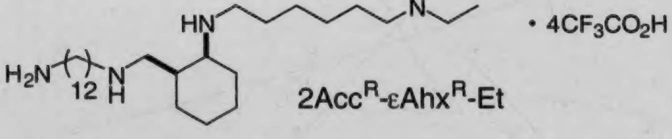
H$_2$N
12
N
H
HN
H
N
• 4CF$_3$CO$_2$H

2Acc^R-εAhx^R-Et

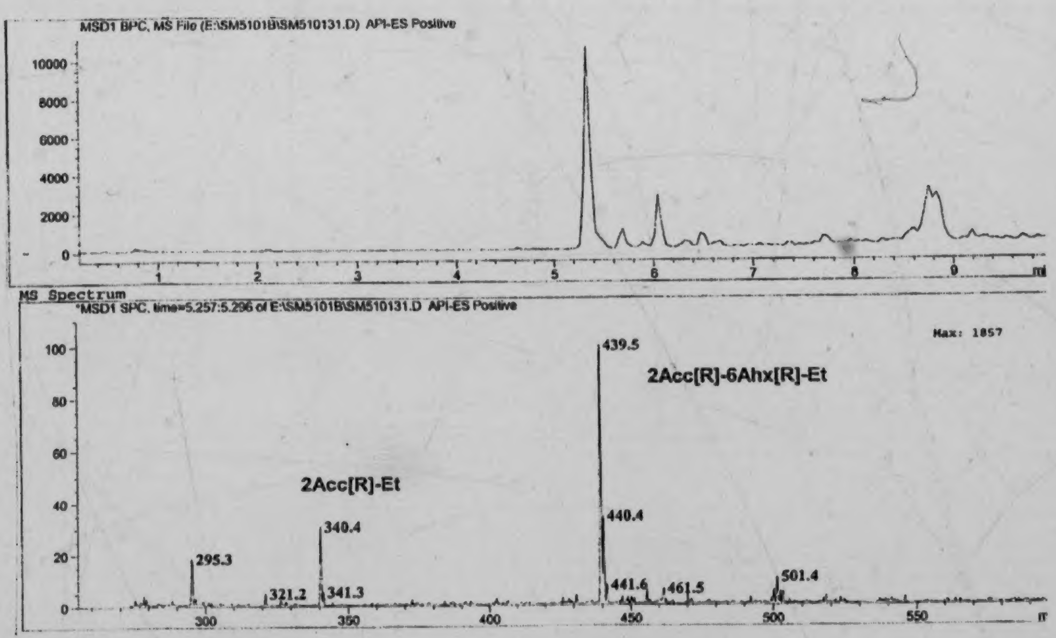

Mass spectrum shown is of LC peaks co-eluting at 5.3 minutes.

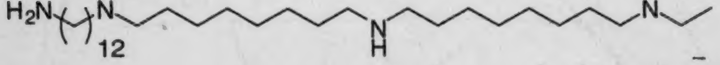

8Aoc^R-8Aoc^R-Et   · 4CF$_3$CO$_2$H

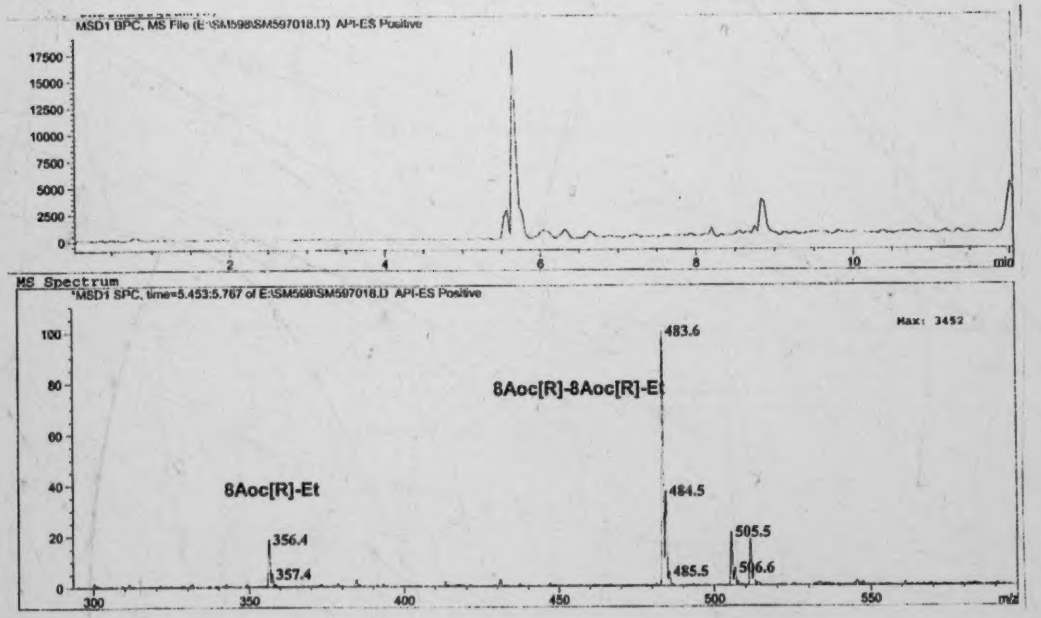

Mass spectrum shown is of LC peaks eluting between 5.5 and 5.8 minutes.

A.3.2. Acetylated polyamines from TentaGel® resin.

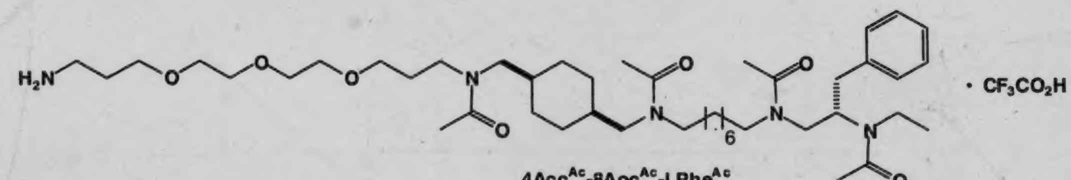

H₂N
O
O
O
N
O
N
O
6
N
O
N
O
• CF₃CO₂H

4Acc^{Ac}-8Aoc^{Ac}-LPhe^{Ac}

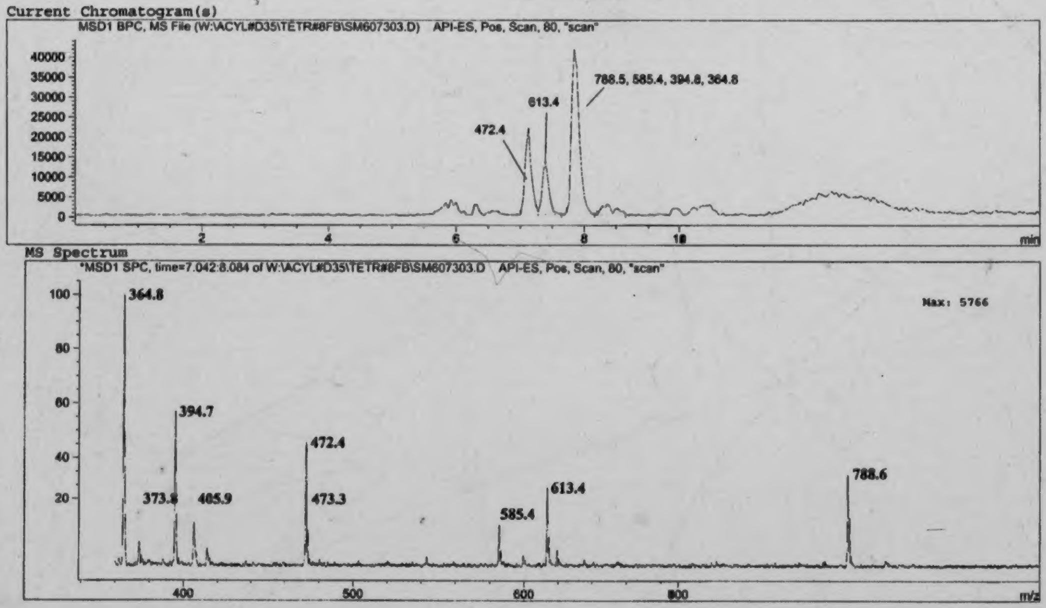

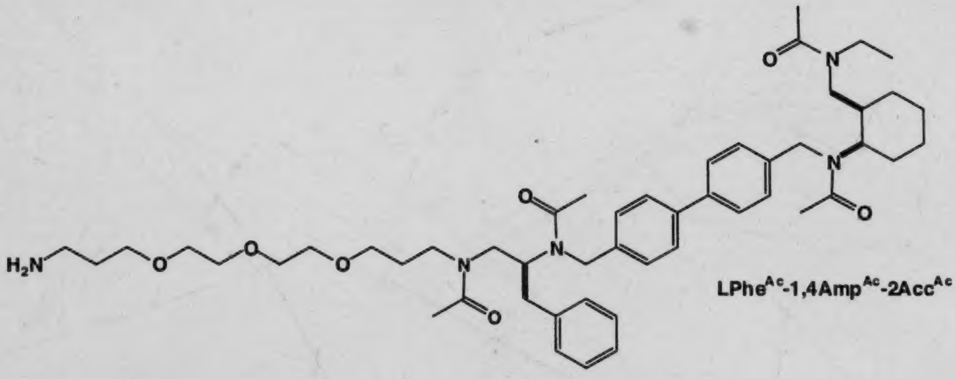
O
N
O
N
N
O
O
H2N
O
O
O
N
O

· CF_3CO_2H

LPhe^{Ac}-1,4Amp^{Ac}-2Acc^{Ac}

Current Chromatogram(s)

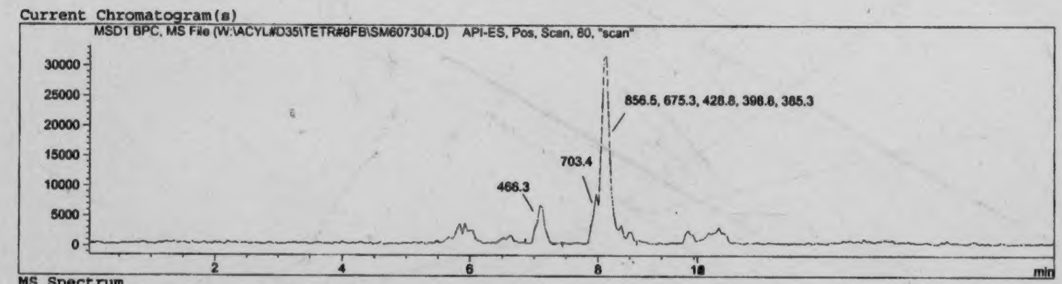

MS Spectrum

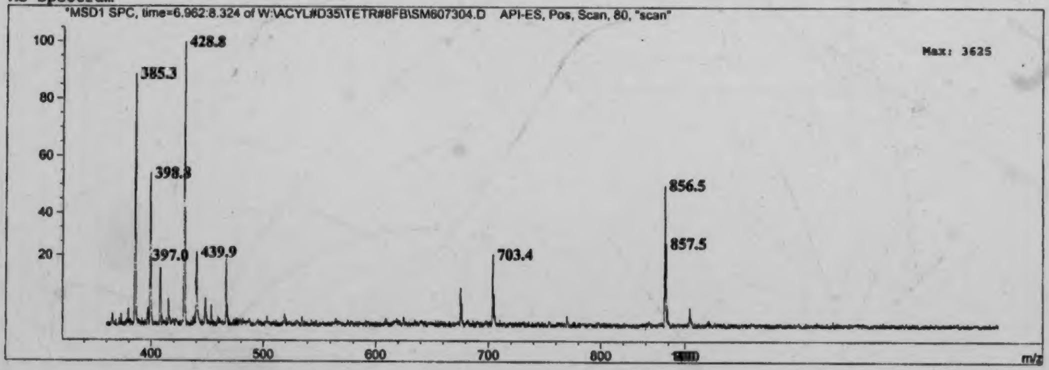

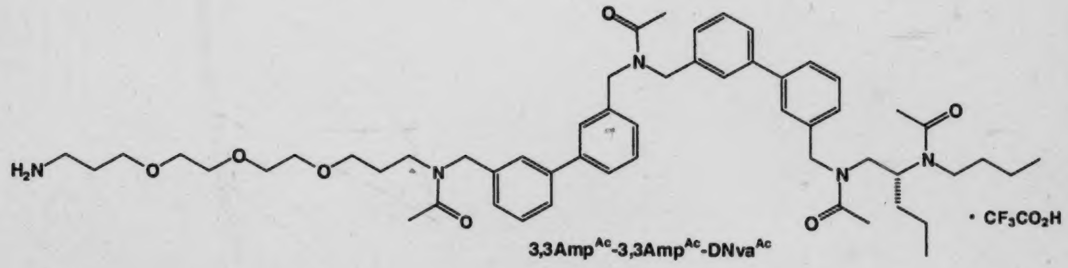
H₂N
O
O
O
N
O
N
O
N
O
N
O
N
O
· CF₃CO₂H

3,3Amp^{Ac}-3,3Amp^{Ac}-DNva^{Ac}

Current Chromatogram(s)

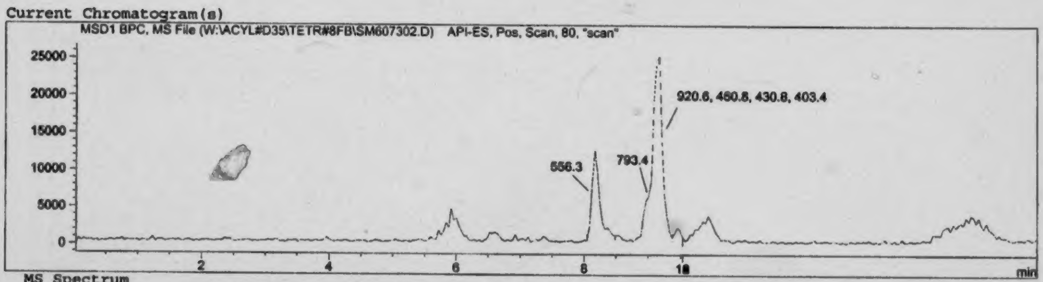

MS Spectrum

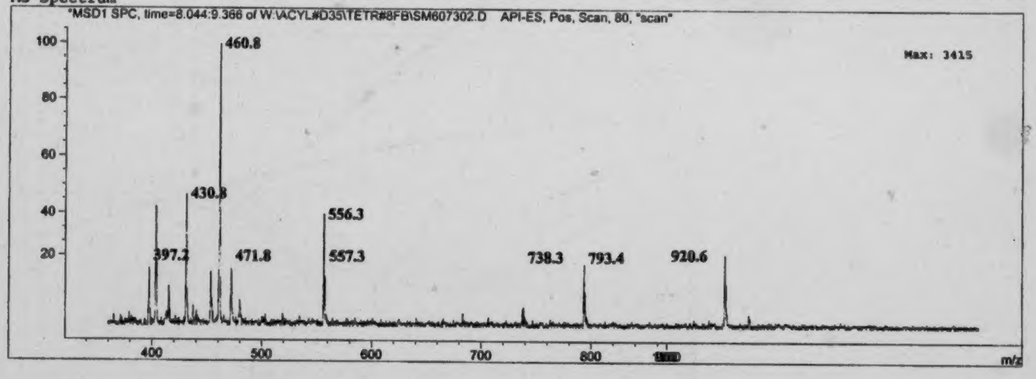

A.3.3. Tetramines from TentaGel® MB resin.

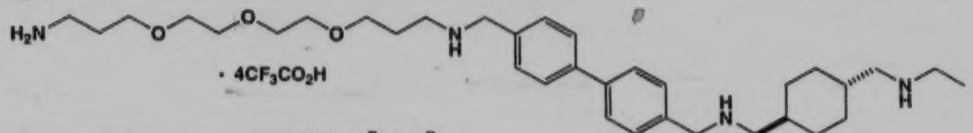
H₂N
O
O
O
N
H
· 4CF₃CO₂H
H
N
N
H

1,4Amp^R-Amc^R

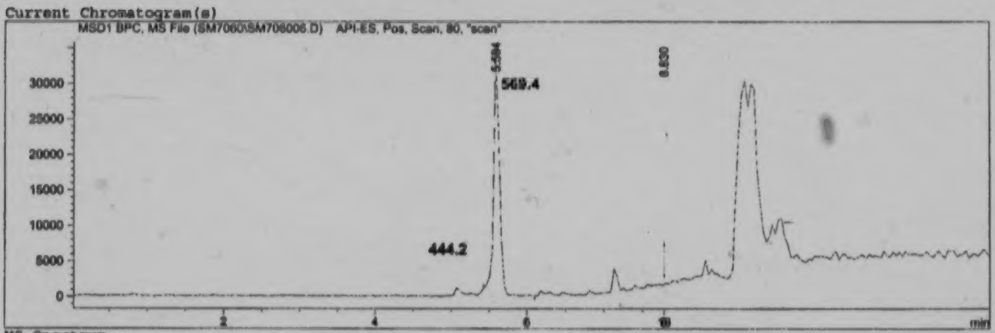

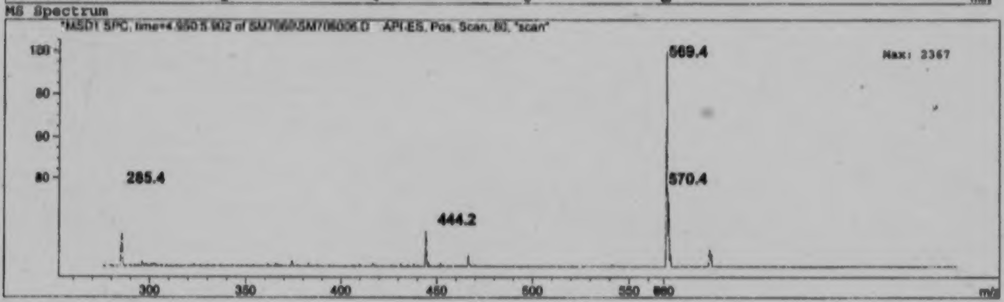

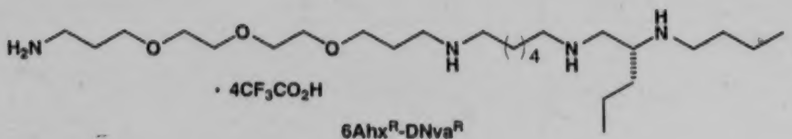
H₂N
O
O
O
N
H
4
N
H
H
N
· 4CF₃CO₂H

6Ahx^R-DNva^R

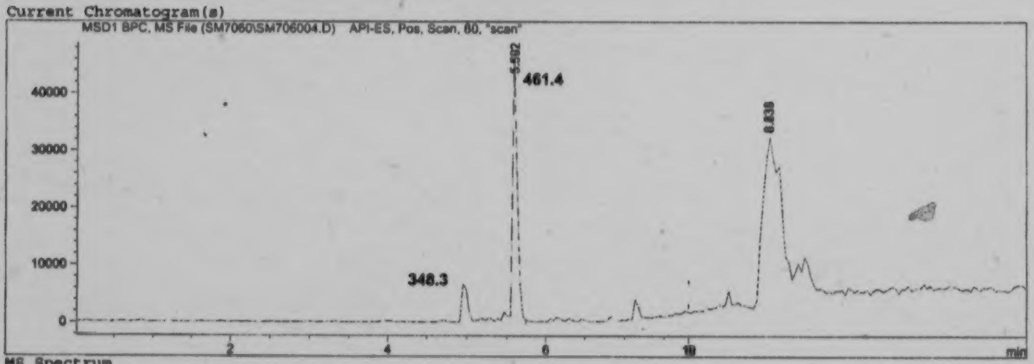
Current Chromatogram(s)
MSD1 BPC, MS File (SM7060\SM706004.D) API-ES, Pos, Scan, 80, "scan"
40000
30000
20000
10000
0
2
4
6
10
min
5.592
461.4
348.3
8.838

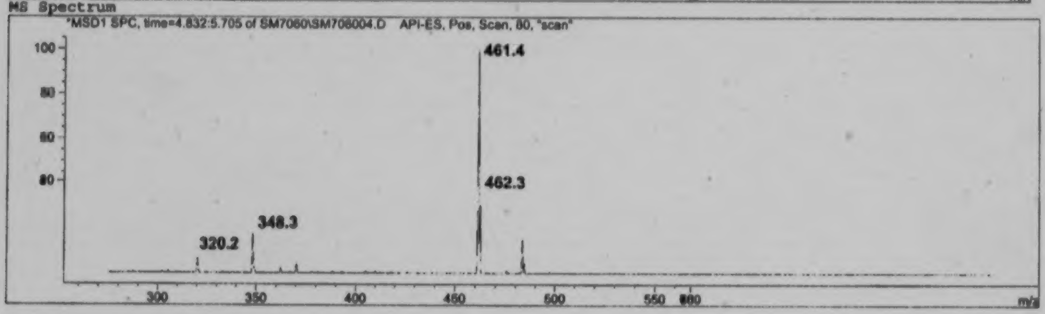
MS Spectrum
*MSD1 SPC, time=4.832:5.705 of SM7060\SM706004.D API-ES, Pos, Scan, 80, "scan"
100
80
60
40
461.4
462.3
348.3
320.2
300
350
400
450
500
550
600
m/z

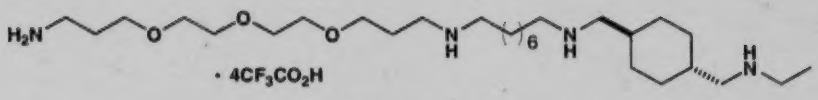
H2N
O
O
O
N H
6
N H
H N
• 4CF3CO2H

8Aoc^R-Amc^R

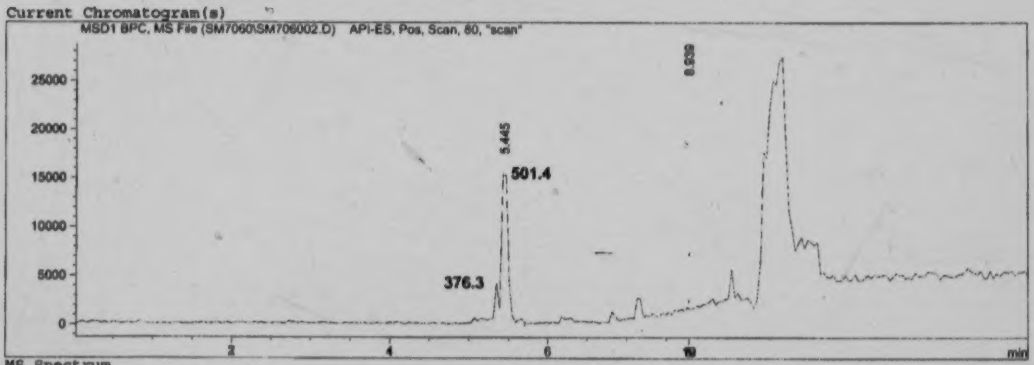
Current Chromatogram(s)

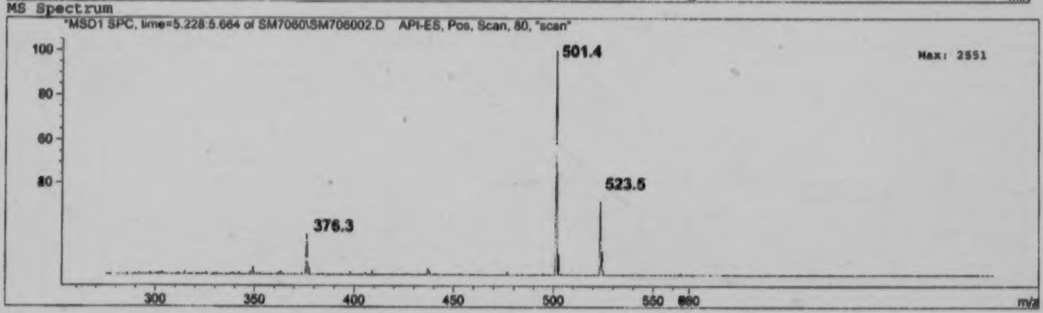
MS Spectrum

A.3.4. Triboronic acids from TentaGel® MB resin.

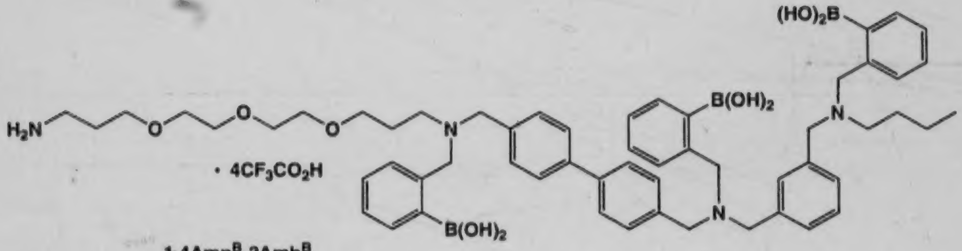

(HO)₂B
B(OH)₂
H₂N
O
O
O
N
N
N
· 4CF₃CO₂H
B(OH)₂

1,4Amp^B-3Amb^B

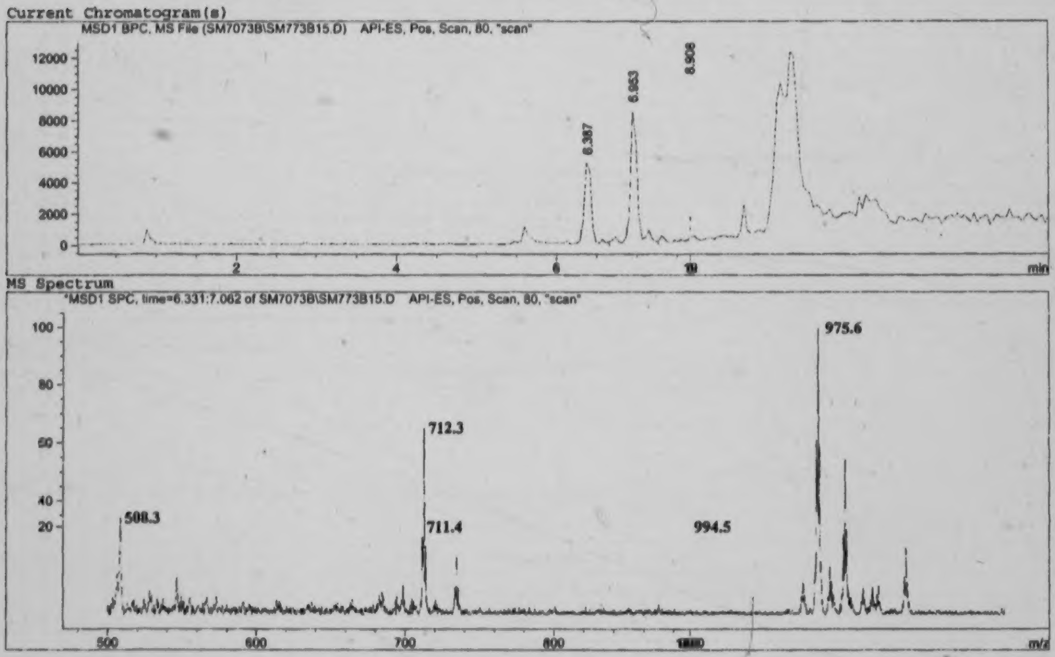

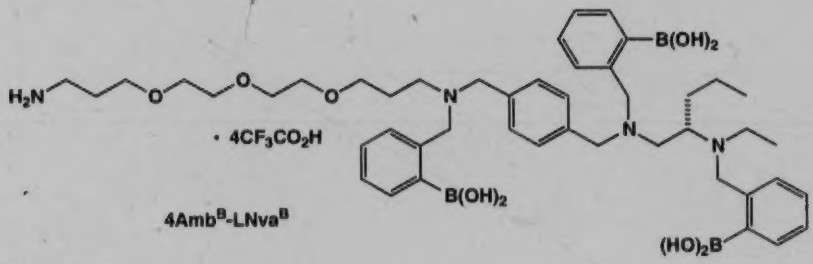
B(OH)2
H2N
O
O
O
N
N
N
· 4CF3CO2H
B(OH)2
(HO)2B

$4Amb^B$-$LNva^B$

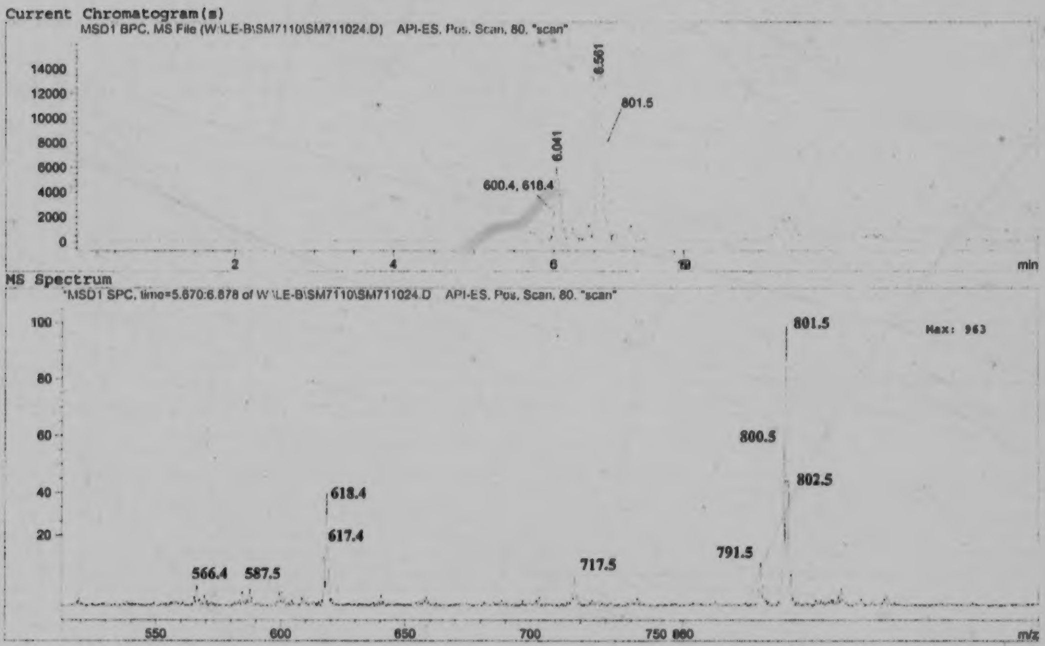
Current Chromatogram(s)
MSD1 BPC, MS File (W:\LE-B\SM7110\SM711024.D) API-ES, Pos, Scan, 80, "scan"
14000
12000
10000
8000
6000
4000
2000
0
2
4
6
10
min
6.561
801.5
6.041
600.4, 618.4
MS Spectrum
*MSD1 SPC, time=5.870:6.878 of W:\LE-B\SM7110\SM711024.D API-ES, Pos, Scan, 80, "scan"
100
80
60
40
20
Max: 963
801.5
800.5
802.5
618.4
617.4
566.4
587.5
717.5
791.5
550
600
650
700
750
800
m/z

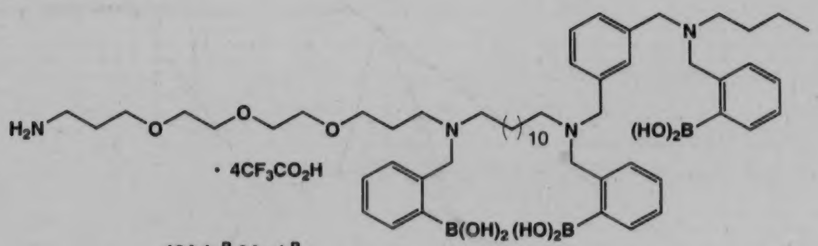
H2N
O
O
O
N
10
N
N
(HO)2B
B(OH)2 (HO)2B
· 4CF3CO2H

12Ado^B-3Amb^B

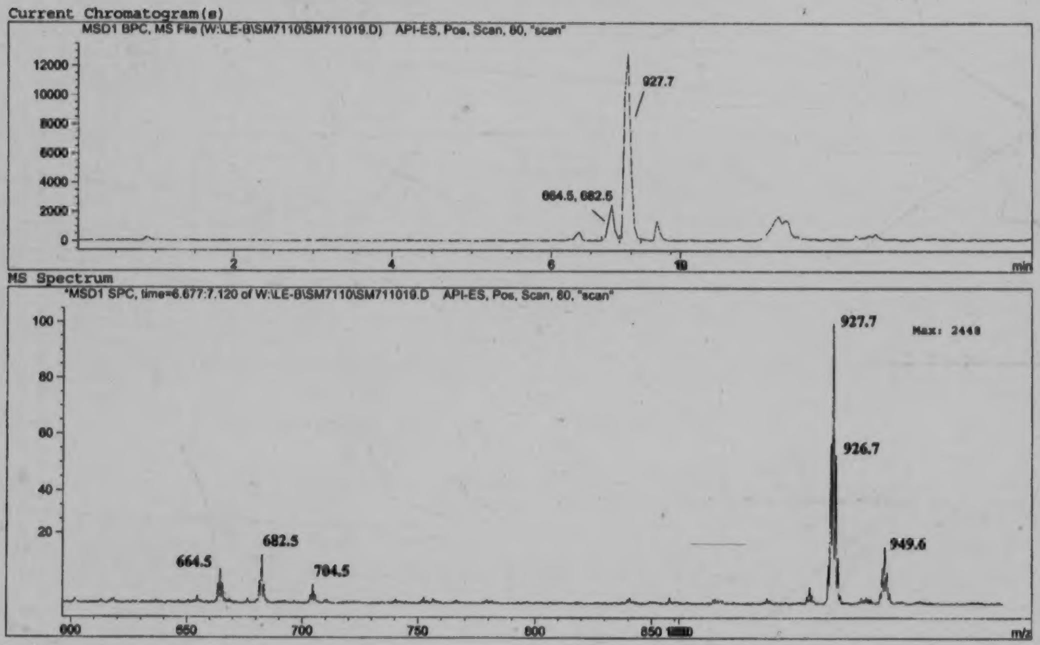

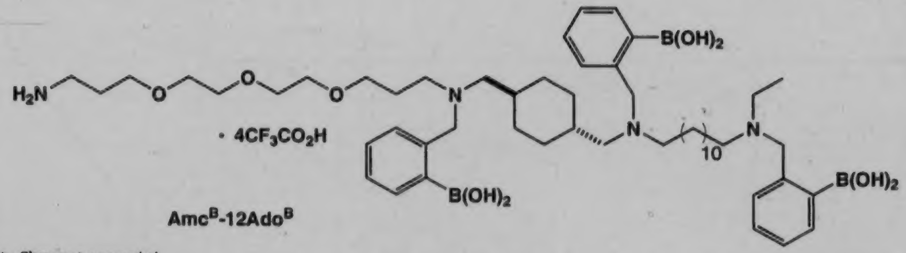
B(OH)$_2$
H_2N
O
O
O
N
N
N
· 4CF$_3$CO$_2$H
10
B(OH)$_2$
B(OH)$_2$

Amc^B-12Ado^B

Current Chromatogram(s)

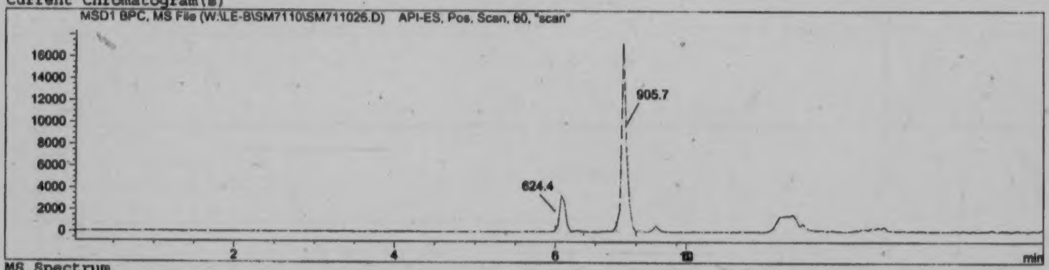

MS Spectrum

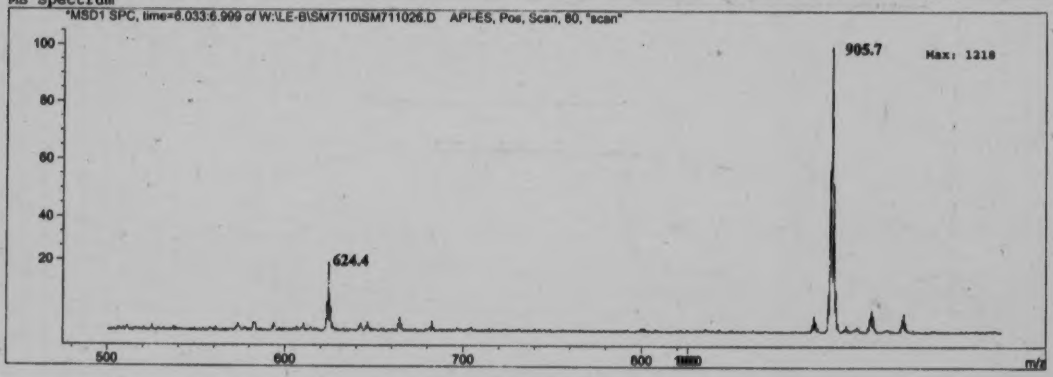

A.4. LC and NMR analyses of anthracenyl triboronic acid, 136.

LC and ESMS of Amb^B-Amb^B-Anth^B

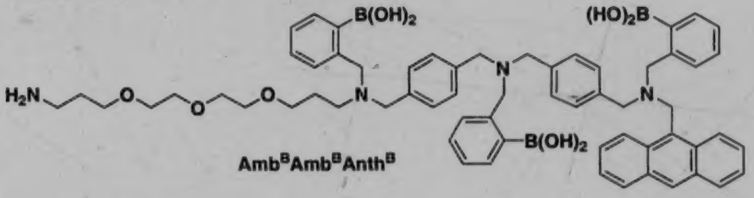
B(OH)2
(HO)2B
H2N
O
O
O
N
N
N
B(OH)2

Amb^{B}Amb^{B}Anth^B

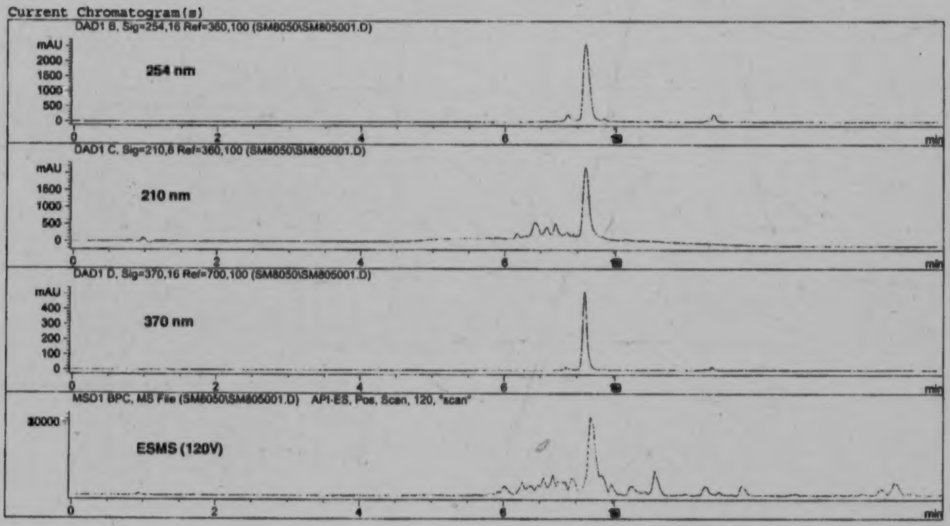

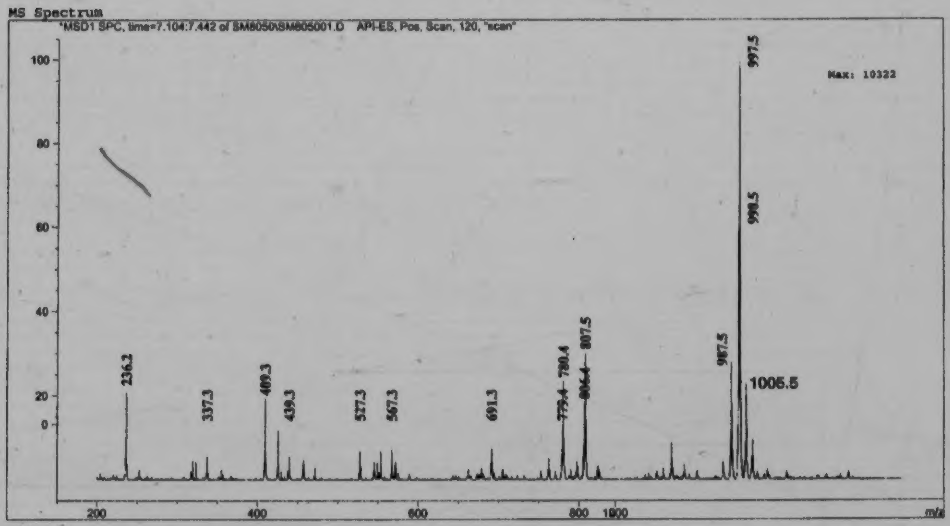

LC and ESMS of εAhx^B-Amb^B-Anth^B

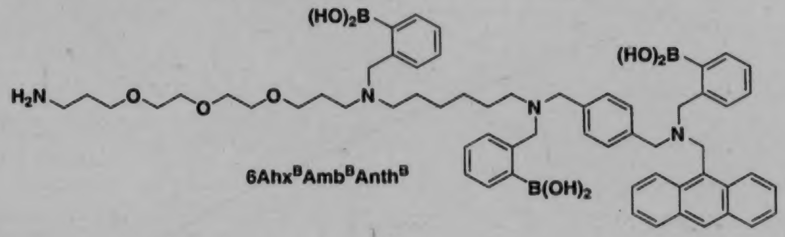
(HO)₂B
(HO)₂B
H₂N
O
O
O
N
N
N
B(OH)₂
6Ahx^B Amb^B Anth^B

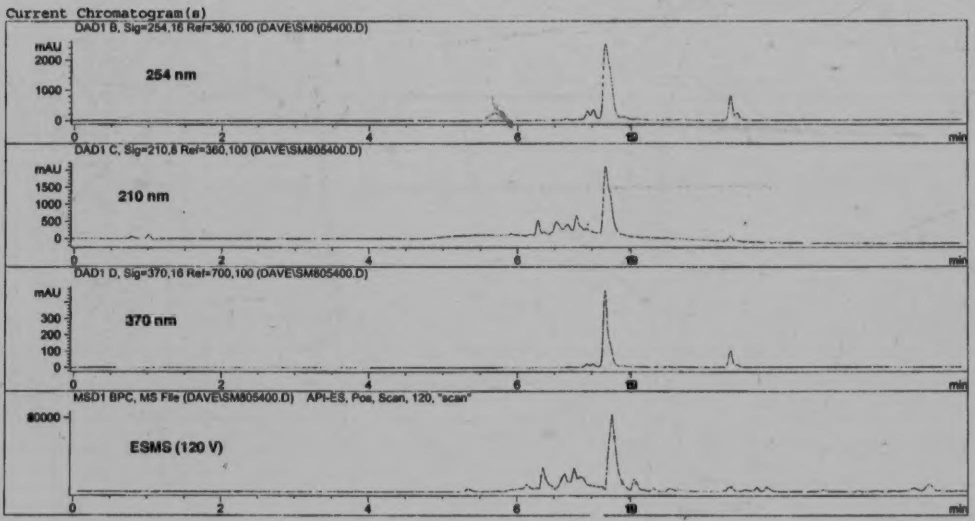

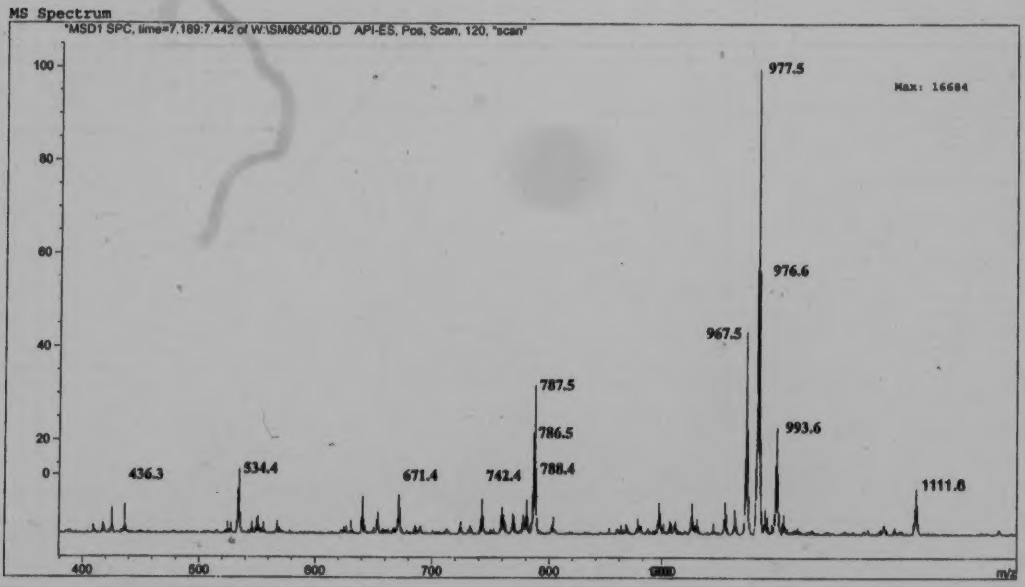

LC and ESMS of 4Acc^B-Amb^B-Anth^B

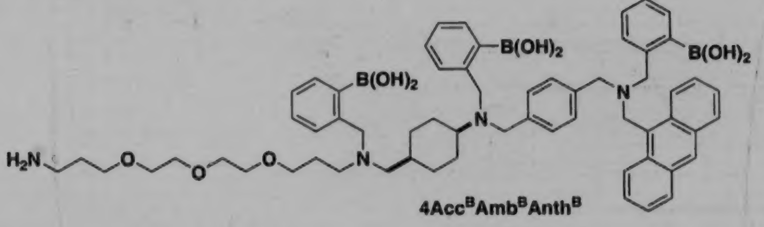
B(OH)₂
B(OH)₂
B(OH)₂
B(OH)₂
H₂N
O
O
O
N
N
N

4Acc^{B}Amb^{B}Anth^B

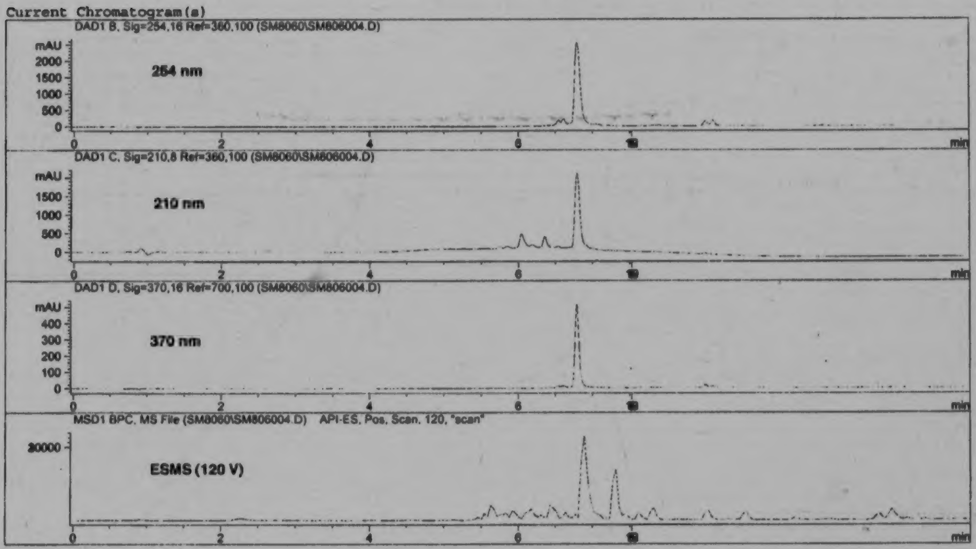

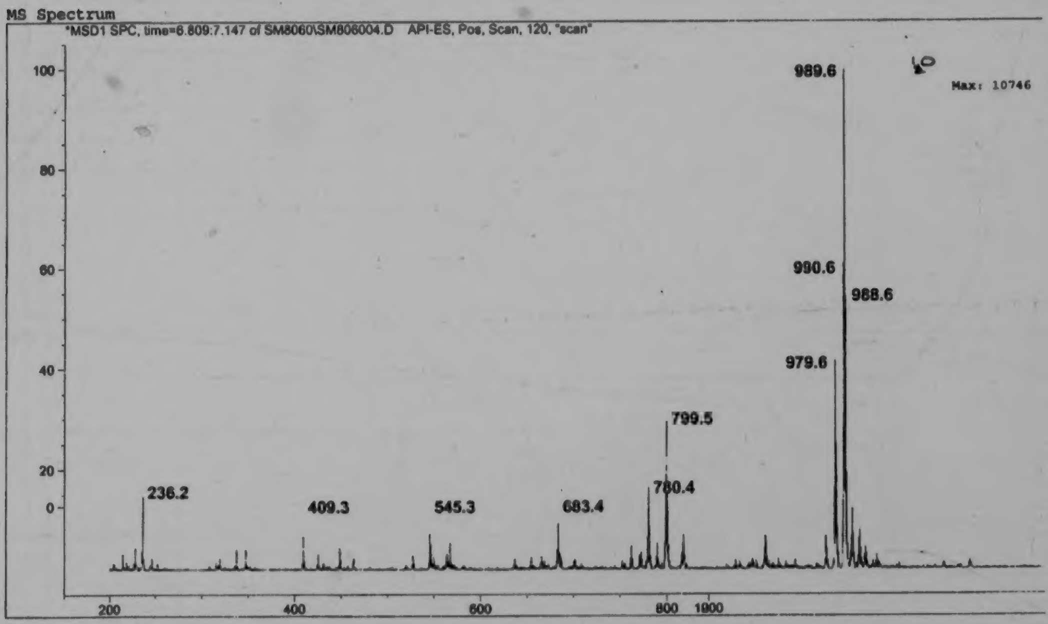

LC and ESMS of Amc^B-Amb^B-Anth^B

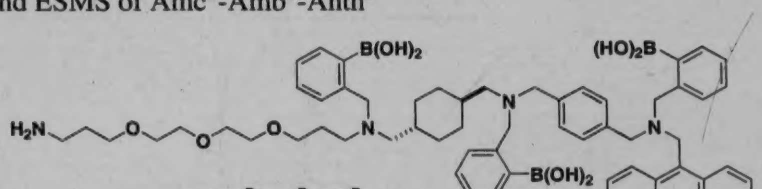
B(OH)2
(HO)2B
H2N
O
O
O
N
N
N
B(OH)2

Amc^{B}Amb^{B}Anth^B

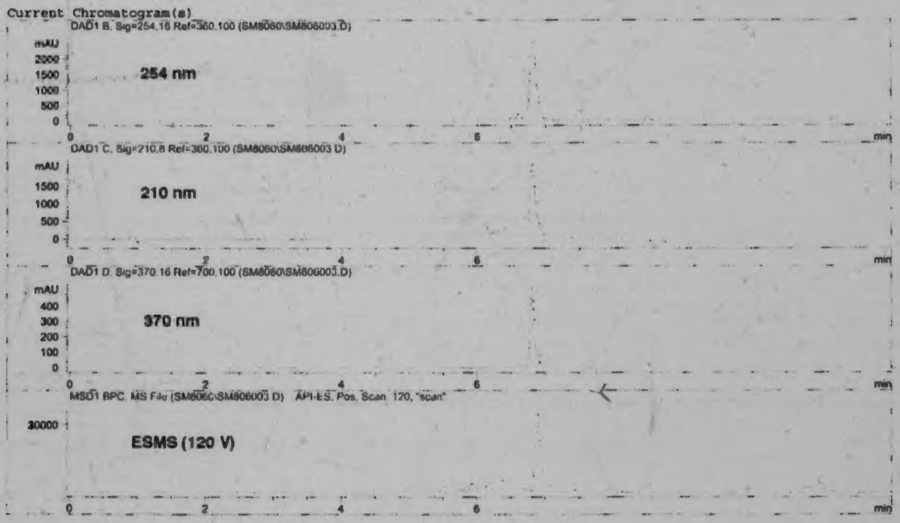

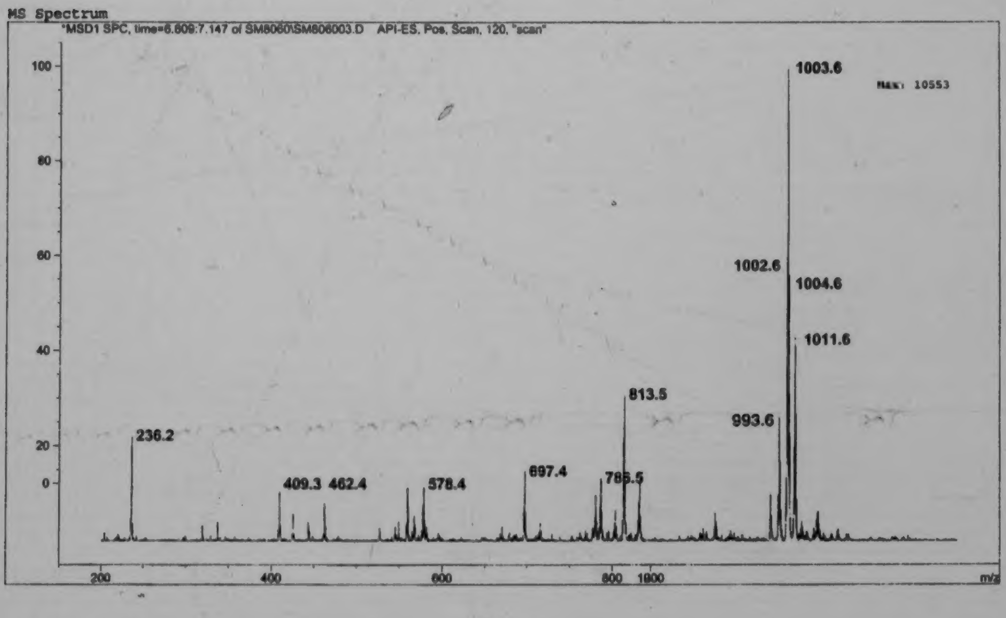

LC of Amb^B-Anth^B

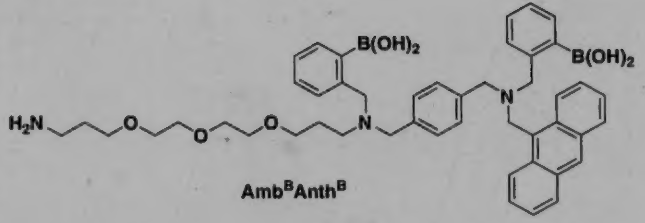
B(OH)$_2$
B(OH)$_2$
H$_2$N
O
O
O
N
N

Amb^{B}Anth^B

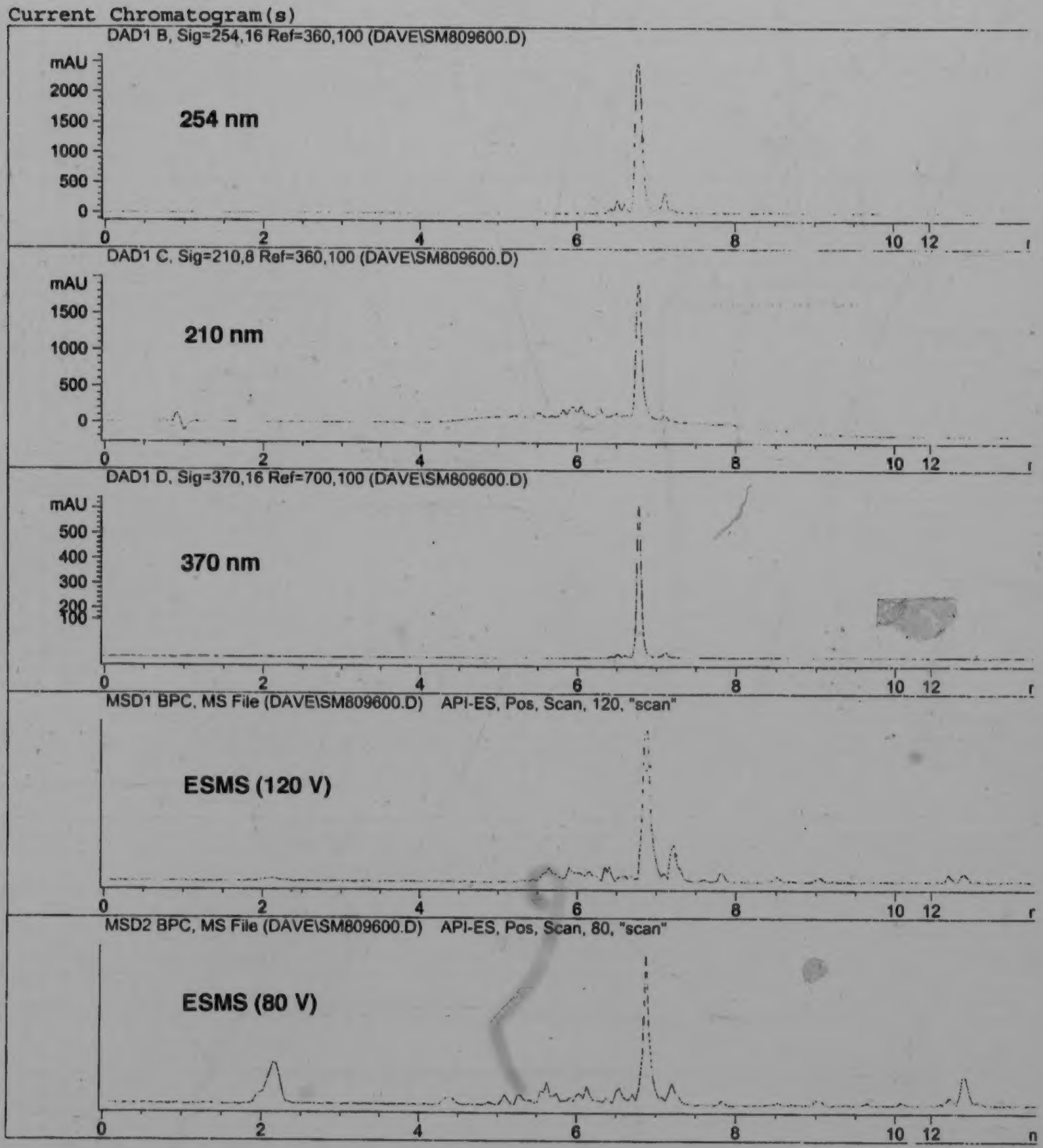

ESMS of Amb^B-Anth^B

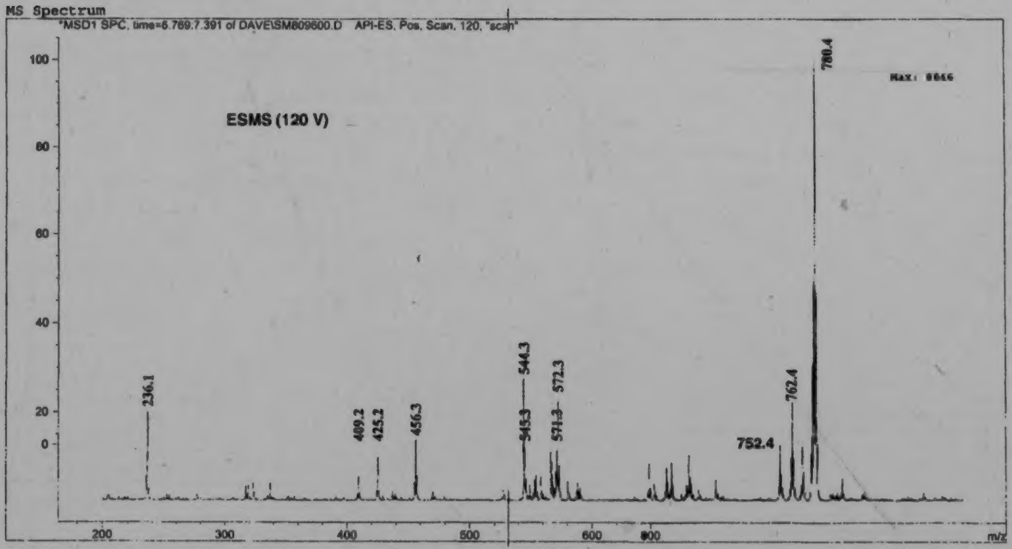

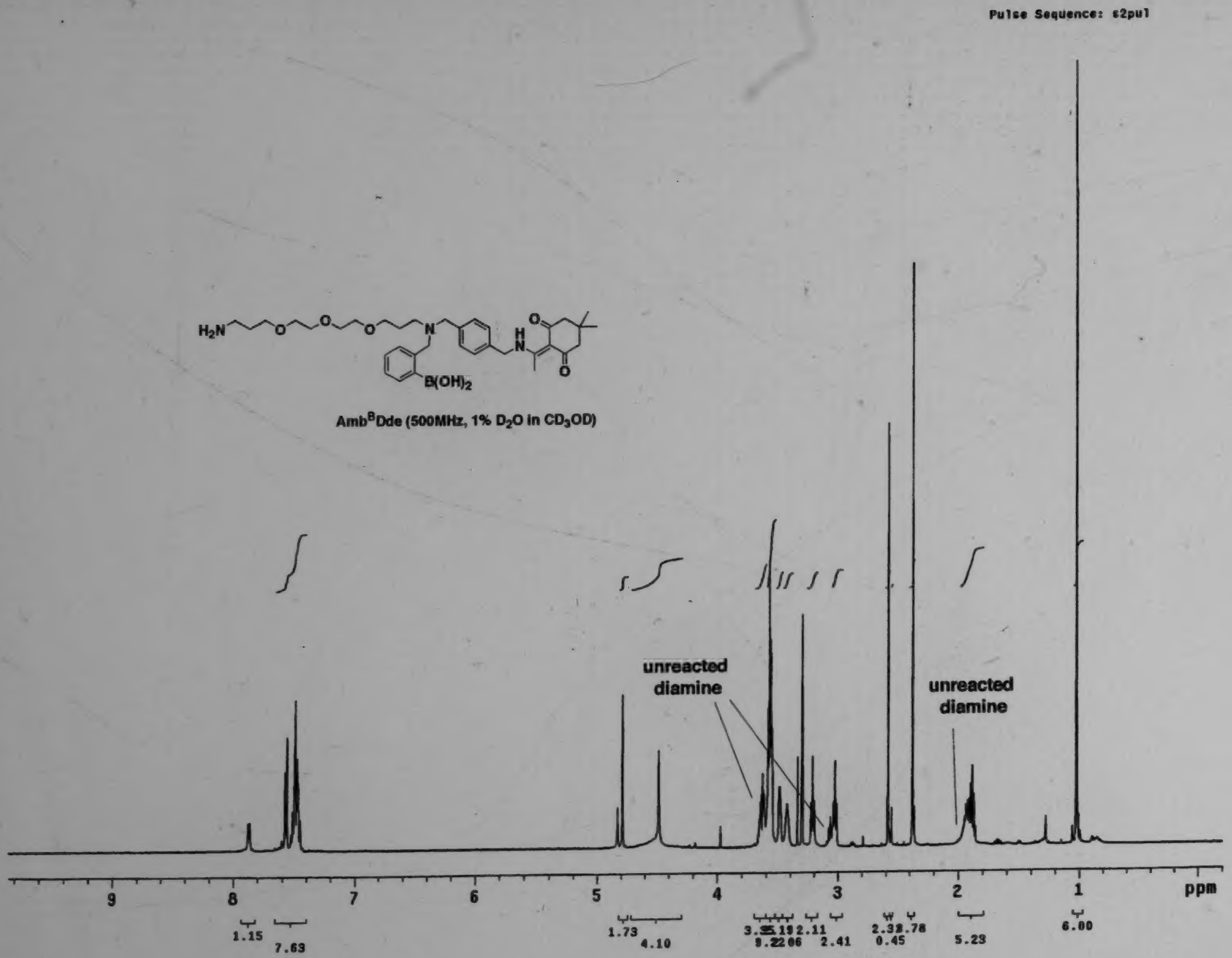

Amb^{B}Dde (500MHz, 1% D_2O in CD_3OD)

1/3,0

sm8115 13C APT 125MHz cd3od 16 sept 2002

Pulse Sequence: apt

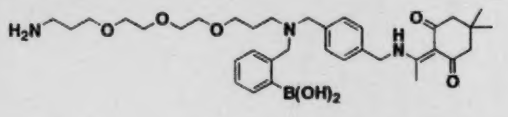

Amb^{B}Dde (500MHz, 1% D_2O in CD_3OD)

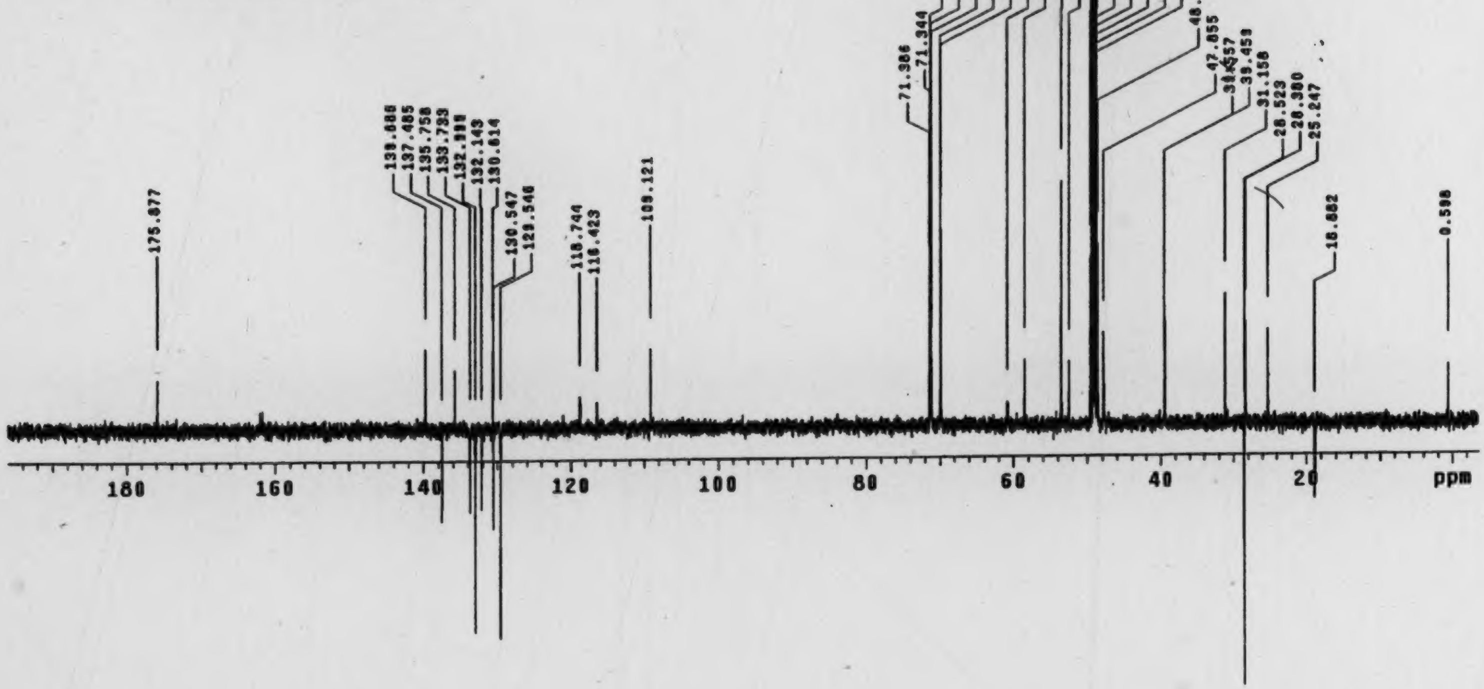

A.5. Fluorescence titrations of 136 with disaccharides.

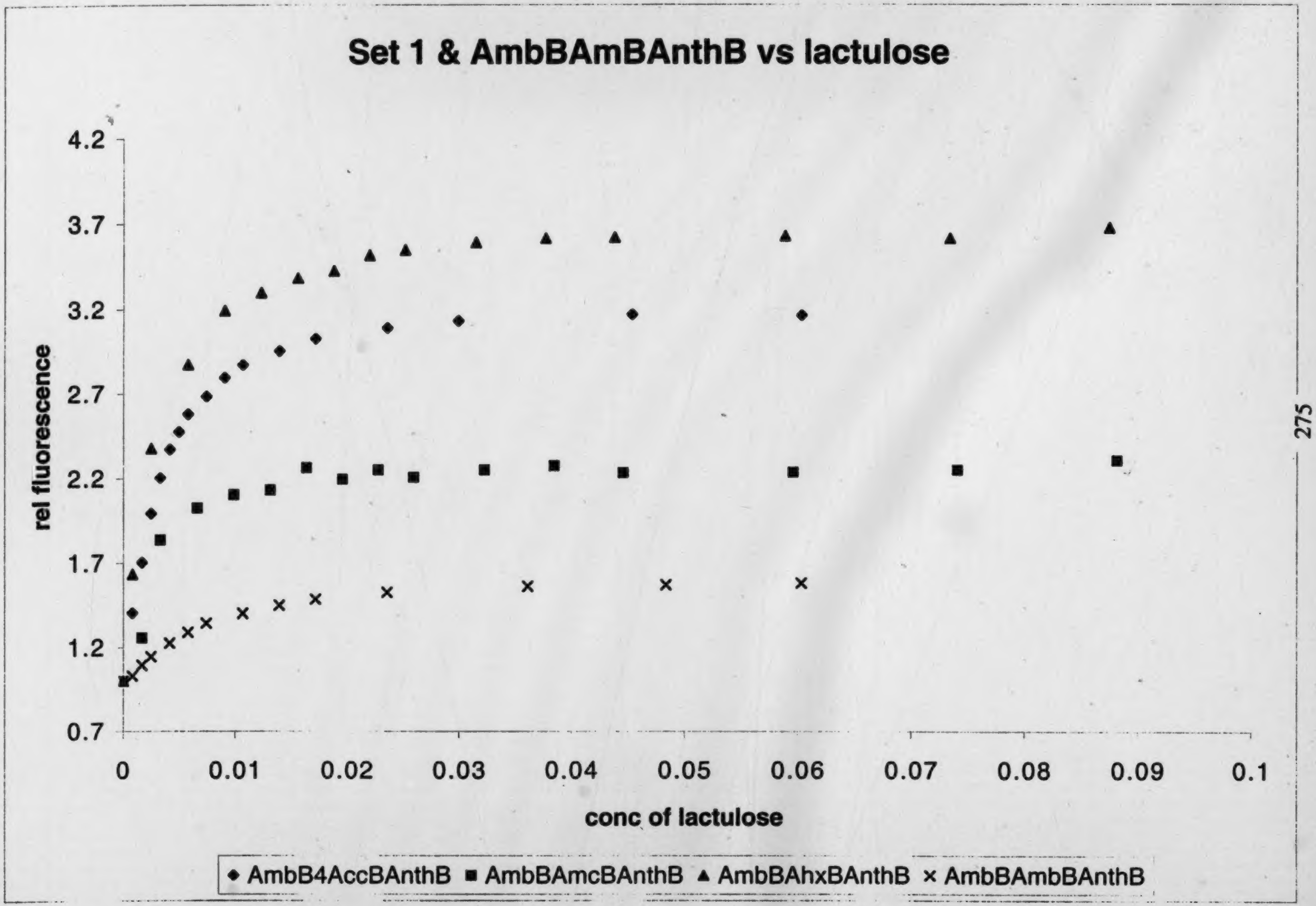
Set 1 & AmbBAmBAnthB vs lactulose
rel fluorescence
4.2
3.7
3.2
2.7
2.2
1.7
1.2
0.7
0
0.01
0.02
0.03
0.04
0.05
0.06
0.07
0.08
0.09
0.1
conc of lactulose
◆ AmbB4AccBAnthB
■ AmbBAmcBAnthB
▲ AmbBAhxBAnthB
× AmbBAmbBAnthB

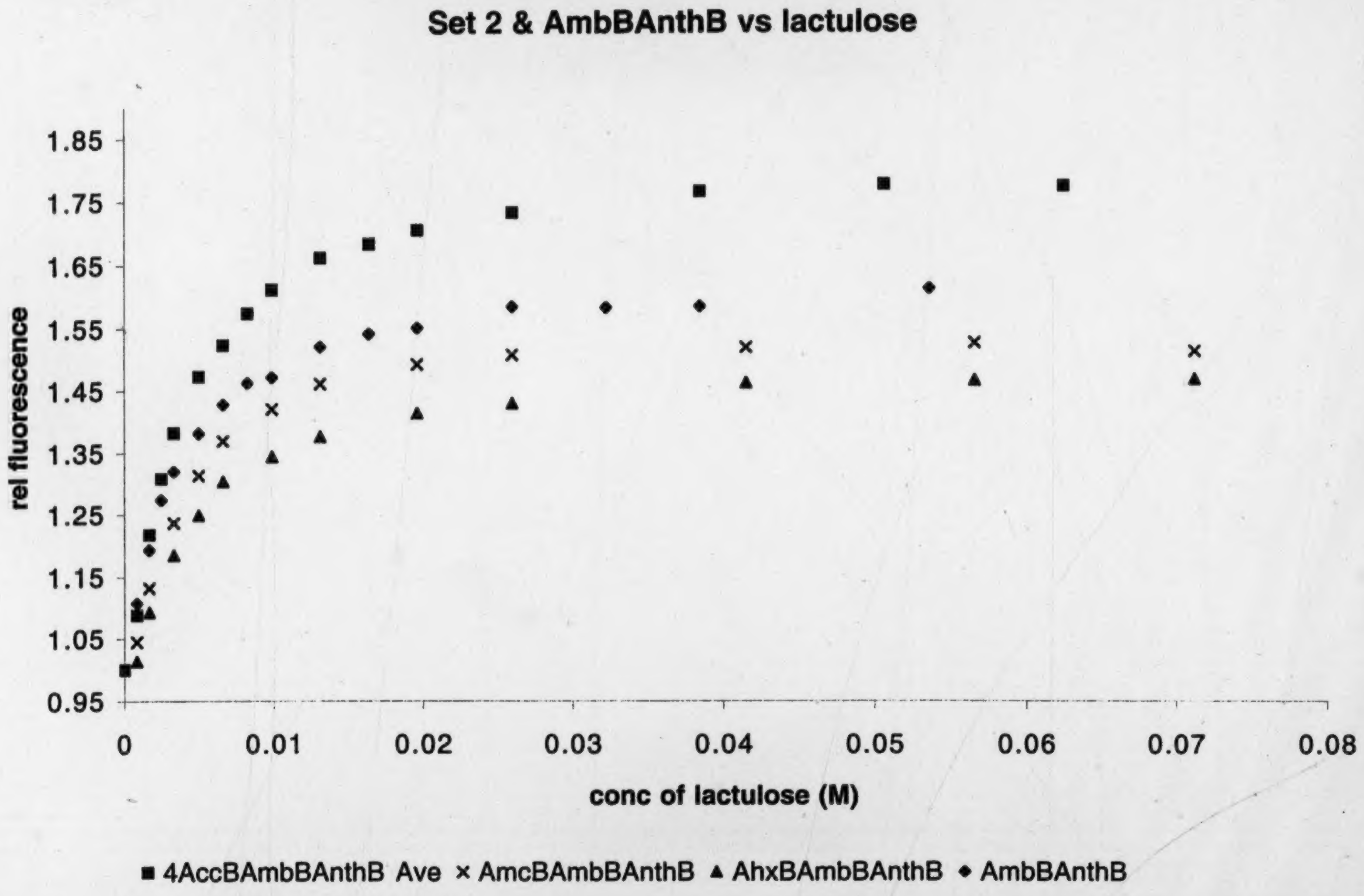
Set 2 & AmbBAnthB vs lactulose
rel fluorescence
1.85
1.75
1.65
1.55
1.45
1.35
1.25
1.15
1.05
0.95
0
0.01
0.02
0.03
0.04
0.05
0.06
0.07
0.08
conc of lactulose (M)
■ 4AccBAmbBAnthB Ave
× AmcBAmbBAnthB
▲ AhxBAmbBAnthB
◆ AmbBAnthB

Set 1 (incl. AmbBAmbBAnthB) vs melibiose

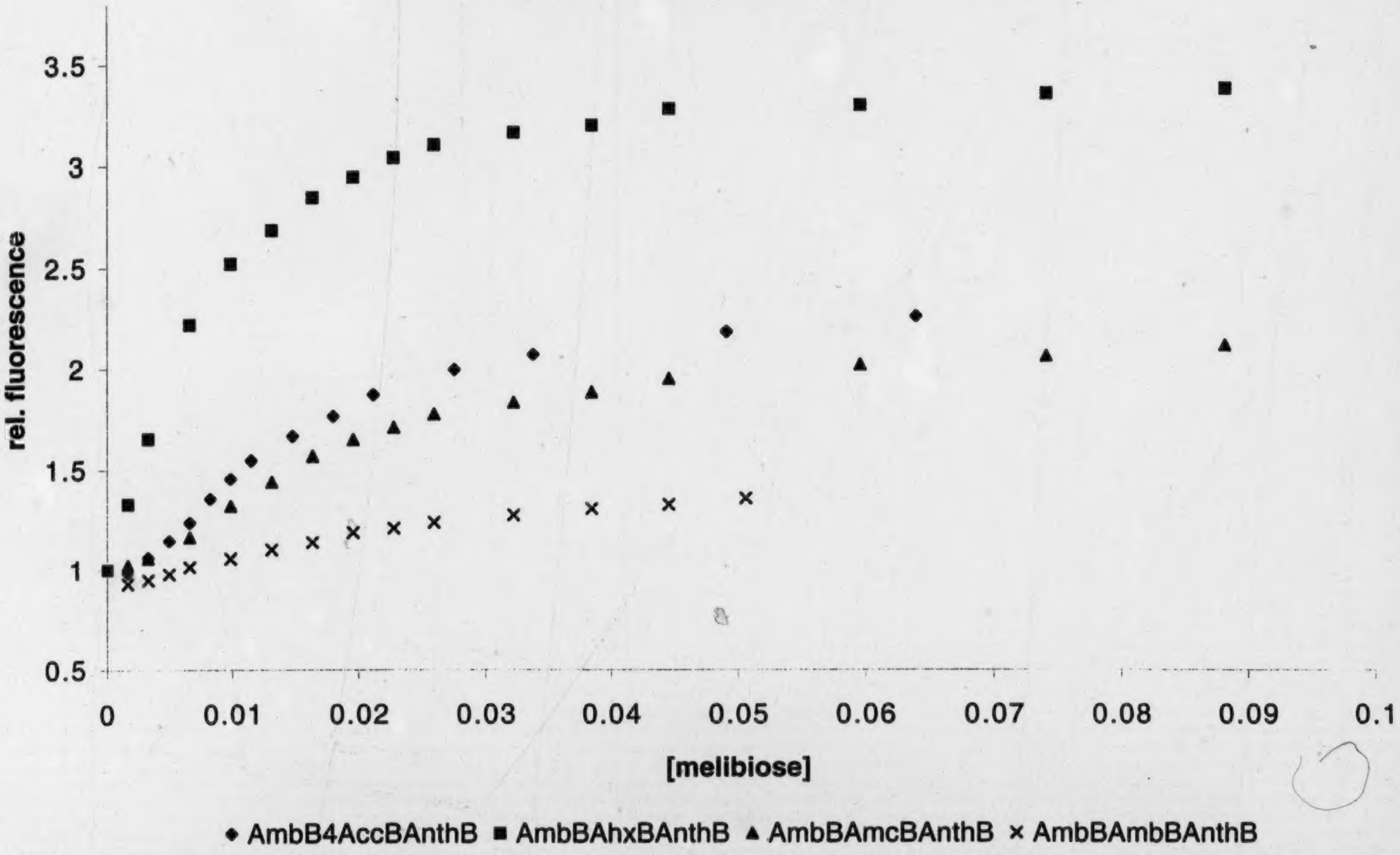

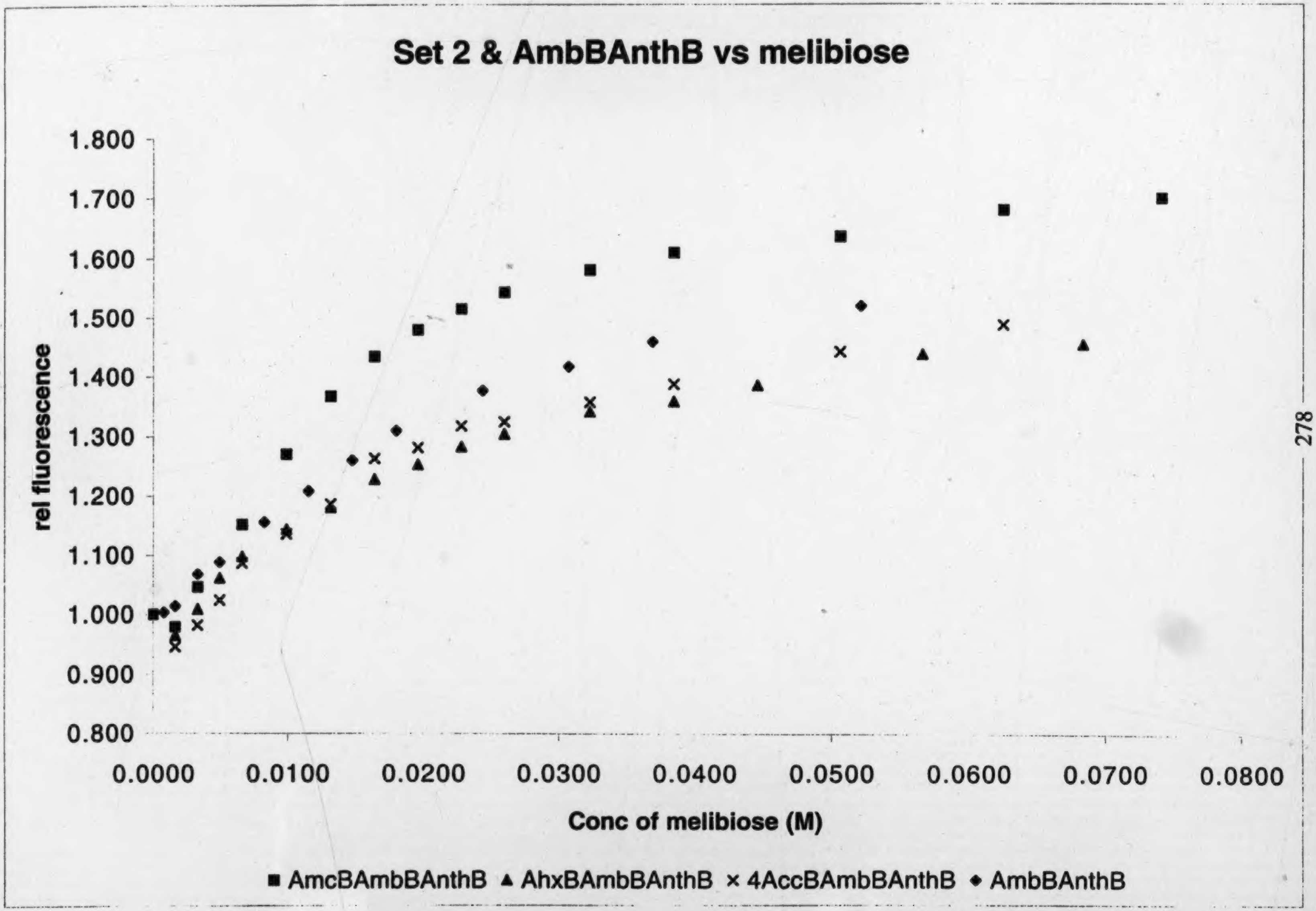
Set 2 & AmbBAnthB vs melibiose
rel fluorescence
1.800
1.700
1.600
1.500
1.400
1.300
1.200
1.100
1.000
0.900
0.800
0.0000
0.0100
0.0200
0.0300
0.0400
0.0500
0.0600
0.0700
0.0800
Conc of melibiose (M)
■ AmcBAmbBAnthB ▲ AhxBAmbBAnthB × 4AccBAmbBAnthB ◆ AmbBAnthB

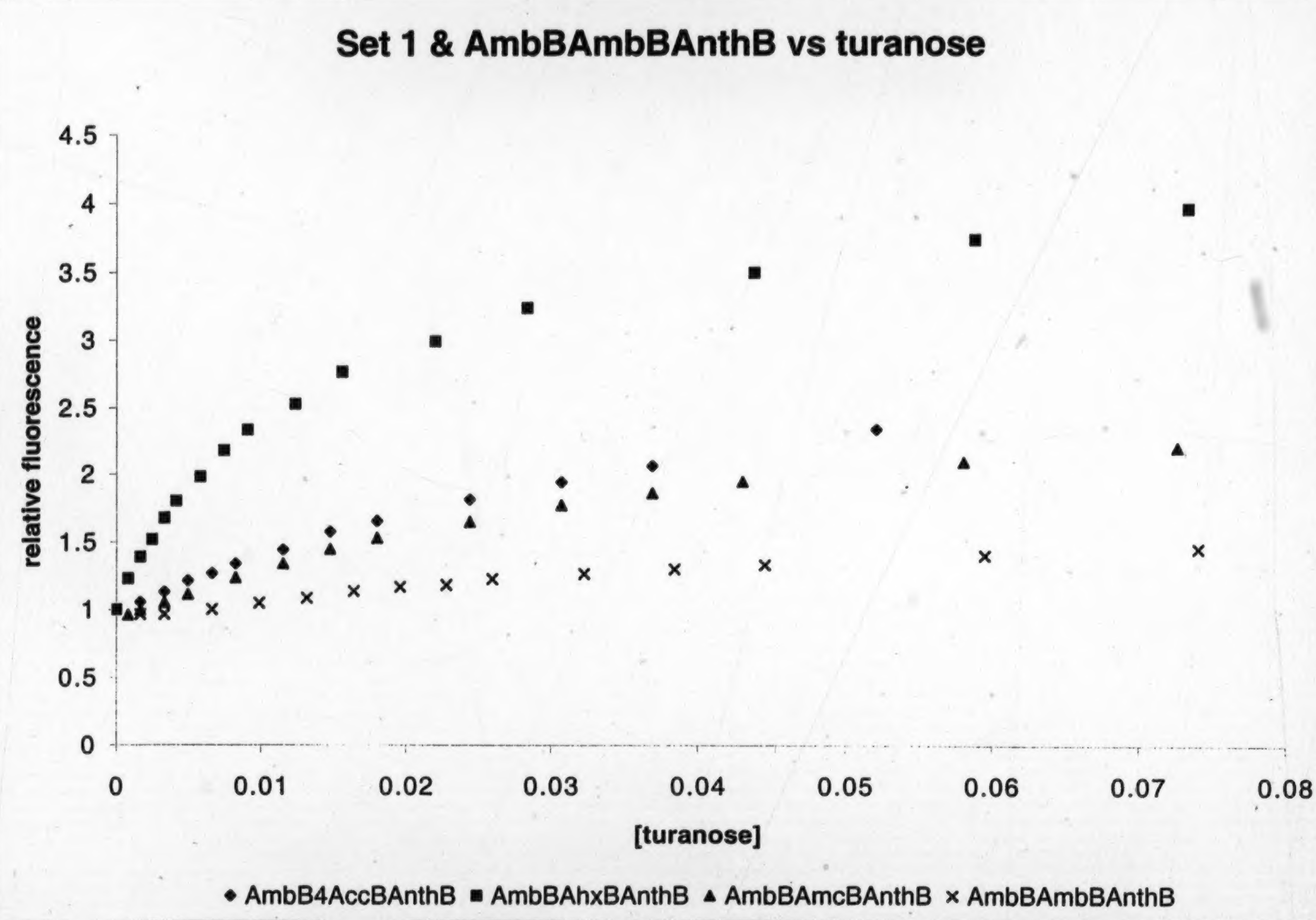
Set 1 & AmbBAmbBAnthB vs turanose
relative fluorescence
4.5
4
3.5
3
2.5
2
1.5
1
0.5
0
0
0.01
0.02
0.03
0.04
0.05
0.06
0.07
0.08
[turanose]
◆ AmbB4AccBAnthB
■ AmbBAhxBAnthB
▲ AmbBAmcBAnthB
× AmbBAmbBAnthB

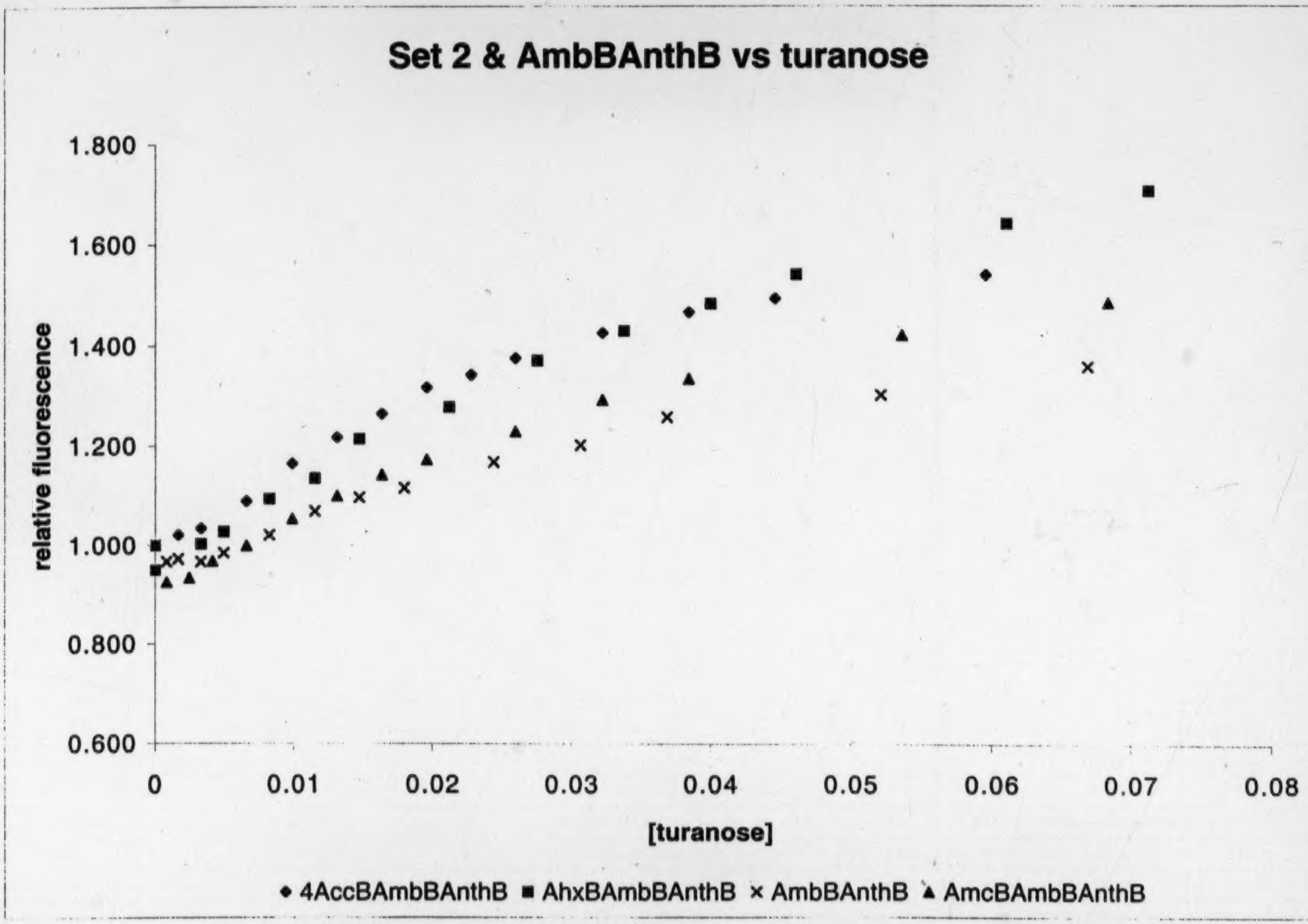
Set 2 & AmbBAnthB vs turanose
relative fluorescence
1.800
1.600
1.400
1.200
1.000
0.800
0.600
0
0.01
0.02
0.03
0.04
0.05
0.06
0.07
0.08
[turanose]
◆ 4AccBAmbBAnthB
■ AhxBAmbBAnthB
× AmbBAnthB
▲ AmcBAmbBAnthB